

STATE OF CALIFORNIA DEPARTMENT OF TRANSPORTATION
TECHNICAL REPORT DOCUMENTATION PAGE
 TR0003 (REV. 10/98)

1. REPORT NUMBER CA18-2544	2. GOVERNMENT ASSOCIATION NUMBER	3. RECIPIENT'S CATALOG NUMBER
4. TITLE AND SUBTITLE Seismic Performance of Precast Full-Depth Decks in Accelerated Bridge Construction	5. REPORT DATE July 2018	6. PERFORMING ORGANIZATION CODE UNR
	8. PERFORMING ORGANIZATION REPORT NO. UNR/CA18-2544	
7. AUTHOR(S) Grishma Shrestha, Ahmad M. Itani, M. Saiid Saiidi	10. WORK UNIT NUMBER	
9. PERFORMING ORGANIZATION NAME AND ADDRESS Department of Civil and Environmental Engineering, MS 258 University of Nevada, Reno 1664 N. Virginia Street Reno, NV 89557	11. CONTRACT OR GRANT NUMBER 65A0423	
	13. TYPE OF REPORT AND PERIOD COVERED Final Report 5/15/2014 – 8/14/2017	
12. SPONSORING AGENCY AND ADDRESS California Department of Transportation Engineering Service Center 1801 30 th Street, MS 9-2/5i Sacramento CA 95816 California Department of Transportation Division of Research and Innovation, MS-83 1227 O Street Sacramento CA 95814	14. SPONSORING AGENCY CODE 913	
	15. SUPPLEMENTAL NOTES Prepared in cooperation with the State of California Department of Transportation.	
16. ABSTRACT <p>Cast-in-place (CIP) concrete construction is time intensive and requires many on-site construction procedures that may create negative impacts on traffic flow, work zone safety, and the environment. Accelerated bridge construction (ABC) offers a viable alternative to CIP construction since significant on-site construction time can be reduced by using prefabricated elements. Full depth R/C deck panels offer unique opportunity for new deck construction or replacement projects. These decks can be quickly assembled minimizing traffic disruption, reducing environmental impact, improving worker and motorist safety, improving constructability, and increasing the quality of the final product. Prefabricated deck panels, if oriented properly, will provide the opportunity to replace decks during the life span of the bridge while keeping part of the bridge in service.</p> <p>The primary objective of this study was to evaluate the ultimate strength and stiffness of headed anchors in connections between prefabricated precast R/C deck panels and girders using different grout types. The study consisted of an experimental and an analytical investigation. The former involved construction and testing shear and pullout specimens to evaluate the shear and pullout strength and stiffness. Various parameters such as group effect of anchor, types of grout, and head area of the anchors were also studied. Experimental results indicated that the type of grout and head area of the anchors had an insignificant effect on the shear and pullout capacity of the anchor. It was concluded that the current provisions in the AASHTO LRFD Specifications for the ultimate shear strength of studs in CIP construction may be used for anchors in precast R/C panels.</p> <p>The second part of the study consisted of an analytical investigation of a two-span bridge to determine the forces in the anchors in precast deck panels when subjected to large ground motions. A computational model for headed anchors was used to investigate the seismic response of decks with rigid shear links between the deck and girders and flexible links with shear pockets spaced at 4 ft and 6 ft spacing. An ensemble of eight earthquake ground motion records were applied in this part of the study, including both far-field and near-fault ground motion records. To achieve spectral compatibility with the design spectrum, the records were scaled to the design spectrum. In addition, the nonlinear response history analysis was performed for earthquake intensities corresponding to 150% of the design level. Insignificant difference was observed in the dynamic properties of the bridge and seismic behavior due to the increase in pocket spacing from 4 ft to 6 ft. It was also found that the forces in the headed anchors for both spacing were well below ultimate strength of the connectors leading to deck connections being capacity protected.</p>		
17. KEY WORDS Seismic, Accelerated Bridge Construction	18. DISTRIBUTION STATEMENT No restrictions. This document is available to the public through the National Technical Information Service, Springfield, VA 22161	
19. SECURITY CLASSIFICATION (of this report) Unclassified	20. NUMBER OF PAGES 304	21. PRICE

DISCLAIMER STATEMENT

This document is disseminated in the interest of information exchange. The contents of this report reflect the views of the authors who are responsible for the facts and accuracy of the data presented herein. The contents do not necessarily reflect the official views or policies of the State of California or the Federal Highway Administration. This publication does not constitute a standard, specification or regulation. This report does not constitute an endorsement by the Department of any product described herein.

For individuals with sensory disabilities, this document is available in alternate formats. For information, call (916) 654-8899, TTY 711, or write to California Department of Transportation, Division of Research, Innovation and System Information, MS-83, P.O. Box 942873, Sacramento, CA 94273-0001.

Final Report No. CA18-2544, CCEER 17-05

**SEISMIC PERFORMANCE OF PRECAST FULL-DEPTH DECKS
IN ACCELERATED BRIDGE CONSTRUCTION**

Grishma Shrestha
Ahmad M. Itani
M. Saiid Saiidi

A report sponsored by the California Department of Transportation

Center for Civil Engineering Earthquake Research

University of Nevada, Reno
Department of Civil and Environmental Engineering, MS 258
1664 N. Virginia St.
Reno, NV 89557

July 2018

Abstract

Cast-in-place (CIP) concrete construction is time intensive and requires many on-site construction procedures that may create negative impacts on traffic flow, work zone safety, and the environment. Accelerated bridge construction (ABC) offers a viable alternative to CIP construction since significant on-site construction time can be reduced by using prefabricated elements. Full depth R/C deck panels offer unique opportunity for new deck construction or replacement projects. These decks can be quickly assembled minimizing traffic disruption, reducing environmental impact, improving worker and motorist safety, improving constructability, and increasing the quality of the final product. Prefabricated deck panels, if oriented properly, will provide the opportunity to replace decks during the life span of the bridge while keeping part of the bridge in service.

The primary objective of this study was to evaluate the ultimate strength and stiffness of headed anchors in connections between prefabricated precast R/C deck panels and girders using different grout types. The study consisted of an experimental and an analytical investigation. The former involved construction and testing shear and pullout specimens to evaluate the shear and pullout strength and stiffness. Various parameters such as group effect of anchor, types of grout, and head area of the anchors were also studied. Experimental results indicated that the type of grout and head area of the anchors had an insignificant effect on the shear and pullout capacity of the anchor. It was concluded that the current provisions in the AASHTO LRFD Specifications for the

ultimate shear strength of studs in CIP construction may be used for anchors in precast R/C panels.

The second part of the study consisted of an analytical investigation of a two-span bridge to determine the forces in the anchors in precast deck panels when subjected to large ground motions. A computational model for headed anchors was used to investigate the seismic response of decks with rigid shear links between the deck and girders and flexible links with shear pockets spaced at 4 ft and 6 ft spacing. An ensemble of eight earthquake ground motion records were applied in this part of the study, including both far-field and near-fault ground motion records. To achieve spectral compatibility with the design spectrum, the records were scaled to the design spectrum. In addition, the nonlinear response history analysis was performed for earthquake intensities corresponding to 150% of the design level. Insignificant difference was observed in the dynamic properties of the bridge and seismic behavior due to the increase in pocket spacing from 4 ft to 6 ft. It was also found that the forces in the headed anchors for both spacing were well below ultimate strength of the connectors leading to deck connections being capacity protected.

Acknowledgement

The research presented in this document was funded by the California Department of Transportation under contract No. 65A0519. The conclusions and recommendations of this study may not necessarily present the views of the sponsor. Special thanks to Mr. Peter S. Lee, Caltrans Research Project Manager and Mr. Ron Bromenschenkel, Caltrans Bridge Design Engineer for their interest and comments.

The research team is indebted to Headed Reinforcement Corp. (HRC) and Kwik Bond Polymers for generously donating materials and providing technical input. The authors are thankful to Dr. Patrick Laplace, Mr. Mark Lattin, Mr. Chad Lyttle and Mr. Todd Lyttle of UNR for their assistance in conducting the experiments.

This report is based on parts of PhD dissertation by the first author supervised by the other co-authors.

Table of Contents

Abstract	i
Acknowledgement	iii
Table of Contents	iv
List of Tables	viii
List of Figures	x
1. Introduction.....	1
1.1 Background	1
1.2 Problem Statement	2
1.3 Literature Review	5
1.3.1 NCHRP Report 407	5
1.3.2 NCHRP Synthesis 324.....	7
1.3.3 Menkulasi and Roberts-Wollmann (2005)	8
1.3.4 Markowski (2005)	9
1.3.5 Ramey and Umphrey (2006)	10
1.3.6 Sullivan (2007)	12
1.3.7 Oliva et al. (2007).....	13
1.3.8 Scholz et al. (2007).....	15
1.3.9 NCHRP 12-65 Project	16
1.3.10 Henley (2009).....	18
1.3.11 Nebraska University Deck (NUDECK) System.....	19
1.3.12 Perry and Royce (2010).....	20
1.3.13 PCI (2011)	21
1.3.14 Assad (2014).....	22
1.3.15 Cao et al. (2016).	22
1.3.16 Tawadrous (2017).....	23
1.4 Research Objectives and Scope of Work	25
1.5 Report Organization	26
2. Experimental Study.....	27

2.1 Introduction	27
2.2 Shear Test of Headed Anchors.....	28
2.2.1 Test Specimens.....	28
2.2.1.1 Deck Section and Pockets.....	30
2.2.1.2 Girder and Footing Section.....	33
2.2.2 Materials.....	37
2.2.2.1 Concrete.....	37
2.2.2.2 Grout.....	39
2.2.2.3 Deck and Girder Reinforcement.....	42
2.2.3 Test Matrix.....	47
2.2.4 Test Setup and Instrumentation.....	48
2.2.5 Construction Process and Testing Procedure.....	56
2.2.6 Shear Test Results.....	59
2.2.6.1 Ultimate Strength and Stiffness.....	59
2.2.6.2 Crack Pattern and Failure Mechanism.....	62
2.2.6.3 Grout Removal.....	65
2.2.7 Discussion of Shear Test Results.....	67
2.2.7.1 Effect of Grout Type.....	67
2.2.7.2 Effect of Number of Headed Anchor.....	69
2.2.7.3 Effect of Anchor Head Area.....	70
2.3 Pullout Test of Headed Anchors.....	72
2.3.1 Specimen Description.....	72
2.3.2 Materials.....	76
2.3.2.1 Concrete.....	76
2.3.2.2 Grout.....	77
2.3.2.3 Pullout Specimen Reinforcement.....	80
2.3.2.4 Headed Anchors.....	81
2.3.3 Test Matrix.....	81
2.3.4 Test Setup and Instrumentation.....	81
2.3.5 Construction process and Testing Procedure.....	83

2.3.6 Pullout Test Results	85
2.3.6.1 Ultimate Strength and Stiffness	85
2.3.6.2 Crack Pattern and Failure Mechanism	88
2.3.7 Discussion of Pullout Test Results	90
2.4.4.1 Effect of Grout Type	90
2.4.4.2 Effect of Anchor Head Area	92
2.4 Implications of Test Results on AASHTO LRFD Bridge Design Specification	94
2.4.1 Lateral Strength	94
2.4.2 Lateral Stiffness	96
2.4.3 Pullout Strength	98
2.4.4 Axial Stiffness	98
2.5 Conclusions and Observations	101
3. Analytical Investigation	103
3.1 Introduction	103
3.2 Bridge Description	103
3.3 Design of Headed Anchors in Precast Decks	110
3.3.1 Current Design Procedure	111
3.3.2 Design Procedure for Headed Anchors in Precast Decks	111
3.3.3 Bridge Computational Model	113
3.3.4 Modeling of Headed Anchors	114
3.3.5 Live Load Analysis	114
3.3.6 Analysis Results	117
3.3.7 Design Spectrum	123
3.4 Nonlinear Analytical Investigation of the Bridge	132
3.4.1 Material Models	133
3.4.2 Bridge Computational Model	135
3.4.3 Model Verification	137
3.4.4 Pushover Analysis	139
3.4.5 Nonlinear Time Response Analysis	143
3.4.5.1 Input Ground Motions	143

3.5 Analytical Results	149
3.5.1 Analytical Results for Model 1	149
3.5.1.1 Hysteresis Response.....	150
3.5.1.2 Displacement Response Histories.....	150
3.5.2 Analytical Results for Model 2.....	153
3.5.2.1 Hysteresis Response.....	153
3.5.2.2 Displacement Response Histories.....	153
3.5.2.3 Behavior of Headed Anchors.....	154
3.5.3 Analytical Results for Model 3.....	158
3.5.3.1 Hysteresis Loop	158
3.5.3.2 Displacement Response Histories.....	158
3.5.3.3 Behavior of Headed Anchors.....	159
3.5.4 Comparison of Model 1, 2 and 3	163
3.5.4.1 Hysteresis Loop	163
3.5.4.2 Displacement Response Histories.....	163
3.5.4.3 Behavior of Headed Anchors.....	163
3.6 Concluding Remarks	167
4. Summary, Conclusions and Recommendations for Future Research.....	248
4.1 Summary	248
4.2 Conclusions	249
4.3 Recommendations for Future Research	251
References.....	252
List of CCEER Publications	256

List of Tables

Table 2-1 Compressive Strength (f'_c) of Deck and Girder Specimen on Test Day.....	38
Table 2-2 Compressive Strength of Grout (f_m) on Test Day	40
Table 2-3 Calculation of Modulus of Elasticity (E) of Grouts	40
Table 2-4 Number 3 Bar Reinforcing Steel Material Test Results.....	43
Table 2-5 Number 4 Bar Reinforcing Steel Material Test Results.....	44
Table 2-6 Test Matrix for Shear Test of Headed Stud.....	48
Table 2-7 Summary of Shear Test Results	60
Table 2-8 Shear Stiffness of Headed Anchors.....	60
Table 2-9 Grout Removal Time.....	67
Table 2-10 Compressive Strength of Pullout Test Specimen.....	76
Table 2-11 Compressive Strength of Grout (Pullout Test).....	78
Table 2-12 Calculation of Modulus of Elasticity (E) of Grouts	78
Table 2-13 Comparison of Modulus of Elasticity.....	78
Table 2-14 Number 5 Bar Reinforcing Steel Material Test Results.....	80
Table 2-15 Test Matrix for Pullout Test of Headed Stud	81
Table 2-16 Summary of Pullout Test Results.....	85
Table 2-17 Axial Stiffness of Headed Anchors	86
Table 2-18 Calculation of Factor (α) for Bending Stiffness.....	97
Table 2-19 Calculation of Factor (α) for Axial Stiffness	100
Table 3-1 Maximum Shear Force, V (Kips) due to Dead Load.....	115
Table 3-2 Maximum Shear Force, V (Kips) due to P15 Truck Loading (1-6 Lane Loaded)	115
Table 3-3 Design of Shear Connectors	116
Table 3-4 Types of Bridge Models for Modal Analysis.....	118
Table 3-5 Period and Modal Participation Mass Ratios (Model 1)	121
Table 3-6 Period and Modal Participation Mass Ratios (Model 2)	122
Table 3-7 Period and Modal Participation Mass Ratios (Model 3)	123
Table 3-8 Maximum Link Demand Force (Model 2).....	131
Table 3-9 Maximum Link Demand Force (Model 3).....	132

Table 3-10 Support Reaction (SAP2000)	138
Table 3-11 Support Reaction (OpenSees)	138
Table 3-12 Pushover Curve	142
Table 3-13 Characteristics of Selected Accelerations Records	144
Table 3-14 Longitudinal and Transverse Components of Selected Earthquakes	145
Table 3-15 Longitudinal and Transverse Components of Selected Earthquakes	146
Table 3-16 Unscaled and Scaled Response Spectrum	147
Table 3-17 Unscaled and Scaled Response Spectrum	148
Table 3-18 Maximum Base Shear and Displacement (Model 1).....	151
Table 3-19 Maximum Displacement and Drift (%) (Model 1).....	152
Table 3-20 Maximum Base Shear and Displacement (Model 2).....	155
Table 3-21 Maximum Displacement and Drift (%) (Model 2).....	156
Table 3-22 Maximum Link Force and Displacement (Model 2).....	157
Table 3-23 Maximum Base Shear and Displacement (Model 3).....	160
Table 3-24 Maximum Displacement and Drift (%) (Model 3).....	161
Table 3-25 Maximum Link Force and Displacement (Model 3).....	162

List of Figures

Figure 1-1 Details for Full-Depth Deck Panel Supported on Prestressed I-Girders.....	3
Figure 1-2 Details for Full-Depth Deck Panel Supported on Steel Plate Girder	4
Figure 1-3 Longitudinal PC Deck Panels Configuration	4
Figure 1-4 Proposed Connectors for Wide Flanged Concrete Girders (Tadros and Baishya, 1998)	6
Figure 1-5 Proposed 1¼ in Shear Stud in Steel Girders (Tadros and Baishya, 1998).....	7
Figure 1-6 Push-off Test Setup (Menkulasi and Roberts-Wollmann, 2005).....	8
Figure 1-7 Isometric Cut-away View of Exodermic Deck Panel (Ramey and Umphrey, 2006).....	11
Figure 1-8 Lab Mockup Details Showing Hooked Reinforcing Bar and Headed Stud (Sullivan, 2007).....	13
Figure 1-9 Shear Stud Cluster: a) Stud Groups at 2 ft. Spacing, and b) Stud Groups at 1 ft. Spacing (Oliva et al., 2007)	14
Figure 1-10 Clustered Steel Studs Welded to Girder in a Typical Shear Pocket (Oliva et al., 2007)	14
Figure 1-11 Connection between Full-Depth Deck Panel and Precast I-Girder (Badie and Tadros, 2008)	17
Figure 1-12 Connection between Full-Depth Deck Panels and Steel Plate Girder (Badie and Tadros, 2008)	17
Figure 1-13 Proposed Precast Deck Panel System (Henley, 2009).....	19
Figure 1-14 General Shear Connectors (Tawadrous, 2017)	24
Figure 1-15 Shear Pocket Layout (Tawadrous, 2017)	25
Figure 2-1 Specimen Details (Shear Test): (a) Specimen 1; (b) Specimen 2 and (c) Specimen 3.....	29
Figure 2-2 Formwork for Deck Specimens with Grout Pockets.....	31
Figure 2-3 Deck Reinforcement Details	31
Figure 2-4 Concrete Pouring on Deck Specimens	32
Figure 2-5 Pocket Detail for 1, 2 and 3 Headed Anchors.....	32
Figure 2-6 Deck Sections with Voided Pockets	33

Figure 2-7 Girder Section (a) 1 Headed Anchor (b) 2 and 4 Headed Anchors	34
Figure 2-8 Girder and Footing Reinforcement Detail.....	35
Figure 2-9 Girder and Footing Reinforcement Details	35
Figure 2-10 Concrete Pouring on Girder Specimens	36
Figure 2-11 Girder and Footing Details.....	36
Figure 2-12 Concrete Cylinders for Compressive Strength Test.....	37
Figure 2-13 Compressive Strength of Deck and Girder Specimen Concrete	38
Figure 2-14 Grout Samples for Compressive Strength Test.....	39
Figure 2-15 Compressive Strength of Grouts (Shear Test)	41
Figure 2-16 Stress-Strain Behavior of #3 Reinforcing Steel	42
Figure 2-17 Stress-Strain Behavior of #4 Reinforcing Steel	43
Figure 2-18 Headed Anchor Details (a) Head Area = $9A_b$; (b) Head Area = $4A_b$	45
Figure 2-19 Headed Anchor (Left: Head Area = $4A_b$; Right: Head Area = $9A_b$).....	45
Figure 2-20 Development Length of Headed Anchor	47
Figure 2-21 Plan and Elevation Schematic of Overall Shear Test Setup	50
Figure 2-22 Shear Test Setup.....	51
Figure 2-23 Transducers on Deck, Girder and Footing	52
Figure 2-24 Placement of Transducers	53
Figure 2-25 Location of Strain Gage in Specimen 1	54
Figure 2-26 Location of Strain Gage in Specimen 2	55
Figure 2-27 Location of Strain Gage in Specimen 3	56
Figure 2-28 Step-by-step Procedure of Shear Test of Headed Anchors.....	57
Figure 2-29 Step-by-step Procedure of Shear Test of Headed Anchors.....	58
Figure 2-30 Force Displacement Curve (Shear Test of Headed Anchors).....	61
Figure 2-31 Failure of Headed Anchor.....	63
Figure 2-32 Crack Pattern of 9 Grout Pockets (Tests 1-6)	64
Figure 2-33 Crack Pattern of 9 Grout Pockets (Tests 7-9)	65
Figure 2-34 Chipping Hammer used for Grout Removal	66
Figure 2-35 Grout Removal	67
Figure 2-36 Force Displacement Curve (Type of Grout)	68

Figure 2-37 Force Displacement Curve (Number of Headed Anchor).....	69
Figure 2-38 Force Displacement Curve per Anchor (Number of Headed Anchor)	70
Figure 2-39 Force Displacement Curve (Head Area).....	71
Figure 2-40 Force Displacement Curve per Anchor (Head Area).....	71
Figure 2-41 Modes of Failure (Pullout test)	72
Figure 2-42 Specimen Details (Pullout Test).....	74
Figure 2-43 Reinforcement Detail of Pullout Specimen.....	75
Figure 2-44 Compressive Strength of Specimen Concrete.....	77
Figure 2-45 Compressive Strength of Grouts (Pullout Test)	79
Figure 2-46 Stress-Strain Behavior of #5 Reinforcing Steel	80
Figure 2-47 Pullout Test Setup	82
Figure 2-48 Step-by-step Procedure of Pullout Test of Headed Anchors	84
Figure 2-49 Force Displacement Curve (Pullout Test of Headed Anchor)	87
Figure 2-50 Crack Pattern of 12 Grout Pockets (Tests 1-4)	88
Figure 2-51 Crack Pattern of 12 Grout Pockets (Tests 5-10)	89
Figure 2-52 Crack Pattern of 12 Grout Pockets (Tests 11-12)	90
Figure 2-53 Force Displacement Curve to Study the Effect of Grout (Head Area 9A _b)..	91
Figure 2-54 Force Displacement Curve to Study the Effect of Grout (Head Area 4A _b)..	91
Figure 2-55 Force Displacement Curve to Study the Effect of Head Area (1428 HP)	92
Figure 2-56 Force Displacement Curve to Study the Effect of Head Area (Concrete)	93
Figure 2-57 Force Displacement Curve to Study the Effect of Head Area (UHPC).....	93
Figure 2-58 Spring Representation of Anchors	99
Figure 3-1 Elevation View of Reigo Road Bridge	104
Figure 3-2 Section of Reigo Road Bridge at Bent	105
Figure 3-3 Girder Layout of Reigo Road Bridge.....	105
Figure 3-4 Cross section of Precast Girder of Reigo Road Bridge.....	106
Figure 3-5 Deck and Girder Connection Detail.....	106
Figure 3-6 Column Section Detail	108
Figure 3-7 Elevation view of Bridge (Model)	109
Figure 3-8 Section of Bridge at Bent (Model)	109

Figure 3-9 Girder Layout of the Bridge (Model).....	109
Figure 3-10 Finite Element Model of Bridge (CsiBridge, 2010-2011)	113
Figure 3-11 Shear Properties of Shear Connectors.....	116
Figure 3-12 FE Modeling of the Links	117
Figure 3-13 Spacing of Headed Connectors along Longitudinal Direction	118
Figure 3-14 Displacement along Longitudinal Direction (SAP2000)	119
Figure 3-15 Design Response Spectrum (LA Downtown: 34.0407 N, 118.2468 W)...	124
Figure 3-16 Axial and Shear Force in the Connectors (Case 1) – Model 1	125
Figure 3-17 Axial and Shear Force in the Connectors (Case 2) – Model 1	126
Figure 3-18 Axial and Shear Force in the Connectors (Case 1) – Model 2.....	127
Figure 3-19 Axial and Shear Force in the Connectors (Case 2) – Model 2.....	128
Figure 3-20 Axial and Shear Force in the Connectors (Case 1) – Model 3.....	129
Figure 3-21 Axial and Shear Force in the Connectors (Case 2) – Model 3.....	130
Figure 3-22 Constitutive Model for Unconfined Concrete.....	134
Figure 3-23 Constitutive Model for Confined Concrete.....	134
Figure 3-24 Constitutive Model for Reinforcing Steel.....	134
Figure 3-25 OpenSees Model at Bent.....	136
Figure 3-26 OpenSees Model at Deck Girder Connection.....	137
Figure 3-27 Displacement along Longitudinal Direction (OpenSees)	139
Figure 3-28 Pushover Curve: (a) Longitudinal Direction; (b) Transverse Direction	140
Figure 3-29 Link Force in Girder 7 (Model 2)	141
Figure 3-30 Link Force in Girder 7 (Model 3)	142
Figure 3-31 Scaled Response Spectrum compared to Design Spectrum.....	149
Figure 3-32 Hysteresis Loop for Imperial Valley-06 "Delta" - Model 1 (a) 100% (b) 150%.....	169
Figure 3-33 Hysteresis Loop for Loma Prieta "Hollister Differential Array" - Model 1 (a) 100% (b) 150%	170
Figure 3-34 Hysteresis Loop for Northridge-01 "LA-Saturn St" - Model 1 (a) 100% (b) 150%.....	171

Figure 3-35 Hysteresis Loop for Imperial Valley-06 "Bonds Corner" - Model 1 (a) 100% (b) 150%.....	172
Figure 3-36 Hysteresis Loop for Chalfant Valley-02 "Zack Brother Ranch" - Model 1 (a) 100% (b) 150%	173
Figure 3-37 Hysteresis Loop for Loma Prieta "Capitola" - Model 1 (a) 100% (b) 150%	174
Figure 3-38 Hysteresis Loop for Northridge-01 "Rinaldi Receiving Sta" - Model 1 (a) 100% (b) 150%	175
Figure 3-39 Hysteresis Loop for Northridge-01 "Sylmar-Converter Sta" - Model 1 (a) 100% (b) 150%	176
Figure 3-40 Displacement History for Imperial Valley-06 "Delta" - Model 1 (a) 100% (b) 150%	177
Figure 3-41 Displacement History for Loma Prieta "Hollister Differential Array" -Model 1 (a) 100% (b) 150%.....	178
Figure 3-42 Displacement History for Northridge-01 "LA-Saturn St" - Model 1 (a) 100% (b) 150%.....	179
Figure 3-43 Displacement History for Imperial Valley-06 "Bonds Corner" - Model 1 (a) 100% (b) 150%	180
Figure 3-44 Displacement History for Chalfant Valley-02 "Zack Brother Ranch" -Model 1 (a) 100% (b) 150%.....	181
Figure 3-45 Displacement History for Loma Prieta "Capitola" - Model 1 (a) 100% (b) 150%	182
Figure 3-46 Displacement History for Northridge-01 "Rinaldi Receiving Sta" - Model 1 (a) 100% (b) 150%.....	183
Figure 3-47 Displacement History for Northridge-01 "Sylmar-Converter Sta" - Model 1 (a) 100% (b) 150%.....	184
Figure 3-48 Hysteresis Loop for Imperial Valley-06 "Delta" - Model 2 (a) 100% (b) 150%	185
Figure 3-49 Hysteresis Loop for Loma Prieta "Hollister Differential Array" - Model 2 (a) 100% (b) 150%	186

Figure 3-50 Hysteresis Loop for Northridge-01 "LA-Saturn St" - Model 2 (a) 100% (b) 150%	187
Figure 3-51 Hysteresis Loop for Imperial Valley-06 "Bonds Corner" - Model 2 (a) 100% (b) 150%.....	188
Figure 3-52 Hysteresis Loop for Chalfant Valley-02 "Zack Brother Ranch" - Model 2 (a) 100% (b) 150%	189
Figure 3-53 Hysteresis Loop for Loma Prieta "Capitola" - Model 2 (a) 100% (b) 150%	190
Figure 3-54 Hysteresis Loop for Northridge-01 "Rinaldi Receiving Sta" - Model 2 (a) 100% (b) 150%	191
Figure 3-55 Hysteresis Loop for Northridge-01 "Sylmar-Converter Sta" - Model 2 (a) 100% (b) 150%	192
Figure 3-56 Displacement History for Imperial Valley-06 "Delta" - Model 2 (a) 100% (b) 150%	193
Figure 3-57 Displacement History for Loma Prieta "Hollister Differential Array" -Model 2 (a) 100% (b) 150%.....	194
Figure 3-58 Displacement History for Northridge-01 "LA-Saturn St" - Model 2 (a) 100% (b) 150%.....	195
Figure 3-59 Displacement History for Imperial Valley-06 "Bonds Corner" - Model 2 (a) 100% (b) 150%	196
Figure 3-60 Displacement History for Chalfant Valley-02 "Zack Brother Ranch" -Model 2 (a) 100% (b) 150%.....	197
Figure 3-61 Displacement History for Loma Prieta "Capitola" - Model 2 (a) 100% (b) 150%	198
Figure 3-62 Displacement History for Northridge-01 "Rinaldi Receiving Sta" - Model 2 (a) 100% (b) 150%.....	199
Figure 3-63 Displacement History for Northridge-01 "Sylmar-Converter Sta" - Model 2 (a) 100% (b) 150%.....	200
Figure 3-64 Maximum Link Force and Displacement for Imperial Valley-06 "Delta" - Model 2 (a) 100% (b) 150%	201

Figure 3-65 Maximum Link Force and Displacement for Loma Prieta "Hollister Differential Array" - Model 2 (a) 100% (b) 150%	202
Figure 3-66 Maximum Link Force and Displacement for Northridge-01 "LA-Saturn St" - Model 2 (a) 100% (b) 150%	203
Figure 3-67 Maximum Link Force and Displacement for Imperial Valley-06 "Bonds Corner" - Model 2 (a) 100% (b) 150%	204
Figure 3-68 Maximum Link Force and Displacement for Chalfant Valley-02 "Zack Brother Ranch" - Model 2 (a) 100% (b) 150%.....	205
Figure 3-69 Maximum Link Force and Displacement for Loma Prieta "Capitola" -Model 2 (a) 100% (b) 150%.....	206
Figure 3-70 Maximum Link Force and Displacement for Northridge-01 "Rinaldi Receiving Sta" - Model 2 (a) 100% (b) 150%	207
Figure 3-71 Maximum Link Force and Displacement for Northridge-01 "Sylmar-Converter Sta" - Model 2 (a) 100% (b) 150%	208
Figure 3-72 Hysteresis Loop for Imperial Valley-06 "Delta" - Model 3 (a) 100% (b) 150%	209
Figure 3-73 Hysteresis Loop for Loma Prieta "Hollister Differential Array" - Model 3 (a) 100% (b) 150%	210
Figure 3-74 Hysteresis Loop for Northridge-01 "LA-Saturn St" - Model 3 (a) 100% (b) 150%	211
Figure 3-75 Hysteresis Loop for Imperial Valley-06 "Bonds Corner" - Model 3 (a) 100% (b) 150%.....	212
Figure 3-76 Hysteresis Loop for Chalfant Valley-02 "Zack Brother Ranch" - Model 3 (a) 100% (b) 150%	213
Figure 3-77 Hysteresis Loop for Loma Prieta "Capitola" - Model 3 (a) 100%.....	214
Figure 3-78 Hysteresis Loop for Northridge-01 "Rinaldi Receiving Sta" - Model 3 (a) 100% (b) 150%	215
Figure 3-79 Hysteresis Loop for Northridge-01 "Sylmar-Converter Sta" - Model 3 (a) 100% (b) 150%	216

Figure 3-80 Displacement History for Imperial Valley-06 "Delta" - Model 3 (a) 100% (b) 150%	217
Figure 3-81 Displacement History for Loma Prieta "Hollister Differential Array" -Model 3 (a) 100% (b) 150%.....	218
Figure 3-82 Displacement History for Northridge-01 "LA-Saturn St" - Model 3 (a) 100% (b) 150%.....	219
Figure 3-83 Displacement History for Imperial Valley-06 "Bonds Corner" - Model 3 (a) 100% (b) 150%	220
Figure 3-84 Displacement History for Chalfant Valley-02 "Zack Brother Ranch" -Model 3 (a) 100% (b) 150%.....	221
Figure 3-85 Displacement History for Loma Prieta "Capitola" - Model 3 (a) 100%	222
Figure 3-86 Displacement History for Northridge-01 "Rinaldi Receiving Sta" - Model 3 (a) 100% (b) 150%.....	223
Figure 3-87 Displacement History for Northridge-01 "Sylmar-Converter Sta" - Model 3 (a) 100% (b) 150%.....	224
Figure 3-88 Maximum Link Force and Displacement for Imperial Valley-06 "Delta" - Model 3 (a) 100% (b) 150%	225
Figure 3-89 Maximum Link Force and Displacement for Loma Prieta "Hollister Differential Array" - Model 3 (a) 100% (b) 150%	226
Figure 3-90 Maximum Link Force and Displacement for Northridge-01 "LA-Saturn St" - Model 3 (a) 100% (b) 150%	227
Figure 3-91 Maximum Link Force and Displacement for Imperial Valley-06 "Bonds Corner" - Model 3 (a) 100% (b) 150%	228
Figure 3-92 Maximum Link Force and Displacement for Chalfant Valley-02 "Zack Brother Ranch" - Model 3 (a) 100% (b) 150%.....	229
Figure 3-93 Maximum Link Force and Displacement for Loma Prieta "Capitola" -Model 3 (a) 100%.....	230
Figure 3-94 Maximum Link Force and Displacement for Northridge-01 "Rinaldi Receiving Sta" - Model 3 (a) 100% (b) 150%	231

Figure 3-95 Maximum Link Force and Displacement for Northridge-01 "Sylmar- Converter Sta" - Model 3 (a) 100% (b) 150%	232
Figure 3-96 Comparison of Hysteresis Loop for Imperial Valley-06 "Delta" (100%)...	233
Figure 3-97 Comparison of Hysteresis Loop for Imperial Valley-06 "Delta" (150%)...	234
Figure 3-98 Comparison of Hysteresis Loop for Loma Prieta "Hollister Differential Array" (100%).....	235
Figure 3-99 Comparison of Hysteresis Loop for Loma Prieta "Hollister Differential Array" (150%).....	236
Figure 3-100 Comparison of Hysteresis Loop for Northridge-01 "LA-Saturn St" (100%)	237
Figure 3-101 Comparison of Hysteresis Loop for Northridge-01 "LA-Saturn St" (150%)	238
Figure 3-102 Comparison of Hysteresis Loop for Imperial Valley-06 "Bonds Corner" (100%).....	239
Figure 3-103 Comparison of Hysteresis Loop for Imperial Valley-06 "Bonds Corner" (150%).....	240
Figure 3-104 Comparison of Hysteresis Loop for Chalfant Valley-02 "Zack Brother Ranch" (100%).....	241
Figure 3-105 Comparison of Hysteresis Loop for Chalfant Valley-02 "Zack Brother Ranch" (150%).....	242
Figure 3-106 Comparison of Hysteresis Loop for Loma Prieta "Capitola" (100%).....	243
Figure 3-107 Comparison of Hysteresis Loop for Northridge-01 "Rinaldi Receiving Sta" (100%).....	244
Figure 3-108 Comparison of Hysteresis Loop for Northridge-01 "Rinaldi Receiving Sta" (150%).....	245
Figure 3-109 Comparison of Hysteresis Loop for Northridge-01 "Sylmar-Converter Sta" (100%).....	246
Figure 3-110 Comparison of Hysteresis Loop for Northridge-01 "Sylmar-Converter Sta" (150%).....	247

1. Introduction

1.1 Background

Cast-in-place (CIP) concrete construction is time intensive, in part because formwork must be used to pour wet concrete and allowed to cure, and then the formwork has to be removed. It also requires many on-site construction procedures that may create negative impacts on work zone safety and the environment. In addition, ageing bridges may require repair, rehabilitation, and/or replacement. The current traditional deck rehabilitation/replacement system in most situations is time consuming and costly. Issues related to work zone safety and traffic disruption are also a major concern. There is significant demand for the development of deck systems that can be constructed quickly while maintaining durability and seismic performance equal to or better than their cast-in-place concrete counterparts.

Accelerated bridge construction (ABC) offers a viable alternative to cast-in-place construction since significant on-site construction time can be reduced by using prefabricated decks. Economic benefits can be achieved through mass production of materials and the repeated use of forms. Prefabricated elements and systems can be quickly assembled and can reduce on-site construction time, minimize traffic disruption, reduce environmental impact, improve worker and motorist safety, improve constructability, and increase the quality of the final product.

Replacement of bridge decks can be one of the most advantages in the uses of ABC. The use of full depth prefabricated deck panels may be the fastest form of deck replacement. The application of ABC methods in seismic regions has been limited thus

far. It is due to the lack of adequate knowledge in seismic detailing, performance of connections, and specifications for seismic design of precast elements. Development of seismically resilient standardized prefabricated precast (PC) bridge decks will provide significant advancements in ABC.

1.2 Problem Statement

One of the attractive solutions to accelerate the construction of new bridges or replacement of deteriorated decks, is the use of full-depth precast deck panels in which the panels cover part of the bridge width. These precast panels can be attached to precast concrete or steel girders by providing voided pockets in these panels. Steel stirrups or headed anchors extending vertically from the girders protrude into the pockets as the panels are placed. These pockets are subsequently filled with a bonding material such as grout. The grouted pockets create composite action between the panels and girders. The main challenges of using full-depth deck panels are: 1) how to connect the deck panels to the longitudinal girders to achieve a ‘full’ composite action and 2) how to connect the panels to each other transversely and longitudinally so that the deck acts as a single unit. This full-depth deck system can be appealing for deck replacement projects since it eliminates the use of overlays. It also eliminates the need of field post-tensioning of precast elements, thus shortening the construction schedule. The connection between the deck and the longitudinal girders has always been one of the shortcomings of utilizing full-depth precast deck panels in new or deck replacement construction projects. Figures 1-1 and 1-2 show schematic diagrams of full-depth deck panel supported on prestressed I-girders and longitudinal steel plate girders, respectively.

Figure 1-3 shows the configuration of longitudinal precast deck panels. The configuration shows the P/C deck panel-to-panel connection as well as pockets used for deck-to-girder connection. This configuration was used in recently conducted research at the University of Reno, Nevada (Saïidi et al., 2017). The main advantage of this configuration is the decrease in closure time and reduction in traffic interruption during deck installation or replacement. This can be achieved by closing lanes on one side for repair or replacement while the lane on other side can be open to traffic.

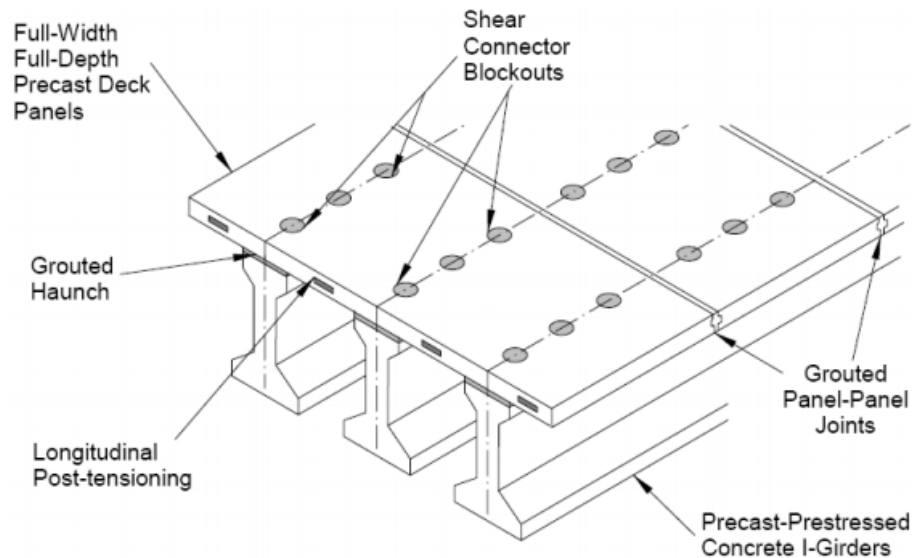


Figure 1-1 Details for Full-Depth Deck Panel Supported on Prestressed I-Griders

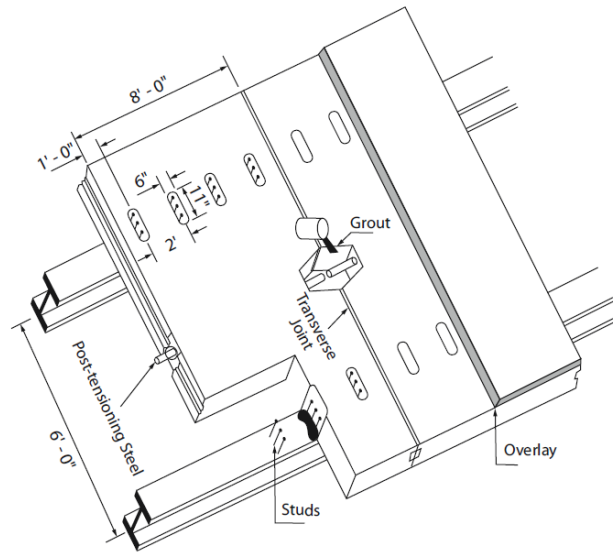


Figure 1-2 Details for Full-Depth Deck Panel Supported on Steel Plate Girder

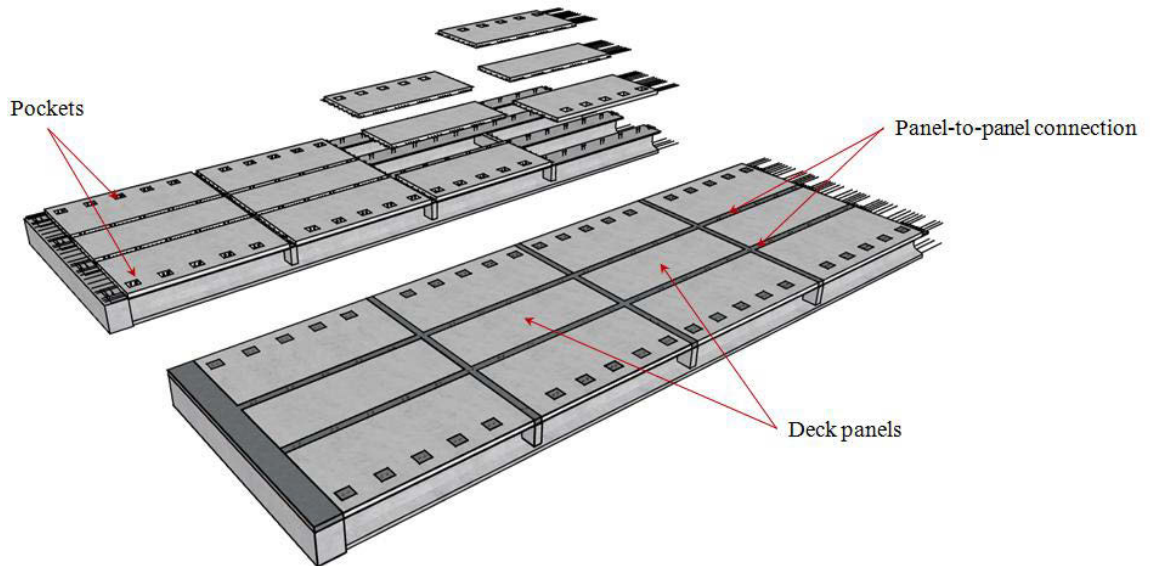


Figure 1-3 Longitudinal PC Deck Panels Configuration

1.3 Literature Review

The main components of the ABC deck system are precast full-depth deck panels, precast prestressed concrete or steel girders, voided pockets in the deck, headed anchors and grout to fill the pockets. Many panel-to-girder connection details have been proposed and used to develop composite action between the precast deck panels and steel/concrete girders. These types of decks have been investigated by many researchers.

1.3.1 NCHRP Report 407

NCHRP Report 407 (Tadros and Baishya, 1998) provided a number of techniques that facilitate rapid deck replacement and included proposed special provisions for deck removal. The report recommended the use of performance based specifications. A full-depth panel system was proposed with panels pretensioned in the transverse direction and post-tensioned in the longitudinal direction, which required least construction time than conventional cast-in-place or precast reinforced concrete. Two new connection systems were developed to study the speed of deck replacement, one for concrete girder-to-concrete deck connection and the other for steel girder-to-concrete deck connection.

For concrete girders, a debonded shear key system, shown in Figure 1-4, was developed that provide composite action and allow for easier deck removal. In addition to the laboratory tests on push-off specimens, full-scale tests were also performed. The test results showed that the system provided adequate composite action as well as the ease of deck removal. For steel girder-to-concrete deck connections, a 1-1/4 in. diameter shear stud, shown in Figure 1-5, was used to replace the commonly used 3/4 in. and 7/8 in. shear studs. A large number of small studs results in increased concrete removal time

and higher probability of damage to the girder top flange or the studs themselves. The new 1-1/4 in. stud, provided approximately twice the capacity of a 7/8 in. stud, allowed the use of a single row over the girder web. The researchers also found that alternating the headed and head-less studs provided adequate anchorage to the concrete deck and facilitated deck removal.

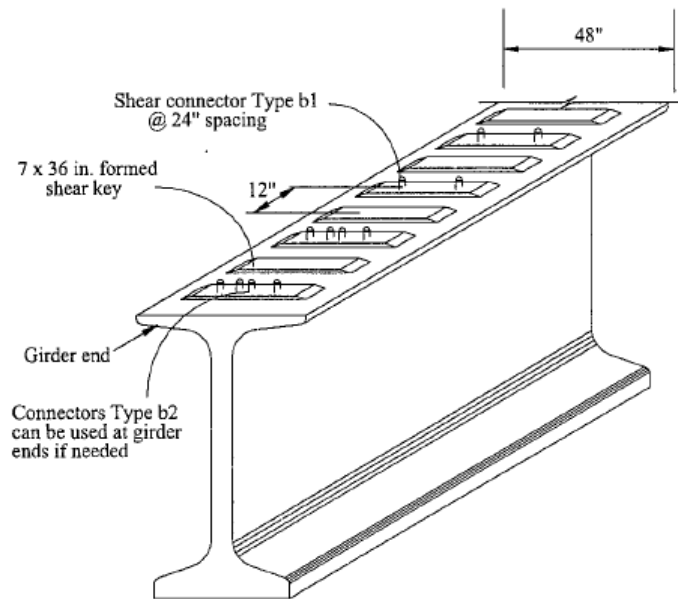


Figure 1-4 Proposed Connectors for Wide Flanged Concrete Girders (Tadros and Baishya, 1998)

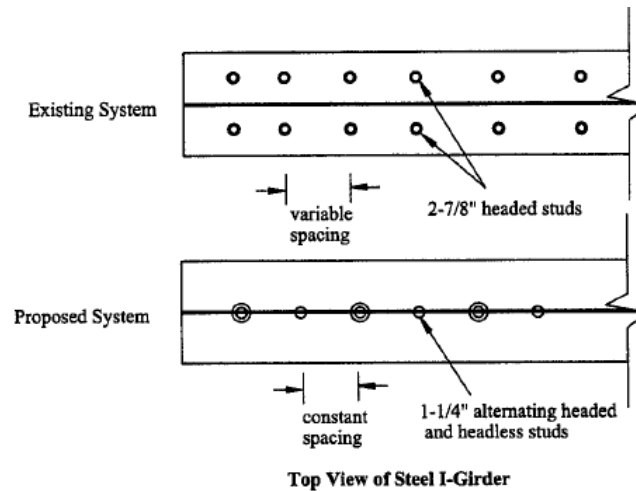


Figure 1-5 Proposed 1¼ in Shear Stud in Steel Girders (Tadros and Baishya, 1998)

1.3.2 NCHRP Synthesis 324

In 2003, the NCHRP published a report titled “Prefabricated Bridge Elements and Systems to Limit Traffic Disruption during Construction.” This report is part of the NCHRP report series, Synthesis of Highway Practice. It provided a review and analysis of using prefabricated elements in both highway and railway bridges. Existing literature and available information were collected and summarized. The research project also included a survey questionnaire, sent to US and Canadian Dots and local agencies, to collect information on the use and the effectiveness of prefabrication technologies. The report was classified as “non-technical” in the sense that no specific information was provided on topics such as design criteria, methods, details, or construction specifications. The report presented various types of prefabrication currently used or in development. The report’s literature review section documented the use of prefabrication bridge components on previous projects and discussed substructure and superstructure elements. It concluded that while prefabricated bridge components are more expensive in

some cases, it reduced the environmental impacts and improved the overall material and construction quality.

1.3.3 Menkulasi and Roberts-Wollmann (2005)

Menkulasi and Roberts-Wollmann (2005) conducted small-scale tests of the panel-to-girder connections to evaluate the effect of different types of grout and haunch heights on the shear strength of the connection. The test specimens are shown in Figure 1-6.

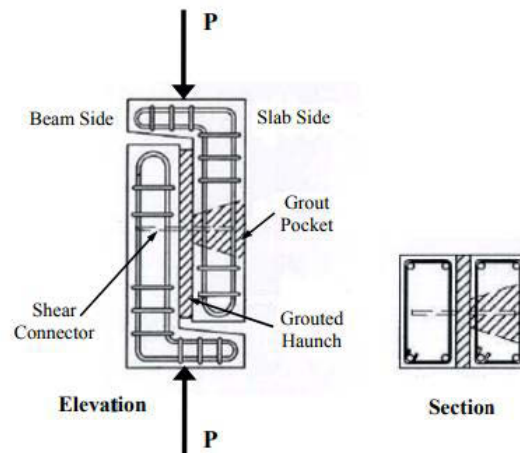


Figure 1-6 Push-off Test Setup (Menkulasi and Roberts-Wollmann, 2005)

From the results, it was observed that Set 45 grout and a latex modified grout performed the best. There was no significant difference in strength when haunch height was varied between 1 in. and 3 in. The shear connector used in these tests were U-shaped stirrups, however, two additional shear connectors were also tested which included post-installed hooked anchors and Dayton-Richmond 6 in. flared coil inserts with 3/4 in.

diameter coil bolts. Both additional shear connectors exhibited ductile behavior and could be used as an alternative to U-shaped stirrups.

1.3.4 Markowski (2005)

Markowski (2005) evaluated the use of full-depth precast deck panels on highway bridges for the Wisconsin Department of Transportation and Federal Highway Administration. Laboratory testing and analysis were conducted to investigate the structural adequacy, failure modes, serviceability, fatigue resistance, and overall behavior of the prefabricated full-depth deck panel system. A series of tests were conducted to investigate several aspects of deck panel behavior including (1) the behavior of the deck panels under edge location, (2) the level of post-tensioning required across transverse and longitudinal joints, and (3) the composite behavior of deck panels placed on a steel plate girder with shear studs spaced at 24 in and 48 in. The panel edge loading behavior and the required post-tensioning levels were evaluated using full-scale panels. Punching shear was identified as the failure mode of panels loaded at their edge. To prevent any cracking at service loads, the required level of post-tensioning across the longitudinal and transverse joints was 370 psi and 250 psi, respectively. A 1/2 scale model was used to evaluate the composite behavior of the system subjected to fatigue and static loading. The behavior of the 1/2 scale specimen indicated that a stud spacing of 48 in. can develop full composite behavior in both elastic and inelastic loading range.

1.3.5 Ramey and Umphrey (2006)

Ramey and Umphrey (2006) monitored and documented the rapid bridge deck replacement work for the Georgia Department of Transportation (GDOT) on two bridges in Gainesville and two bridges in the Atlanta. They identified the design and construction problems, and corrective actions to eliminate these problems in any future rapid deck replacement. Precast Exodermic or “unfilled composite steel grid,” panels were evaluated and the problems and pitfalls were identified.

The Exodermic bridge deck is comprised of a reinforced concrete slab on top of a composite unfilled steel grid. The upper portion of the main bearing bars extend up into the reinforced concrete slab, making the slab composite with the steel grid. This composite action is accomplished by drilling holes into the upper portion of the main bearing bars. The concrete portion of the Exodermic deck can either be cast-in-place (the grid panels act as the formwork), or precast, where rapid construction is critical.

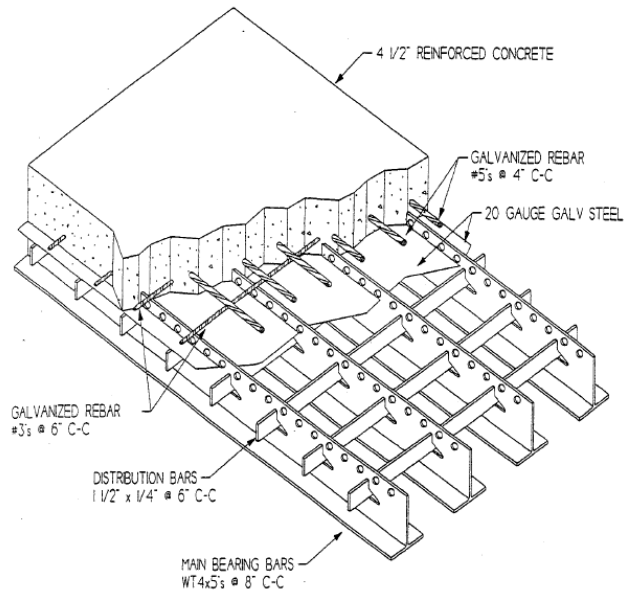


Figure 1-7 Isometric Cut-away View of Exodermic Deck Panel (Ramey and Umphrey, 2006)

The researchers concluded that the use of precast Exodermic deck panels allowed deck replacement work to be executed during the permitted work windows. The rehabilitation work for four bridge decks were accomplished effectively and efficiently within the imposed time limits while maintaining minimum traffic interruption. The researchers had also monitored the construction sequence adopted by the contractors and the problems observed during the rapid bridge deck replacement. They provided recommendations concerning the design and/or construction practices with Exodermic deck replacement panels.

1.3.6 Sullivan (2007)

Sullivan (2007) investigated the behavior of full-depth, large-scale, precast bridge deck panels on concrete girders. A bridge with precast bridge deck panels was built to examine constructability issue, creep and shrinkage behavior, and strength and fatigue performance of transverse joints, different shear connectors, and different shear pocket spacings. Two of the transverse joints were epoxied male-female joints and the other two transverse joints were grouted female-female joints. Two different pocket spacings were studied: 4 ft pocket spacing and 2 ft pocket spacing. Two different shear connector types were studied: hooked reinforcing bars and a new shear stud detail that can be used with concrete girders (Figure 1-8).

Cyclic loading tests, and shear and flexural strength tests were performed to examine the performance of the different pocket spacings, shear connector types and transverse joint configurations. The transverse joints proved to be more for a constructability issue than a strength or fatigue issue when subjected to moments that cause compression in the deck. The grouted female-female joint configuration prevented leaking at the joints and allowed for rapid placement of the panels on the girders during construction. Both types of pocket spacings and shear connectors performed exceptionally well. Both 2 ft and 4 ft pocket spacings produced composite action to reach the required flexural strength and the required vertical shear strength. Using shear studs as shear connectors allowed for more rapid placement of panels on the girders. When hooked reinforcing bars were used as shear connectors, the size of the shear pockets should be increased to compensate for casting tolerances. Based on the live load test results, both hooked reinforcing bars and shear stud had axial strains less than 50% of

the nominal yield strain. A recommended design and detailing procedure was also provided for the shear connectors and shear pockets.

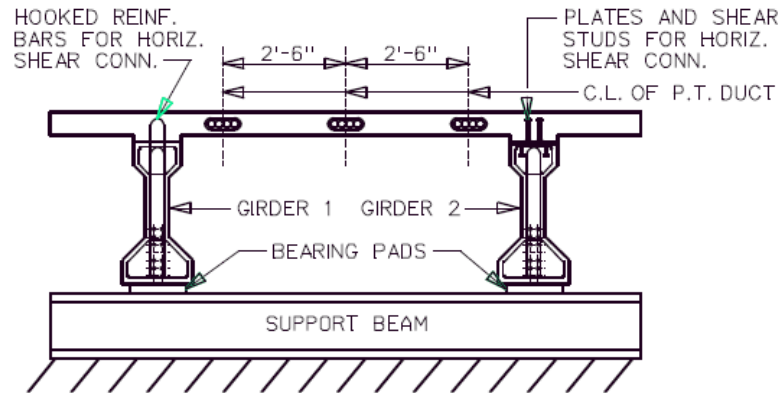


**Figure 1-8 Lab Mockup Details Showing Hooked Reinforcing Bar and Headed Stud
(Sullivan, 2007)**

1.3.7 Oliva et al. (2007)

Oliva et al. (2007) used a 1/2 scale model to investigate the composite action between steel girders and precast concrete panels with different shear pocket spacings. The deck panels on one half of the bridge span had shear stud block-outs spaced at 2 ft center-to-center, while the other side of the beam had shear stud block-outs spaced at 1 ft center-to-center (4 ft and 2 ft spacing in a full scale bridge, respectively) as shown in Figure 1-9. The specimen was subjected to 2 million cycles of load at 2 Hz and static tests were performed every 400,000 cycles to check for any degradation in stiffness due to cyclic loading. Figure 1-10 shows the dimension details and cross section of the shear pocket. No special shear pocket confinement was provided, instead, the shear pocket blowouts were 0.5 in. tapered from each side (wedged shear pockets).

girder had 95% of the theoretical fully composite section properties. Thus, the shear stud spacing was found to provide adequate composite action. Upon completion of load testing on the composite girder, the girder flange was disassembled in an exploratory manner by creating saw cuts at critical locations. There was no visible deformation of the shear studs at the block-outs, which would have been expected if significant slip had developed between the steel beam and concrete flange.

1.3.8 Scholz et al. (2007)

Scholz et al. (2007) provided a set of recommendations for the design, detail, and construction of the connection between full-depth precast deck panels and prestressed concrete I-beams. He developed performance specifications for the grout that fills the haunch between the top of the beam and the bottom of the deck panel, as well as the horizontal shear connector pockets and the panel-to-panel joints. Tests were performed using standard or modified ASTM tests to determine basic material properties on eight types of grout. Based on these tests, requirements for shrinkage, compressive strength, and flow were established for the grouts. Four grouts were analyzed through a series of tests to develop grout recommendations. Four grouts without aggregate and four grouts with 3/8 in. pea gravel aggregate were evaluated. The two grouts that were found to be suitable for the use in full-depth deck panel system were: Five Star Highway Patch and Set 45 Hot Weather.

To examine the horizontal shear strength of a precast-full depth bridge deck panel system on precast beam, 29 push-off tests were conducted. Various parameters that were studied included the grout type, the type of connectors, the slab bottom surface treatment

and the pocket type. The slab surface treatments were smooth and exposed aggregate. The connectors used were either reinforcing bar stirrups or headed shear studs. The double leg stirrups were either No. 4 bars or No. 5 bars. Arrangements of two, three and four headed shear studs were used. The studs were $\frac{3}{4}$ in. diameter and 7 in. in length. The headed shear stud system utilized welded stud connectors on a plate that was embedded in the top flange of the beam had successful results. The specimens performed very similar to the test specimens that utilized the typical reinforcement bar stirrups. Headed shear studs do have a lower yield stress, so an increased number of studs may be required.

1.3.9 NCHRP 12-65 Project

Badie and Tadros (2008), as a part of NCHRP project 12-65, developed two full-depth precast concrete bridge panel systems, a transversely pretensioned system and a transversely conventionally reinforced system. They proposed guidelines for the design, fabrication, and construction of full-depth precast concrete bridge deck panel systems without the use of post-tensioning or overlays. The study also proposed and tested innovative connections between full-depth deck panels to steel and precast longitudinal girders and connections between the panels. Experimental testing was conducted on these panels under fatigue and gravity loading. Figures 1-11 and 1-12 show the connection details between the deck panel and precast and steel plate girders, respectively.

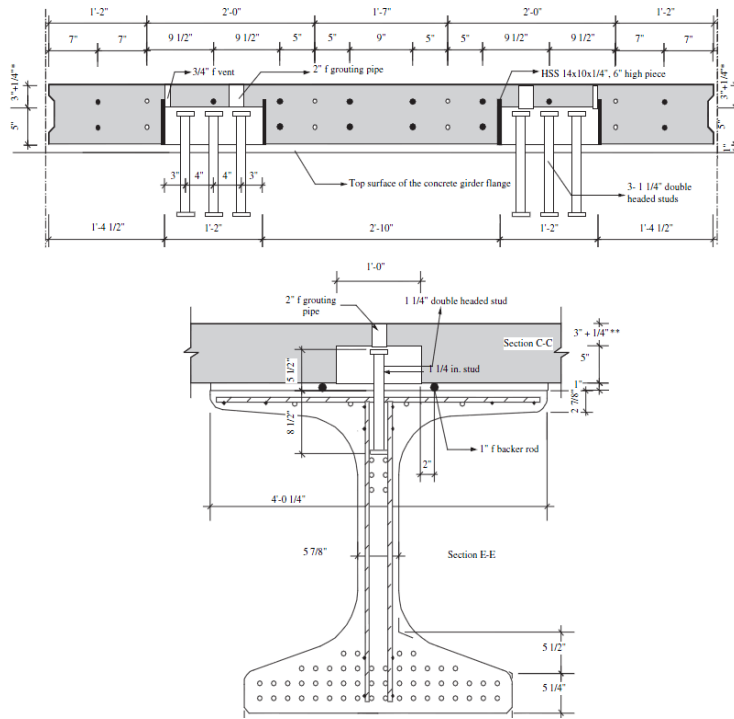


Figure 1-11 Connection between Full-Depth Deck Panel and Precast I-Girder (Badie and Tadros, 2008)

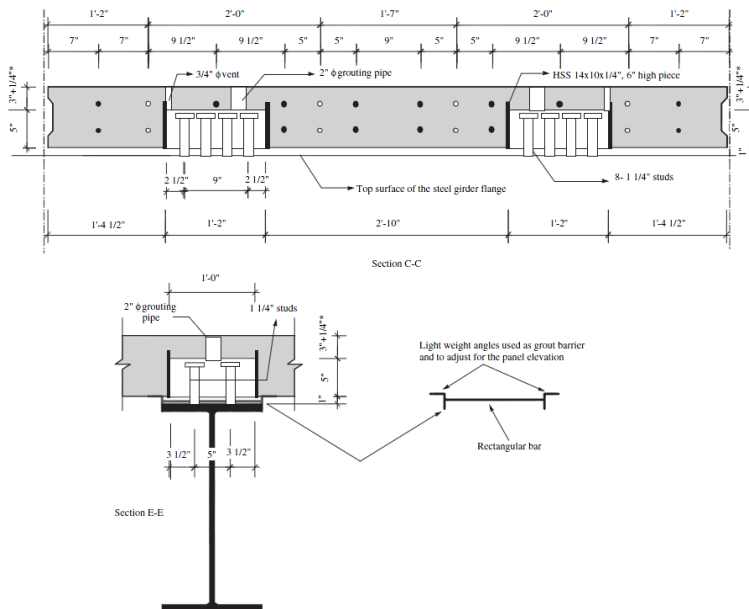


Figure 1-12 Connection between Full-Depth Deck Panels and Steel Plate Girder (Badie and Tadros, 2008)

A new panel to concrete girder connection detail was developed, where clusters of three double-headed studs 1-1/4 in. were used. The longitudinal spacing between the clustered studs was 4 ft. This type of connection was found to achieve a full composite action for bridges with spans up to 130 ft and girder spacing up to 11 ft. Significant fatigue testing was also performed on this connection and found to be adequate.

A new panel to steel girder connection detail was developed, with clusters of eight double-headed 1-1/4 in. studs at 48 in. spacing. Hollow Structural Steel (HSS) tubes were shown to be effective in confining the grout surrounding the studs. Extensive analytical and experimental investigation proved that this connection was adequate for strength and fatigue.

In addition, recommended guidelines for design, detailing, fabrication, and construction of full-depth concrete bridge deck panel systems were developed. It was found that the connection details using 1-1/4 in. shear stud cluster spaced at 48 in., instead of the 24 in. that is currently specified in Section 6 of the current AASHTO LRFD Bridge Design Specifications (AASHTO, 2012), was sufficient. Also, Article 5.8.4.1 in the AASHTO LRFD specifications can be used to estimate the horizontal shear capacity of the proposed panel-to girder detail on both concrete and steel girders.

1.3.10 Henley (2009)

Henley (2009) explored the shear connection between a full-depth precast deck and a precast concrete girder via a pocket-haunch-connector system, as shown in Figure 1-13. He performed experiments on 24 shear push-off samples that were simulated as a precast concrete girder with precast slab on top. The effects of various pre-and post-

installed shear connectors, haunch heights, surface roughness, grouping effects, and grout compositions were compared to cast-in-place specimens. Of these specimens, 16 had pre-installed connectors and the remaining 8 were post-installed specimens. Two threaded rods with end nuts were tested, with and without couplers. Similarly, four specimens using conventional R-bar shear connections were tested with haunch heights of 2 in. and 3.5 in. The remainder of the pre-installed connectors used both one and two high strength bolted connections per composite pocket. Two threaded rods per composite pocket had similar performance (5% superior peak force) as that of the current CIP shear connector (R-bars). The 8 specimens assembled with post-installed shear connectors were tested to investigate the feasibility of post-installed options, should the pre-installed connectors not align with the composite pockets during construction. They concluded that post-installed shear connections provided inferior shear capacity.

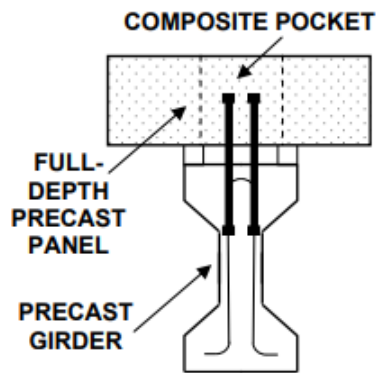


Figure 1-13 Proposed Precast Deck Panel System (Henley, 2009)

1.3.11 Nebraska University Deck (NUDECK) System

Hanna et al. (2010) developed the second generation of precast concrete deck system to simplify precast panel/girder production, speed up bridge superstructure

construction, and improve deck durability. This new generation of NUDECK consisted of full-width full-depth precast concrete deck panels, that were 12 ft long, to minimize the number of deck panels and transverse joints. It also utilizes covered individual pockets and bundled shear connectors at 4 ft spacing to simplify panel and girder production and eliminate the need for deck overlay. Precast deck panels were pre-tensioned in transverse direction and post-tensioned in the longitudinal to enhance deck durability and to achieve the same service life of other bridge components. Post-tensioning strands were placed underneath the deck panels (at the haunch area) to eliminate threading strands through ducts and grouting operations.

This system was first implemented in the Kearney East Bypass project in Kearney, NE (Morcous et al., 2013). The project consisted of twin bridges: the south bound bridge constructed using conventional cast-in-place deck; and the north bound bridge constructed using the second generation NUDECK system. Each bridge is a two-span continuous bridge that is 41 ft 8 in. wide and 332 ft long. Each span is 166 ft long and consists of five precast/prestressed concrete girders (NU1800) at 8 ft 6 in. spacing. Several experimental investigations were conducted to evaluate the practicality, economic feasibility and structural performance of Second Generation NUDECK system. The results of these investigations indicated that this system is an efficient deck system for implementation in the Kearney East Bypass project.

1.3.12 Perry and Royce (2010)

Perry and Royce (2010) investigated a new method for the replacement of deteriorating highway bridge decks by using UHPC joint filled with full-depth precast

deck panels. They used precast concrete deck panels with filed-cast UHPC joints to develop the continuity in the deck panels. The UHPC joint fill material showed excellent bond development length. It also showed superior freeze/thaw resistance, extremely low porosity, higher than normal flexural strength and superior toughness, which provided improved resistance to climatic conditions and continuous flexing from truck loadings across the joints. It was also observed that the total shrinkage of UHPC was distributed throughout the system and the UHPC/HPC deck interface was bonded with no potential for leaking.

1.3.13 PCI (2011)

PCI (2011) provided state-of-the-art guidance relative to selecting, designing, detailing, and constructing precast full-depth decks for bridge construction. The information provided in the report is applicable for new bridge deck construction or bridge deck replacement. A typical practice for design of panel thickness, longitudinal and transverse reinforcement, overhang design, impact to barrier, panel-to-girder connection, and longitudinal post-tensioning along with design examples are provided in the report. Examples included successful detailing including transverse joints, horizontal shear connections, leveling and temporary supports, and haunch details between the beams and decks. Various connection details used in full-depth precast deck panel systems built in the United States during the past 30 years were also presented in the report. Information on the production, handling, and construction of full-depth precast deck panels were also provided in the report. This included quality control, construction operations, and wearing and protection systems.

1.3.14 Assad (2014)

Assad (2014) investigated different deck removal methods and their impacts on the structural performance of precast/prestressed concrete I-girders with wide and thin top flange. Different saw cutting and jack hammering techniques were investigated to study the damage to the girders, duration, cost and impact on the environment. These methods were implemented on the Camp Creek Bridge over I-80 in Lancaster County, NE. Two girders from the bridge were also tested in flexure after applying different levels of deck removals around shear connectors and re-decking. Data obtained from using similar techniques on three other projects were also collected and analyzed.

Based on the results from the field, and analytical and experimental investigations, the most common methods for deck removal for re-decking were saw cutting, jack hammering and hydro demolition. Debonding the edges of the top flange was found to be an effective way for lifting saw-cut deck panels between girders without damaging the thin top flange of the girders. Moreover, they indicated that the most cost effective method of deck removal was highly dependent on the quantity, environmental restriction, and type of girder and its shear connectors. It was observed that leaving approximately 50% of the old deck concrete around shear connectors does not significantly affect the horizontal shear capacity of the new composite section.

1.3.15 Cao et al. (2016).

Cao et al. (2016) developed and evaluated the performance of self-consolidating concrete (SCC) for connecting precast concrete deck panels to supporting bridge girders. SCC was found to maintain a high filling and passing ability for 2 hours and exhibit

adequate stability. The use of SCC for the filling of shear pockets and haunches in precast concrete deck system proved to be an economical as well as a superior alternative to commercial grouts in bridge construction.

The developed SCC mixture was also implemented in the construction of the Kearney East Bypass Bridge Project in Kearney, Nebraska. The SCC was used to fill the shear pockets and haunches between the deck and the girders. The SCC used for the field implementation had high flowability, adequate stability, and high compressive strength. The developed SCC also had adequate frost durability. The SCC was found to completely fill the shear pockets and haunches between the deck and the girders. This successful implementation proved that the developed SCC for the filling of shear pockets and haunches in precast concrete deck systems can be used as an economical and superior alternative to commercial grouts in bridge construction.

1.3.16 Tawadrous (2017)

Tawadrous (2017) developed methods for designing HSS-formed shear pockets with clustered shear connectors for full-depth precast concrete deck systems. These methods were intended to assist in sizing shear connectors, selecting shear pocket dimensions and HSS thickness, and determining pocket anchorage and reinforcement necessary to maximize the connection capacity while allowing adequate construction tolerance. Experimental investigation (push-off testing) and finite element analysis (FEA) were performed to validate the developed design procedures. Figures 1-14 and 1-15 show a general shear connector and shear pocket configuration for a clustered shear connection, respectively. A combination of rectangular and circular HSS shear pockets

were used to verify a wide range of shear pocket shapes and dimensions. The mode of failure in push-off specimens was primarily the shearing off the shear connectors. However, concrete failure was experienced when the shear pocket dimensions exceeded the recommended upper limits of shear pocket dimensions and/or when transverse reinforcement was not provided. Analysis and testing results validated the adequacy of the developed design method for HSS-formed shear pocket connections. In addition, a clustered shear connector database consisting of 162 shear tests obtained from the literature was created. The database was used to evaluate the feasibility of using current interface shear prediction models provided by AASHTO LRFD, fib MC 2010, Eurocode-2, and CSA-S6 design codes. Comparisons indicated that the existing code provisions are applicable to predict the interface shear resistance of clustered shear connectors with different levels of accuracy.

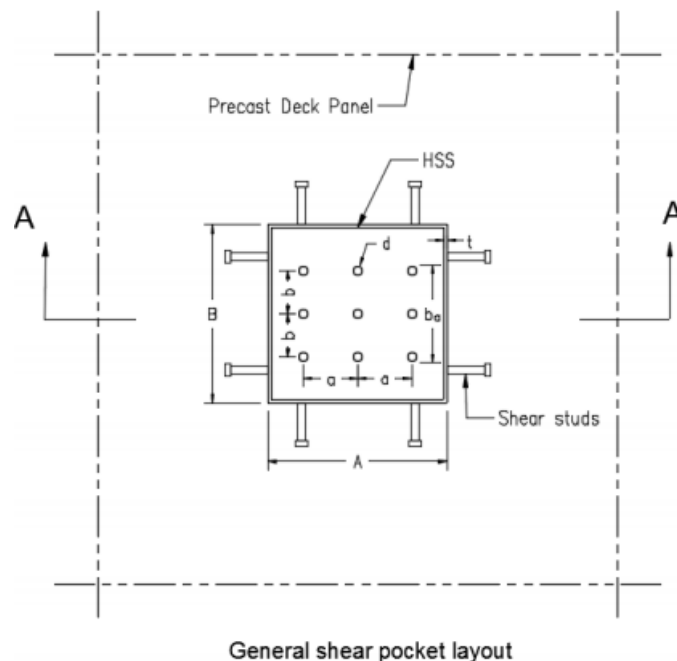


Figure 1-14 General Shear Connectors (Tawadrous, 2017)

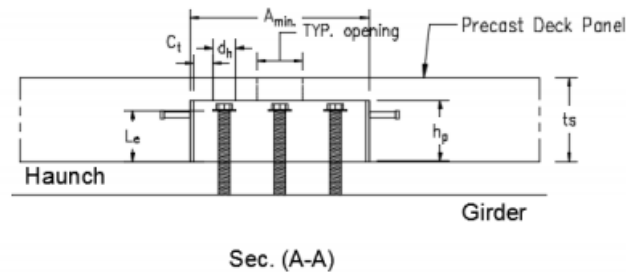


Figure 1-15 Shear Pocket Layout (Tawadrous, 2017)

1.4 Research Objectives and Scope of Work

The current provisions in AASHTO LRFD bridge design specifications are for cast-in-place decks and do not address the seismic design of composite full depth precast deck panels. The primary objective of this study was to develop and design a prefabricated composite precast bridge deck that can be used in high seismic zones. These prefabricated decks also offer the ability to be replaced during the life span of the bridge while maintaining the serviceability and seismic resiliency of the newly replaced decks.

The study conducted literature review on shear connector research and accelerated bridge construction as discussed in Section 1.3 of this report. Experiments were conducted to investigate the shear and pull-out behavior of headed anchors. Shear and pull-out specimens were constructed and tested to evaluate the effect of grout type, head area and group effect on the ultimate capacity and the stiffness of anchors. The results from these experiments were then used to perform nonlinear analyses of a two-span bridge. The AASHTO provisions used for CIP construction were utilized for the seismic design of precast deck panels. From the nonlinear analysis, seismic forces on the anchor

and the effect of anchor spacing on the overall seismic response of the bridge were also evaluated.

1.5 Report Organization

This report is organized as follows:

Chapter 1 introduces the background, problem statement, objectives and literature review of current precast concrete deck systems;

Chapter 2 describes the experimental investigation carried out to evaluate the shear and pullout strength of the selected headed anchor;

Chapter 3 presents the seismic computational model for headed anchors and their seismic response using nonlinear response history analysis. The anchor seismic forces and the effect of the anchor spacing on the overall bridge seismic response are also presented;

Chapter 4 presents the summary and conclusions of the conducted research, as well as recommendations for future research.

2. Experimental Study

2.1 Introduction

The anchors that connect prefabricated deck panels to longitudinal girders of a bridge could have a major impact on the gravity and seismic load performance of bridges. Without these anchors, the deck will act independently and will thus increase the live load stresses in the longitudinal girders due to the non-composite action. Furthermore, if the deck is not adequately attached to the longitudinal girders, it will slip over the longitudinal girders during seismic events. The current AASHTO Specifications (AASHTO 2012) do not have explicit requirements for the connection of precast deck panels to precast, prestressed (P/S) concrete girders.

For CIP decks, the stirrups of the precast girder are extended into the deck to provide composite action in the deck girders system. Previous earthquakes did not expose any vulnerabilities in CIP deck and precast girders. Therefore, it is implied that the shear reinforcement designed for gravity load is adequate to connect the CIP deck to the girders to resist seismic loads. However, when precast deck panels are used, it is necessary to attach the deck panels to the longitudinal girders through headed anchors or other shear connectors. This is achieved by leaving voided pockets along the depth of the precast deck and a cluster of anchors or other shear connectors that are already embedded in girders, extending into the pockets. These pockets are then be filled with grout to connect the precast deck to the girders.

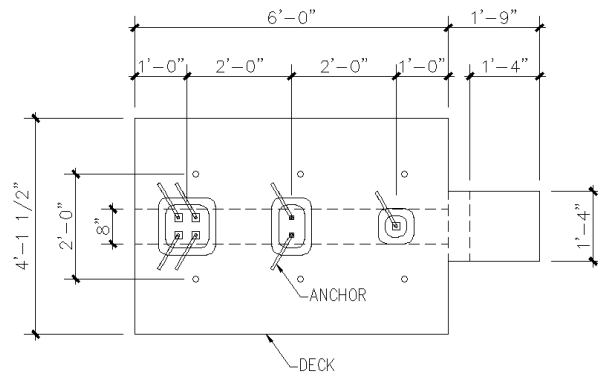
This study used headed anchors to connect the deck to the longitudinal girders. Shear and pullout tests of the anchors were carried out to study the shear and pullout behavior of these anchors.

2.2 Shear Test of Headed Anchors

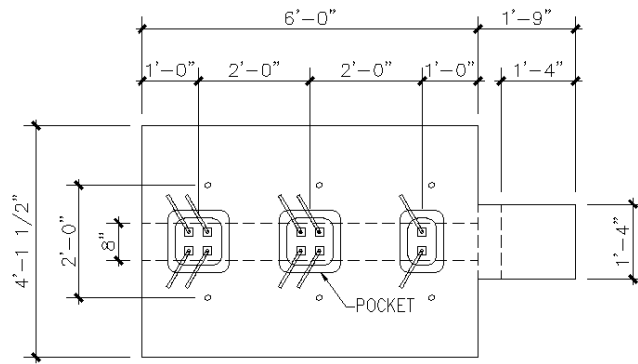
The objective of this investigation was to determine the shear strength and stiffness of the anchors by performing a push-out test, in which shear force is applied directly at the interface between deck and girder. These tests help identify the strength and stiffness of anchors embedded in different types of grout, the group effect of headed anchors, and the effect of the anchor head area. Nine push-out shear experiments were performed to better understand the effect of these parameters on the shear strength and stiffness.

2.2.1 Test Specimens

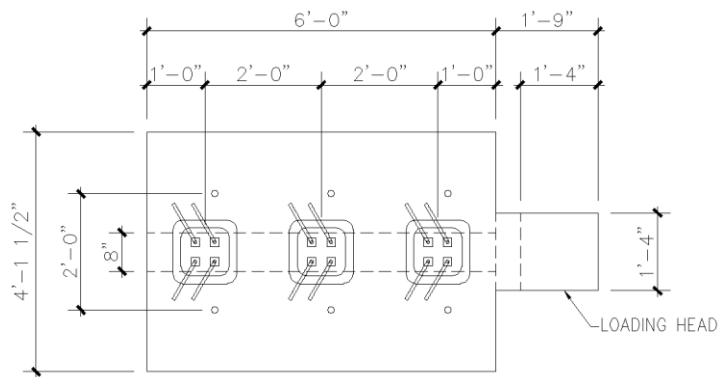
Three shear specimens, with three shear pockets in each specimen, were constructed each with three combination of number of anchors, types of grout, and head area of the anchors. Thus a total of nine experiments were conducted. Figure 2-1 shows the details of all the specimens. The geometry of the test specimens was selected to represent full-scale deck-girder connection. Each specimen consisted of an 8 in. thick concrete deck and the upper part of a precast concrete girder, and a concrete footing. The footing base was used to connect the girder web to the strong floor of the lab. A loading head at the deck was used to apply the load along the interface of the deck and girder.



(a)



(b)



(c)

Figure 2-1 Specimen Details (Shear Test): (a) Specimen 1; (b) Specimen 2 and (c) Specimen 3

2.2.1.1 Deck Section and Pockets

The deck section consisted of a nominal 6'x4.125'x8" slab with pockets of various sizes. Figure 2-2 shows the formwork for deck sections with pockets. Figure 2-3 shows the reinforcement detail of the deck section that consisted of top and bottom layers with #4 bars in the longitudinal direction, and #5 bars in the transverse direction. All the deck segments were cast at the same time from the same mix of concrete with a target 28-day compressive strength of 5,000 psi. Figure 2-4 shows the casting of concrete.

Each deck specimen was constructed with three voided pockets through the entire depth of the deck. The pocket sizes were different depending on the number of anchors used. The pocket details are shown in Figure 2-5. Rounded corners were provided in the pockets to minimize cracking potential and minimize potential for grout voids. Out of the nine pockets, there were one, two and six pockets with 1, 2, and 4 anchors, respectively. Figure 2-6 shows the deck section with the pockets before placement of the filler material.



Figure 2-2 Formwork for Deck Specimens with Grout Pockets



Figure 2-3 Deck Reinforcement Details



Figure 2-4 Concrete Pouring on Deck Specimens

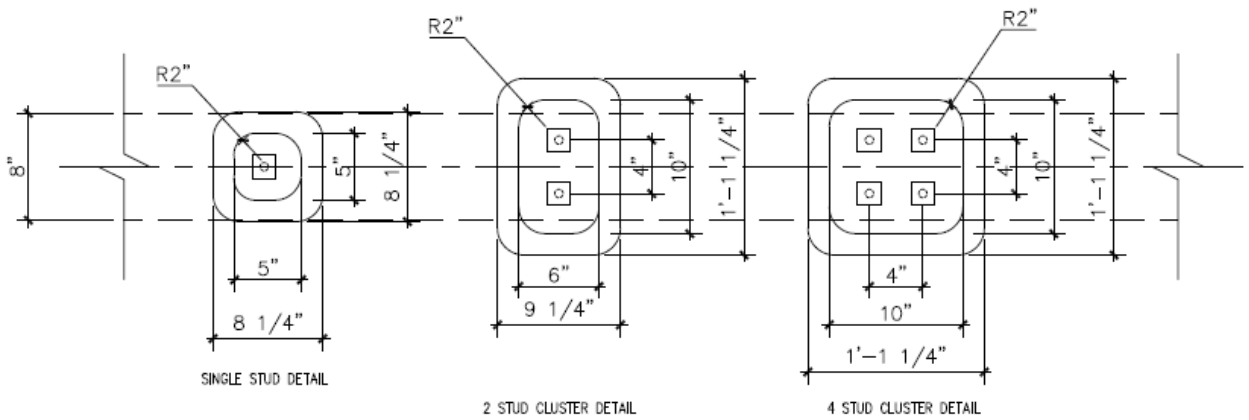


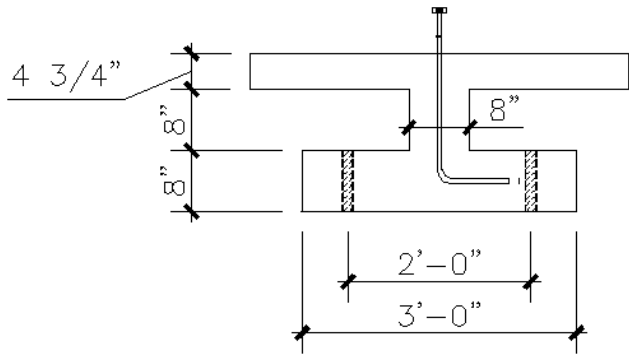
Figure 2-5 Pocket Detail for 1, 2 and 3 Headed Anchors



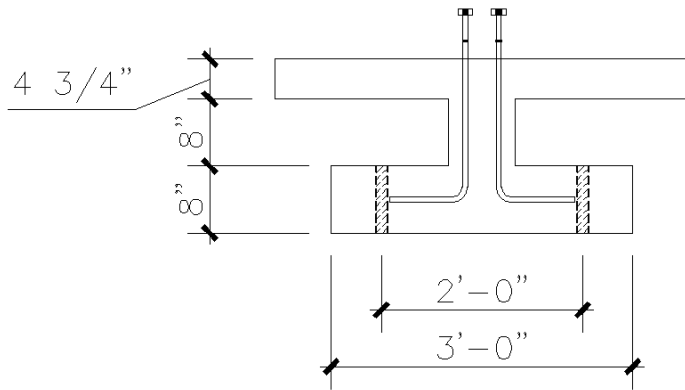
Figure 2-6 Deck Sections with Voided Pockets

2.2.1.2 Girder and Footing Section

The girder section consisted of a top flange and an upper part of web connected to a footing as shown in Figure 2-7. The total height of 16.75 in. was used based on the development length required for the anchor. Figures 2-8 and 2-9 show reinforcement details of the girder and the footing. Headed anchors in each pocket were installed in the girder before casting concrete such that 6 in. of the anchor extended beyond the top surface of the girder. All girder segments were cast at the same time using the same mix of concrete with a target 28-day compressive strength of 8,000 psi. Figure 2-10 shows the girder and the footing during casting. Figure 2-11 shows the completed girder and footing specimen with anchors extended above the top surface of the girder.

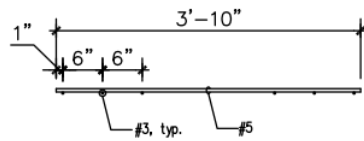
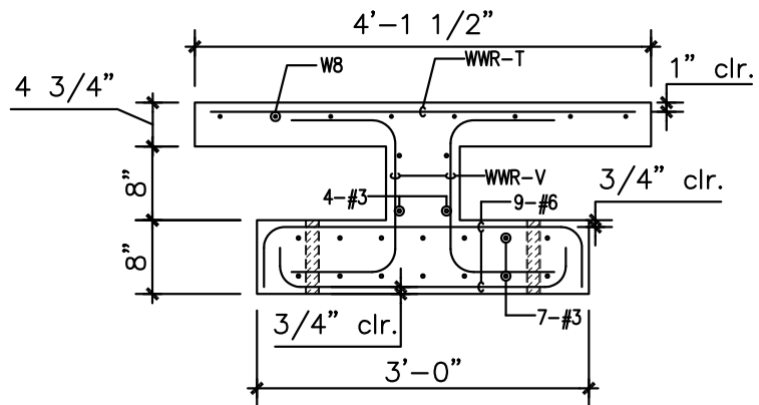


(a)

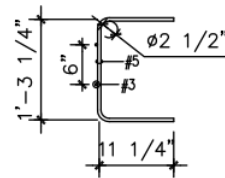


(b)

Figure 2-7 Girder Section (a) 1 Headed Anchor (b) 2 and 4 Headed Anchors



WWR-T



WWR-V

Figure 2-8 Girder and Footing Reinforcement Detail



Figure 2-9 Girder and Footing Reinforcement Details



Figure 2-10 Concrete Pouring on Girder Specimens



Figure 2-11 Girder and Footing Details

2.2.2 Materials

2.2.2.1 Concrete

Conventional concrete was used for the construction of the deck and girder for shear test specimens. Standard 6" x 12" concrete cylinders, as shown in Figure 2-12, were tested under compression at 7 days, 28 days, and the day of testing. At least three cylinders were tested according to ASTM C39/C39M-17a. Only the average of test data was reported. The measured 28-day compressive strength of deck and girder specimens were 4.2 ksi and 3.8 ksi, respectively. The measured strength history of the concrete used for deck and girder specimens is shown in Figure 2-13, and test day compressive strength of concrete is presented in Table 2-1.



Figure 2-12 Concrete Cylinders for Compressive Strength Test

Table 2-1 Compressive Strength (f'_c) of Deck and Girder Specimen on Test Day

Test	Strength (ksi)	
	Deck	Girder
1	5.15	4.87
2	5.23	4.59
3	5.12	4.78
4	5.26	4.87
5	5.47	5.00
6	5.40	5.00
7	5.80	5.29
8	6.03	5.45
9	5.71	5.28

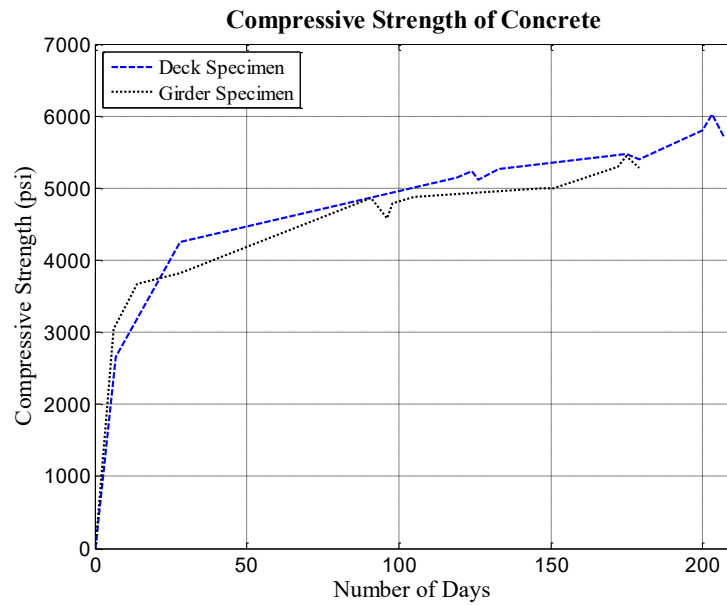


Figure 2-13 Compressive Strength of Deck and Girder Specimen Concrete

2.2.2.2 Grout

Various types of grout and concrete materials were used to fill the deck pockets. The grout used are: 1428 HP, EucoSpeed, Latex concrete (HD 50) and Polyester Concrete (PPC 1121). In addition to grout, Concrete (Sakrete 5000 Plus High Strength Concrete Mix) and Ultra High Performance Concrete (UHPC) were also used. The compressive strength of 1428 HP, EucoSpeed and Latex concrete grouts were measured according to ASTM C109/C109M using 2 in. cube specimens as shown in Figure 2-14. Plastic cylinders with 4 in. diameter and 8 in. height were used for concrete and polyester concrete samples and cylinders with 3 in. diameter and 6 in. height were used for UHPC sampling. The measured strengths of the grouts and concrete are shown in Figure 2-15, and the test day compressive strength of the grouts is presented in Table 2.2. The modulus of elasticity (E) of each grout was calculated according to ASTM C469/C469M and is listed in Table 2-3. The modulus of elasticity of the remaining four grouts were found to be between 3600 to 4300 psi.



Figure 2-14 Grout Samples for Compressive Strength Test

Table 2-2 Compressive Strength of Grout (f_m) on Test Day

Test	Specimen	Pocket	Grout	No. of Days	Strength (ksi)
1	1	1	1428 HP	9	10.72
2	2	1	1428 HP	14	11.23
3	3	1	1428 HP	16	11.15
4	1	3	EucoSpeed	8	7.92
5	2	2	Concrete	32	6.62
6	3	2	Latex Concrete	19	8.87
7	3	3	Polyester Concrete	8	5.55
8	2	3	UHPC	7	17.46
9	1	2	UHPC	12	21.78

Table 2-3 Calculation of Modulus of Elasticity (E) of Grouts

Grout	Specimen 1	Specimen 2	Specimen 3	Average E (psi)
1428 HP	4,055	4,420	4,405	4,293
EucoSpeed	4,262	4,117	-	4,189
Concrete	3,421	3,990	3,834	3,749
Latex Concrete	3,702	3,487	3,887	3,692
Polyester Concrete	1,419	1,415	1,421	1,418
UHPC	8,917	8,602	9,139	8,886

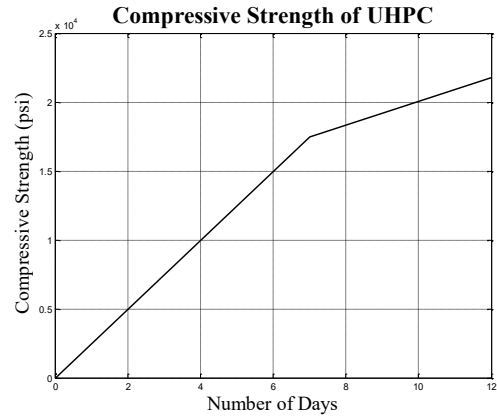
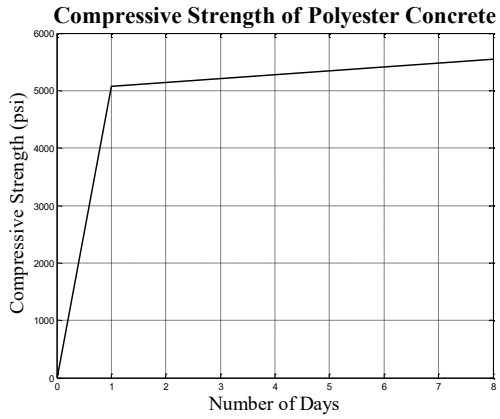
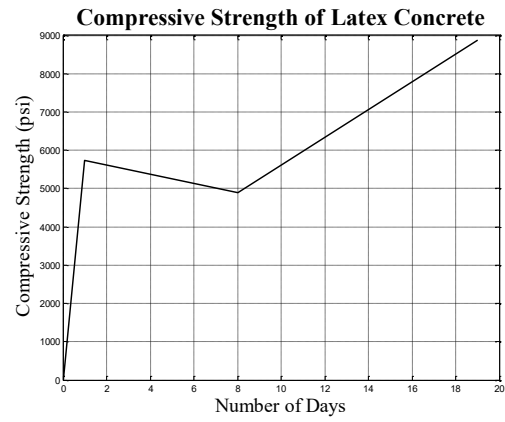
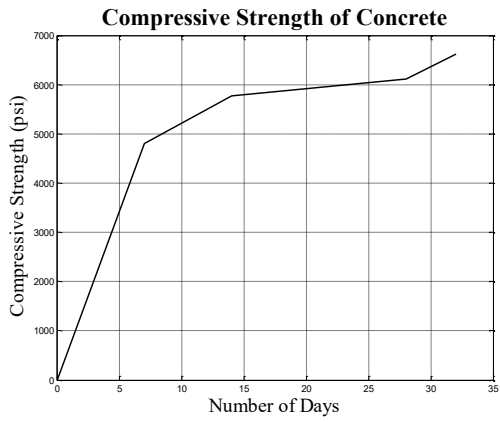
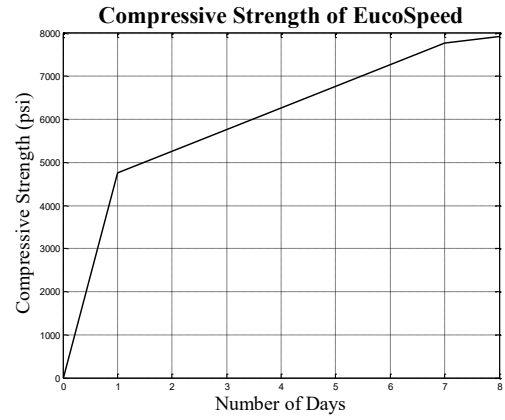
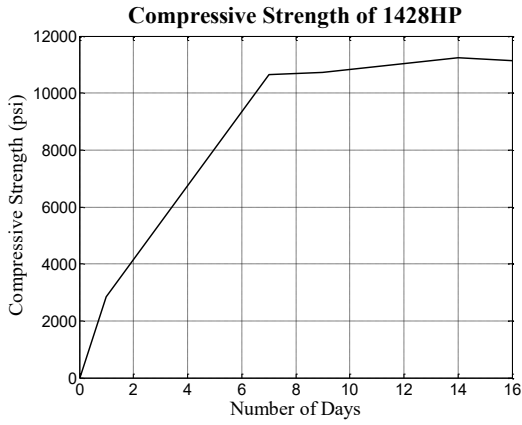


Figure 2-15 Compressive Strength of Grouts (Shear Test)

2.2.2.3 Deck and Girder Reinforcement

Standard Gr. 60, ASTM A615 deformed mild reinforcing steel bars were used in this study. Samples of the No. 3 and No. 4 reinforcing bars used in the test specimen were tested under tension according to ASTM E8/E8M-16a. The average measured yield stress and ultimate strength for No. 3 bars were 72.1 ksi and 111.8 ksi. For No. 4 bars, the average measured yield stress and ultimate strength were 73.7 ksi and 101.8 ksi. The measured stress-strain relationships of the #3 and #4 samples are shown in Figures 2-16 and 2-17. A summary of the measured material properties is listed in Tables 2-4 and 2-5.

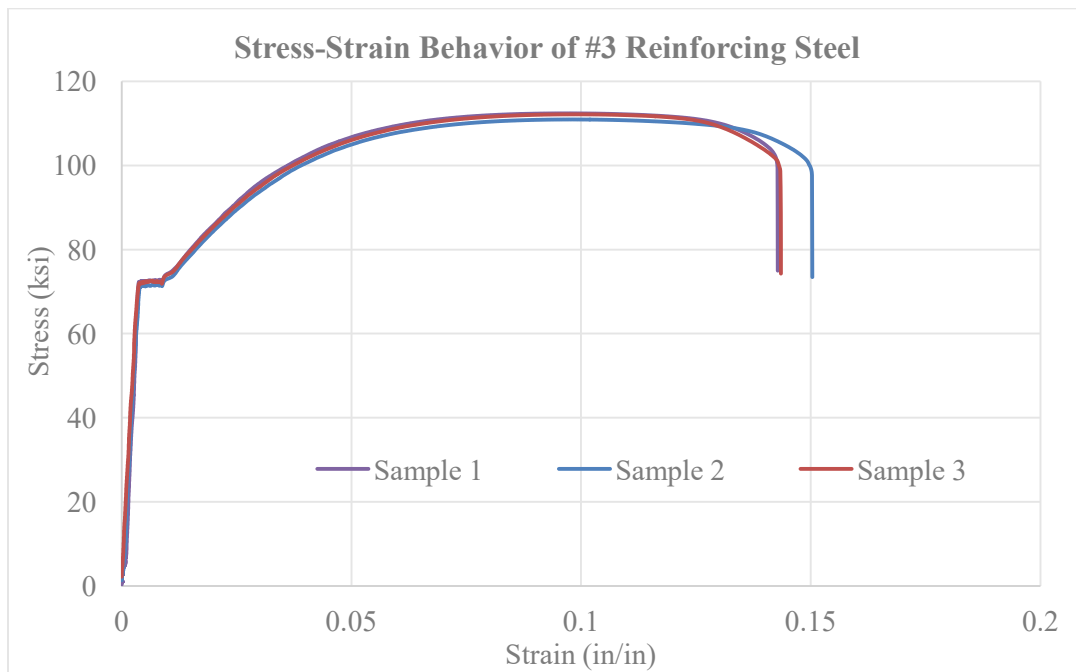


Figure 2-16 Stress-Strain Behavior of #3 Reinforcing Steel

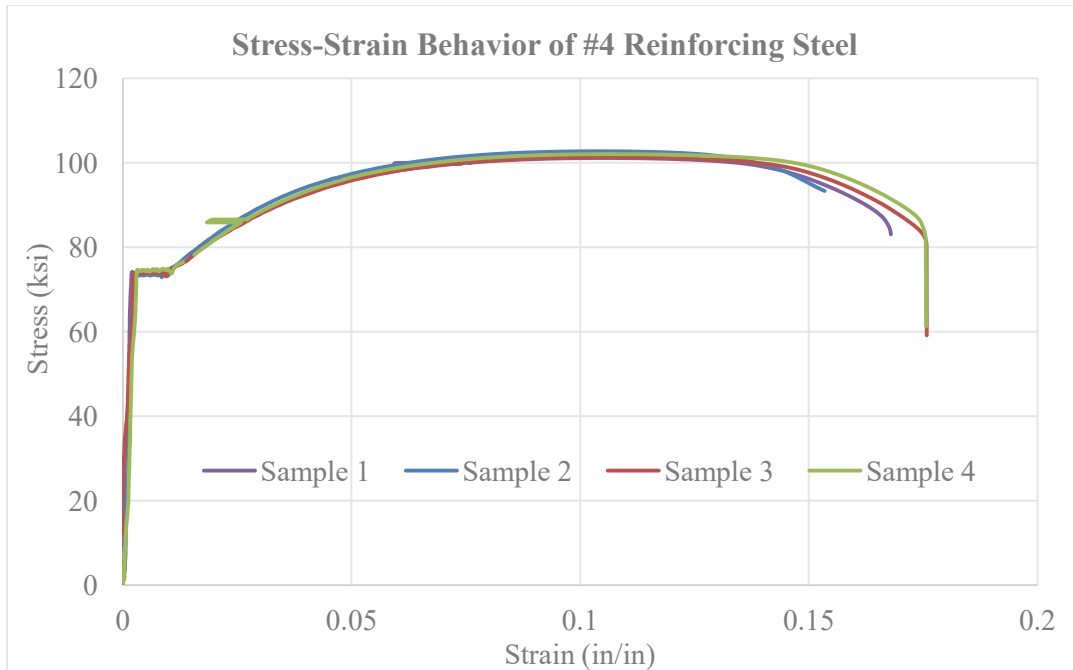


Figure 2-17 Stress-Strain Behavior of #4 Reinforcing Steel

Table 2-4 Number 3 Bar Reinforcing Steel Material Test Results

Sample	Yield Stress (ksi)	Ultimate Stress (ksi)
1	72.5	112.4
2	71.6	111.0
3	72.2	112.1
Average	72.1	111.8

Table 2-5 Number 4 Bar Reinforcing Steel Material Test Results

Sample	Yield Stress (ksi)	Ultimate Stress (ksi)
1	73.8	101.1
2	73.4	102.7
3	73.7	101.3
4	73.9	102.0
Average	73.7	101.8

2.2.2.4 Headed Anchors

The headed anchors used in this study were #5 Standard Gr. 60, ASTM A706 deformed mild steel reinforcing bar. These anchors were supplied by Headed Reinforcement Corporation (HRC). Two different head areas, 9A_b and 4A_b, were used. Figures 2-18 and 2-19 show the details and photos of the headed anchor for two head bars, respectively. The head and # 5 bars connected using a coupler. The bar was friction-welded to the coupler. The head was square and was threaded inside with 5/8 in – 11 UNC thread size.

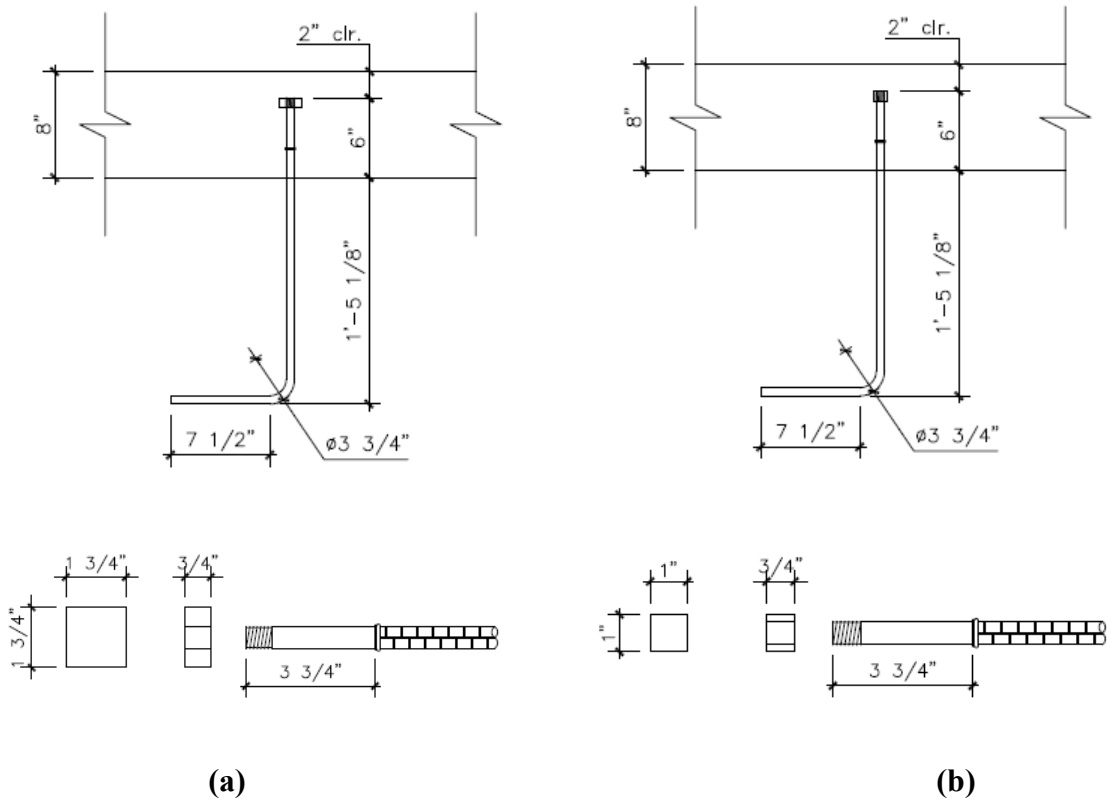


Figure 2-18 Headed Anchor Details (a) Head Area = $9A_b$; (b) Head Area = $4A_b$



Figure 2-19 Headed Anchor (Left: Head Area = $4A_b$; Right: Head Area = $9A_b$)

Figure 2-20 shows the elevation of the headed anchors. The development length of the bar embedded into the girder was calculated according to AASHTO Section 5.11.2.4 for a standard hook, l_{dh} , is defined as:

$$\frac{38}{\underline{\quad}} \text{ sing}$$

Therefore, $l_{dh} = 11.2$ in. was used.

The development length of the rebar embedded into the girder was increased to 17 in. to provide sufficient workable space between flange of girder and footing.

AASHTO provisions do not have equations for determining the development length of headed anchor. Therefore, ACI 318-11, Section 12.6 was used to calculate the development length for headed anchors into deck. The development length in tension for headed bars (l_{dt}) is defined as:

$$\frac{0.016}{\underline{\quad}} \text{ 6 sing}$$

Therefore, $l_{dt} = 6$ in. controls.

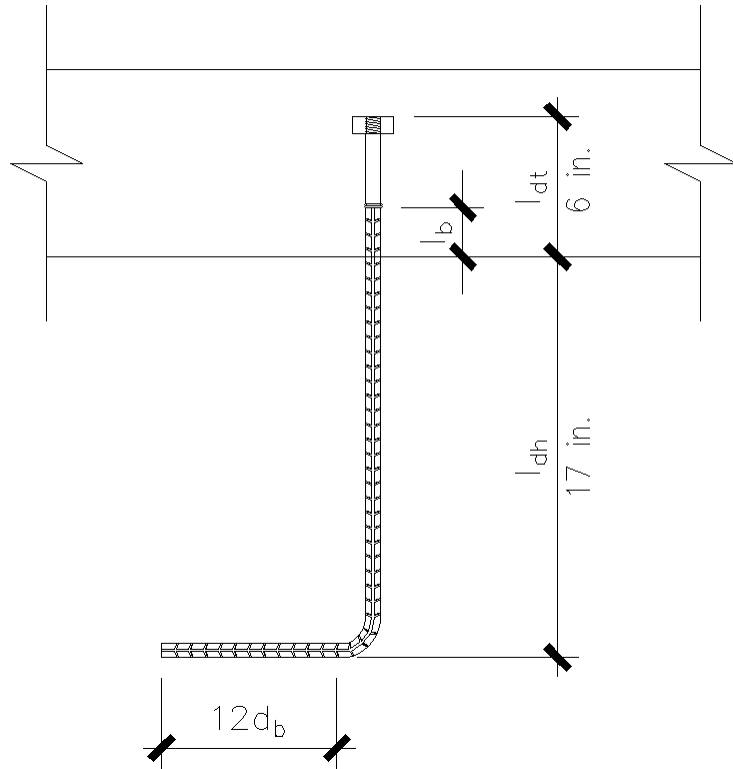


Figure 2-20 Development Length of Headed Anchor

2.2.3 Test Matrix

A test matrix, shown in Table 2-6, was developed to study various parameters used in the nine experiments. The small head was used only in combination with UHPC to determine if the high strength of UHPC would improve the anchorage mechanism and would allow for a smaller heads, which could simplify construction. The test was performed such that only one pocket in each specimen was filled with grout at a time to ensure that only the anchors in that pocket were engaged during the test. Note that the term “grout” used in this document refers to the pocket filler material, which in some cases was concrete as stated in the test matrix. After each test, grout was removed before

placing grout in the next pocket. A detailed step-by-step procedure of the testing is discussed in Section 2.2.5.

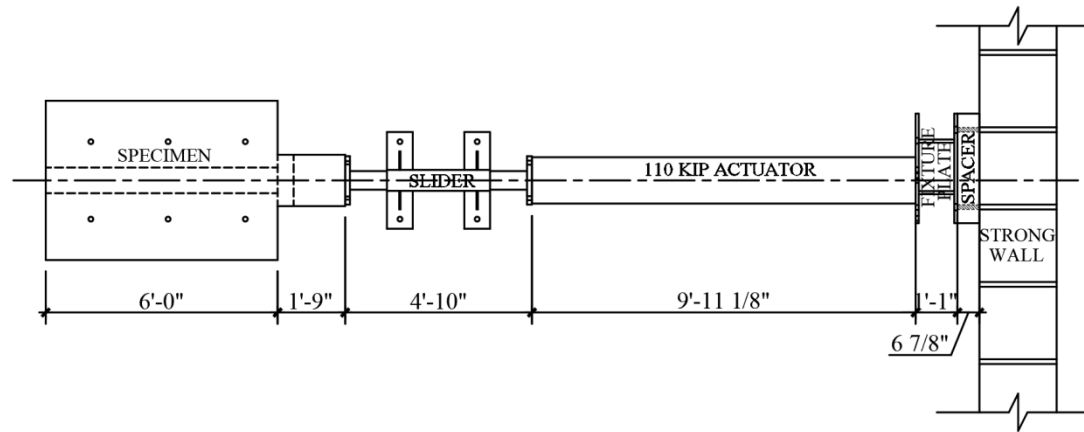
Table 2-6 Test Matrix for Shear Test of Headed Stud

Test	Specimen	Pocket	Grout	Number of Anchors	Head Area
1	1	1	1428 HP	1	9A _b
2	2	1	1428 HP	2	9A _b
3	3	1	1428 HP	4	9A _b
4	1	3	EucoSpeed	4	9A _b
5	2	2	Concrete	4	9A _b
6	3	2	Latex Concrete	4	9A _b
7	1	3	Polyester Concrete	4	9A _b
8	2	3	UHPC	4	9A _b
9	3	2	UHPC	2	4A _b

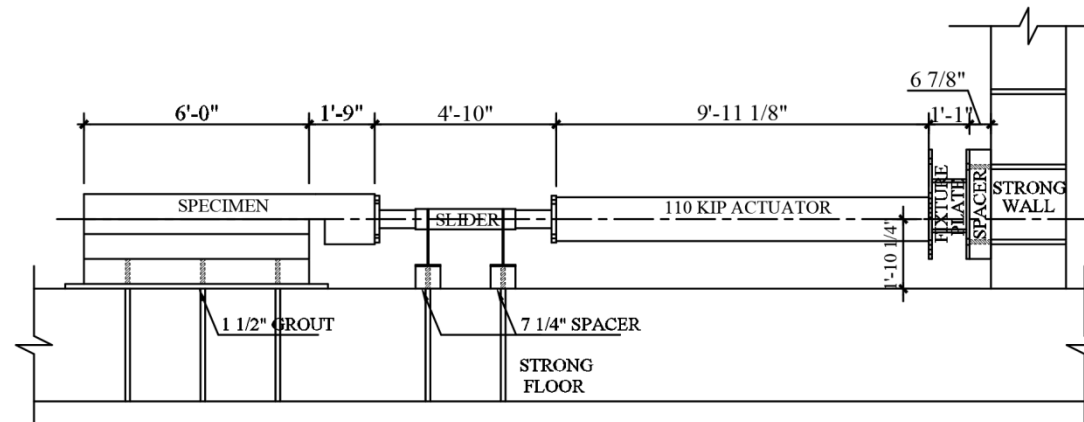
2.2.4 Test Setup and Instrumentation

The schematic of the test set up is shown in Figures 2-21 and 2-22. A hydraulic actuator was used to apply load on the loading head of each specimen. A displacement controlled loading scheme was utilized where a horizontal compressive load was applied on the loading head at an average rate of 0.5 in/min until failure of the anchors. The load and horizontal displacement were monitored and recorded at an interval of 0.1 in. displacement until the displacement was 0.6 in. Afterward, the load and displacement were recorded at an interval of 0.2 in. up to 1 in. displacement. The interval was increased to 0.4 in. afterward. The intervals were adjusted during the test depending on

the observed behavior. Figure 2-23 shows the location of transducers in deck, girder and footing segments. Two Novotechnik transducers (LWG series) were mounted on each side of the deck and girder section to measure any horizontal slippage of the deck relative to the girder as shown in Figure 2-24 (a). Figure 2-24 (b) shows the placement of transducers (TR series) between the test specimen and the laboratory strong floor to measure any relative slip between the girder and strong floor. Cracks and signs of failure were noted and recorded during each test. Strain gages were also placed on the anchor rebar to measure the strain in the connectors. Figures 2-25, 2-26, and 2-27 show the location of strain gages in specimens 1, 2 and 3, respectively. The strain gages were placed at the level of deck and girder interface and also at the level of girder web and flange interface.



(a) Plan View

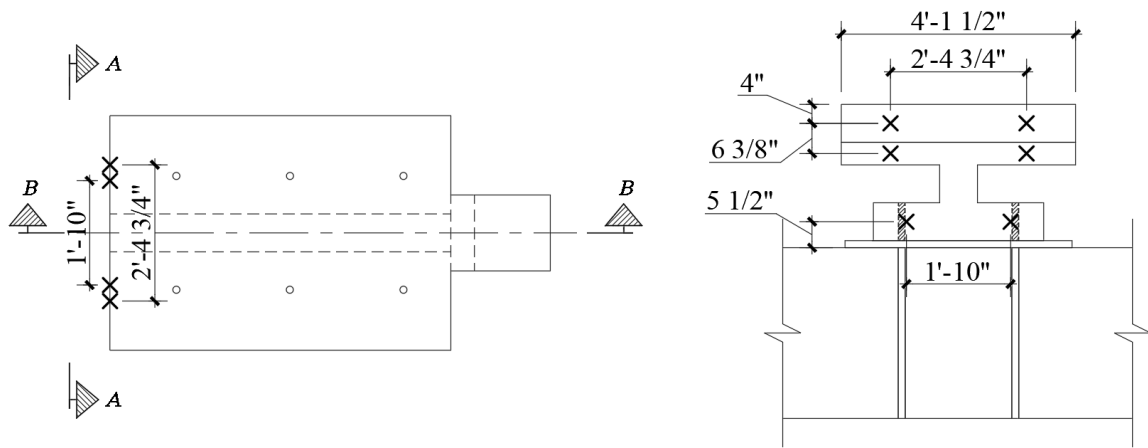


(b) Elevation View

Figure 2-21 Plan and Elevation Schematic of Overall Shear Test Setup

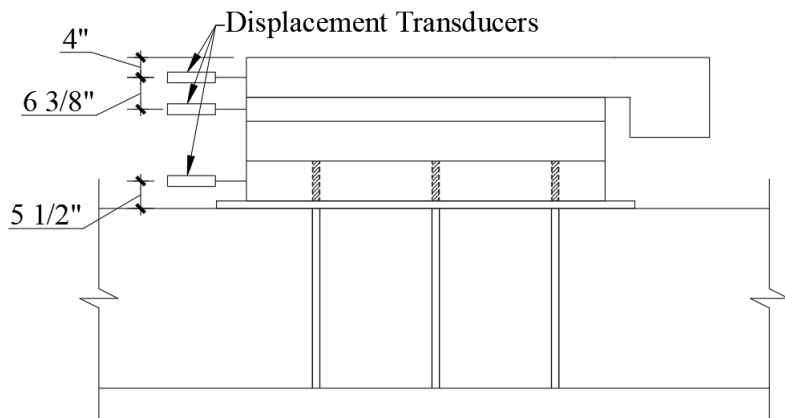


Figure 2-22 Shear Test Setup



PLAN VIEW

ELEVATION VIEW A-A



ELEVATION VIEW B-B

Figure 2-23 Transducers on Deck, Girder and Footing

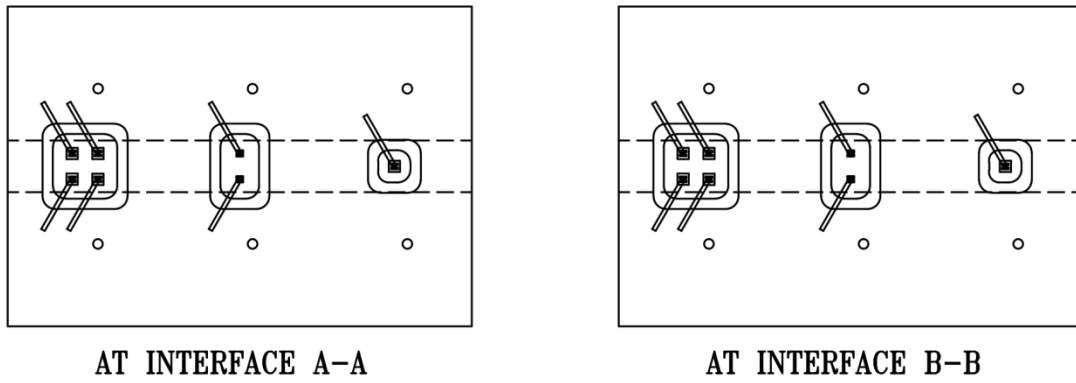


(a)

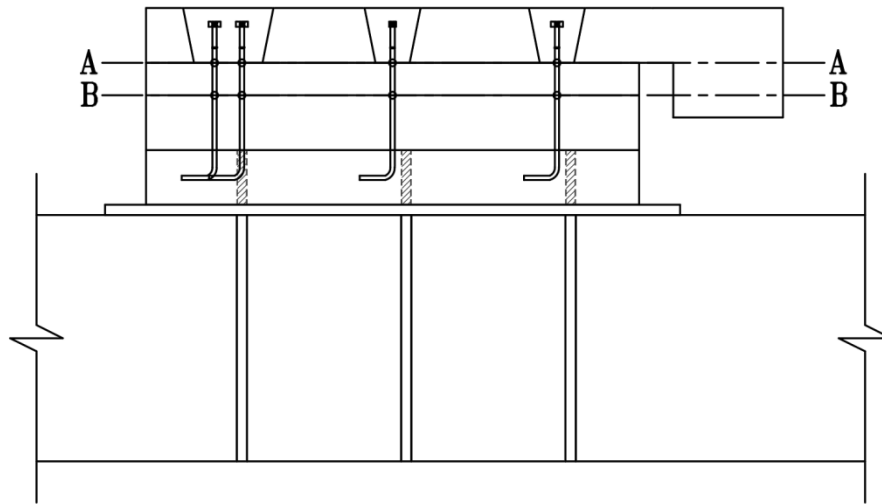


(b)

Figure 2-24 Placement of Transducers

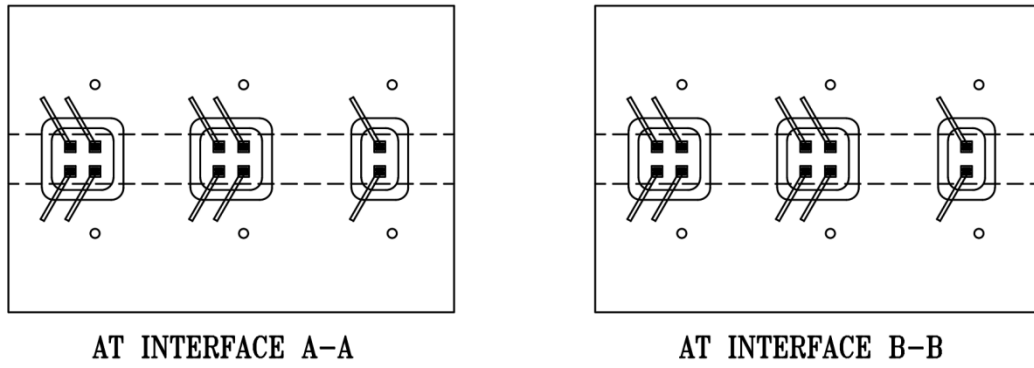


(a) Plan View

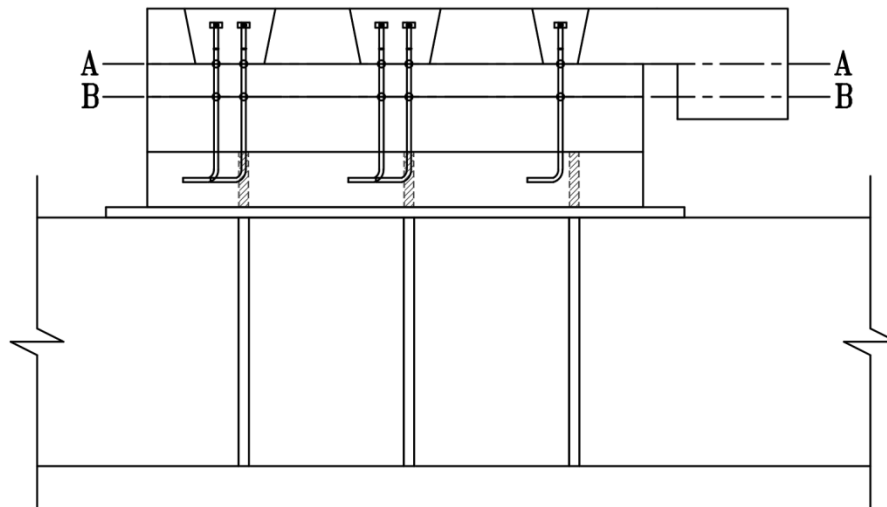


(b) Elevation View

Figure 2-25 Location of Strain Gage in Specimen 1

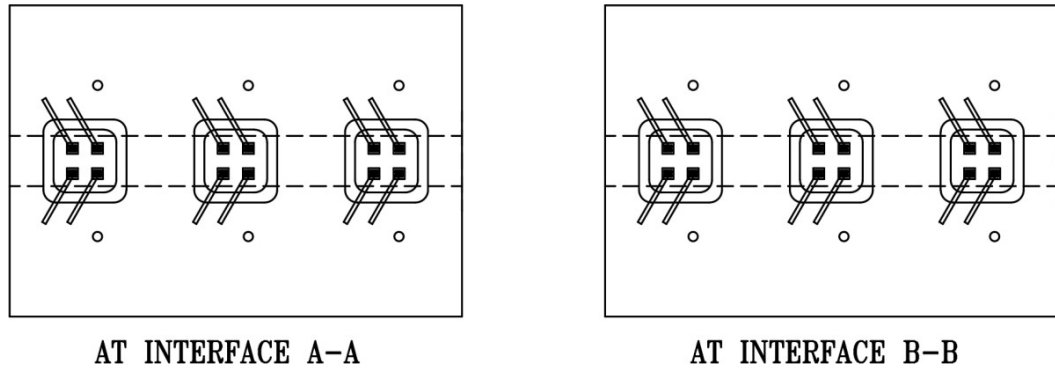


(a) Plan View

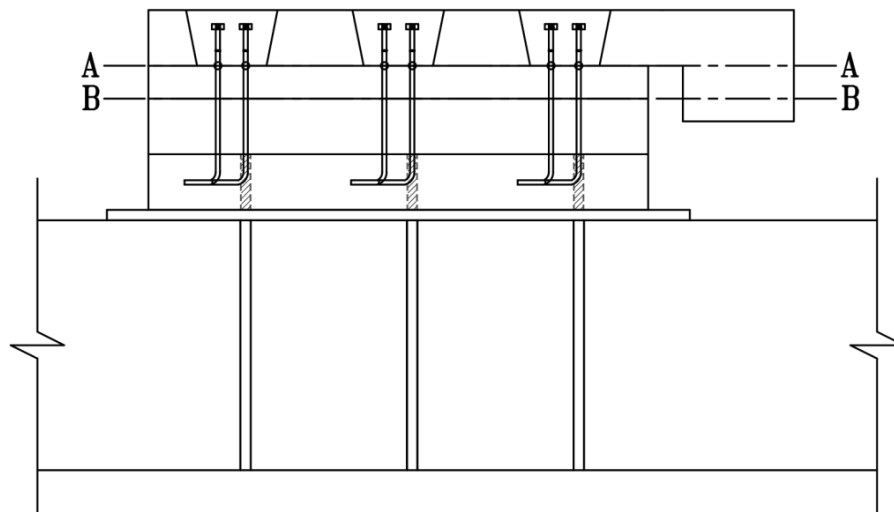


(b) Elevation View

Figure 2-26 Location of Strain Gage in Specimen 2



(a) Plan View



(b) Elevation View

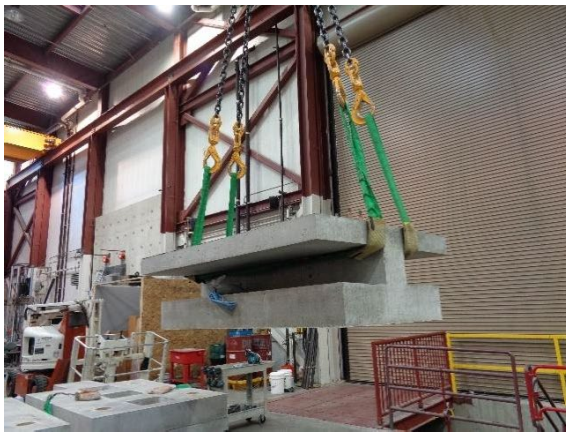
Figure 2-27 Location of Strain Gage in Specimen 3

2.2.5 Construction Process and Testing Procedure

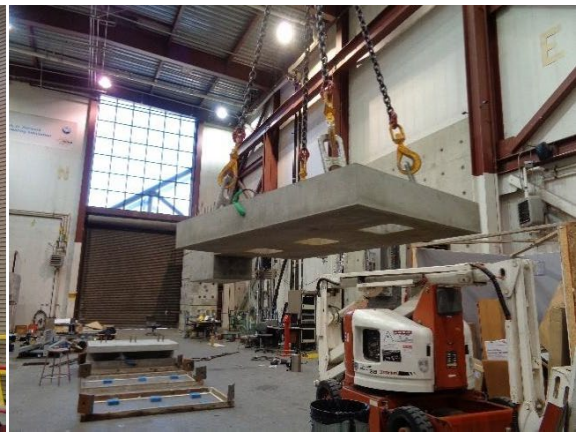
The step-by-step testing procedure followed for the construction and testing of all shear test specimens is explained below and illustrated in Figure 2-28.

- a) Cast the deck, the girder, and the footing.

- b) After 28 days of placing concrete in the deck and girder segments, the specimens were crane lifted, Figure 2-28 (a), to the test location and were connected to the strong floor. The deck segments were placed on the top of the girders, Figure 2-28 (b). Grout was then poured under footing as shown in Figure 2-28 (c).
c) 1428 HP grout was placed in the first pocket of each specimen to ensure only the first anchor was engaged during the test as shown in Figure 2-28 (d).



(a)



(b)



(c)



(d)

Figure 2-28 Step-by-step Procedure of Shear Test of Headed Anchors

- d) After the grout reached the required strength, the first specimen was prepared for testing. A load slider was connected to the loading head of the first specimen to prevent any potential of actuator uplift [Figure 2-29 (a)]. The actuator was then connected to the strong wall using fixture plate and a spacer [Figure 2-29 (b)]. The actuator and the load slider were connected and aligned with the loading head of the deck. Shear test was performed on the first pocket of first specimen.



(a)

(b)

Figure 2-29 Step-by-step Procedure of Shear Test of Headed Anchors

- e) After completing testing the first specimen, the second specimen was prepared. All the testing equipment was moved from specimen 1 to specimen 2 according to the procedure explained in step (d).
- f) Step (e) was repeated for specimen 3.
- g) After each test, grout was removed from the pockets using chipping hammer and recorded the time needed for that. The grout removal process and results are discussed in more detail in Section 2.2.6.3. After completely removing the grout, the deck was lifted and positioned along the girder.

- h) EucoSpeed, Concrete and Latex Concrete were then placed in third, second and second pockets of Specimens 1, 2 and 3, respectively. After the pocket grout had reached the required strength, the testing was repeated for specimens 1, 2 and 3 according to the steps explained earlier. After completing the tests, grout was removed, the deck was lifted and positioned on the girder.
- i) Polyester Concrete, UHPC and UHPC were then poured in the second, third and third pocket of Specimens 1, 2 and 3, respectively. After the grout reached the required strength, the testing was repeated for specimens 1, 2 and 3 according to the steps explained earlier.

2.2.6 Shear Test Results

2.2.6.1 Ultimate Strength and Stiffness

Table 2-7 summarizes the key test results such as peak loads and displacements at the peak loads. Figure 2-30 shows the load-displacement curves for all nine specimens. The average ultimate shear capacity per anchor was found to be 25.42 kips, as shown in Table 2-7. The measured force displacement curves were used to calculate the stiffness of the headed anchor for each test by computing the slope in the linear region of the force-displacement response. The stiffness of the headed anchor for each test is listed in Table 2-8. The stiffness of each anchor ranged between 41 to 63 kip/in.

Table 2-7 Summary of Shear Test Results

Test	Grout	Number of Anchors	Head Area	Displacement (in)	Force (kips)	Force per Headed Stud (kips)
1	1428 HP	1	9A _b	1.820	25.82	25.82
2	1428 HP	2	9A _b	1.430	55.45	27.73
3	1428 HP	4	9A _b	1.440	101.43	25.36
4	EucoSpeed	4	9A _b	1.540	99.36	24.84
5	Concrete	4	9A _b	1.780	107.83	26.96
6	Latex Concrete	4	9A _b	1.670	102.19	25.55
7	Polyester Concrete	4	9A _b	1.460	106.59	26.65
8	UHPC	4	9A _b	1.330	94.41	23.60
9	UHPC	2	4A _b	1.220	44.62	22.31

Table 2-8 Shear Stiffness of Headed Anchors

Test	Grout	No. of Anchors	Total Stiffness (kip/in)	Stiffness/Anchor (kip/in)
1	1428 HP	1	40	40
2	1428 HP	2	124	62
3	1428 HP	4	225	56
4	EucoSpeed	4	178	44
5	Concrete	4	182	45
6	Latex Concrete	4	253	63
7	Polyester Concrete	4	238	60
8	UHPC	4	188	47
9	UHPC	2	83	41

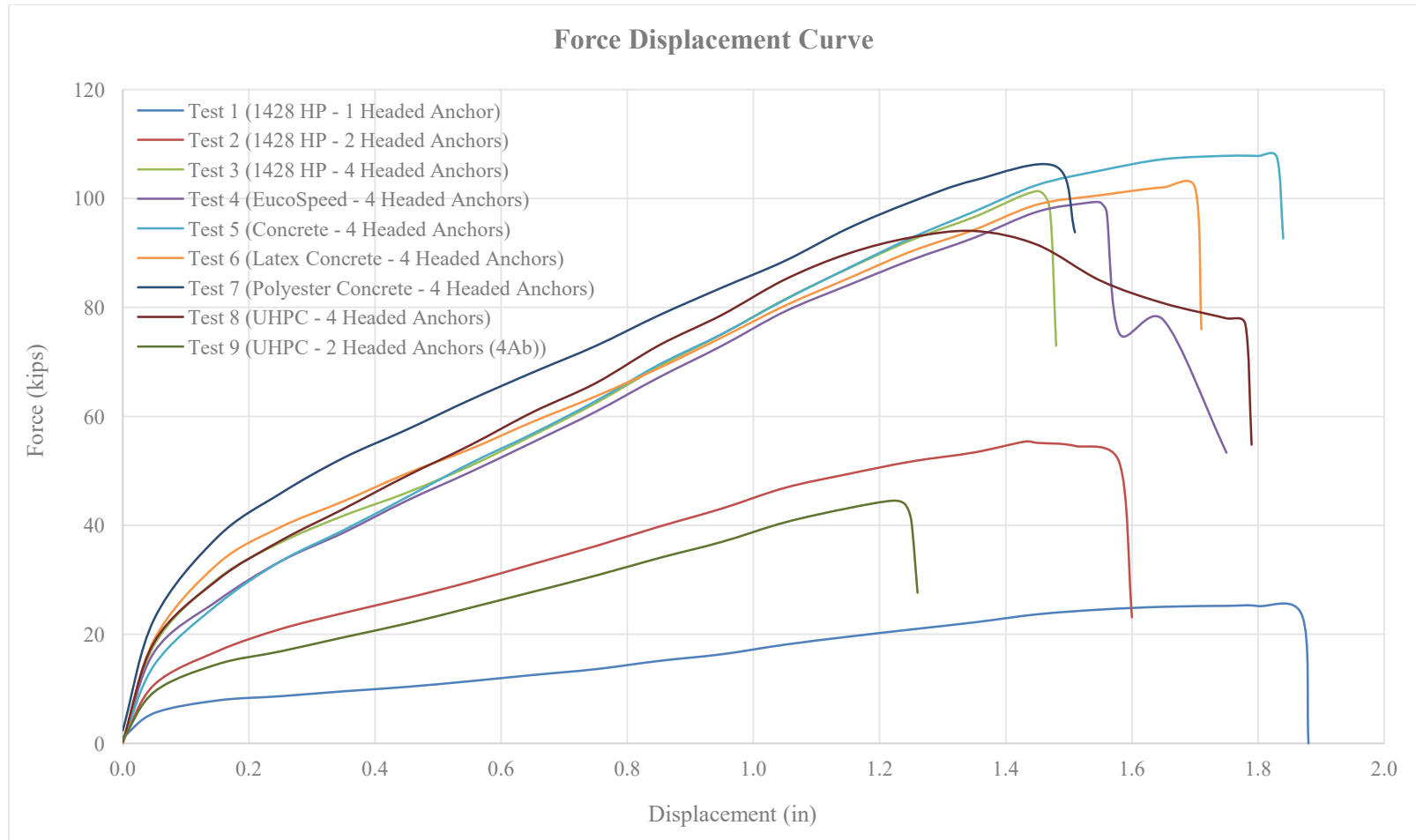


Figure 2-30 Force Displacement Curve (Shear Test of Headed Anchors)

2.2.6.2 Crack Pattern and Failure Mechanism

The crack patterns during each load increment were carefully studied and recorded to determine the failure mechanism. In all nine specimens, the failure mode was the fracture of the headed anchor at the deck girder interface. In some pockets with four anchors, the test was stopped before the fracture of all four anchors in order not to damage the anchors in the adjacent pockets. Figure 2-31 shows the fractured headed anchors and the pocket with the failed anchors. Figures 2-31 (a), (b) and (c) show the fractured headed anchors from 1-, 2- and 4-anchors pockets, respectively. Figure 2-31 (d) shows the girder surface where the anchors were fractured. Figure 2-31 (e) shows the un-fractured headed anchor in one of the 4-anchor pockets.

Figures 2-32 and 2-33 show the crack pattern in various pockets at the end of the test. Cracking was observed around the grout concrete interface while testing the first pocket in each specimen. For the second and third pockets, additional cracks were observed at the corner of the grout pocket across the width of the specimen.



(a)



(b)



(c)



(d)



(e)

Figure 2-31 Failure of Headed Anchor



Test 1



Test 2



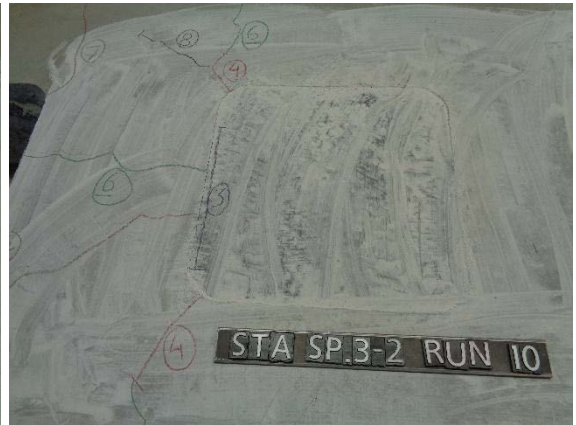
Test 3



Test 4



Test 5



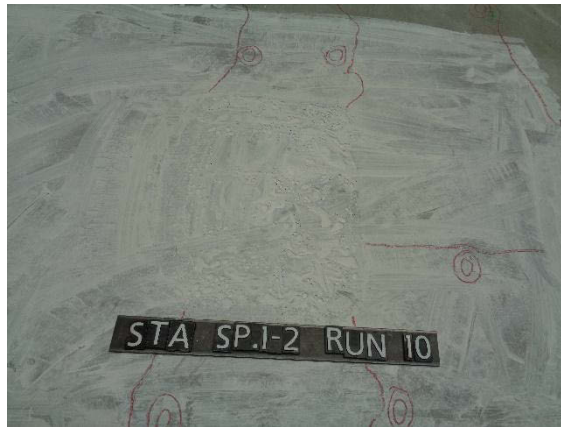
Test 6

Figure 2-32 Crack Pattern of 9 Grout Pockets (Tests 1-6)



Test 7

Test 8



Test 9

Figure 2-33 Crack Pattern of 9 Grout Pockets (Tests 7-9)

2.2.6.3 Grout Removal

One of the parameters for this study was to investigate the ease of removing the grout from the pocket. This issue was studied to identify the more feasible grouts for future deck replacement or rehabilitation. After each test, the grout in the pockets was removed using a Makita 1 9/16 HR 4041C chipping hammer shown in Figure 2-34. Figures 2-35 (a) and (b) show the pocket during and after completely removing the grout.

The time required to remove the grout was recorded. Table 2-9 shows the time required for the removal of grout in each pocket with 4 anchors. The time required for tests 1, 2 and 9 are not included since only the pockets with same quantity of grout were studied. It was observed that the latex concrete took the least amount of time (52 minutes) to be removed, while the times for 1428 HP, EucoSpeed grout and conventional concrete were 62, 86, and 72 minutes, respectively. The 1428 HP, EucoSpeed and conventional concrete required 19.2%, 65.4%, and 38.5% more time for removal than the time needed for latex concrete. The polyester concrete and UHPC required the longest time to remove. In fact, these grout were not completely removed from the pockets since it took approximately 90 minutes to remove the first 1/3rd of the each grout. Based on the time required and ease in removing the grout, 1428 HP, EucoSpeed, conventional concrete and latex concrete can be recommended for use when future deck replacement is a concern.



Figure 2-34 Chipping Hammer used for Grout Removal



Figure 2-35 Grout Removal

Table 2-9 Grout Removal Time

Test	Grout	Number of Anchors	Time	Notes
3	1428 HP	4	1 hr 2 min	
4	EucoSpeed	4	1 hr 26 min	
5	Concrete	4	1 hr 12 min	
6	Latex Concrete	4	52 min	
7	Polyester Concrete	4	1 hr 30 min	Only 1/3 removed
8	UHPC	4	1 hr 30 min	Only 1/3 removed

2.2.7 Discussion of Shear Test Results

2.2.7.1 Effect of Grout Type

The goal of the first test series was to investigate the performance of different types of grout. Results of tests 3, 4, 5, 6, 7 and 8 were compared to study the effect of six different types of grout. All these tests have 4 headed anchors in the shear pockets. The

results from test 1, 2 and 9 were not included in this study since these tests had less than 4 headed anchors. Figure 2-36 shows the measured force displacement curves for the six headed anchors. From these curves, it can be concluded that the grout type had a negligible effect in the shear strength of headed anchors. The maximum capacity of 108 kips was observed in the anchor with concrete grout and the minimum capacity of 94 kips was observed in the anchor with UHPC filled grout pocket. It was also observed that the anchors yielded at lower displacement in UHPC filled grout pockets than other grout pockets causing small drop in the force. This is due to the higher stiffness of UHPC and higher bond strength between UHPC and the anchors. Due to the higher stiffness and bond strength that the UHPC provided, it appears that shear strains were concentrated over a relatively small portion of anchor, which caused the bar to yield at a lower displacement.

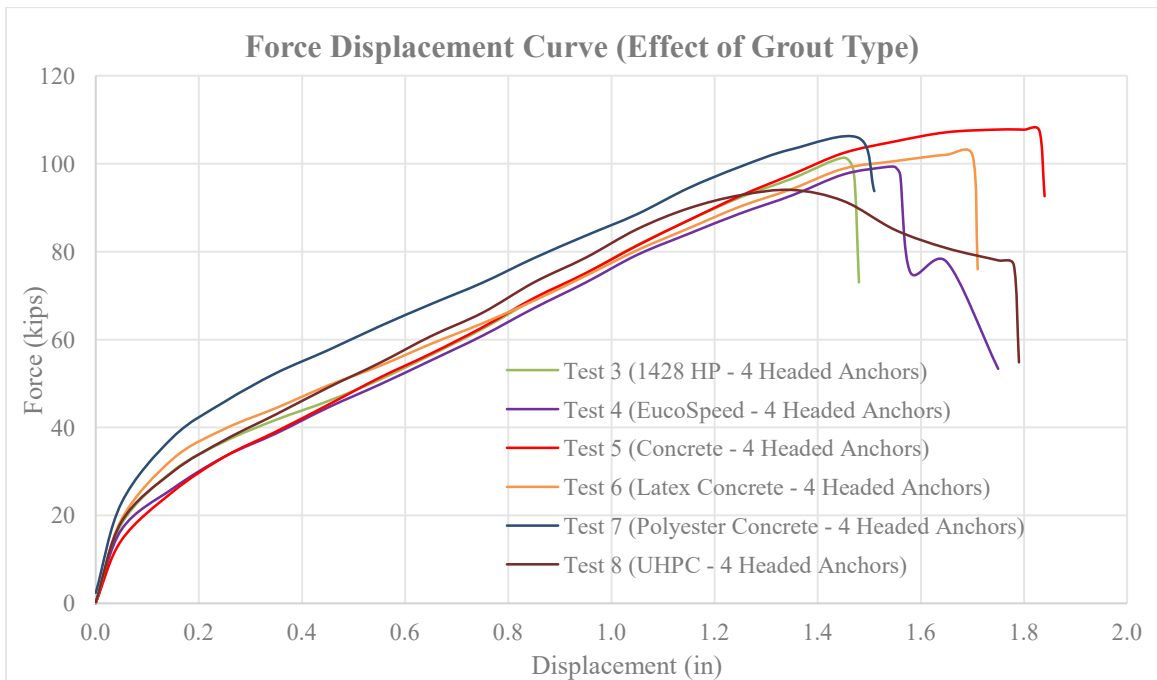


Figure 2-36 Force Displacement Curve (Type of Grout)

2.2.7.2 Effect of Number of Headed Anchor

The second test parameter was the anchor group effect. The test results of pockets with 1, 2 and 4 anchors with HP 1428 grout were compared. Figure 2-37 shows the force displacement response for pockets with various numbers of headed anchors. To isolate the effect of the number of anchors, the curves for the specimens with 2 and 4 number of anchors were normalized by dividing the forces by number of anchors and presented in Figure 2-38. It was observed that the number of headed anchor had negligible effect on the force displacement relationships and the ultimate shear strength of the headed anchor. However, the maximum displacement at which the headed anchor failed decreased with the increase in the number of anchors. This could be attributed to the increased stiffness in the anchor group.

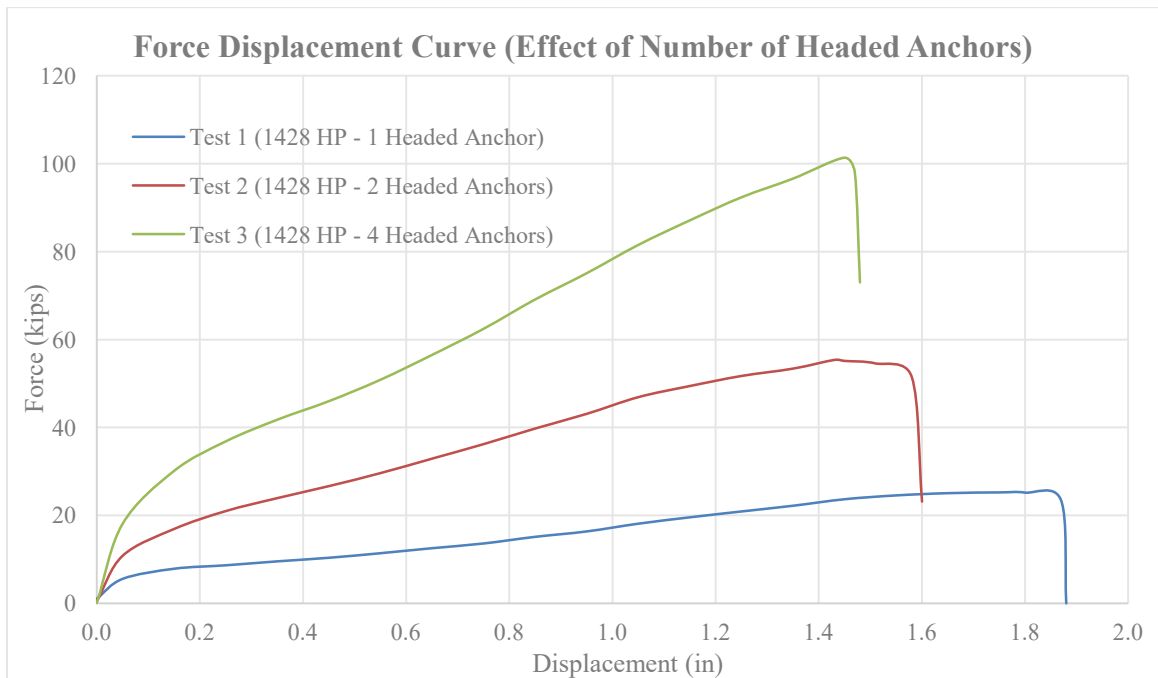


Figure 2-37 Force Displacement Curve (Number of Headed Anchor)

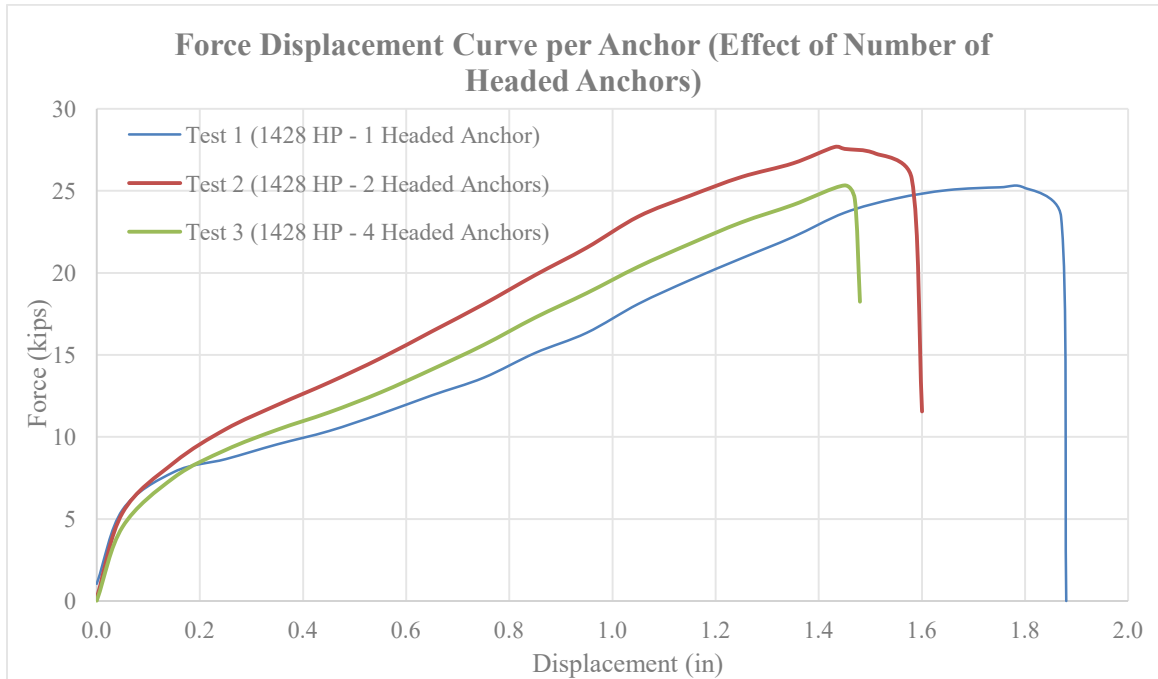


Figure 2-38 Force Displacement Curve per Anchor (Number of Headed Anchor)

2.2.7.3 Effect of Anchor Head Area

The effect of the head area on the ultimate shear strength of the anchors was also studied. The force displacement curves of the anchor with head area of $9A_b$ (4 anchors) and $4A_b$ (2 anchors) are compared in Figure 2-39. Both pockets were filled with UHPC. The forces were then normalized by the number of anchors as shown in Figure 2-40. No significant force difference was observed when the size of the head was reduced. However, it was observed that the maximum displacement at which the anchors failed decreased with the reduction in the head area of the anchors.

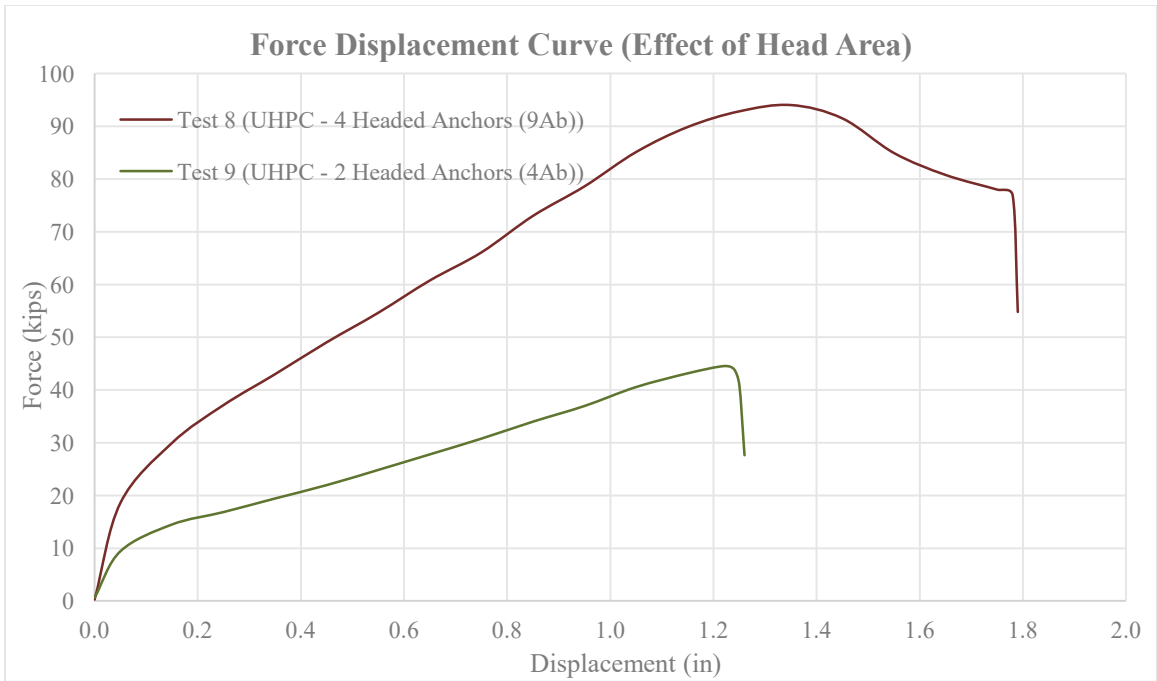


Figure 2-39 Force Displacement Curve (Head Area)

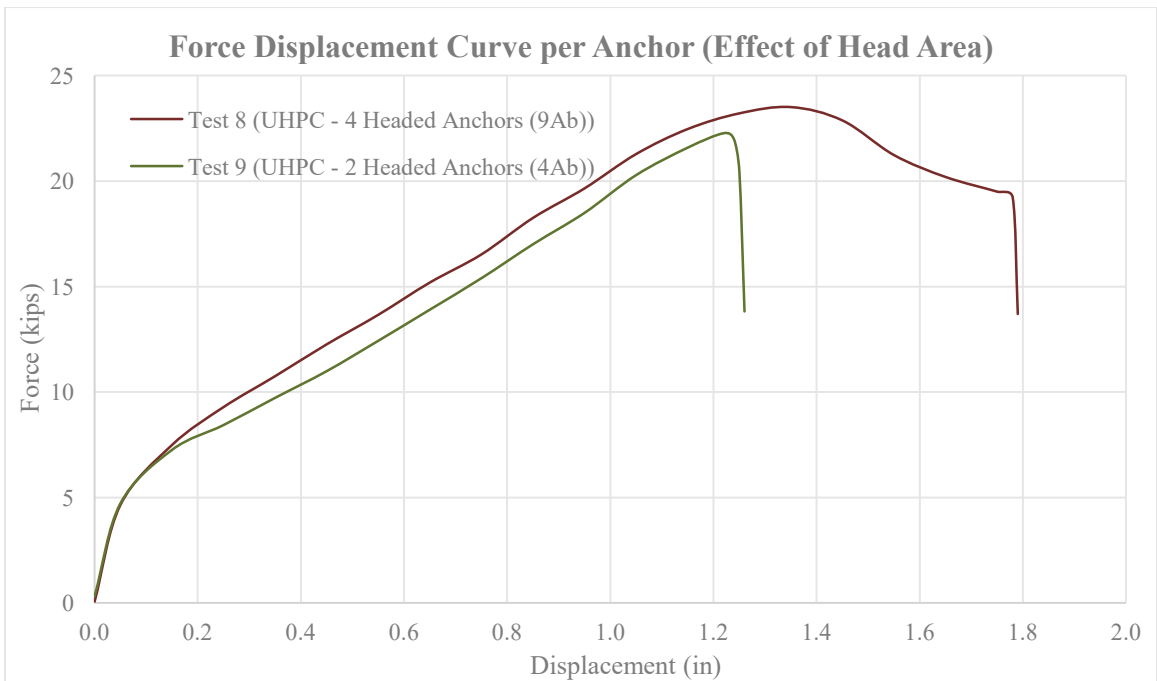


Figure 2-40 Force Displacement Curve per Anchor (Head Area)

2.3 Pullout Test of Headed Anchors

The objective of this part of the investigation was to study the pull-out behavior of the headed anchors and to determine the rebar pullout strength using various grouts. These tests were also used to identify the mode of failure for anchors embedded in various grouts. The potential failure modes in rebar embedded in concrete are shown in Figure 2-41 and can be summarized as: (a) Steel failure, (b) Grout breakout of the anchors and the surrounding concrete, and (c) pullout of the anchors from the grout.

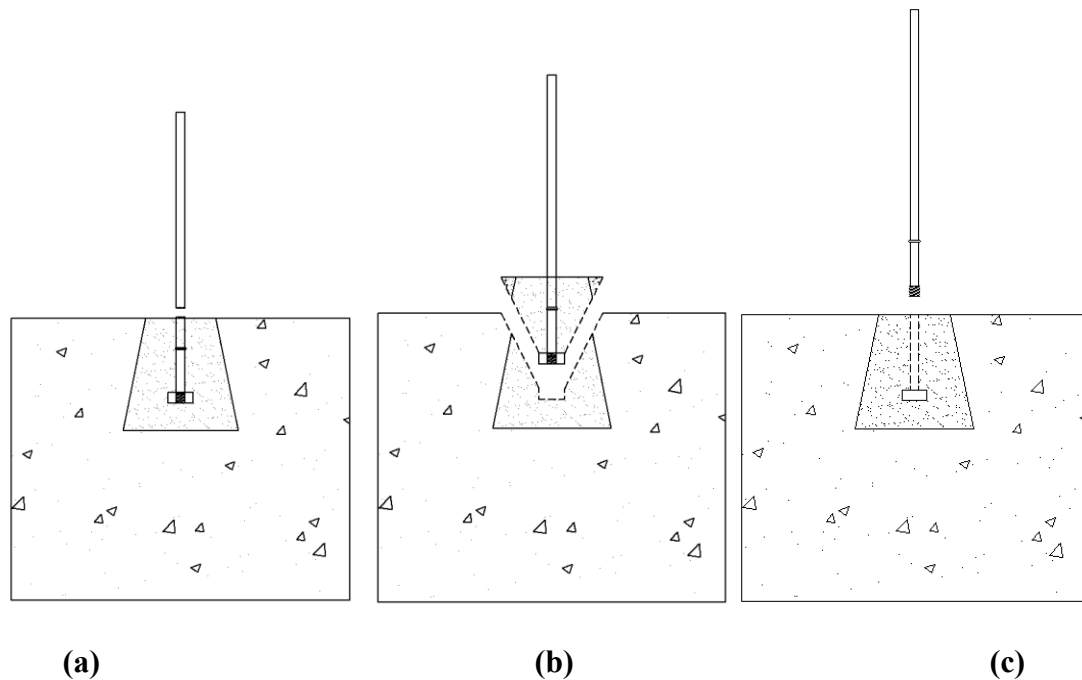


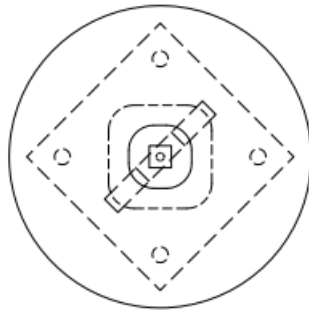
Figure 2-41 Modes of Failure (Pullout test)

2.3.1 Specimen Description

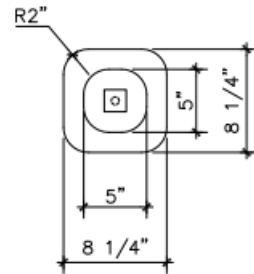
The geometry of the test specimens was selected to represent the headed anchor embedded in pockets in the precast deck. A total of 12 specimens were constructed to study the pullout behavior of headed anchors. Each specimen was constructed with one

pocket with different types of grout and head area. Section 2.3.3 discuss the 12 types of pullout tests and the related parameters for this study.

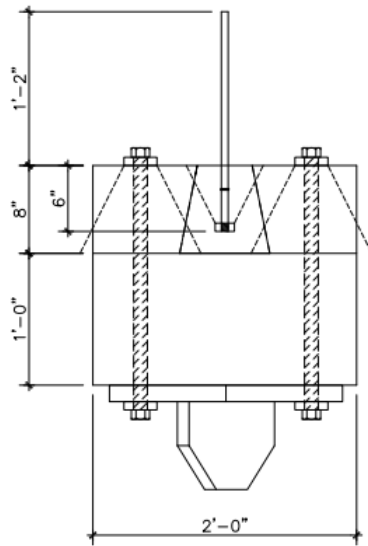
Figure 2-42 shows the details of the test specimens. Each specimen consisted of a 20 in. high cylinder with a 24 in. diameter. The top 8 in. of the cylinder represented the depth of concrete deck. The top surface of the specimen represented the interface of the deck and girder. All specimens were lightly reinforced longitudinally with 6-#3 bars and transversely with #3 spiral at 3 in. pitch. Figure 2-43 shows the reinforcement detail of the specimens. All 12 pullout test specimens were cast at the same time from the same mix of concrete with a target 28-day compressive strength of 5,000 psi.



PLAN VIEW



POCKET DETAILS



ELEVATION VIEW

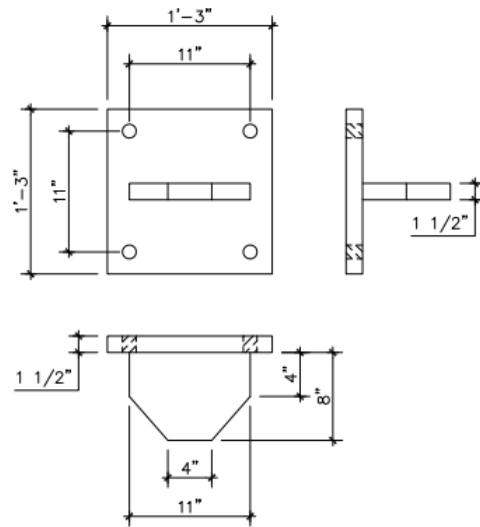
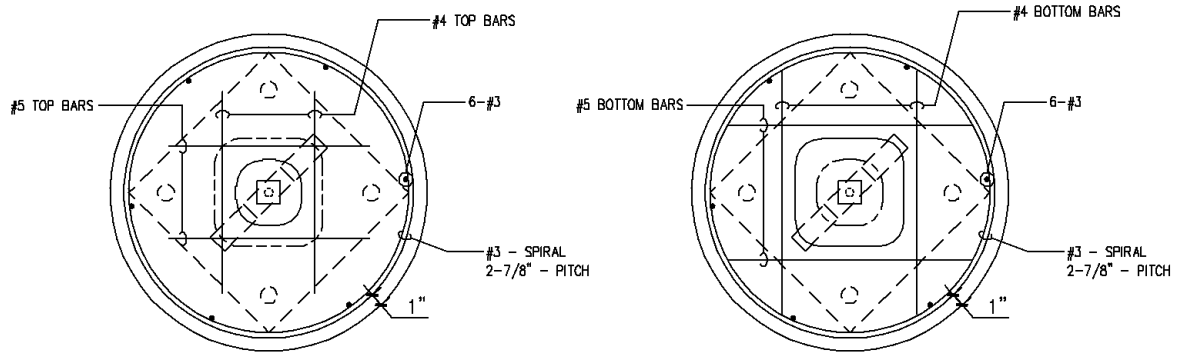
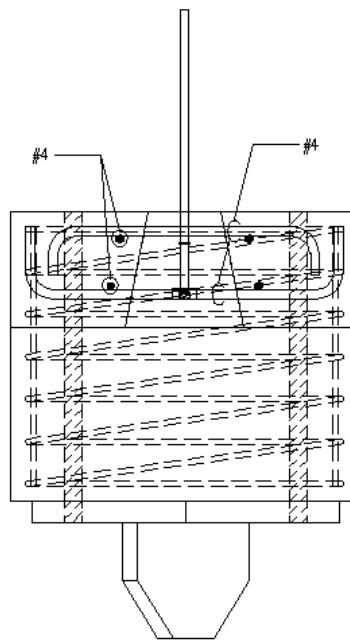


PLATE DETAILS

Figure 2-42 Specimen Details (Pullout Test)



PLAN VIEW



ELEVATION VIEW

Figure 2-43 Reinforcement Detail of Pullout Specimen

2.3.2 Materials

2.3.2.1 Concrete

Conventional concrete was used for the construction of the pullout test specimens. Standard 6" x 12" concrete cylinders were tested under compression at 7 days, 28 days, and day of testing. At least three cylinders were tested according to ASTM C39/C39M-17a. Only the average of test data was reported. The measured 28-day compressive strength of specimens was 3.8 ksi. The measured strength of the concrete used for deck and girder specimens is shown in Figure 2-44, and test day compressive strength of concrete is presented in Table 2-10.

Table 2-10 Compressive Strength of Pullout Test Specimen

Test	Strength (ksi)
1, 2, 3	4.81
4, 5, 6, 7	4.62
8, 9, 10, 11, 12	4.68

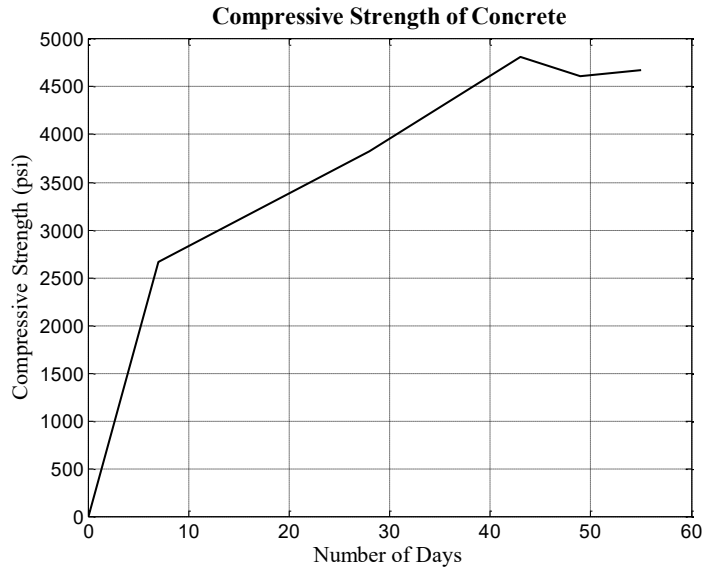


Figure 2-44 Compressive Strength of Specimen Concrete

2.3.2.2 Grout

Various types of grout materials have been used to fill the pockets such as 1428 HP, EucoSpeed and Latex concrete (HD 50). In addition to the grout material, Concrete (Sakrete 5000 Plus High Strength Concrete Mix) and Ultra High Performance Concrete (UHPC) were also used as the grout material. The compressive strength of 1428 HP, EucoSpeed and Latex concrete grouts were measured according to ASTM C109/C109M using 2 in. cube specimen. Plastic cylinders with 3 in. diameter and 6 in. height were used for UHPC sampling. The measured strength of the grouts is shown in Figure 2-45, and the compressive strength of the grouts on each test day are presented in Table 2-11. The modulus of elasticity (E) of each grout was calculated according to ASTM C469/C469M and is listed in Table 2-12. The modulus of elasticity of each grouts calculated from shear test and pullout test were compared in Table 2-13. It was observed that the values were similar for EucoSpeed and UHPC with a difference of 1.92% and

1.38%, respectively. There was 6.43%, 8.25% and 13.36% difference between the modulus of elasticity for 1428 HP, Concrete and Latex Concrete, respectively.

Table 2-11 Compressive Strength of Grout (Pullout Test)

Grout	No. of Days	Strength (ksi)	Test
HP 1428	17	11.43	1, 2, 3
Latex Concrete	14	6.18	4, 5
UHPC	13	21.69	6, 7
EucoSpeed	12	8.47	8, 9
Concrete	32	6.59	10, 11, 12

Table 2-12 Calculation of Modulus of Elasticity (E) of Grouts

Grout	Specimen 1	Specimen 2	Specimen 3	Average E (ksi)
1428 HP	4,119	4,003	3,929	4,017
EucoSpeed	3,878	-	4,340	4,109
Concrete	-	3,844	4,272	4,058
Latex Concrete	4,166	4,376	4,014	4,185
UHPC	9,058	8,393	8,840	8,764

Table 2-13 Comparison of Modulus of Elasticity

Grout	Modulus of Elasticity, E (ksi)			
	Shear Test	Pullout Test	Difference	%
1428 HP	4,293	4,017	276	6.43
EucoSpeed	4,189	4,109	80	1.92
Concrete	3,749	4,058	309	8.25
Latex Concrete	3,692	4,185	493	13.36
UHPC	8,886	8,764	122	1.38

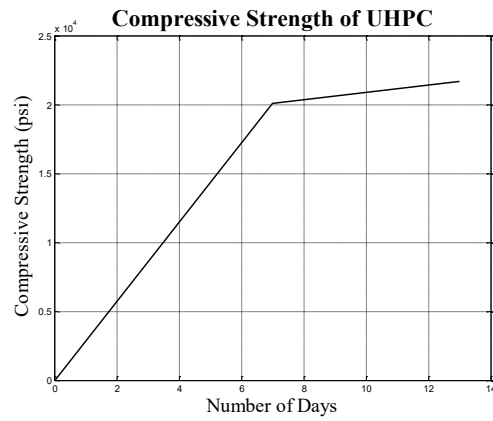
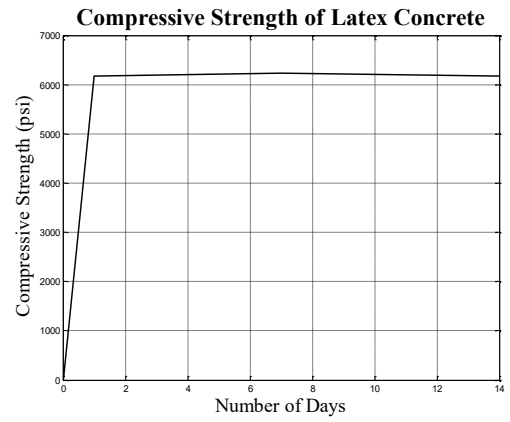
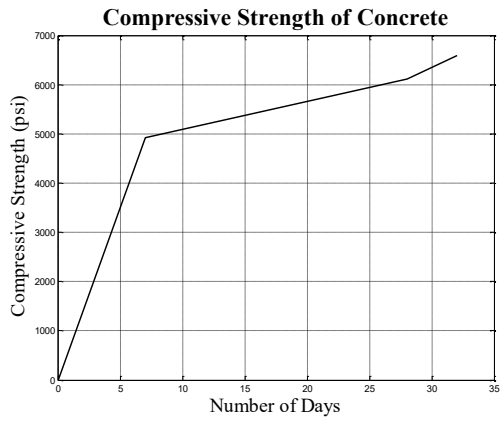
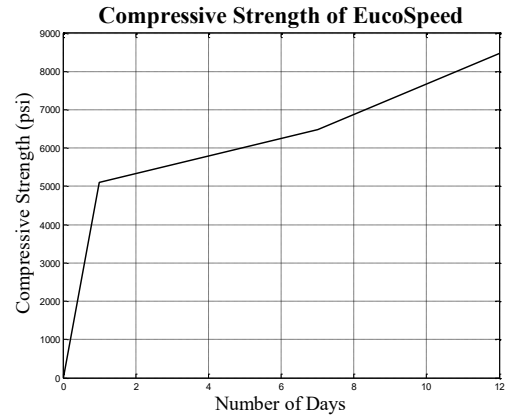
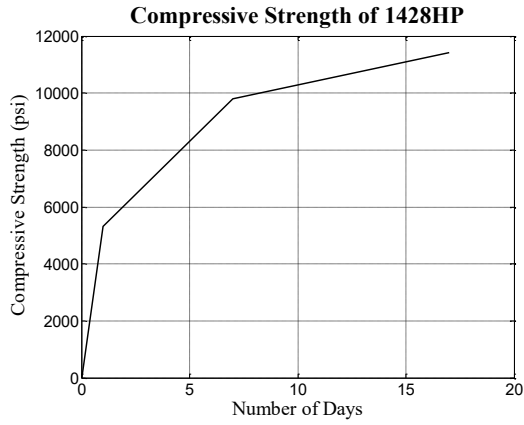


Figure 2-45 Compressive Strength of Grouts (Pullout Test)

2.3.2.3 Pullout Specimen Reinforcement

Standard Gr. 60, ASTM A615 deformed mild reinforcing steel bars were used in this study. The No. 5 reinforcing bars used in construction of the test specimen were tested under tension according to ASTM E8/E8M-16a. The average measured yield stress and ultimate strength were 66.8 ksi and 96.5 ksi. The measured stress-strain relationship of the #5 sample is shown in Figure 2-46. A summary of the measured properties for different samples is listed in Table 2-14.

Table 2-14 Number 5 Bar Reinforcing Steel Material Test Results

Sample	Yield Stress (ksi)	Ultimate Stress (ksi)
1	64.7	96.4
2	67.0	96.7
3	68.8	96.5
Average	66.8	96.5

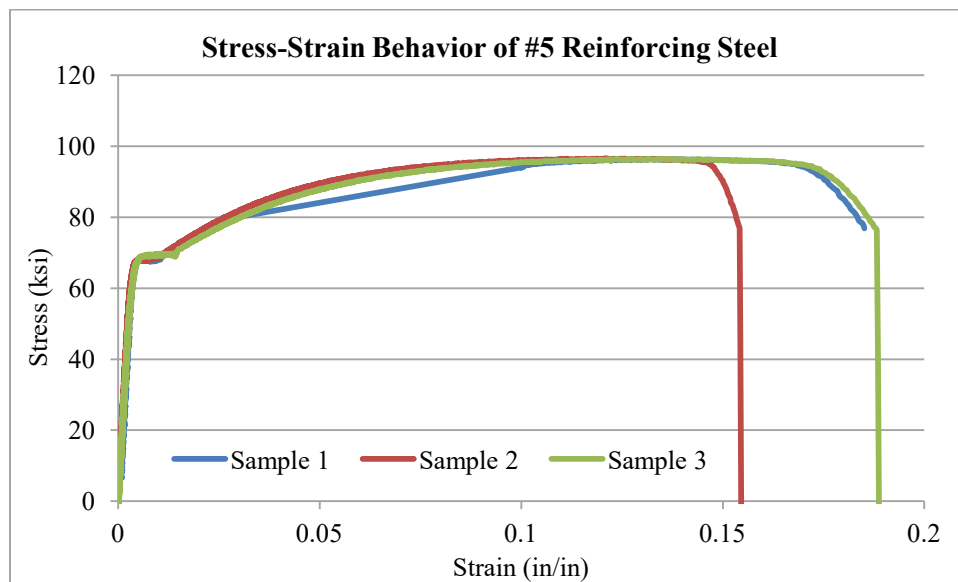


Figure 2-46 Stress-Strain Behavior of #5 Reinforcing Steel

2.3.2.4 Headed Anchors

The details and development length of headed anchors used in pullout test are the same as those discussed in Section 2.2.2.4.

2.3.3 Test Matrix

A testing matrix was developed to summarize the parameters of the 12 pullout tests, as listed in Table 2-15.

Table 2-15 Test Matrix for Pullout Test of Headed Stud

Specimen	Head Area	Grout
1	9A _b	1428 HP
2	9A _b	1428 HP
3	9A _b	EucoSpeed
4	9A _b	EucoSpeed
5	9A _b	Concrete
6	9A _b	Concrete
7	9A _b	Latex Concrete
8	9A _b	Latex Concrete
9	9A _b	UHPC
10	4A _b	UHPC
11	4A _b	Concrete
12	4A _b	1428 HP

2.3.4 Test Setup and Instrumentation

The test set up is shown in Figure 2-47. An MTS Load Frame with 647 Hydraulic Wedge Grip was used to test the specimens. A loading rate of 1.2 in/min was applied on

the anchor rod. A slip gage was used to measure any slippage between the steel plate under the specimen and the testing machine. Two strain gages were also placed on each headed anchor to measure the strain in the connectors. They were placed at the top of the grout which would match the interface of deck and girder in bridge application. Cracks were marked and evidence of failure was recorded for each test.



Figure 2-47 Pullout Test Setup

2.3.5 Construction process and Testing Procedure

The step-by-step procedure of the testing is shown in Figure 2-48 and are explained in the following steps:

- a) Cast specimen for pullout test.
- b) After 28 days of concrete curing, the specimens were prepared for casting grout in the pockets. The headed anchors were placed such that the anchors were embedded 6 in. into the deck as shown in Figure 2-48 (a). Respective grout was placed in the pockets according the test matrix of the pullout test. Figure 2-48 (b) shows one of the specimens after the grout was poured in the pocket.
- c) After the pocket grout had reached the required strength, the specimens were prepared for testing. A base plate was first connected to the bottom part of the testing machine [Figure 2-48 (c)]. The specimen was then lifted to place on top of the loading frame base plate as shown in Figure 2-48 (d). The grip of the testing machine would then hold the rebar of the headed anchor as shown in Figure 2-48 (e).
- d) The process was repeated for all the specimens.



(a)



(b)



(c)



(d)



(e)

Figure 2-48 Step-by-step Procedure of Pullout Test of Headed Anchors

2.3.6 Pullout Test Results

2.3.6.1 Ultimate Strength and Stiffness

Table 2-16 presents the peak axial loads and corresponding displacements. Figure 2-49 shows the measured load-displacement curves for all test specimens. The anchors showed fairly stiff, linear behavior at lower loads with stiffness decreasing as the load reached approximately 20 kips. The average ultimate pullout force for the headed anchors was 27.26 kips. The axial stiffness of the headed anchor for each test are listed in Table 2-17 and had an average value of 320.1 kip/in.

Table 2-16 Summary of Pullout Test Results

Test	Grout	Head Area	Displacement (in)	Force (kips)
1	1428 HP	9A _b	1.20	27.06
2	1428 HP	9A _b	1.24	27.27
3	1428 HP	4A _b	1.15	27.26
4	Latex Concrete	9A _b	1.17	27.31
5	Latex Concrete	9A _b	1.16	27.15
6	UHPC	9A _b	1.19	27.32
7	UHPC	4A _b	1.26	27.34
8	EucoSpeed	9A _b	1.39	27.24
9	EucoSpeed	9A _b	1.16	27.24
10	Concrete	9A _b	1.17	27.25
11	Concrete	9A _b	1.20	27.26
12	Concrete	4A _b	1.44	27.37

Table 2-17 Axial Stiffness of Headed Anchors

Test	Grout	Stiffness/Anchor (kip/in)
1	1428 HP	295.80
2	1428 HP	313.81
3	1428 HP	257.14
4	Latex Concrete	308.13
5	Latex Concrete	336.26
6	UHPC	307.19
7	UHPC	376.15
8	EucoSpeed	342.67
9	EucoSpeed	341.77
10	Concrete	351.62
11	Concrete	250.11
12	Concrete	360.51

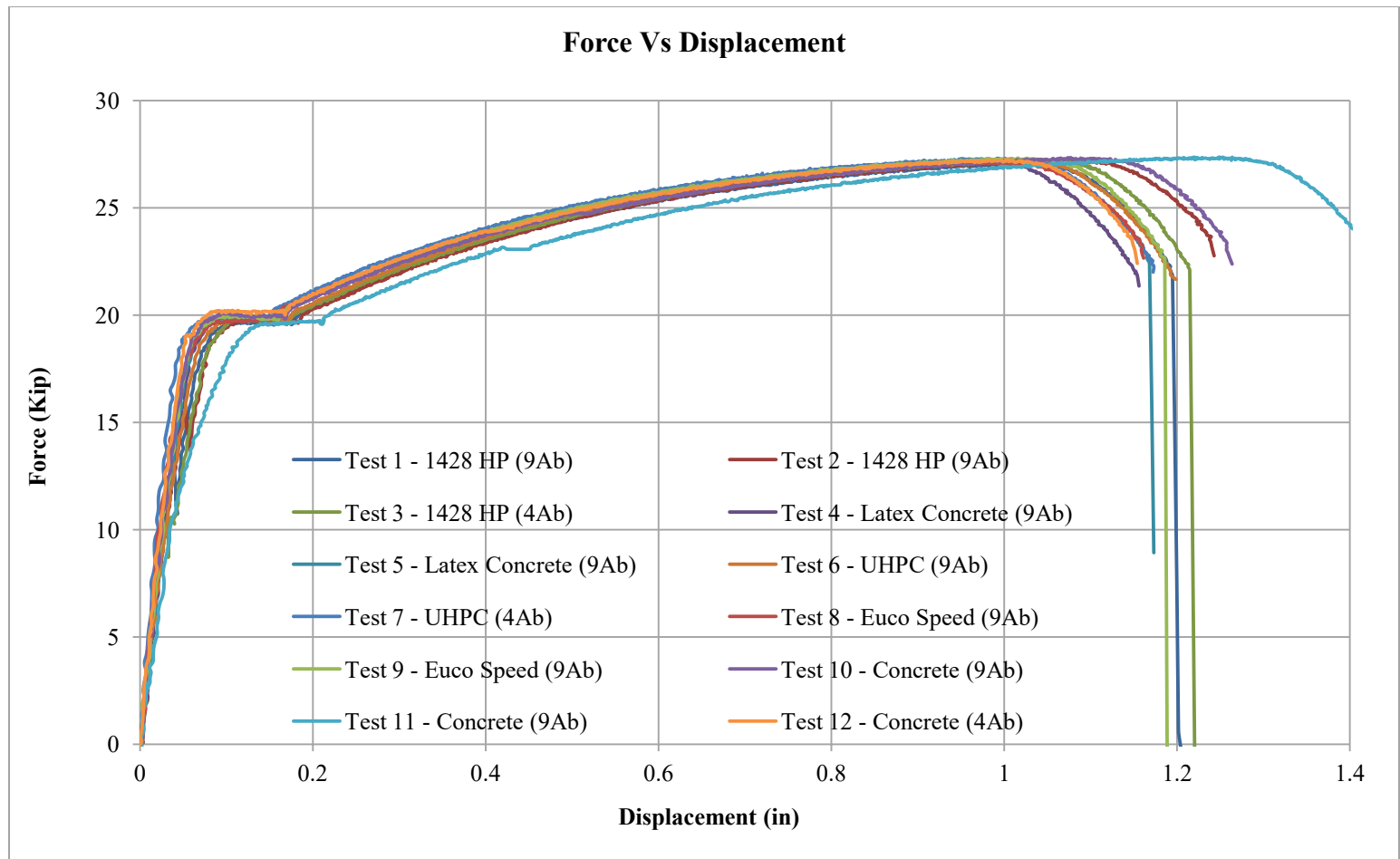


Figure 2-49 Force Displacement Curve (Pullout Test of Headed Anchor)

2.3.6.2 Crack Pattern and Failure Mechanism

The crack patterns during each load increment were carefully marked to study the failure mechanism. The failure mode in all test specimens was the breakage of anchor bar at the top of the grout. This matches the interface of deck and girder in bridge application indicating adequate embedment length of headed anchor. Figures 2-50 to 2-52 show the crack patterns in 12 grout pockets at the end of the test.

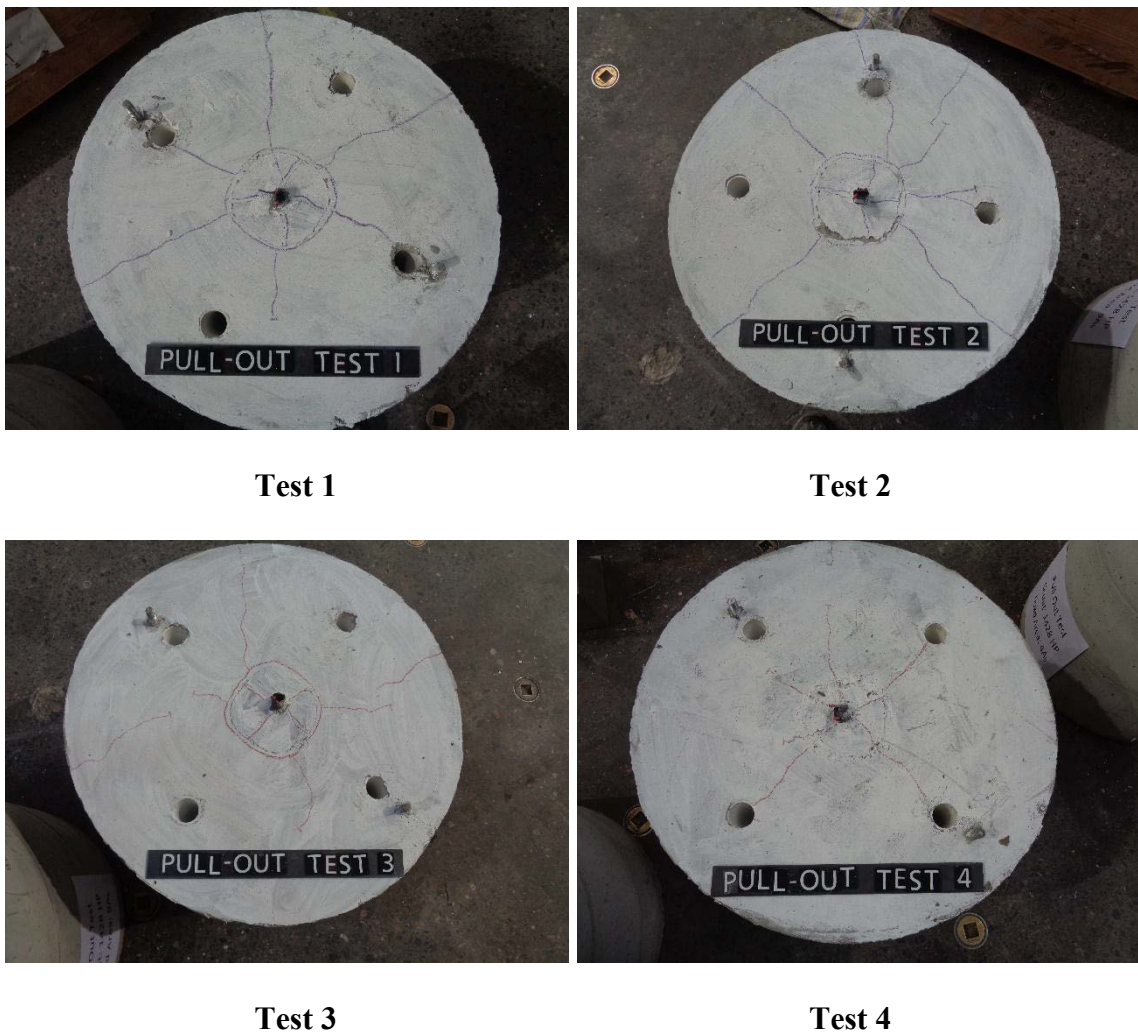


Figure 2-50 Crack Pattern of 12 Grout Pockets (Tests 1-4)



Test 5



Test 6



Test 7



Test 8



Test 9



Test 10

Figure 2-51 Crack Pattern of 12 Grout Pockets (Tests 5-10)



Test 11

Test 12

Figure 2-52 Crack Pattern of 12 Grout Pockets (Tests 11-12)

2.3.7 Discussion of Pullout Test Results

2.4.4.1 Effect of Grout Type

Five different types of grout were used to investigate their effect on the pullout capacity of the anchor. Figures 2-53 and 2-54 show the force displacement curves for five different types of grout with anchor head areas of $9A_b$ and $4A_b$, respectively. For anchors with head area of $9A_b$, the maximum capacity of 27.32 kips was observed in the anchor with UHPC grout and the minimum capacity of 27.06 kips was observed in the anchor with 1428 HP grout pocket. For anchor with head area of $4A_b$, the maximum capacity of 27.37 kips was observed in the anchor with conventional concrete grout and the minimum capacity of 27.26 kips was observed in the anchor with 1428 HP grout pocket. From the force displacement curves, it can be concluded that the type of grout had a negligible effect on the strength of headed anchors.

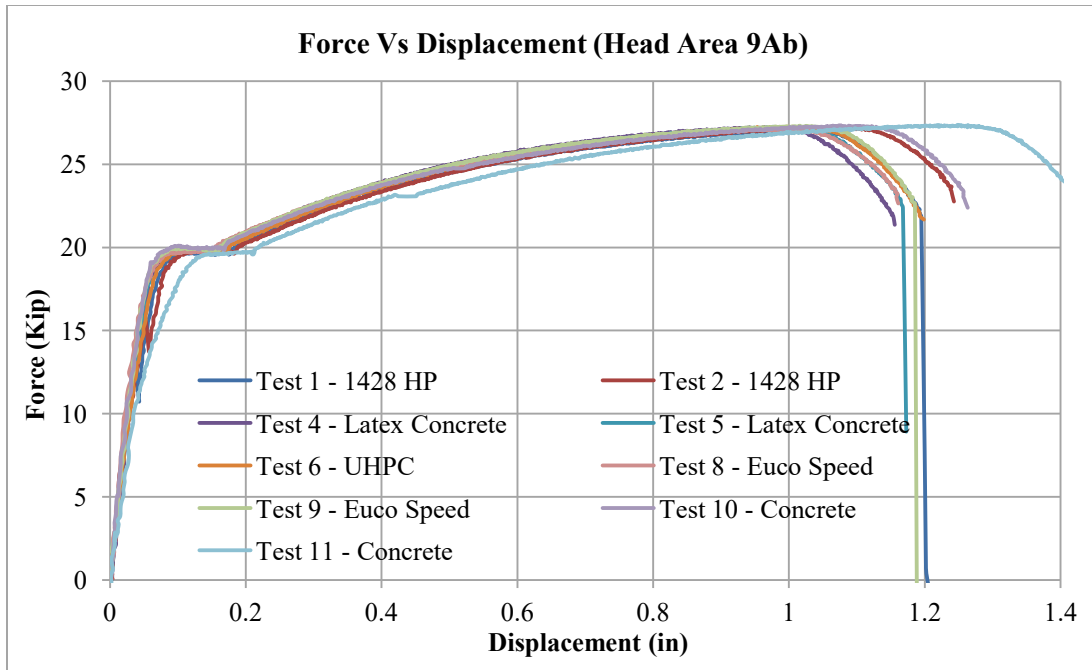


Figure 2-53 Force Displacement Curve to Study the Effect of Grout (Head Area 9Ab)

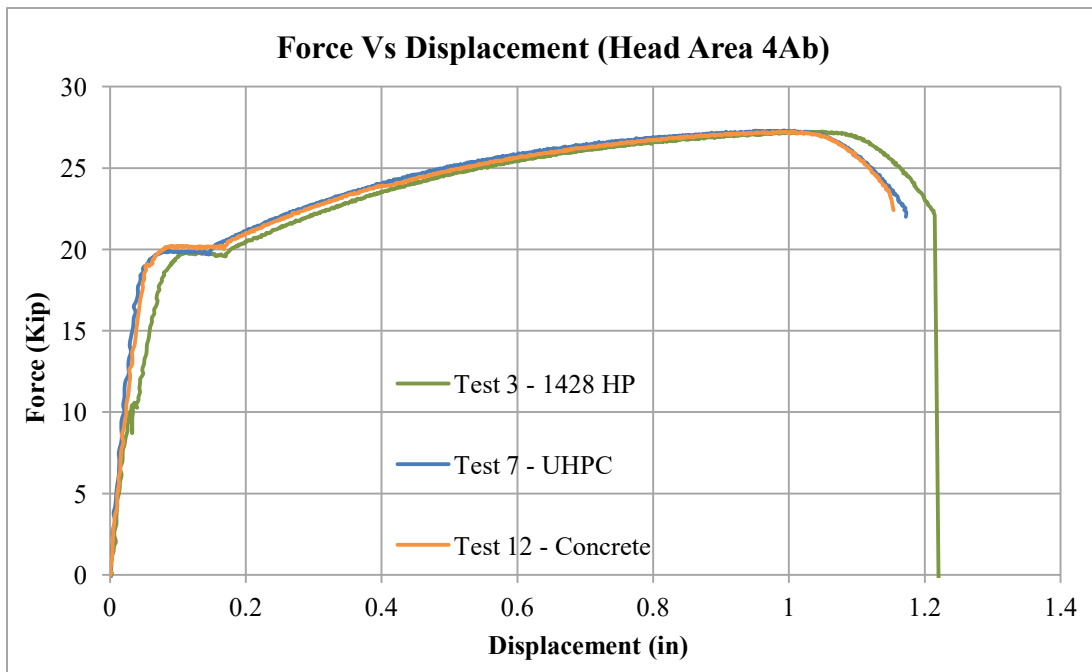


Figure 2-54 Force Displacement Curve to Study the Effect of Grout (Head Area 4Ab)

2.4.4.2 Effect of Anchor Head Area

Anchors with two different head areas of $9A_b$ and $4A_b$ were tested to investigate effect of head size on the strength of headed anchors. Figures 2-55, 2-56 and 2-57 show the force displacement curves for the different head area anchors with 1428 HP, concrete, and UHPC grouts, respectively. It can be observed that the head area had negligible effect on the anchor strength regardless of the grout types.

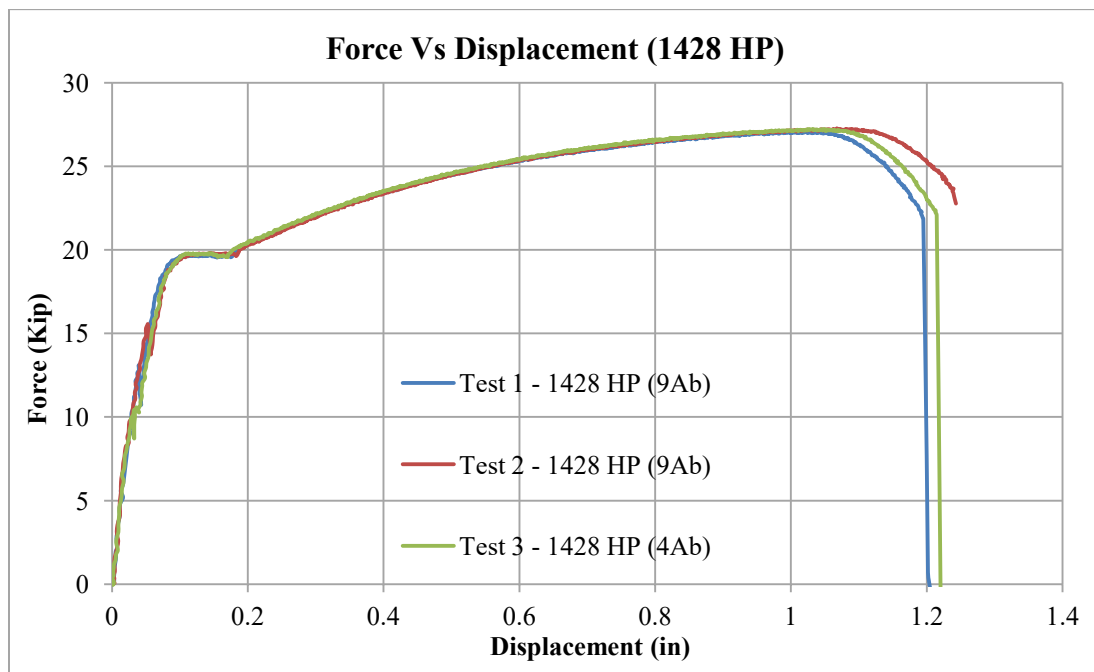


Figure 2-55 Force Displacement Curve to Study the Effect of Head Area (1428 HP)

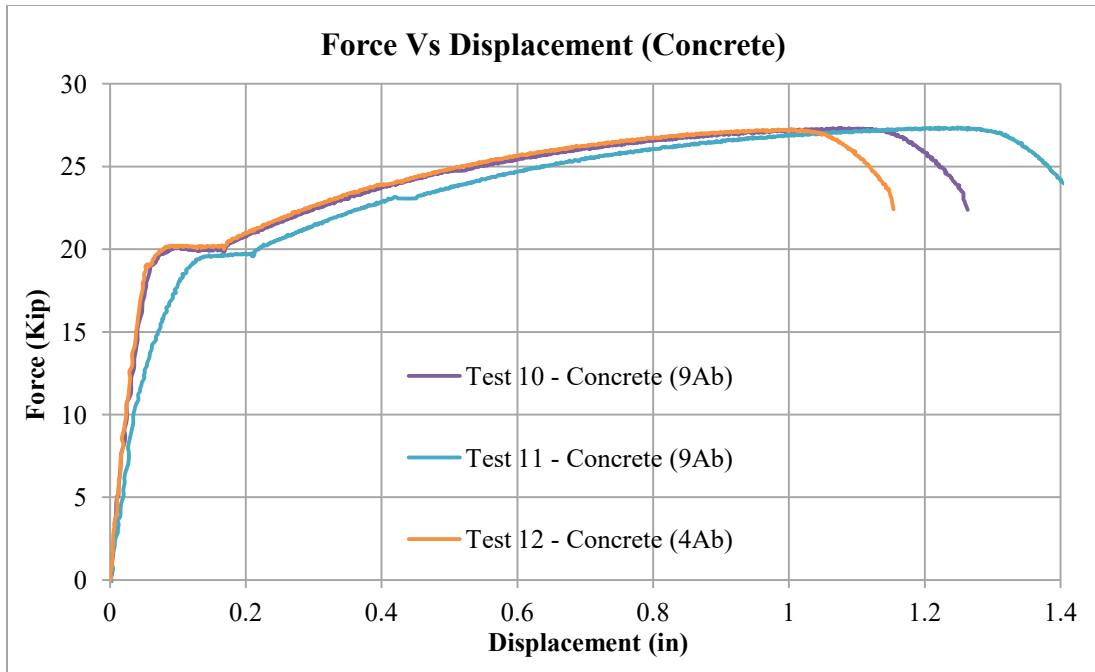


Figure 2-56 Force Displacement Curve to Study the Effect of Head Area (Concrete)

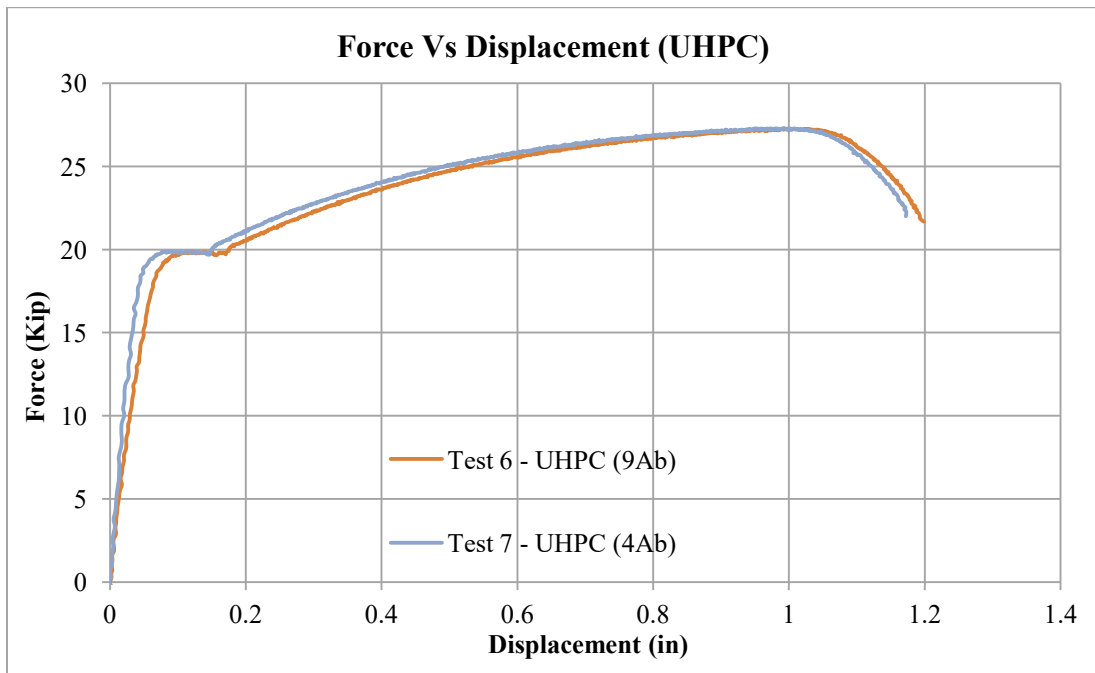


Figure 2-57 Force Displacement Curve to Study the Effect of Head Area (UHPC)

2.4 Implications of Test Results on AASHTO LRFD Bridge Design Specification

2.4.1 Lateral Strength

The AASHTO LRFD Bridge Design Specification Section 5.8.4 presents the interface shear transfer by shear friction. The commentary states “*Composite section design utilizing full-depth precast deck panels is not addressed by these provisions. Design specifications for such systems should be established by, or coordinated with, the Owner.*” The shear resistance at the interface plane, V_{ni} , can be determined by Equation 5.8.4.1-3 as

where c is the cohesion factor, A_{cv} is the concrete interface area, μ is coefficient of friction, A_{vf} is the area of interface shear reinforcement crossing the shear plane within the area A_{cv} , f_y is the yield stress of reinforcement not to be taken greater than 60 ksi, and P_c is the permanent net compressive force normal to the shear plane.

The nominal shear resistance, V_{ni} , used in the design shall not be greater than the lesser of:

where, K_1 is the fraction of concrete strength available to resist interface shear and K_2 is the limiting interface shear resistance.

Using AASHTO LRFD Equation 5.8.4.1-3 for No. 5 anchors and the specified steel yield stress of 60 ksi, the nominal shear resistance of the interface plane is:

where, $c = 0.075$ ksi and $\mu = 0.6$ (for concrete placed against a clean concrete surface, free of laitance, but not intentionally roughened).

The above equation is a modified shear-friction model accounting for a contribution from cohesion and/or aggregate interlock depending on the nature of interface. The strength of stud shear connector can also be calculated as a function of concrete modulus of elasticity and concrete strength using AASHTO Article 6.10.10.4.3. AASHTO LRFD Equation 6.10.10.4.3-1 presents the nominal shear resistance of headed shear stud connector embedded in a CIP concrete deck.

where,

A_{sc} = cross-sectional area of a stud shear connector

E_c = modulus of elasticity of the deck concrete determined as specified in Article 5.4.2.4

F_u = specified minimum tensile strength of a stud shear connector as specified in Article 6.4.4.

Using AASHTO Equation 6.10.10.4.3-1,

The horizontal shear calculated from equation 5.8.4.1-3 underestimated the ultimate shear capacity by 56.1%, whereas, the equation 6.10.10.4.3-1 overestimated the ultimate shear capacity by 9.8%. Comparing the horizontal shear predicted by the AASHTO equations using all the measured properties from the experimental tests with the actual measured horizontal shear values, it was concluded that the equation 6.10.10.4.3-1 in LRFD Specifications best predicted the test loads in this research.

2.4.2 Lateral Stiffness

The bending stiffness, k_b , of anchor that bends in double and single curvature is given by:

$$k_b = \frac{3EI_a}{L_{eff}^3}$$

where, E is the modulus of elasticity of anchor (29,000 ksi), I_a is the moment of inertia of anchor (0.00749 in^4), and L_{eff} is the effective length of the anchor that is unrestrained for bending.

The pictures of fractured headed anchors shown in Figures 2-31 (a), (b) and (c) show that the bending in the anchor during shear test does not occur at the coupler region of the anchor. In addition, single curvature bending of rebar region of the anchor is observed from the shape of the fractured headed anchor. Therefore, length of rebar region embedded in the deck, l_b , shown in Figure 2-20 was used as effective length in the equation of the single curvature. Using $L_{eff} = l_b = 2 \text{ in}$, the calculated bending stiffness is 81.5 kip/in. The equation overestimated the stiffness of the anchor by 31.5% to 103.8%

obtained from nine test results. Thus, the results from experiment was used to calculate a factor (α) to determine an equivalent bending stiffness of the anchor in pocket regions.

—

The value of the factor (α) calculated for each test is presented in Table 2-18. Thus, the equivalent bending stiffness for the anchor can be given by:

—

Table 2-18 Calculation of Factor (α) for Bending Stiffness

Test	Grout	No. of Anchors	Total Stiffness (kip/in)	Stiffness/Anchor (kip/in)	α
1	1428 HP	1	40	40	1.6
2	1428 HP	2	124	62	2.5
3	1428 HP	4	225	56	2.2
4	EucoSpeed	4	178	44	1.7
5	Concrete	4	182	45	1.8
6	Latex Concrete	4	253	63	2.6
7	Polyester Concrete	4	238	60	2.4
8	UHPC	4	188	47	1.9
9	UHPC	2	83	41	1.6
			Average	51	2.0

2.4.3 Pullout Strength

The failure mode in all the pullout tests was the fracture of the anchor above the grout. Therefore, the pullout strength can be defined as the tensile resistance of a single connector that is determined by:

The pullout strength calculated from the above equation overestimated the pullout strength capacity by 2.3%.

2.4.4 Axial Stiffness

The total axial stiffness of the anchors used in the pullout tests is the combination of stiffness of embedded and free part of anchor. The embedded and free part of anchor can be modeled as springs in series to represent the total stiffness of the anchor. The axial stiffness of the free part (K_1) and embedded part (K_2) of anchor is defined by:

$$\frac{1}{K} = \frac{L_1}{EA} + \frac{L_2}{EA}$$

where, L_1 is the length of free part of anchor (14 in) and L_2 is the length of embedded part of anchor (6 in). The calculated stiffness of the unembedded part of anchor was 642 kip/in.

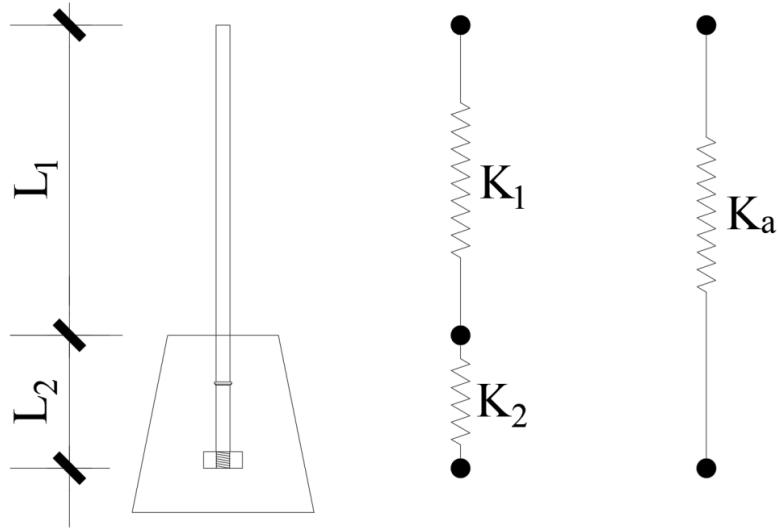


Figure 2-58 Spring Representation of Anchors

The total stiffness of the anchor, K_a , can be calculated as:

$$\frac{1}{K_a} = \frac{1}{K_1} + \frac{1}{K_2}$$

Using the total stiffness, K_a , and stiffness of free part of anchor, K_1 , the stiffness of the embedded part of anchor, K_2 , was calculated. The results are listed in Table 2-19. The results from experiment was used to calculate a factor (α) to determine an equivalent axial stiffness of the anchor in pocket regions. The value of the factor (α) calculated for each test is presented in Table 2-19. Thus, the equivalent axial stiffness for the anchor can be given by:

$$K_{a,eq} = \alpha K_a$$

Table 2-19 Calculation of Factor (α) for Axial Stiffness

Test	Grout	Head Area	K_a (kip/in)	K₂ (kip/in)	α in $\alpha EA/L_2$
1	1428 HP	9A _b	295.80	548.4	0.37
2	1428 HP	9A _b	313.81	613.7	0.41
3	Latex Concrete	9A _b	308.13	592.4	0.39
4	Latex Concrete	9A _b	336.26	705.9	0.47
5	UHPC	9A _b	307.19	588.9	0.39
6	Euco Speed	9A _b	342.67	734.8	0.49
7	Euco Speed	9A _b	341.77	730.6	0.49
8	Concrete	9A _b	351.62	777.2	0.52
9	Concrete	9A _b	250.11	409.7	0.27
10	1428 HP	4A _b	257.14	428.9	0.28
11	UHPC	4A _b	376.15	908.1	0.61
12	Concrete	4A _b	360.51	822.0	0.55
			Average	655.0	0.44

2.5 Concluding Remarks

The experimental investigation involved testing the shear and pullout specimens with headed anchors in grout materials. The key observations and conclusions on the shear and pullout capacity of the headed anchors are:

- The failure mode of all shear test specimens was the fracture of the headed anchor at the interface of deck and girder.
- Failure in all the pullout test specimens was due to the fracture of the rebar at the face of the grout, which represented the deck-girder interface.
- The shear and pullout failure of the headed anchor with #5 rebar occurred at 25.42 and 27.26 kips, respectively.
- The type of grout had an insignificant effect on the shear capacity of headed anchors.
- The shear capacity of the headed anchor increased almost linearly with the increase in number of anchors.
- The head area of the anchor had an insignificant effect on the ultimate shear capacity of headed anchors.
- The type of grout and head area of the anchor had an insignificant effect on the pullout strength of headed anchors.
- Out of six different types of grout, Latex Concrete took the least amount of time to be removed from the pocket. Polyester Concrete and UHPC were the most difficult grouts to be removed. Based on the time required and ease in removing the grout, 1428 HP, EucoSpeed, conventional concrete and latex concrete were recommended to be used to fill the deck pockets.

- Equation 6.10.10.4.3-1 of the LRFD specification may be used to estimate the ultimate shear resistance of headed anchor in grouted pockets.
- Based on the test data, the shear stiffness of headed anchor was:

$$\text{---}$$

where, E is the modulus of elasticity of anchor, I_a is the moment of inertia of anchor, and L_{eff} is the effective length that is unrestrained for bending in anchor.

- Based on the test data, the axial stiffness of the headed anchor was:

$$\text{---}$$

where, A is the area of anchor, E is the modulus of elasticity of anchor, and L_2 is the length of the anchor embedded into the deck.

3. Analytical Investigation

3.1 Introduction

This chapter presents the seismic analysis of a highway bridge and the response of headed anchors. The objective of the analytical investigation was to determine the headed anchor seismic forces and the effect of the longitudinal anchor spacing on the overall bridge seismic response. This investigation was aimed at shedding light on the level of composite action of the precast girders when using realistic values of headed anchor stiffness.

A two-span precast girder bridge was analyzed to accomplish these objectives. Three different computational models for headed anchors were used to investigate the seismic response of decks with rigid shear links between the deck and girders and flexible links with shear pockets spaced at 4 ft and 6 ft spacing. A nonlinear response history analyses was performed with eight earthquake ground motions, including both far-field and near-fault ground motion records.

3.2 Bridge Description

The Reigo Road Bridge, located on State Route 99 at Reigo Road in Sutter County near the North border of Sacramento County, was used for this investigation. The bridge was designed according to the 2006 Caltrans Bridge Design Specifications. The AASHTO HL-93 design and California P15 truck were used as the design live load. The bridge is a two-span continuous precast girder bridge with an overall length of 295 ft

with two unequal span lengths of 154 ft and 141 ft, respectively. The bridge has a skew angle of 8°. Figure 3-1 shows an elevation view of the bridge.

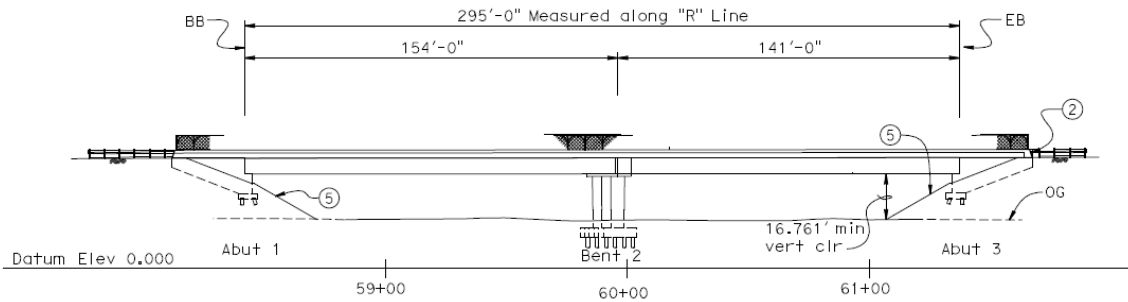


Figure 3-1 Elevation View of Reigo Road Bridge

The total width of the bridge is 154 ft 4 in. The barrier is Type 26 concrete barrier with chain link railing Type 6. The deck thickness is 8.25 in. CIP reinforced concrete slab. Figure 3-2 shows a cross sectional view of the bridge. The bridge deck and girders are placed at a 2% gradient. The reinforced concrete deck is supported by 14 wide-flange, 5.5 feet deep precast concrete girders spaced at 11 ft 3 in. The top and bottom flanges are 4.1 ft and 3.8 ft wide, respectively, and a web thickness of 8 in. Figures 3-3 and 3-4 show the girders layout and cross section of the girder. The girders were designed to be composite with the cast-in-place concrete deck by extending all girder shear reinforcement into the deck. Welded Wire Reinforcement (WWR) was used as vertical stirrups as well as in top and bottom flange of girder. The vertical girder stirrups have three different spacings along the girder length. They were placed at a spacing of 2 in. at the supports and 12 in. at the center of each span. In between these

two regions, the stirrups are placed at a spacing of 4 in. Figure 3-5 shows the deck and girder connection detail.

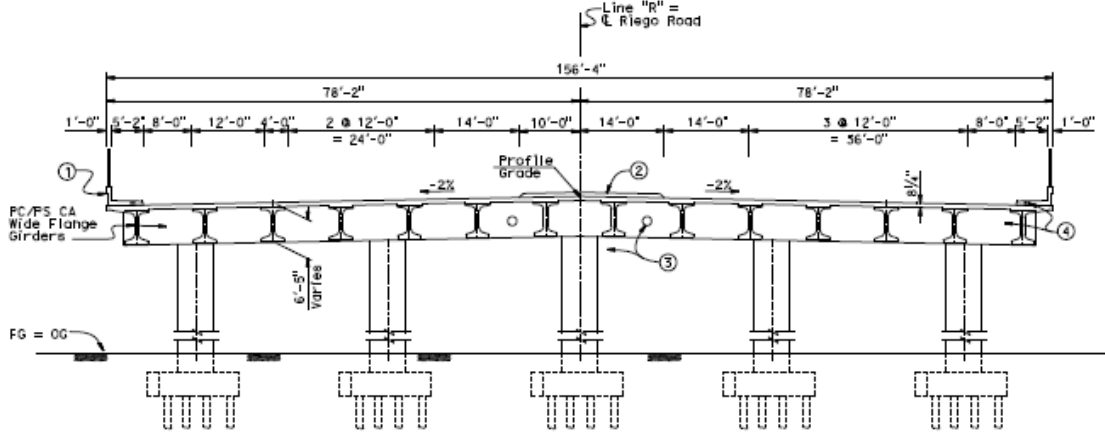


Figure 3-2 Section of Reigo Road Bridge at Bent

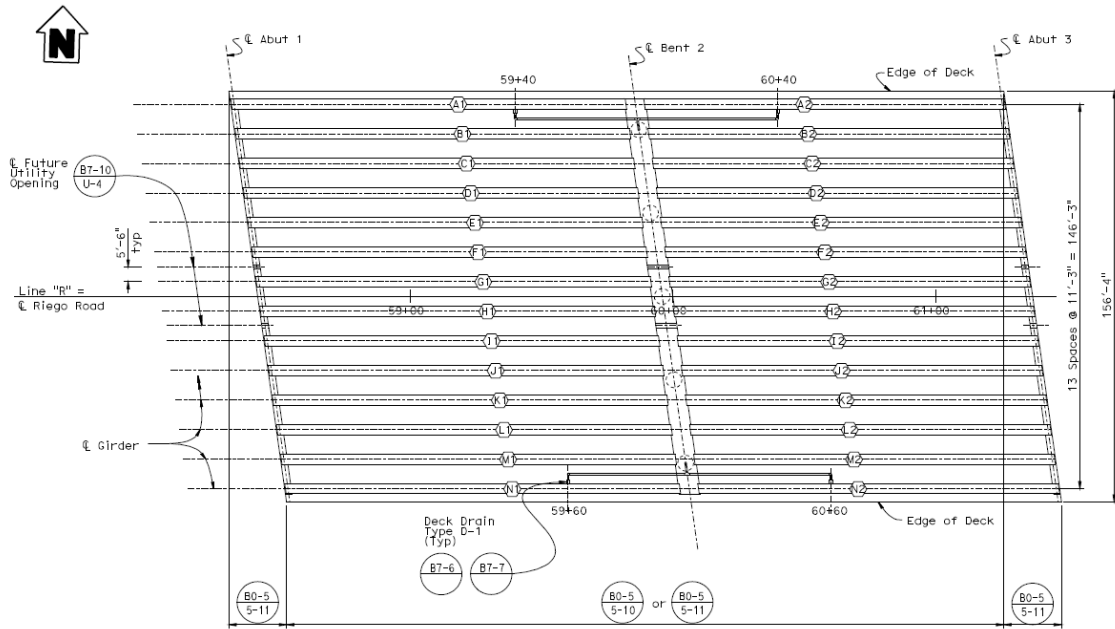


Figure 3-3 Girder Layout of Reigo Road Bridge

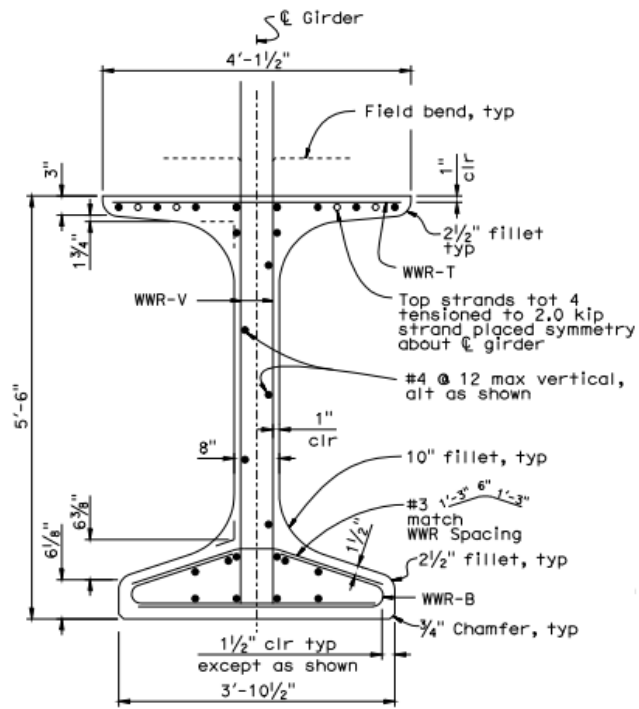


Figure 3-4 Cross section of Precast Girder of Reigo Road Bridge

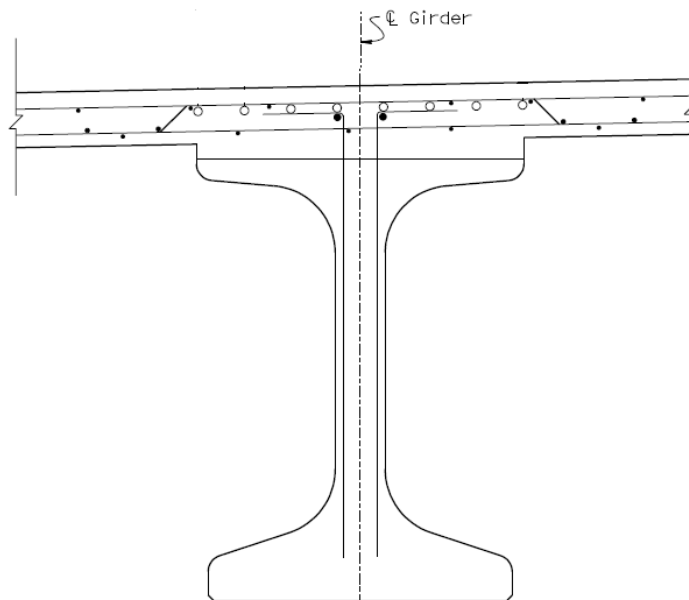


Figure 3-5 Deck and Girder Connection Detail

Each girder was post-tensioned using two stage post-tensioning. Straight pretensioned strands were used along with draped post-tensioning tendons. The girders for span 1 were pretensioned with 36-0.6 in. diameter strand and girders for span 2 were pretensioned with 30 strands. One-third of the strands were debonded for 15 ft at each end, and four 3/8 in. diameter top strands were added to reduce tensile stress in the top flange at the girder ends. The strands used for the post tensioning were 270 ksi low relaxation strands.

The 3 ft R/C end diaphragms of the bridge connect the girders at each abutments. The bridge is supported at the mid-span by an integral bent cap. The cap is supported on five 6 ft diameter columns spaced at 32 ft center to center. They are approximately 26 ft in height, rigidly connected to the cap and pinned at the bottom. The column's longitudinal reinforcements are 28#10 bars (0.9%). The transverse reinforcements of the column are #6 welded hoops spaced at 4.0 in. on center along the height of the column (0.65%). Figure 3-6 shows the cross section of the column. The columns are supported by a foundation with dimensions of 15 ft x 15 ft x 4 ft. Each foundation is supported by 25-Class 140 Concrete Pile. (Hida, 2015)

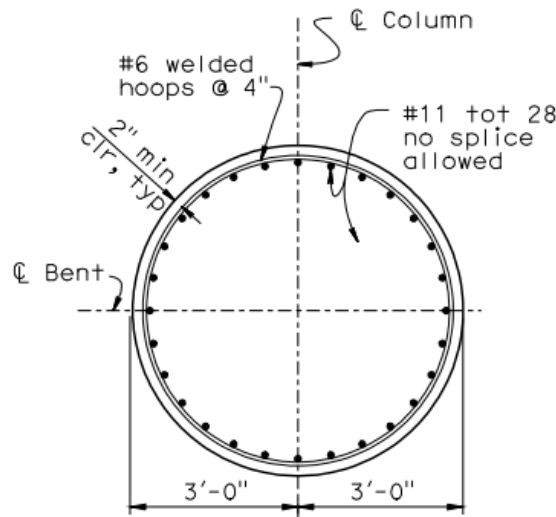


Figure 3-6 Column Section Detail

Several assumptions were made to simplify the bridge for the analytical investigation. Two equal spans of 160 ft were used in this study. The 2% deck gradient and the skew angle of the bridge were ignored. The concrete haunch that separates the girders from the bottom surface of the deck was not included in the computational model. Precast R/C deck panels were used in place of the cast-in-place deck. Pockets along the length of the precast deck were used. Headed anchors that are designed for gravity and seismic forces were placed in the pockets and were spaced along the longitudinal direction of the girders. The longitudinal spacing between the pockets which will be discussed later. Figures 3-7, 3-8 and 3-9 show the elevation, section and girders layout of the bridge used for analytical investigation.

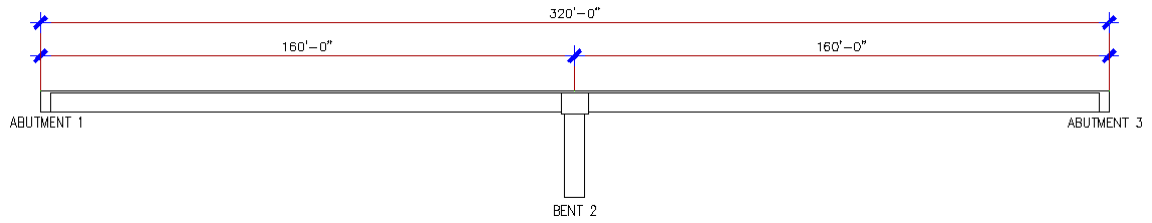


Figure 3-7 Elevation view of Bridge (Model)

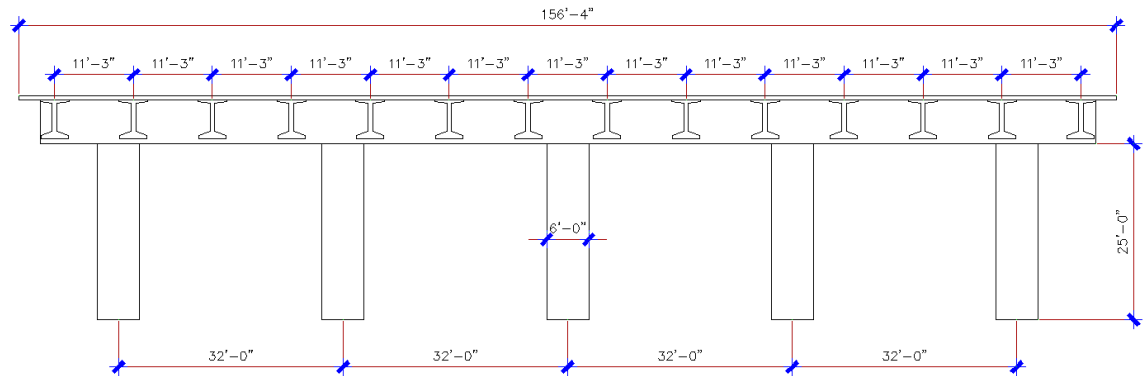


Figure 3-8 Section of Bridge at Bent (Model)

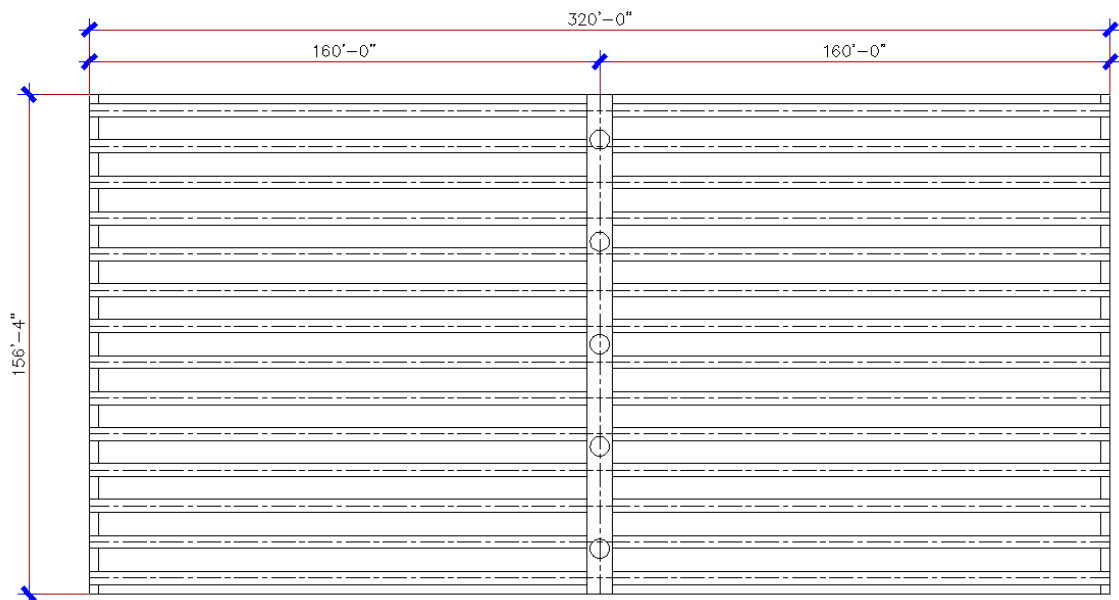


Figure 3-9 Girder Layout of the Bridge (Model)

3.3 Design of Headed Anchors in Precast Decks

Headed anchors are provided to connect the precast concrete deck panels and the supporting P/S girders. These anchors extend vertically from the girders and protrude into the pockets provided in deck panels. The anchors connecting deck panels and girders are required to create composite action between the deck and the girders, which enhances structural efficiency of the bridge superstructure. The headed anchors prevent the slippage between the deck and the longitudinal girders, thus they are subjected to longitudinal interface shear. Bridge designers compute this horizontal interface shear, between the slab and girders, under gravity load based on full composite section. Section 5 of the AASHTO LRFD Specifications provide a simple way relating the interface shear to the vertical shear that is derived from static equilibrium. For CIP deck, the shear reinforcement in the longitudinal girders are extended into the R/C deck. When the deck is hardened, this reinforcement resists the interface shear creating a composite action between the deck and the longitudinal girders. However, in precast decks the shear reinforcement in the longitudinal girders are not extended in the deck, thus headed anchors are used. These anchors are placed along the longitudinal girders. Pockets in the precast deck are blocked-out so the headed anchors are extended through them. High strength grouts are then poured in these pockets. The headed anchors in precast decks provide the connection between the deck and the longitudinal girders, thus they are subjected to interface shear due to live load and seismic forces.

3.3.1 Current Design Procedure

Headed anchors in precast decks are designed to resist the interface shear due to the live loads and the seismic forces generated in the deck. The interface shear occurs when vertical shear is transferred across a plane that is made up of two components of different materials. The seismic design of the R/C deck is performed according to Section 6.16.4.2 of the AASHTO seismic provisions. Article 6.16.4.2 specifies that the deck can be considered to act as a rigid horizontal diaphragm if the span-to-width ratio of the deck is not more than 3.0 and net mid-span lateral substructure displacement is less than twice the average of the adjacent lateral support displacements. Otherwise, the deck is considered to act as a flexible diaphragm and must be designed to resist shear and bending stresses. Rigid diaphragm, on the other hand, requires no special seismic design, but must have sufficient shear resistance to transfer the seismic shear to the support.

3.3.2 Design Procedure for Headed Anchors in Precast Decks

The current design provisions for stud connectors in cast-in-place construction was adopted in this research for the design of headed anchors in full-depth precast deck panels. A step-by-step procedure to achieve a composite precast deck and precast girders is listed below:

1. Perform live load analysis to obtain the maximum shear force along the bridge. The forces obtained due to future overlays, barrier load and live load are combined according to AASHTO LRFD Table 3.4.1-1, Strength I and II.

$$\text{Strength I: } U = 1.25 DC_2 + 1.5 DW + 1.75 LL$$

$$\text{Strength II: } U = 1.25 DC_2 + 1.5 DW + 1.35 LL$$

where, DC_2 is the weight of the railing that will be placed after the deck pockets are filled. Based on the vertical shear, interface shear is calculated along the length of the girder.

2. The number of headed anchors should be designed for the maximum interface shear forces obtained from step 1.
3. The live load analysis is performed again using the actual properties of the designed anchors. If the shear demands on the anchor are higher than the capacity of the anchor, the number of anchors should be increased.
4. Perform a modal response spectrum analysis using the design response spectrum in both the longitudinal and transverse directions for Extreme Event I.

$$\text{Extreme Event I: } 1.25 DC_2 + 1.5 DW + 1.00 EQ$$

The resulting orthogonal responses are then combined using the 100/30 percent rule for elastic seismic force effect specified in the AASHTO LRFD Bridge Design Specification (AASHTO 2012).

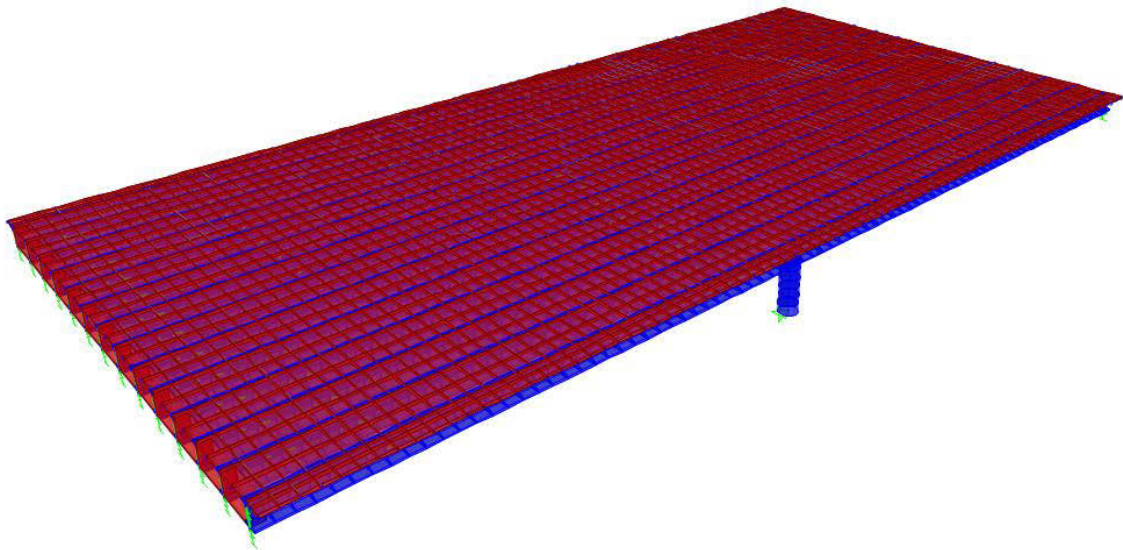
$$\text{Case I: } 100\% \text{ Longitudinal} + 30\% \text{ Transverse}$$

$$\text{Case II: } 30\% \text{ Longitudinal} + 100\% \text{ Transverse}$$

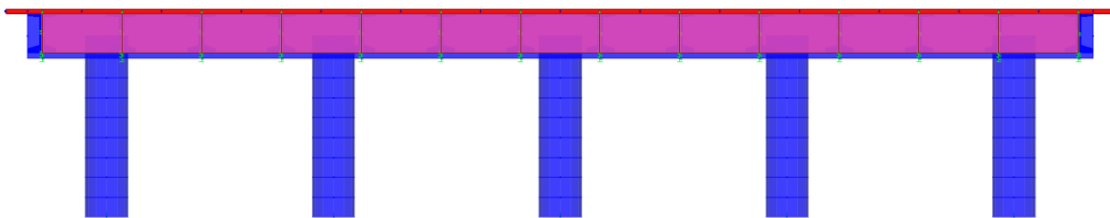
The forces in the headed anchor should be checked for both cases and it should be ensured that the maximum force on the headed anchor does not exceed the total anchor's design capacity. If the capacity of the anchors is less than the demand forces, the anchors should be redesigned and reanalyzed.

3.3.3 Bridge Computational Model

Elastic and inelastic analysis of a 3-D bridge model were carried to verify the design procedure. A computational model of the entire bridge was created and analyzed using CSiBridge software (CSiBridge, 2010-2011). The bridge model was built as the combination of shell and frame elements. Shell elements were used to model the precast concrete deck. The girders, cap beams at bents, diaphragms at the abutments and column were modeled using Frame elements. The deck mesh was generated automatically by CSiBridge. Figure 3-10 shows the 3-D and sectional view of the bridge model.



(a) 3-D View



(b) Section View

Figure 3-10 Finite Element Model of Bridge (CsiBridge, 2010-2011)

Rigid links were used to connect the column and the beam cap. Abutment bearing links (link elements) were used to model the abutments by fixing the vertical translation of the abutment bearing. All other abutment bearing components were modeled as free since the bridge is assumed to be supported on seat-type abutments. Bent bearing links (link elements) were used to model the connection between the girders and the beam cap by fixing all the translations and rotational components of the link element.

3.3.4 Modeling of Headed Anchors

The concrete deck and girder connection is a critical detail to be modeled properly for the effective utilization of the composite connection. The headed anchors were modeled using two different assumptions in three computational models. In the first model, the headed anchors were assumed rigid connections between the deck and the girders. The rigid connection was modeled using the CSiBridge auto-generated rigid constraints at deck and girder nodes. In the second and third models, the headed anchors were modeled using flexible link elements and assigning the measured shear and axial stiffness values for the elements based on the experimental results presented in Chapter 2. The difference between Model 2 and 3 was the spacing of the pockets.

3.3.5 Live Load Analysis

Structural analysis of the bridge was performed in CSiBridge to obtain the moments and shear effects due to live loads. The design live loads, LL, were the AASHTO HL-93 and Caltrans P15 vehicular live loads.

Tables 3-1 and 3-2 list the analysis results for the exterior girder and three interior girders, which includes the maximum shear force due to live load.

Table 3-1 Maximum Shear Force, V (Kips) due to Dead Load

	Wearing Surface	Concrete Barrier
Right Exterior Girder	37.3	0.035
Interior Girder 12	39.4	0
Interior Girder 11	39.4	0
Interior Girder 10	39.4	0

Table 3-2 Maximum Shear Force, V (Kips) due to P15 Truck Loading (1-6 Lane Loaded)

	1 Lane	2 Lane	3 Lane	4 Lane	5 Lane	6 Lane
Right Exterior Girder	207.71	196.58	168.78	130.26	131.45	132.67
Interior Girder 12	210.71	311.48	289.20	223.02	224.73	226.41
Interior Girder 11	60.54	228.27	298.83	244.35	246.02	247.62
Interior Girder 10	10.95	64.65	207.47	232.15	246.02	247.65

Based on the analysis results and load combinations, the maximum shear force of 480 kips was obtained for Strength II Combination in Interior Girder 12, which resulted in an interface shear of 6.88 kip/in. This value was used to design the number of headed anchors. In order to investigate the effect of pocket spacing, anchors were designed for pocket spacing of 4 ft and 6 ft. The summary of headed anchor design is presented in Table 3-3. Based on the interface shear demand, 12-#5 and 18-#5 connectors were used

for 4 ft and 6 ft pocket spacing, respectively. The designed connectors resulted in the total capacity of 512.3 kips and 725.7 kips, respectively.

Table 3-3 Design of Shear Connectors

Pocket Spacing	Required Shear Connectors
4 ft	12-#5
6 ft	18-#5

Based on the results from Chapter 2 and the design of the connectors, the axial stiffness of the link element for Models 2 and 3 was equal to 3,796 kip/in and 5,695 kip/in, respectively. The shear stiffness of the link element for Models 2 and 3 was equal to 630 kip/in and 945 kip/in, respectively. Figure 3-11 shows the shear properties of Models 2 and 3 used in the model, respectively. Figure 3-12 illustrates the link connecting the deck to girder, girder to diaphragm, abutment bearings and the substructure.

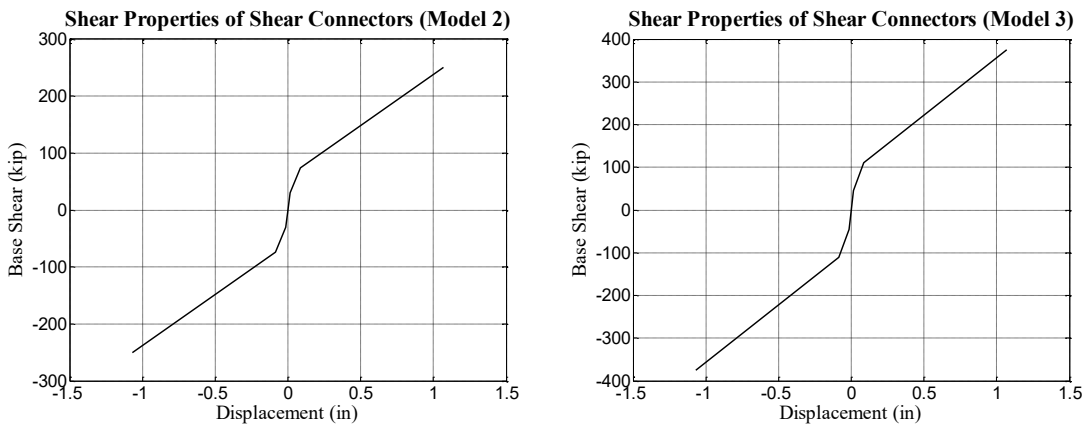


Figure 3-11 Shear Properties of Shear Connectors

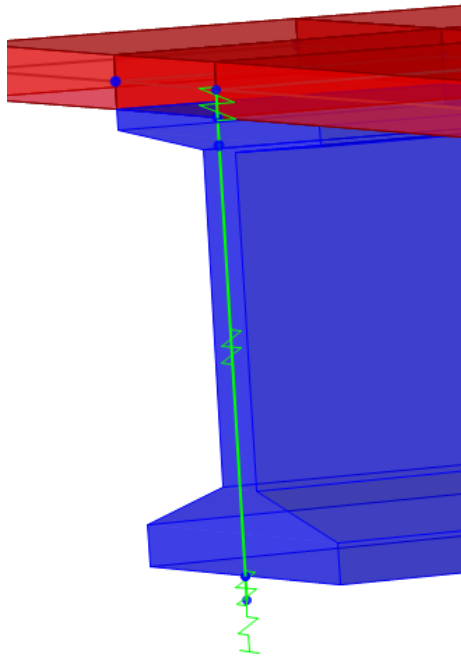


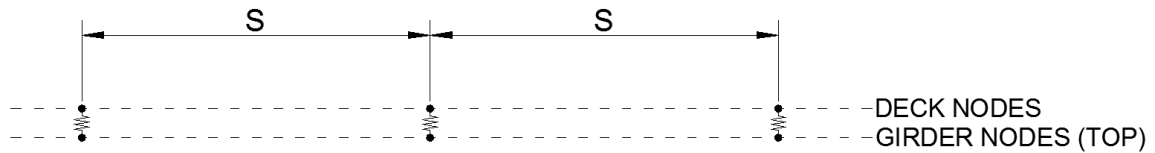
Figure 3-12 FE Modeling of the Links

3.3.6 Analysis Results

SAP2000 was used to perform the structural analysis of the three models. These models were developed considering the variations in pocket spacing and properties of the element connecting the deck and girders. The different types of models used in the analysis are presented in Table 3-4. The deck and girders in Model 1 were connected with a rigid link element representing a full composite section. In Model 2 and Model 3, the deck and girders elements were connected using a link element with axial and shear properties obtained from Chapter 2 and using the number of headed anchors from Table 3-3. The link elements were defined at a spacing of 4 ft and 6 ft in Model 2 and Model 3, respectively. Figure 3-13 shows the headed connectors spacing along longitudinal direction.

Table 3-4 Types of Bridge Models for Modal Analysis

Model	Pocket Spacing (ft)	Description of Connectors
1	4	Linear Rigid Connectors
2	4	Linear Connectors with stiffness equivalent to 12-#5
3	6	Linear Connectors with stiffness equivalent to 18-#5



Notes:
 Model 2: S = 4 ft
 Model 3: S = 6 ft

Figure 3-13 Spacing of Headed Connectors along Longitudinal Direction

Gravity load analysis was performed on all three models. The results from the gravity load analysis were checked against hand-calculation to verify the results. Figure 3-14 shows the displacement profile along the longitudinal direction of the bridge due to dead load for the models. A maximum displacement of 1.8 in. was observed in Model 1 whereas a maximum deflection of 2.6 in. was observed in both Models 2 and 3. The use of flexible links increased the vertical deflection of the bridge by 44%. Using the deflections of the bridge, the moment of inertia of Models 1, 2 and 3 were calculated. It was concluded that the moment of inertia of Models 2 and 3 were 32% lower than the moment of inertia of Model 1. Therefore, Models 2 and 3 provided 68% of a full composite section. The decrease in vertical stiffness in Models 2 and 3 can also be verified using the vertical period of the bridge. The moment of inertia of Models 2 and 3,

calculated using vertical period of the bridge, were 28% and 25% lower than the moment of inertial of Model 1. Therefore, Models 2 and 3 provided 72% and 75% of a full composite section. This indicated that the connectors spaced at 4 ft and 6 ft were not able to provide a full composite action.

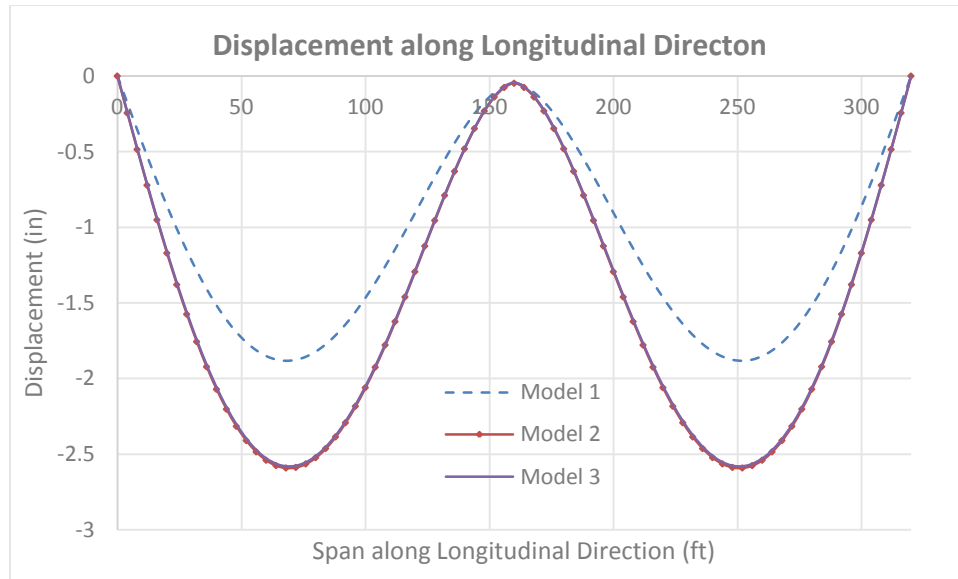


Figure 3-14 Displacement along Longitudinal Direction (SAP2000)

A modal analysis of the three models was also conducted to determine the natural periods of pertinent modes of vibration. Eleven modes were considered in the analysis to capture at least 90% mass participation in each orthogonal direction of displacement. The period and modal participating mass ratios for Models 1, 2 and 3 are summarized in Tables 3-5, 3-6 and 3-7, respectively. The second and third modes of each model represents the period of the bridge in the longitudinal and transverse directions, respectively. The longitudinal periods of the bridge were 1.31 sec, 1.38 sec and 1.33 sec and the modal participation mass ratios for these mode were 94.9%, 93.9% and 92.6% for

models 1, 2 and 3, respectively. The transverse periods of the bridge were 1.10 sec, 1.13 sec and 1.05 sec for models 1, 2 and 3, respectively. The modal participation mass ratios for these mode were 99.9% for all three models. The vertical periods of the bridges were 0.39 sec, 0.46 sec and 0.45 sec for models, 1, 2 and 3, respectively. The increase in the vertical periods reduce the stiffness by 28.4% and 23.8% in models 2 and 3, respectively. Using the vertical periods of the bridge, the moment of inertia of Models 1, 2 and 3 were calculated. It was concluded that the moment of inertia of Models 2 and 3 were 28.2% and 25% lower than the moment of inertia of Model 1. Therefore, Models 2 and 3 provided 71.8% and 75% of a full composite action, respectively.

Table 3-5 Period and Modal Participation Mass Ratios (Model 1)

Mode	Period (sec)	UX	UY	UZ	Sum UX	Sum UY	Sum UZ
1	1.31	0.9487	0.0000	0.0000	0.9487	0.0000	0.0000
2	1.10	0.0000	0.9997	0.0000	0.9487	0.9997	0.0000
3	0.53	0.0503	0.0000	0.0000	0.9990	0.9997	0.0000
4	0.50	0.0000	0.0000	0.0000	0.9990	0.9997	0.0000
5	0.40	0.0000	0.0000	0.0000	0.9990	0.9997	0.0000
6	0.39	0.0000	0.0000	0.6591	0.9990	0.9997	0.6591
7	0.38	0.0000	0.0000	0.0000	0.9990	0.9997	0.6591
8	0.34	0.0000	0.0000	0.0008	0.9990	0.9997	0.6600
9	0.33	0.0000	0.0000	0.0000	0.9990	0.9997	0.6600
10	0.30	0.0000	0.0000	0.0000	0.9990	0.9997	0.6600
11	0.28	0.0000	0.0000	0.0000	0.9990	0.9997	0.6600

Table 3-6 Period and Modal Participation Mass Ratios (Model 2)

Mode	Period (sec)	UX	UY	UZ	Sum UX	Sum UY	Sum UZ
1	1.38	0.9392	0.0000	0.0000	0.9392	0.0000	0.0000
2	1.13	0.0000	0.9992	0.0000	0.9392	0.9992	0.0000
3	0.58	0.0587	0.0000	0.0000	0.9980	0.9992	0.0000
4	0.56	0.0000	0.0000	0.0000	0.9980	0.9992	0.0000
5	0.49	0.0001	0.0000	0.0000	0.9980	0.9992	0.0000
6	0.46	0.0000	0.0000	0.6597	0.9980	0.9992	0.6597
7	0.45	0.0000	0.0000	0.0000	0.9980	0.9992	0.6597
8	0.43	0.0000	0.0000	0.0000	0.9980	0.9992	0.6597
9	0.43	0.0000	0.0000	0.0008	0.9980	0.9992	0.6605
10	0.40	0.0000	0.0000	0.0000	0.9980	0.9993	0.6605
11	0.38	0.0000	0.0000	0.0000	0.9980	0.9993	0.6605

Table 3-7 Period and Modal Participation Mass Ratios (Model 3)

Mode	Period (sec)	UX	UY	UZ	Sum UX	Sum UY	Sum UZ
1	1.33	0.9262	0.0000	0.0000	0.9262	0.0000	0.0000
2	1.05	0.0000	0.9990	0.0000	0.9262	0.9990	0.0000
3	0.57	0.0713	0.0000	0.0000	0.9975	0.9990	0.0000
4	0.55	0.0000	0.0000	0.0000	0.9975	0.9990	0.0000
5	0.49	0.0001	0.0000	0.0000	0.9975	0.9990	0.0000
6	0.45	0.0000	0.0000	0.6584	0.9975	0.9990	0.6584
7	0.45	0.0000	0.0000	0.0000	0.9975	0.9991	0.6584
8	0.43	0.0000	0.0000	0.0000	0.9975	0.9991	0.6584
9	0.43	0.0000	0.0000	0.0009	0.9975	0.9991	0.6593
10	0.40	0.0000	0.0000	0.0000	0.9975	0.9991	0.6593
11	0.38	0.0000	0.0000	0.0000	0.9975	0.9991	0.6593

3.3.7 Design Spectrum

A design response (acceleration) spectrum was used to determine the maximum structural response parameters such as displacements and member forces for each mode of vibration.

The modal responses were combined using the complete quadratic combination (CQC) method. The resulting orthogonal responses were then combined using the 100/30 rule for elastic seismic force effect specified in the AASHTO LRFD Bridge Design Specification (AASHTO 2012).

The design response spectrum diagram, shown in Figure 3-15, of downtown LA (34.0407°N, 118.2468°W) was selected. The maximum forces in the anchors determined from the response spectrum analysis of the bridge were compared to the capacity of the

headed anchors to ensure that there was no failure in the anchors. Figures 3-16 through 3-21 show the distribution of axial and shear forces in the headed anchors along the longitudinal span of the bridge for Models 1, 2 and 3. Due to the rigid properties of the link element connecting the cap beam and girders, large forces were developed in the link element at the bent section. Tables 3-8 and 3-9 list the maximum force in the link, excluding the link forces in the bent region, in Models 2 and 3, respectively. Due to the symmetry of the bridge, only the maximum link forces in girders 1 through 7 are listed in Tables 3-8 and 3-9. As shown in these tables, the demand forces on the anchors are less than the ultimate strength of the connector.

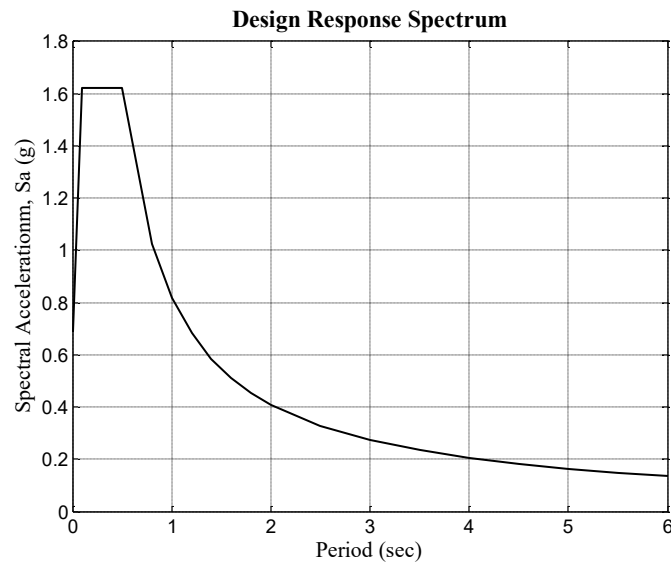


Figure 3-15 Design Response Spectrum (LA Downtown: 34.0407°N, 118.2468°W)

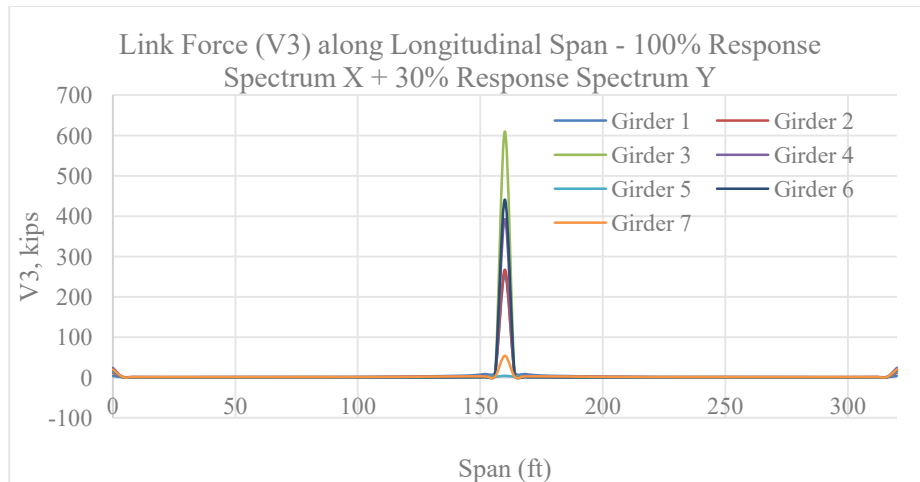
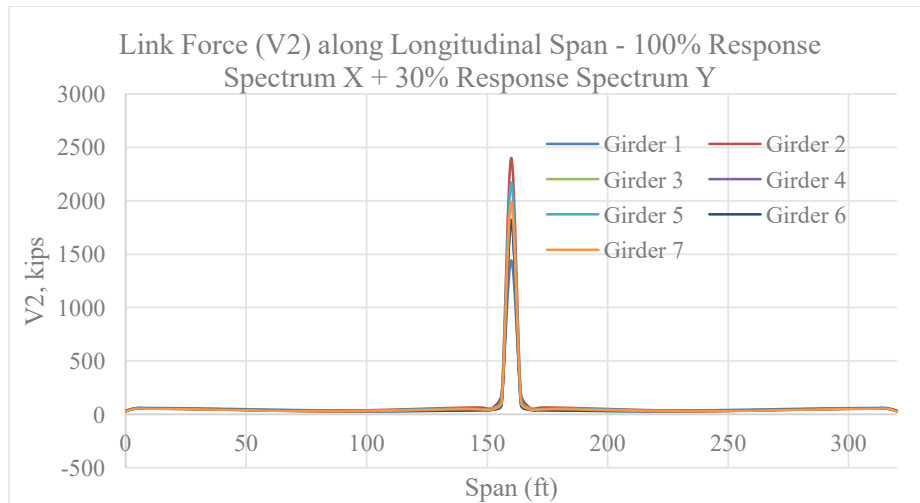
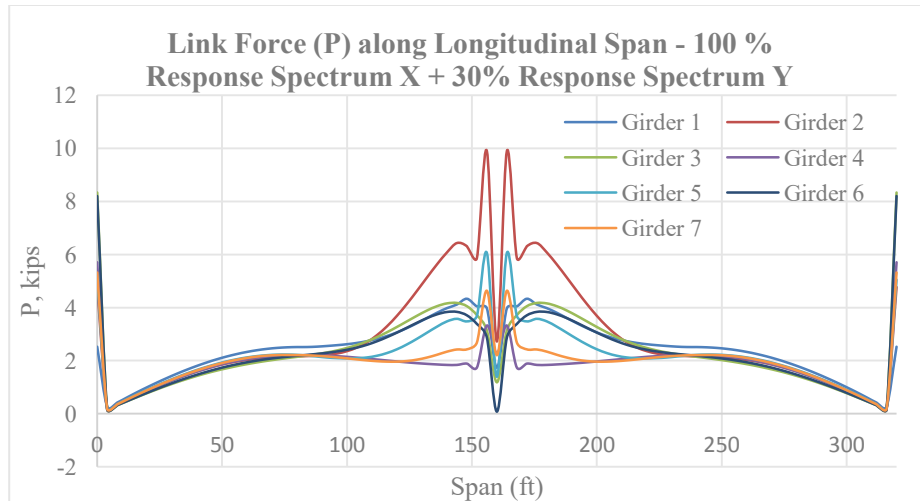


Figure 3-16 Axial and Shear Force in the Connectors (Case 1) – Model 1

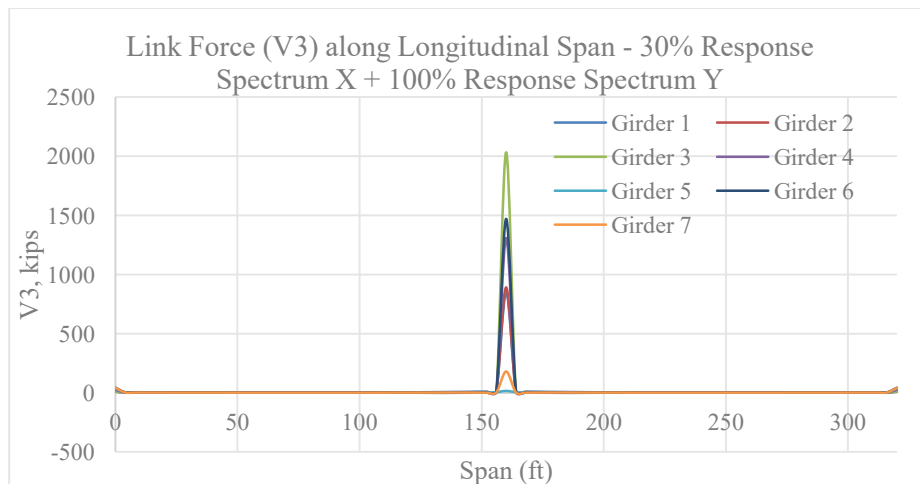
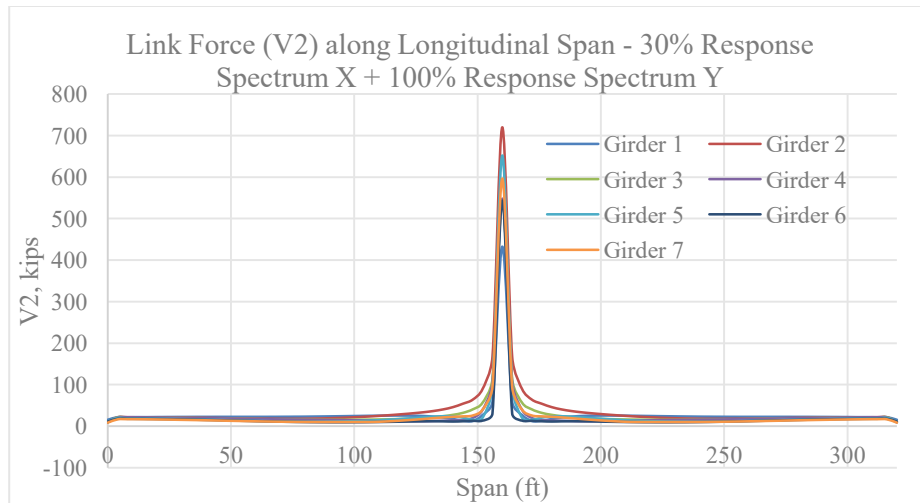
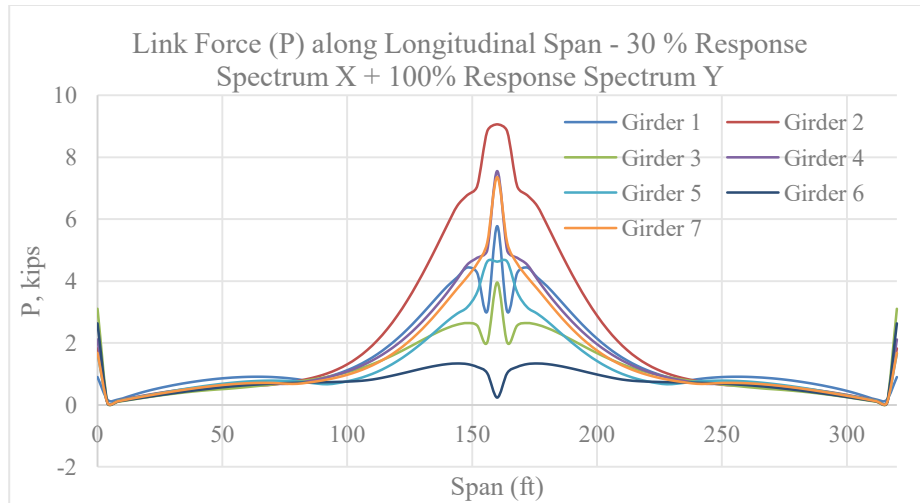


Figure 3-17 Axial and Shear Force in the Connectors (Case 2) – Model 1

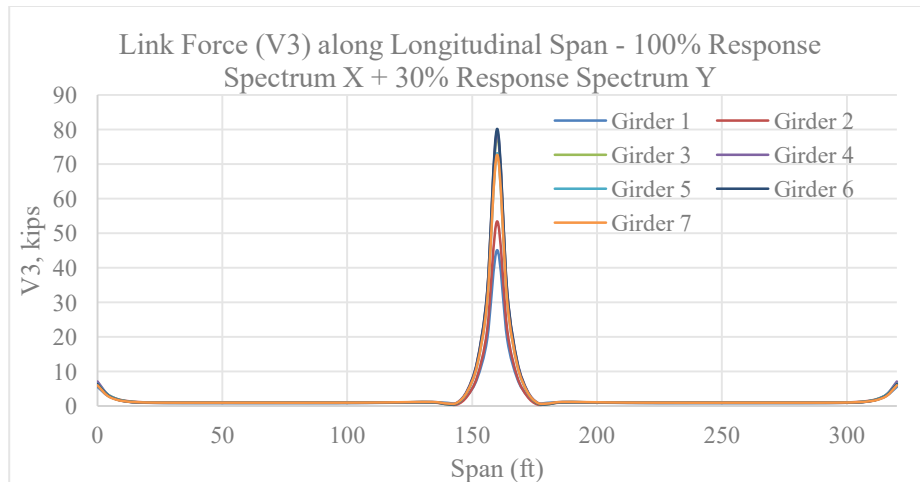
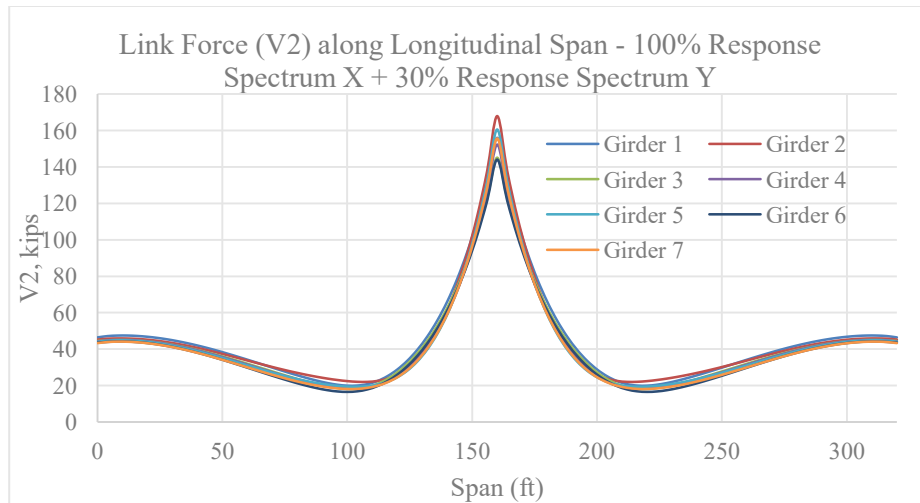
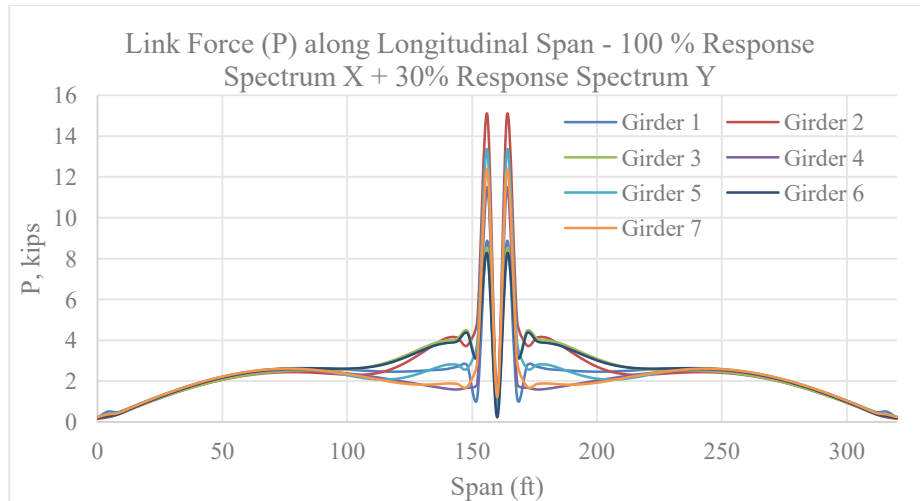


Figure 3-18 Axial and Shear Force in the Connectors (Case 1) – Model 2

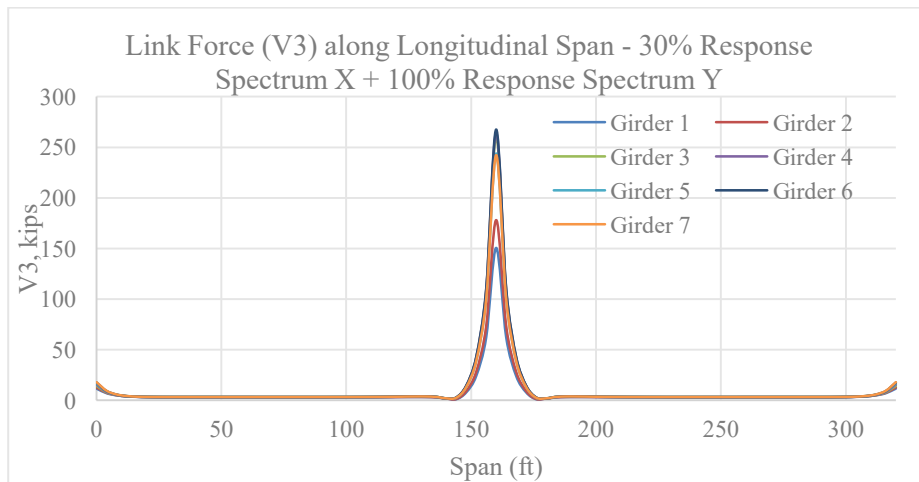
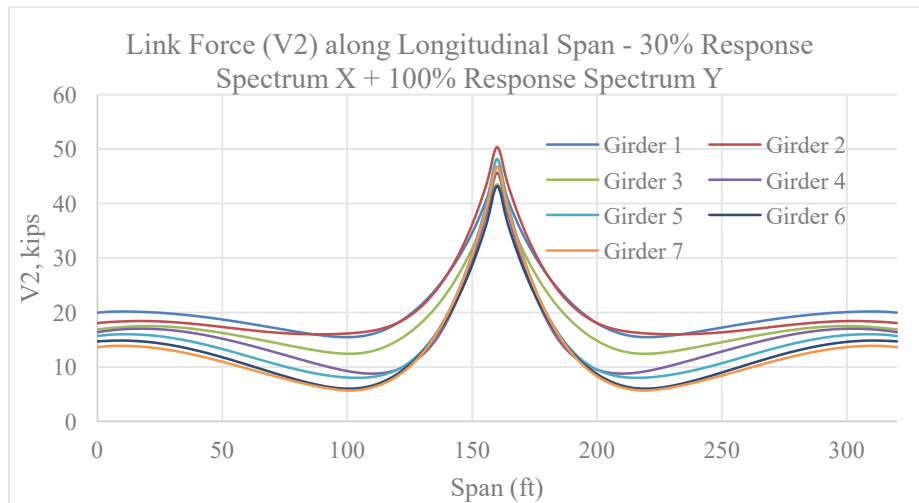
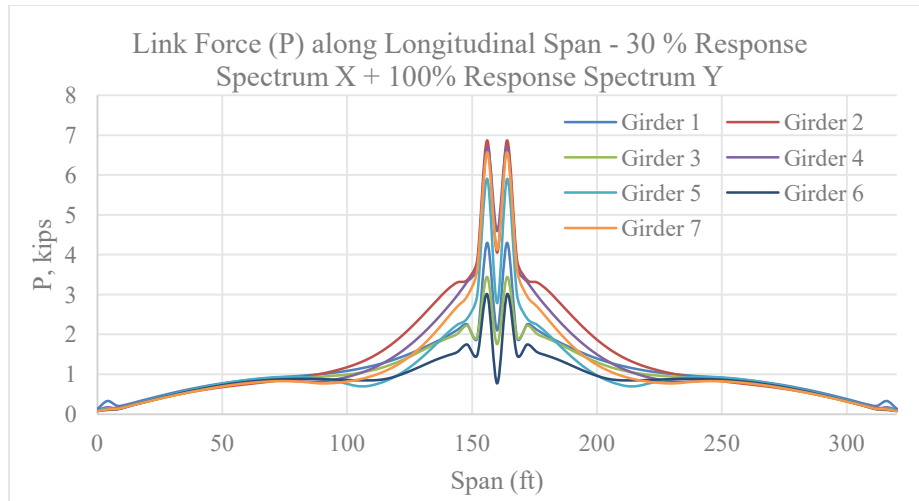


Figure 3-19 Axial and Shear Force in the Connectors (Case 2) – Model 2

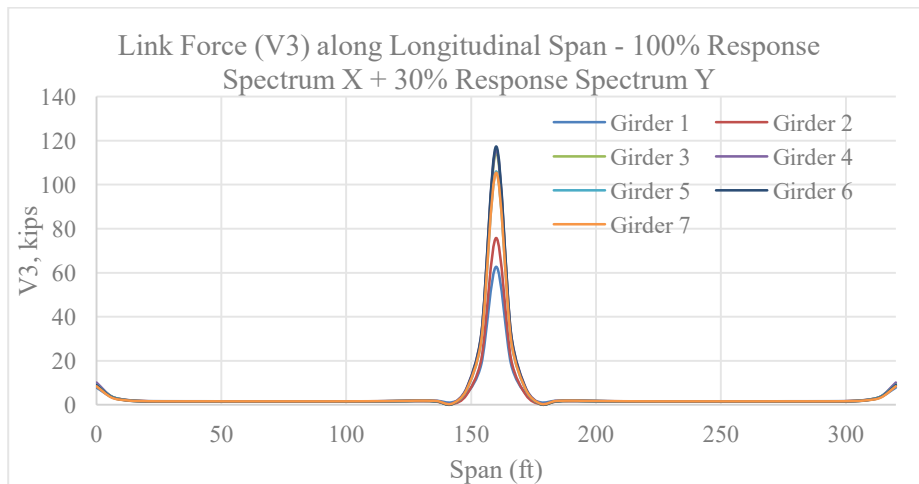
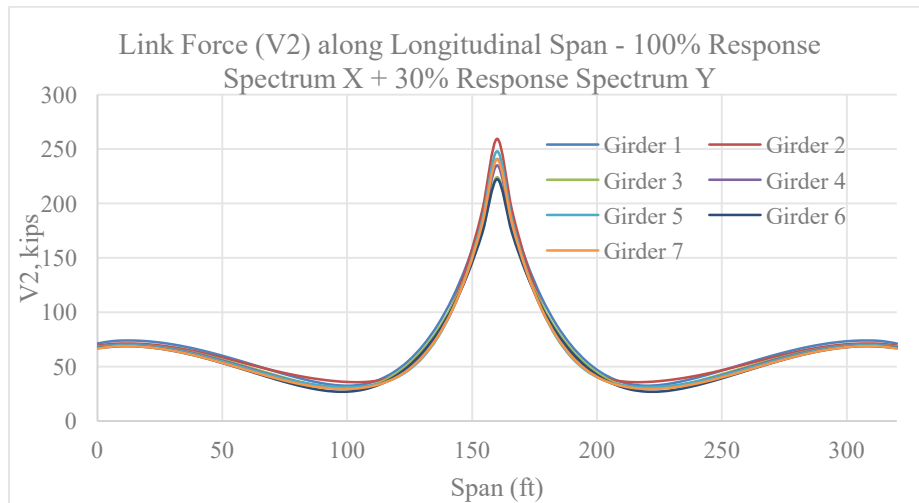
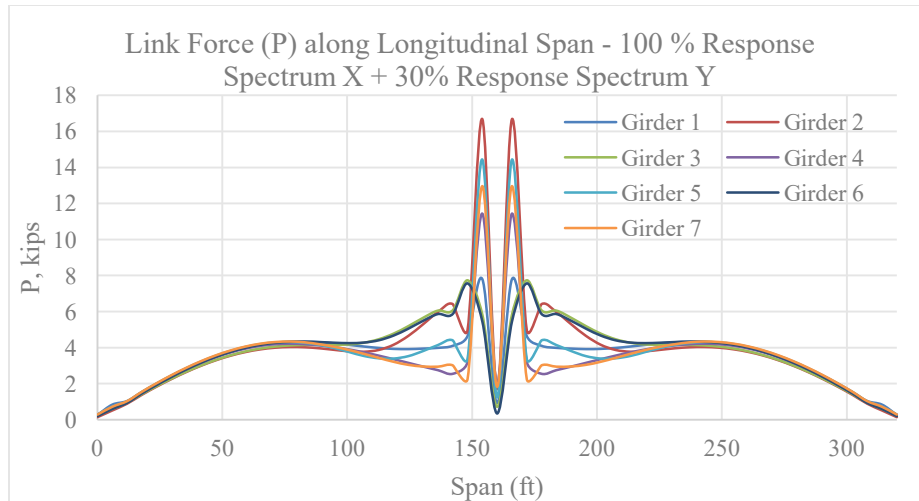


Figure 3-20 Axial and Shear Force in the Connectors (Case 1) – Model 3

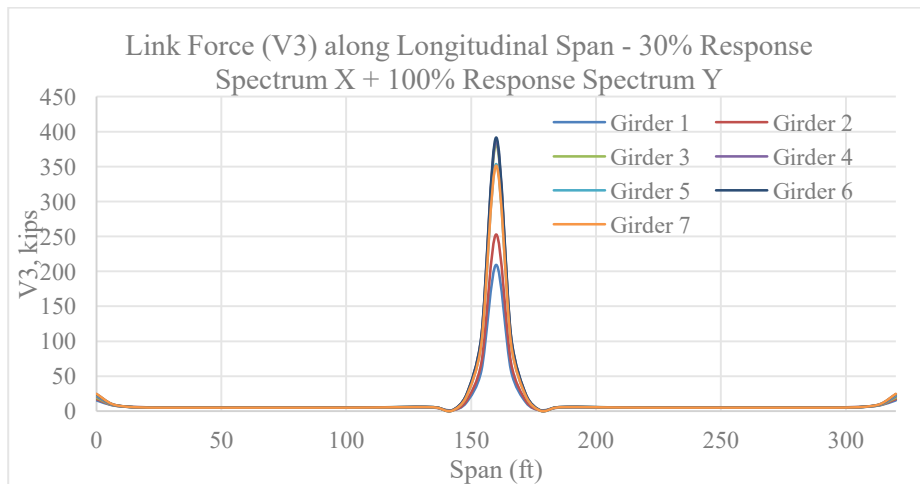
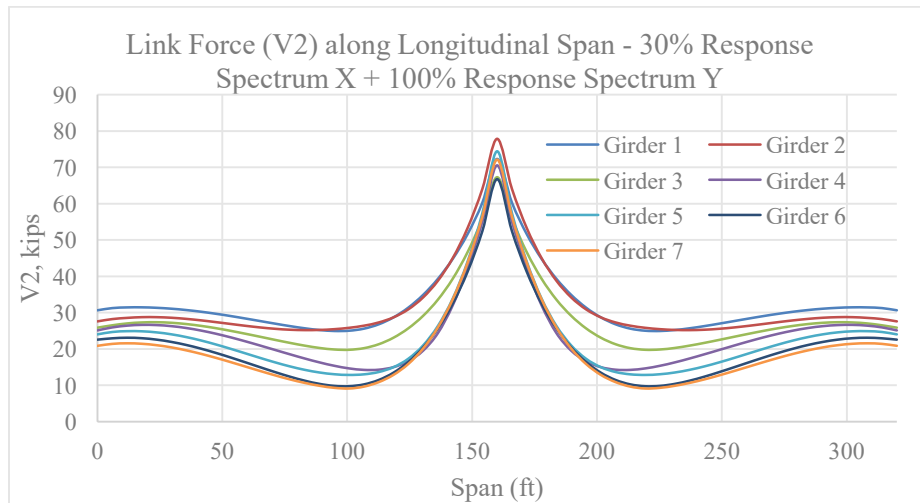
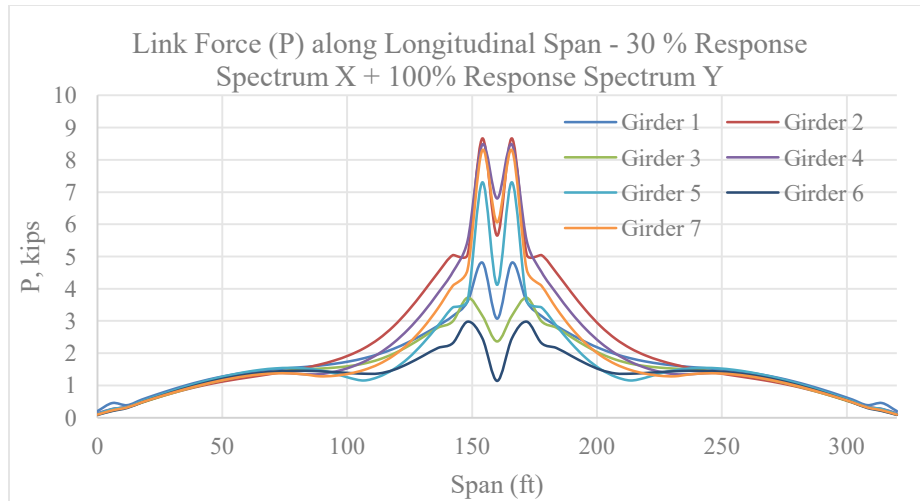


Figure 3-21 Axial and Shear Force in the Connectors (Case 2) – Model 3

Table 3-8 Maximum Link Demand Force (Model 2)

	Case I			Case II		
Girder	P (kips)	V2 (kips)	V3 (kips)	P (kips)	V2 (kips)	V3 (kips)
1	3	111	8	2	37	24
2	5	113	9	4	39	28
3	4	104	13	2	34	42
4	3	105	13	4	32	42
5	4	108	12	3	34	39
6	4	102	13	2	31	43
7	3	106	12	4	33	39
Maximum Force	5	113	13	4	39	43

Note:

Case I = 100% Longitudinal + 30% Transverse

Case II = 30% Longitudinal +100% Transverse

P = Axial Force in Link

V2 = Shear Force in Link along Longitudinal Direction

V3 = Shear Force in Link along Transverse Direction

Table 3-9 Maximum Link Demand Force (Model 3)

Girder	Case I			Case II		
	P (kips)	V2 (kips)	V3 (kips)	P (kips)	V2 (kips)	V3 (kips)
1	8	187	19	5	60	58
2	17	194	21	9	64	69
3	8	175	32	4	56	105
4	11	179	33	8	55	107
5	14	186	30	7	57	97
6	8	173	32	3	52	107
7	13	182	30	8	56	97
Maximum Force	17	194	33	9	64	107

Note:

Case I = 100% Longitudinal + 30% Transverse

Case II = 30% Longitudinal +100% Transverse

P = Axial Force in Link

V2 = Shear Force in Link along Longitudinal Direction

V3 = Shear Force in Link along Transverse Direction

3.4 Nonlinear Analytical Investigation of the Bridge

OpenSees (2017) was used to determine the nonlinear seismic response of the bridge and to verify the headed anchors remain as capacity protected element. OpenSees is a software framework for simulating the seismic response of structural and geotechnical systems. It utilizes advanced capabilities for modeling and analyzing the

nonlinear response of systems using a wide range of material models, elements, and solution algorithms.

3.4.1 Material Models

The material "Concrete04" from OpenSees library was used to represent the unconfined concrete properties. The unconfined concrete material property was assigned to the cover concrete with a maximum compressive strain of 0.002 and ultimate unconfined compressive strain of 0.005, and a specified concrete compressive strength. Due to the presence of the transverse confinement around the core and the cage effect, the core compressive strength and ultimate strain are higher than those of the unconfined concrete. The material "Concrete02" was used to represent the confined concrete properties. Confined concrete has a strain of 0.005 at a stress of 6.38 kip/in² and a strain of 0.05 at a stress of 5.11 kip/in². The unconfined and confined concrete stress-strain models are shown in Figures 3-22 and 3-23, respectively. Longitudinal steel reinforcement was represented by "Reinforcing Steel" that captures the yield plateau as well as the strain hardening of the rebar. Figure 3-24 shows the general monotonic curve for a mild reinforcing bar under tensile loading, and the six required input parameters for reinforcing steel.

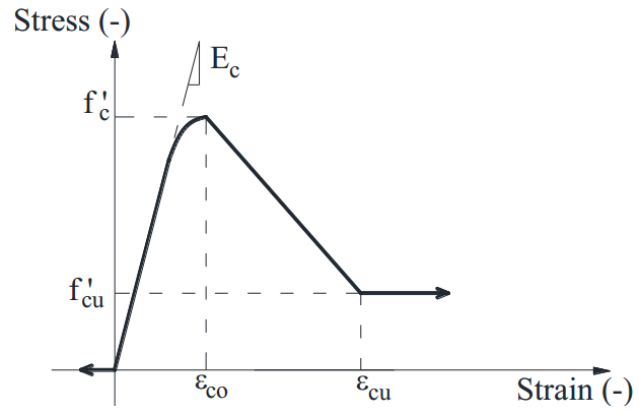


Figure 3-22 Constitutive Model for Unconfined Concrete

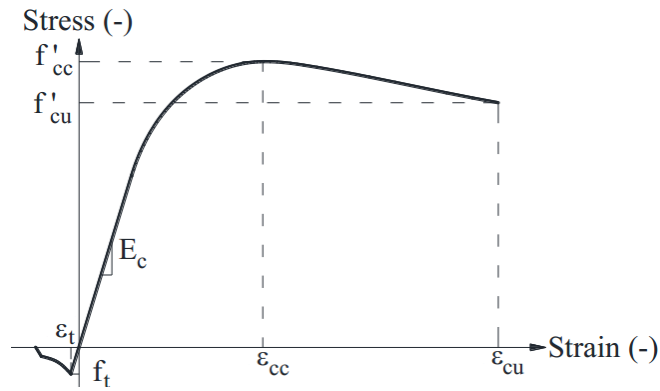


Figure 3-23 Constitutive Model for Confined Concrete

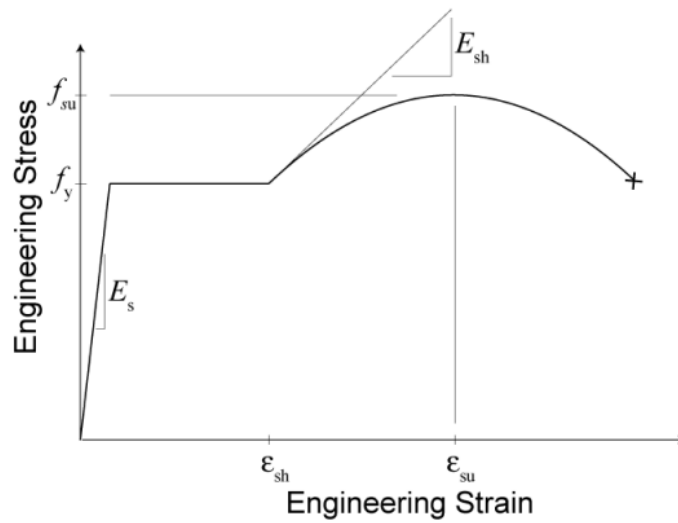


Figure 3-24 Constitutive Model for Reinforcing Steel

When the concrete strain in one of the core fibers (with confined property) reaches the concrete ultimate strain (concrete crushing), concrete strength drops to zero in the fiber. When the strain in one of the longitudinal rebar passes the ultimate strain at breaking stress, the analysis is interrupted due to the rebar fracture.

3.4.2 Bridge Computational Model

The bridge was modeled as an elastic superstructure supported on nonlinear columns. The deck, girders, diaphragms, and cap beam are expected to remain elastic and thus were modeled using equivalent elastic beam-column elements with mass concentrated at their nodes. Rigid elements at each end of the deck were used to connect the decks to the bearing nodes on the bents or abutments. The column element was modeled using three dimensional "forceBeamColumn" element that is based on an iterative force-based formulation. This element enables the user to model the distributed plasticity along the element without the need for defining the plastic hinge length and cracked section modifier. The column was finely discretized along the height, with five integration points, for a better distribution of mass. Nonlinear material properties were assigned to the section, which consist of confined and unconfined concrete and reinforcing steel to account for the axial and flexural stiffness of the column. Cracked shear and torsional stiffness of the column were included in the element by aggregating the uniaxial elastic material with each element. The cover and core areas of the sections were defined by assigning unconfined and confined concrete properties to them, respectively. The core, which is confined by hoops, consists of 80 subdivisions in the circumferential direction and 80 subdivisions in the radial direction. The cover has 80

and 10 subdivisions in the circumferential and radial directions, respectively. Figure 3-25 shows the OpenSees model at the bent.

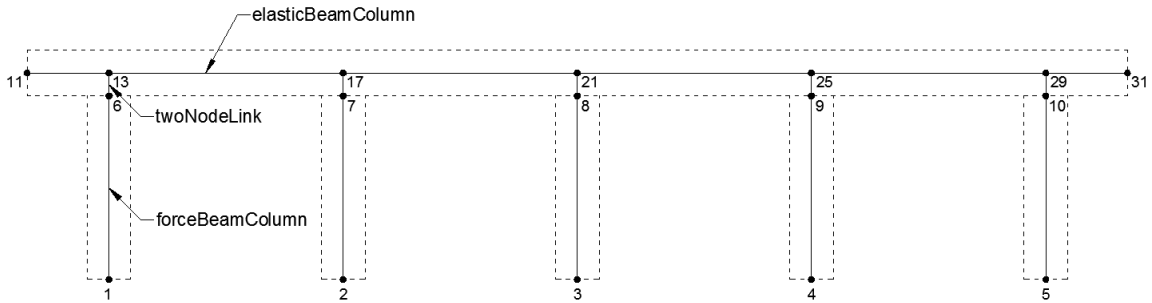


Figure 3-25 OpenSees Model at Bent

The headed anchors were modeled with a “twoNodeLink” object that connects the girder and deck nodes. The deck girder connection detail is shown in Figure 3-26. Axial and horizontal shear properties were defined for the twoNodeLink element. The axial stiffness of the link element was defined using elastic bilinear uniaxial material object with stiffness of 3,796 kip/in and 5,695 kip/in for Models 2 and 3, respectively. The shear stiffness of the link element for Models 2 and 3 was 630 kip/in and 945 kip/in, respectively. The shear stiffness of the link element was defined using multi-linear elastic uniaxial material object. Figure 3-11 shows the shear properties of Models 2 and 3, respectively.

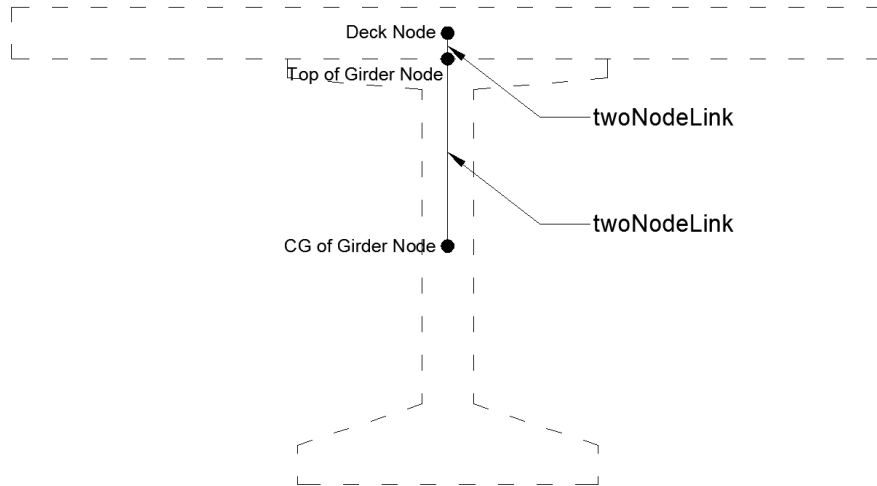


Figure 3-26 OpenSees Model at Deck Girder Connection

3.4.3 Model Verification

Linear modal analysis was performed in both OpenSees and SAP2000 to verify the OpenSees model. The models were verified for gravity loads, support reactions, and displacement. The gravity loads included the weight of the superstructure, the cap beam, and the columns. The results from the gravity analysis from SAP2000 and OpenSees models were checked against hand-calculation values.

The support reaction at Abutment 1, Bent 2 and Abutment 3 from the SAP2000 and OpenSees Model are listed in Tables 3-10 and 3-11, respectively. The results from SAP2000 and OpenSees model were compared with those from hand calculations to validate the finite element models.

Table 3-10 Support Reaction (SAP2000)

	Reaction (kips)			
	Abutment 1	Bent 2	Abutment 3	Total
Model 1	2,189	7,570	2,189	11,948
Model 2	2,210	7,528	2,210	11,948
Model 3	2,189	7,570	2,189	11,948
Model 4	2,210	7,528	2,210	11,948

Table 3-11 Support Reaction (Opensees)

	Reaction (kips)			
	Abutment 1	Bent 2	Abutment 3	Total
Model 1	2,188	7,572	2,188	11,948
Model 2	2,207	7,534	2,207	11,948
Model 3	2,188	7,572	2,188	11,948
Model 4	2,207	7,534	2,207	11,948

Figure 3-27 shows the displacement profile of the entire bridge for Models 1, 2 and 3. The displacement profiles of Model 2 and Model 3 show that the displacement along the longitudinal span of the bridge were same for the pocket spacing of 4 ft and 6 ft. Model 2 and Model 3 experienced a 31.25% higher displacement at the center of span than Model 1. Model 1 represented the fully composite deck girders connection, whereas, Model 2 and Model 3 represented partially composite deck girders connection.

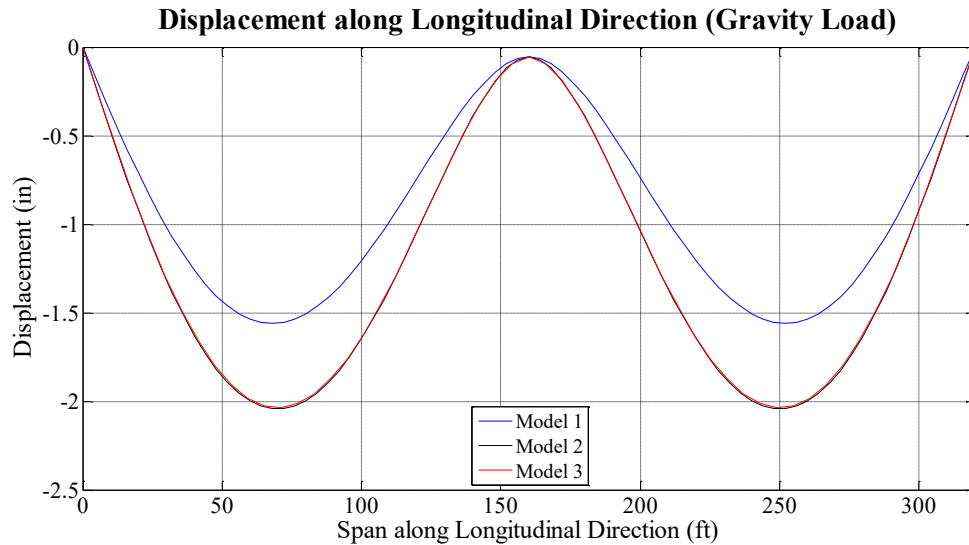
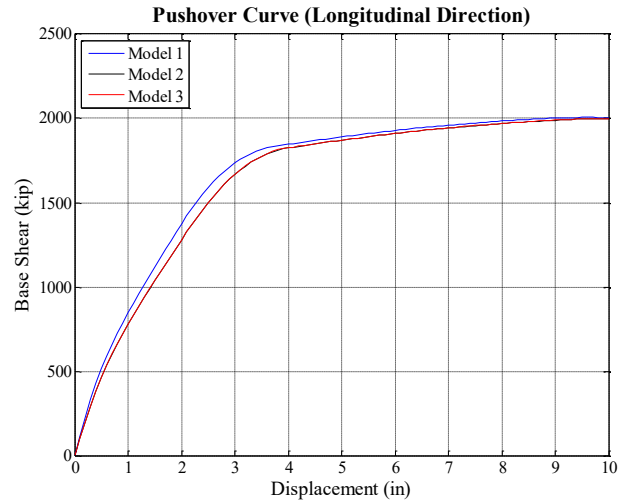


Figure 3-27 Displacement along Longitudinal Direction (OpenSees)

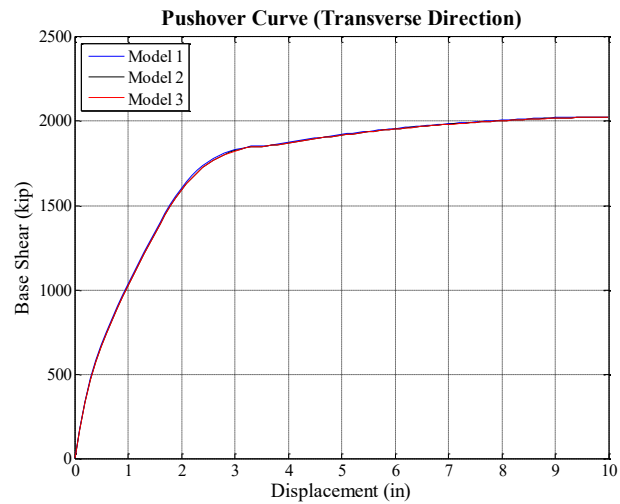
3.4.4 Pushover Analysis

Pushover analyses of the bridge were conducted in the two orthogonal directions to capture the behavior of the structure by monitoring the displacement at a point of reference. The lateral shear capacity of the bridge and the forces in the anchors monitored were reported.

Figures 3-28 (a) and 3-28 (b) show the capacity curves for the pushover analyses in longitudinal and transverse direction for all three models (Models 1, 2 and 3). During the pushover analysis, the reference node for displacement was taken as the central point of the cap beam. The displacement capacity for all three models were approximately equal in both directions. The pushover curves show that significant yielding start at about 3 in. displacement or 1% drift ratio in case of longitudinal pushover. In the case of transverse pushover, similar yielding is observed at 2.5 in. displacement or 0.8 % drift ratio. The lateral force was 1,800 kips when this yielding occurred in both directions.



(a)

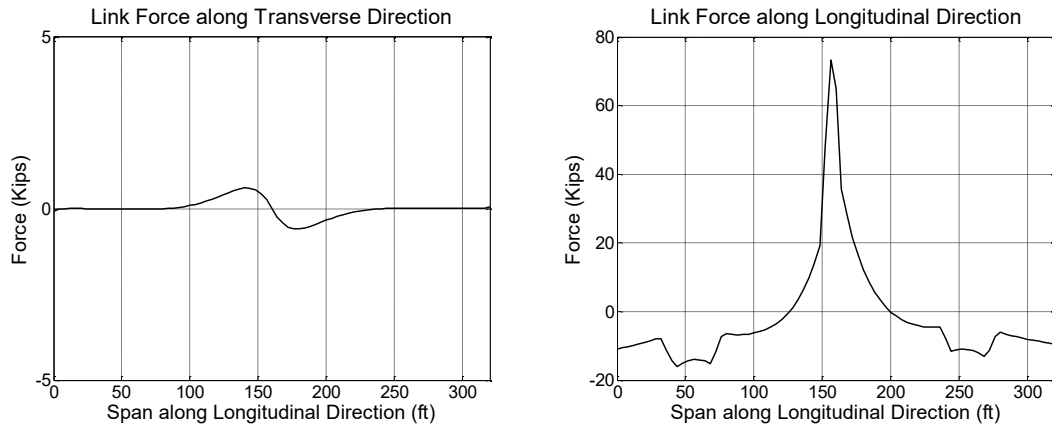


(b)

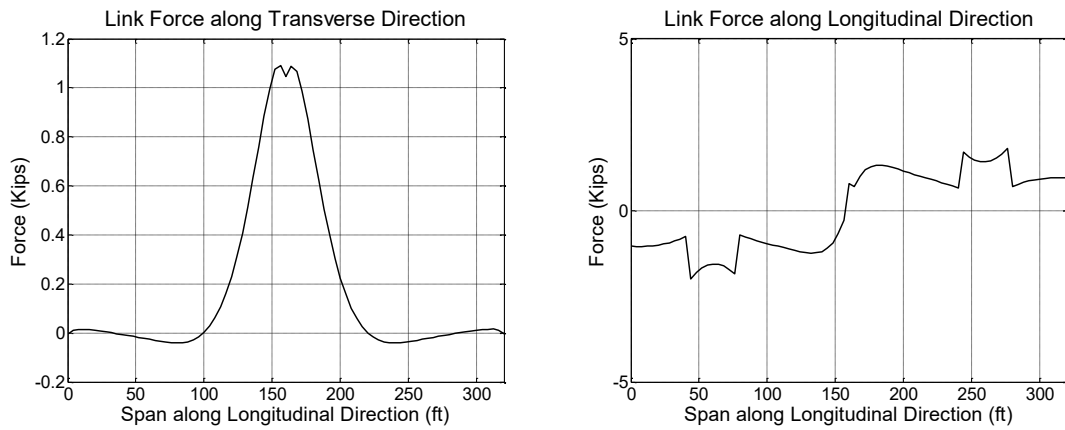
Figure 3-28 Pushover Curve: (a) Longitudinal Direction; (b) Transverse Direction

Figures 3-29 and 3-30 show the longitudinal and transverse shear forces in the link due to longitudinal and transverse pushover in Models 2 and 3. Negligible forces in the links were observed for transverse pushover in Models 2 and 3. For longitudinal pushover, negligible forces were observed in transverse direction for both models. The

maximum forces in longitudinal direction were 70 kips and 100 kips for Model 2 and Model 3, respectively, which are well below the ultimate capacity of the link. Anchor spacing had a negligible effect in the overall response of the bridge.

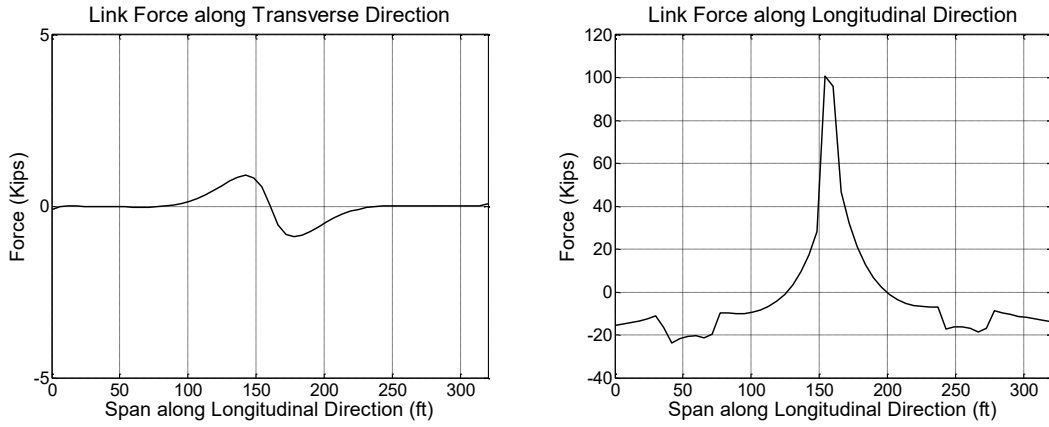


(a) Longitudinal Pushover

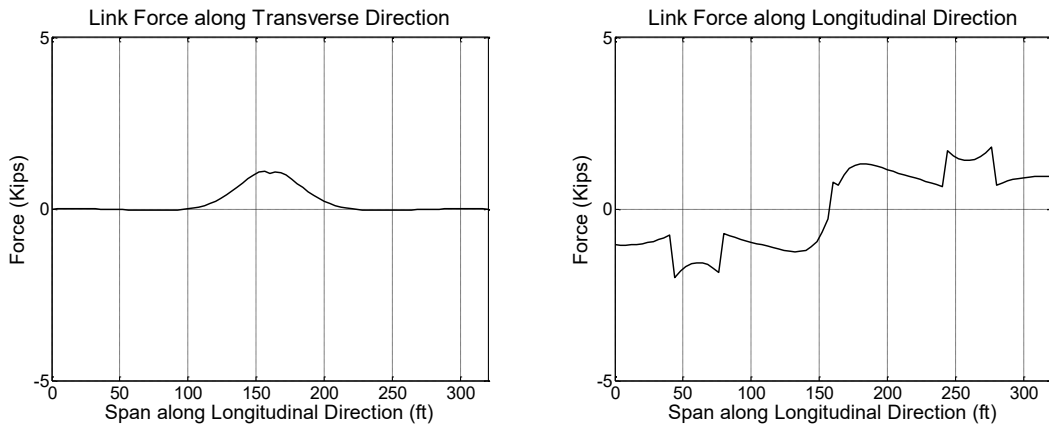


(b) Transverse Pushover

Figure 3-29 Link Force in Girder 7 (Model 2)



(a) Longitudinal Pushover



(b) Transverse Pushover

Figure 3-30 Link Force in Girder 7 (Model 3)

Table 3-12 Pushover Curve

Model	Maximum Force (kips)	
	Longitudinal Direction	Transverse Direction
1	2006	2026
2	1997	2023
3	1997	2023

3.4.5 Nonlinear Response History Analysis

Nonlinear response history analysis was performed to determine the seismic response of the bridge using a large suite of ground motions.

3.4.5.1 Input Ground Motions

The AASHTO Seismic Guide Specifications (AASHTO, 2011) require at least seven sets of independent ground motion records to be applied in orthogonal directions.

An ensemble of eight earthquake ground motion records were selected for this study, including both far-field and near-fault ground motion records. The ground motions were selected for magnitude greater than 6, soil class D and range of V_{S30} of 600 ft/s to 1,200 ft/sec. Table 3-13 shows the selected acceleration history from the Pacific Earthquake Engineering Research Center (PEER). Tables 3-14 and 3-15 show the eight ground motion profiles in both longitudinal and transverse direction.

To achieve spectral compatibility with the design spectrum, the records were scaled to the design response spectrum at the transverse period of the bridge. The scaled and unscaled response spectrums of selected ground motions are shown in Tables 3-16 and 3-17, respectively. Figure 3-31 compares the scaled response spectrum of all ground motions with the design spectrum.

Table 3-13 Characteristics of Selected Accelerations Records

Type	RSN	Event	Station Name	Magnitude (Richter)	Rjb (km)	V_{S30} (m/s)
Near Fault	169	Imperial Valley-06	Delta	6.53	22.03	242.05
	778	Loma Prieta	Hollister Differential Array	6.93	24.52	215.54
	1003	Northridge-01	LA - Saturn St	6.69	21.17	308.71
Far Field	160	Imperial Valley-06	Bonds Corner	6.53	0.44	223.03
	558	Chalfant Valley-02	Zack Brothers Ranch	6.19	6.44	316.19
	752	Loma Prieta	Capitola	6.93	8.65	288.62
	1063	Northridge-01	Rinaldi Receiving Sta	6.69	0	282.25
	1084	Northridge-01	Sylmar - Converter Sta	6.69	0	251.24

Note: RSN = Record Serial Number in PEER NGA-West2 ground motion database.

Table 3-14 Longitudinal and Transverse Components of Selected Earthquakes

Event	Longitudinal	Transverse
Imperial Valley-06 "Delta"		
Loma Prieta "Hollister Differential Array"		
Northridge-01 "LA - Saturn St"		
Imperial Valley-06 "Bonds Corner"		

Table 3-15 Longitudinal and Transverse Components of Selected Earthquakes

Event	Longitudinal	Transverse
Chalfant Valley-02 "Zack Brothers Ranch"		
Loma Prieta "Capitola"		
Northridge-01 "Rinaldi Receiving Sta"		
Northridge-01 "Sylmar - Converter Sta"		

Table 3-16 Unscaled and Scaled Response Spectrum

Event	Scale Factor	Unscaled	Scaled
Imperial Valley-06 "Delta"	1.7		
Loma Prieta "Hollister Differential Array"	1.5		
Northridge-01 "LA - Saturn St"	1.7		
Imperial Valley-06 "Bonds Corner"	1.8		

Table 3-17 Unscaled and Scaled Response Spectrum

Event	Scale Factor	Unscaled	Scaled
Chalfant Valley-02 "Zack Brothers Ranch"	1.4		
Loma Prieta "Capitola"	1.7		
Northridge-01 "Rinaldi Receiving Sta"	0.4		
Northridge-01 "Sylmar - Converter Sta"	0.6		

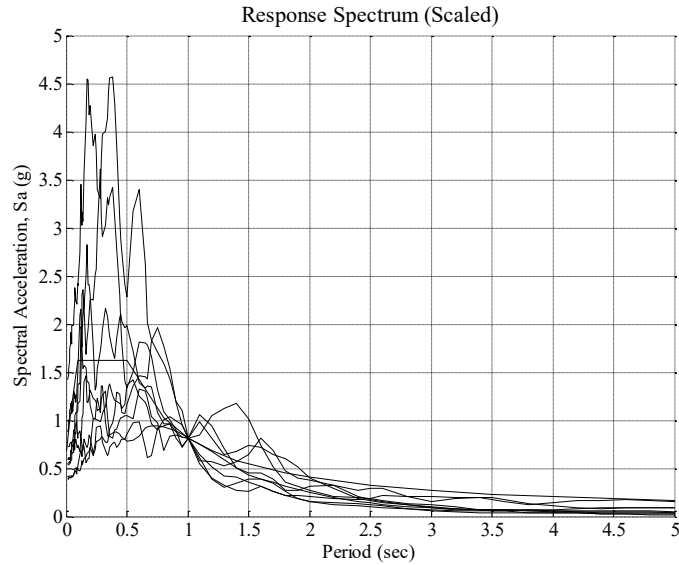


Figure 3-31 Scaled Response Spectrum compared to Design Spectrum

Nonlinear response history analysis was performed simultaneously in both the longitudinal and transverse directions of the bridge using the scaled ground motions. The bridge was also analyzed for earthquake intensities corresponding to 150% of the design earthquake (DE). The 150 % DE was assumed as the maximum considered earthquake (MCE) (Monzon et. al.).

3.5 Analytical Results

3.5.1 Analytical Results for Model 1

Results from Model 1 are shown in Figures 3-32 through 3-47 and Tables 3-18 and 3-19.

3.5.1.1 Hysteretic Response

The hysteretic base shear-displacement response at the center of cap beam are shown in Figures 3-32 to 3-39. The maximum base shear and displacement for 100% and 150% design motions in the longitudinal and transverse directions are summarized in Table 3-18.

3.5.1.2 Displacement Response Histories

Table 3-19 shows the maximum displacement and the corresponding drift at the center of cap beam for all ground motions. The maximum longitudinal and transverse displacement are also presented in Figures 3-40 to 3-47 corresponding to seismic excitations scaled to two intensity levels, 100% and 150% of design motions. From the figures, it can be observed that the displacements at the top of all five columns are almost identical. The maximum displacements varied from 4.5 in. (1.5% drift) to 10.6 in. (3.53% drift) along the longitudinal direction and 4.3 in. (1.43% drift) to 11.8 in. (3.93% drift) along the transverse direction for 100% design earthquake. In the longitudinal direction, the maximum displacements were 10.6 in. for the Design Level and 18.4 in. for MCE level. In the transverse direction, the maximum displacements of 11.8 in. and 16.52 in. were observed for design and MCE level earthquakes, respectively. At the Design Level, the transverse displacement is higher than that of the longitudinal displacement. This trend was reversed at MCE Level.

Table 3-18 Maximum Base Shear and Displacement (Model 1)

Earthquake	Station	RSN	Scale	Transverse		Longitudinal	
				Displacement (in)	Base Shear (kips)	Displacement (in)	Base Shear (kips)
Imperial Valley-06	Delta	169	1	4.29	1810.33	9.04	1980.21
Loma Prieta	Hollister Differential Array	778		5.53	1909.85	4.43	1655.85
Northridge-01	LA - Saturn St	1003		6.41	1576.06	7.86	2000.21
Imperial Valley-06	Bonds Corner	160		6.60	1896.43	7.06	1861.37
Chalfant Valley-02	Zack Brothers Ranch	558		5.81	1882.66	7.46	1727.09
Loma Prieta	Capitola	752		11.85	2161.38	5.67	1656.23
Northridge-01	Rinaldi Receiving Sta	1063		10.13	1877.87	4.84	1585.42
Northridge-01	Sylmar - Converter Sta	1084		7.30	1781.04	10.56	1922.79
Imperial Valley-06	Delta	169	1.5	6.99	1893.46	18.41	2064.75
Loma Prieta	Hollister Differential Array	778		10.20	1933.67	8.26	1702.92
Northridge-01	LA - Saturn St	1003		9.33	1830.85	9.89	2009.95
Imperial Valley-06	Bonds Corner	160		12.66	2105.99	8.52	1858.97
Chalfant Valley-02	Zack Brothers Ranch	558		8.20	1943.29	8.75	1741.34
Loma Prieta	Capitola	752		10.11	2216.83	6.97	1768.13
Northridge-01	Rinaldi Receiving Sta	1063		16.52	1987.28	7.70	1344.55
Northridge-01	Sylmar - Converter Sta	1084		8.10	1818.34	12.88	1796.27

Table 3-19 Maximum Displacement and Drift (%) (Model 1)

Earthquake	Station Name	RSN	Scale	Max. Transverse Displacement (in)	Drift (%)	Max. Longitudinal Displacement (in)	Drift (%)
Imperial Valley-06	Delta	169	1	4.3	1.43	9.5	3.17
Loma Prieta	Hollister Differential Array	778		5.5	1.83	4.5	1.50
Northridge-01	LA - Saturn St	1003		6.4	2.13	8	2.67
Imperial Valley-06	Bonds Corner	160		6.6	2.20	7.3	2.43
Chalfant Valley-02	Zack Brothers Ranch	558		5.8	1.93	7.5	2.50
Loma Prieta	Capitola	752		11.8	3.93	5.8	1.93
Northridge-01	Rinaldi Receiving Sta	1063		10.1	3.37	5	1.67
Northridge-01	Sylmar - Converter Sta	1084		7.3	2.43	10.6	3.53
Imperial Valley-06	Delta	169	1.5	7	2.33	18.8	6.27
Loma Prieta	Hollister Differential Array	778		10.2	3.40	8.3	2.77
Northridge-01	LA - Saturn St	1003		9.3	3.10	10	3.33
Imperial Valley-06	Bonds Corner	160		12.7	4.23	8.9	2.97
Chalfant Valley-02	Zack Brothers Ranch	558		8.2	2.73	8.8	2.93
Loma Prieta	Capitola	752		12.8	4.27	7.8	2.60
Northridge-01	Rinaldi Receiving Sta	1063		16.5	5.50	7.9	2.63
Northridge-01	Sylmar - Converter Sta	1084		8.1	2.70	13.2	4.40

3.5.2 Analytical Results for Model 2

Model 2 computational model connector configuration is identical to that in Model 1, except that the Model 1 used a rigid connectors whereas Model 2 used the properties of the connectors described in Section 3.3.4. The results of Model 2 are illustrated in Figures 3-48 through 3-71 and Tables 3-20 through 3-22.

3.5.2.1 Hysteretic Response

The hysteretic base shear force-displacement response at the center of cap beam for the ground motions (100% and 150%) are shown in Figures 3-48 to 3-55. The maximum base shears and displacements for 100% and 150% design motions in the longitudinal and transverse direction are summarized in Table 3-20.

3.5.2.2 Displacement Response Histories

Table 3-21 shows the maximum displacement and corresponding drift ratios at the center of cap beam for all ground motions. The maximum longitudinal and transverse displacements are also presented in Figures 3-56 to 3-63 corresponding to seismic excitations scaled to two intensity levels, 100% and 150% of design motion. From the figures, it can be observed that the displacements at the top of all five columns are almost identical. The displacements varied from 4.4 in. (1.47% drift) to 11.3 in. (3.77% drift) along the longitudinal direction and 4.3 in. (1.43% drift) to 11.6 in. (3.87% drift) along the transverse direction for 100% design earthquake. In the longitudinal direction, the maximum displacements were 11.3 in. for the Design Level and 19.4 in. for MCE level. In the transverse direction, the maximum displacements of 11.6 in. and 16.7 in. were

observed for design and MCE level earthquakes, respectively. At the Design Level, the transverse displacement is higher than that of the longitudinal displacement. This trend was reversed at MCE Level.

3.5.2.3 Behavior of Headed Anchors

The forces and displacements in the links are presented along the longitudinal direction of the girders. Negligible difference between the force and displacement in the link were observed among the 14 girders. Therefore, only results of girder 7 are presented in Table 3-22. The maximum forces and displacements are also shown in Figures 3-64 to 3-71. The response is plotted along the longitudinal span of the bridge. It can be seen that the anchor displacements were negligible. From the figures, it can be ascertained that the peak link displacement occurred close to the bent for all the eight earthquakes. The maximum force in the anchors when subjected to 100% design level and MCE level were 83 kips in longitudinal direction and 7.2 kips in transverse direction, which are substantially lower than the ultimate capacity of the connectors (250 kips).

Table 3-20 Maximum Base Shear and Displacement (Model 2)

Earthquake	Station	RSN	Scale	Transverse		Longitudinal	
				Displacement (in)	Base Shear (kips)	Displacement (in)	Base Shear (kips)
Imperial Valley-06	Delta	169	1	4.34	1800.31	10.70	2000.67
Loma Prieta	Hollister Differential Array	778		5.77	1971.63	4.38	1608.04
Northridge-01	LA - Saturn St	1003		6.65	1401.86	9.21	1964.52
Imperial Valley-06	Bonds Corner	160		6.45	1885.01	7.03	1882.66
Chalfant Valley-02	Zack Brothers Ranch	558		5.73	1851.04	7.53	1688.36
Loma Prieta	Capitola	752		11.64	2157.71	5.78	1631.02
Northridge-01	Rinaldi Receiving Sta	1063		10.12	1910.70	4.92	1615.31
Northridge-01	Sylmar - Converter Sta	1084		7.43	1755.87	11.26	1926.31
Imperial Valley-06	Delta	169	1.5	7.12	1902.87	18.89	2012.49
Loma Prieta	Hollister Differential Array	778		10.16	1935.97	8.69	1758.69
Northridge-01	LA - Saturn St	1003		9.00	1823.91	9.31	1971.25
Imperial Valley-06	Bonds Corner	160		12.31	2115.12	9.16	1888.54
Chalfant Valley-02	Zack Brothers Ranch	558		8.34	1928.13	8.81	1686.94
Loma Prieta	Capitola	752		9.94	2253.67	6.93	1735.68
Northridge-01	Rinaldi Receiving Sta	1063		16.73	2000.22	7.81	1420.58
Northridge-01	Sylmar - Converter Sta	1084		8.23	1814.52	13.32	1758.25

Table 3-21 Maximum Displacement and Drift (%) (Model 2)

Earthquake	Station Name	RSN	Scale	Max. Transverse Displacement (in)	Drift (%)	Max. Longitudinal Displacement (in)	Drift (%)
Imperial Valley-06	Delta	169	1	4.3	1.43	10.9	3.63
Loma Prieta	Hollister Differential Array	778		5.8	1.93	4.4	1.47
Northridge-01	LA - Saturn St	1003		6.7	2.23	9.2	3.07
Imperial Valley-06	Bonds Corner	160		6.4	2.13	7.1	2.37
Chalfant Valley-02	Zack Brothers Ranch	558		5.7	1.90	7.5	2.50
Loma Prieta	Capitola	752		11.6	3.87	5.9	1.97
Northridge-01	Rinaldi Receiving Sta	1063		10.1	3.37	5.2	1.73
Northridge-01	Sylmar - Converter Sta	1084		7.4	2.47	11.3	3.77
Imperial Valley-06	Delta	169		7.1	2.37	19.4	6.47
Loma Prieta	Hollister Differential Array	778	1.5	10.2	3.40	8.8	2.93
Northridge-01	LA - Saturn St	1003		9	3.00	9.4	3.13
Imperial Valley-06	Bonds Corner	160		12.3	4.10	9.2	3.07
Chalfant Valley-02	Zack Brothers Ranch	558		8.3	2.77	8.8	2.93
Loma Prieta	Capitola	752		12.6	4.20	7.7	2.57
Northridge-01	Rinaldi Receiving Sta	1063		16.7	5.57	8	2.67
Northridge-01	Sylmar - Converter Sta	1084		8.2	2.73	13.7	4.57

Table 3-22 Maximum Link Force and Displacement (Model 2)

Earthquake	Station	RSN	Scale	Transverse		Longitudinal	
				Maximum Displacement (in)	Maximum Force (kips)	Maximum Displacement (in)	Maximum Force (kips)
Imperial Valley-06	Delta	169	1	0.02	6.80	0.10	75.90
Loma Prieta	Hollister Differential Array	778		0.02	6.95	0.10	75.80
Northridge-01	LA - Saturn St	1003		0.02	6.70	0.11	77.50
Imperial Valley-06	Bonds Corner	160		0.02	6.92	0.12	79.50
Chalfant Valley-02	Zack Brothers Ranch	558		0.01	6.70	0.09	75.00
Loma Prieta	Capitola	752		0.02	6.73	0.10	76.50
Northridge-01	Rinaldi Receiving Sta	1063		0.02	6.90	0.09	74.50
Northridge-01	Sylmar - Converter Sta	1084		0.01	6.75	0.09	75.10
Imperial Valley-06	Delta	169		1.5	0.02	6.80	0.11
Loma Prieta	Hollister Differential Array	778	0.02		7.00	0.09	75.50
Northridge-01	LA - Saturn St	1003	0.02		6.80	0.12	79.40
Imperial Valley-06	Bonds Corner	160	0.02		7.04	0.14	82.90
Chalfant Valley-02	Zack Brothers Ranch	558	0.02		6.73	0.10	76.50
Loma Prieta	Capitola	752	0.02		7.18	0.13	81.50
Northridge-01	Rinaldi Receiving Sta	1063	0.02		7.00	0.09	74.60
Northridge-01	Sylmar - Converter Sta	1084	0.02		6.90	0.10	76.20

3.5.3 Analytical Results for Model 3

The purpose of Model 3 was to study the effect of pocket spacing on bridge response by comparing the results with Model 2. The results of Model 3 are illustrated in Figures 3-72 through 3-95 and Tables 3-23 through 3-25.

3.5.3.1 Hysteretic Response

The hysteretic response base shear-displacement response at the center of cap beam are shown in Figures 3-72 to 3-79. The maximum base shear and displacement for 100% and 150% design motions in the longitudinal and transverse direction are summarized in Table 3-23.

3.5.3.2 Displacement Response Histories

Table 3-24 shows the maximum displacement and corresponding drift at the center of cap beam for all ground motions. The maximum longitudinal and transverse displacement are also presented in Figures 3-80 to 3-87 corresponding to seismic excitations scaled to two intensity levels, 100% and 150% of design motions. From the figures, it can be observed that the displacements at the top of all five columns are almost identical. The displacements varied from 4.4 in. (1.47% drift) to 11.3 in. (3.7% drift) along the longitudinal direction and 4.3 in. (1.43% drift) to 11.7 in. (3.9% drift) along the transverse direction for 100% design earthquake. In the longitudinal direction, the maximum displacements were 11.3 in. for the Design Level and 19.4 in. for MCE level. In the transverse direction, the maximum displacements of 11.7 in. and 16.7 in. were observed for design and MCE level earthquakes. At the Design Level, the transverse

displacement is higher than that of the longitudinal displacement. This trend was reversed at MCE Level.

3.5.3.3 Behavior of Headed Anchors

The forces and displacements in the links are presented along the longitudinal direction of the girders. Negligible difference between the force and displacement profile of the links were observed among 14 girders. Therefore, only the results for girder 7 are presented in Table 3-25. The maximum forces and displacements are also shown in Figures 3-88 to 3-95. The response is plotted along the longitudinal span of the bridge. It can be seen that the anchor displacements were negligible. From the figures, it can be ascertained that the peak link displacement occurred was close to the bent for all the eight earthquakes. The maximum force in the anchors when subjected to 100% design level and MCE level were 124 kips in longitudinal direction and 10.2 kips in transverse direction, which are substantially lower than the ultimate capacity of the connectors (375 kips).

Table 3-23 Maximum Base Shear and Displacement (Model 3)

Earthquake	Station	RSN	Scale	Transverse		Longitudinal	
				Displacement (in)	Base Shear (kips)	Displacement (in)	Base Shear (kips)
Imperial Valley-06	Delta	169	1	4.34	1800.15	10.66	2000.67
Loma Prieta	Hollister Differential Array	778		5.77	1969.09	4.38	1608.69
Northridge-01	LA - Saturn St	1003		6.73	1407.68	9.22	1965.62
Imperial Valley-06	Bonds Corner	160		6.48	1886.76	7.01	1878.35
Chalfant Valley-02	Zack Brothers Ranch	558		5.73	1850.58	7.57	1692.69
Loma Prieta	Capitola	752		11.65	2157.03	5.79	1630.87
Northridge-01	Rinaldi Receiving Sta	1063		10.13	1912.61	4.93	1617.77
Northridge-01	Sylmar - Converter Sta	1084		7.43	1755.84	11.26	1925.16
Imperial Valley-06	Delta	169	1.5	7.11	1903.75	18.88	2012.54
Loma Prieta	Hollister Differential Array	778		10.22	1935.22	8.69	1760.92
Northridge-01	LA - Saturn St	1003		9.33	1807.33	9.25	1965.82
Imperial Valley-06	Bonds Corner	160		12.30	2113.18	9.13	1885.82
Chalfant Valley-02	Zack Brothers Ranch	558		8.38	1926.60	8.80	1685.69
Loma Prieta	Capitola	752					
Northridge-01	Rinaldi Receiving Sta	1063		16.74	2001.98	7.81	1418.86
Northridge-01	Sylmar - Converter Sta	1084		8.22	1814.53	13.32	1757.48

Table 3-24 Maximum Displacement and Drift (%) (Model 3)

Earthquake	Station Name	RSN	Scale	Max. Transverse Displacement (in)	Drift (%)	Max. Longitudinal Displacement (in)	Drift (%)
Imperial Valley-06	Delta	169	1	4.3	1.43	10.8	3.60
Loma Prieta	Hollister Differential Array	778		5.8	1.93	4.4	1.47
Northridge-01	LA - Saturn St	1003		6.7	2.23	9.2	3.07
Imperial Valley-06	Bonds Corner	160		6.5	2.17	7.1	2.37
Chalfant Valley-02	Zack Brothers Ranch	558					
Loma Prieta	Capitola	752		11.7	3.90	5.9	1.97
Northridge-01	Rinaldi Receiving Sta	1063		10.1	3.37	5.2	1.73
Northridge-01	Sylmar - Converter Sta	1084		7.4	2.47	11.3	3.77
Imperial Valley-06	Delta	169					
Imperial Valley-06	Delta	169	1.5	7.1	2.37	19.4	6.47
Loma Prieta	Hollister Differential Array	778		10.2	3.40	8.8	2.93
Northridge-01	LA - Saturn St	1003		9.3	3.10	9.3	3.10
Imperial Valley-06	Bonds Corner	160		12.3	4.10	9.2	3.07
Chalfant Valley-02	Zack Brothers Ranch	558		8.4	2.80	8.8	2.93
Loma Prieta	Capitola	752					
Northridge-01	Rinaldi Receiving Sta	1063		16.7	5.57	8	2.67
Northridge-01	Sylmar - Converter Sta	1084		8.2	2.73	13.7	4.57

Table 3-25 Maximum Link Force and Displacement (Model 3)

Earthquake	Station	RSN	Scale	Transverse		Longitudinal	
				Maximum Displacement (in)	Maximum Force (kips)	Maximum Displacement (in)	Maximum Force (kips)
Imperial Valley-06	Delta	169	1	0.02	9.93	0.10	113.30
Loma Prieta	Hollister Differential Array	778		0.02	10.20	0.10	113.10
Northridge-01	LA - Saturn St	1003		0.02	9.85	0.10	115.70
Imperial Valley-06	Bonds Corner	160		0.02	10.20	0.11	118.50
Chalfant Valley-02	Zack Brothers Ranch	558		0.02	9.78	0.09	112.00
Loma Prieta	Capitola	752		0.02	10.20	0.10	114.20
Northridge-01	Rinaldi Receiving Sta	1063		0.02	10.14	0.09	111.44
Northridge-01	Sylmar - Converter Sta	1084		0.02	9.89	0.09	112.20
Imperial Valley-06	Delta	169		1.5	0.02	10.00	0.11
Loma Prieta	Hollister Differential Array	778	0.02		10.23	0.09	112.60
Northridge-01	LA - Saturn St	1003	0.02		10.05	0.11	117.90
Imperial Valley-06	Bonds Corner	160	0.03		10.30	0.13	123.70
Chalfant Valley-02	Zack Brothers Ranch	558	0.02		9.90	0.10	114.10
Loma Prieta	Capitola	752					
Northridge-01	Rinaldi Receiving Sta	1063	0.03		10.26	0.09	111.52
Northridge-01	Sylmar - Converter Sta	1084	0.02		10.10	0.10	113.80

3.5.4 Comparison of Model 1, 2 and 3

3.5.4.1 Hysteretic Response

The hysteresis loop for Models 1, 2 and 3 are shown in Figures 3-96 through 3-110. From the hysteresis loop, it can be observed that all three models show similar seismic behavior. All three models show inelastic response of the bridge substructure.

3.5.4.2 Displacement Response Histories

Negligible difference was observed in the displacement at the top of the columns among the models with connectors spaced at 4 ft (Model 2) and 6 ft (Model 3). The results are not presented herein.

3.5.4.3 Behavior of Headed Anchors

The behavior of the headed anchors when placed at the spacing of 4 ft and 6 ft was determined by comparing the link force and displacement results from Model 2 and Model 3. Tables 3-26 and 3-27 present the maximum force and displacement in the link in Model 2 and 3 in longitudinal and transverse direction, respectively. No significant difference was observed in the link element representing the headed anchors between Models 2 and 3. A significant increase in the forces in the link element was observed between these models in the longitudinal direction. The maximum link forces in the longitudinal direction increased from 83 kips to 124 kips, when the link spacing was increased from 4 ft to 6 ft. In the transverse direction, the maximum forces increased from 7.2 kips to 10.2 kips. In both models, the maximum link forces were lower than the ultimate strength by at least 67% in the longitudinal direction and 97% in the transverse

direction. Therefore, there was no failure in the link element under MCE motion level even when the spacing was increased to 6 ft.

Table 3-26 Comparison of Maximum Link Force and Displacement in Model 2 and 3 in Longitudinal Direction

Earthquake	Station	RSN	Scale	Model 2		Model 3	
				Maximum Displacement (in)	Maximum Force (kips)	Maximum Displacement (in)	Maximum Force (kips)
Imperial Valley-06	Delta	169	1	0.10	75.90	0.10	113.30
Loma Prieta	Hollister Differential Array	778		0.10	75.80	0.10	113.10
Northridge-01	LA - Saturn St	1003		0.11	77.50	0.10	115.70
Imperial Valley-06	Bonds Corner	160		0.12	79.50	0.11	118.50
Chalfant Valley-02	Zack Brothers Ranch	558		0.09	75.00	0.09	112.00
Loma Prieta	Capitola	752		0.10	76.50	0.10	114.20
Northridge-01	Rinaldi Receiving Sta	1063		0.09	74.50	0.09	111.44
Northridge-01	Sylmar - Converter Sta	1084		0.09	75.10	0.09	112.20
Imperial Valley-06	Delta	169		1.5	0.11	77.80	0.11
Loma Prieta	Hollister Differential Array	778	0.09		75.50	0.09	112.60
Northridge-01	LA - Saturn St	1003	0.12		79.40	0.11	117.90
Imperial Valley-06	Bonds Corner	160	0.14		82.90	0.13	123.70
Chalfant Valley-02	Zack Brothers Ranch	558	0.10		76.50	0.10	114.10
Loma Prieta	Capitola	752	0.13		81.50		
Northridge-01	Rinaldi Receiving Sta	1063	0.09		74.60	0.09	111.52
Northridge-01	Sylmar - Converter Sta	1084	0.10		76.20	0.10	113.80

Table 3-27 Comparison of Maximum Link Force and Displacement in Model 2 and 3 in Transverse Direction

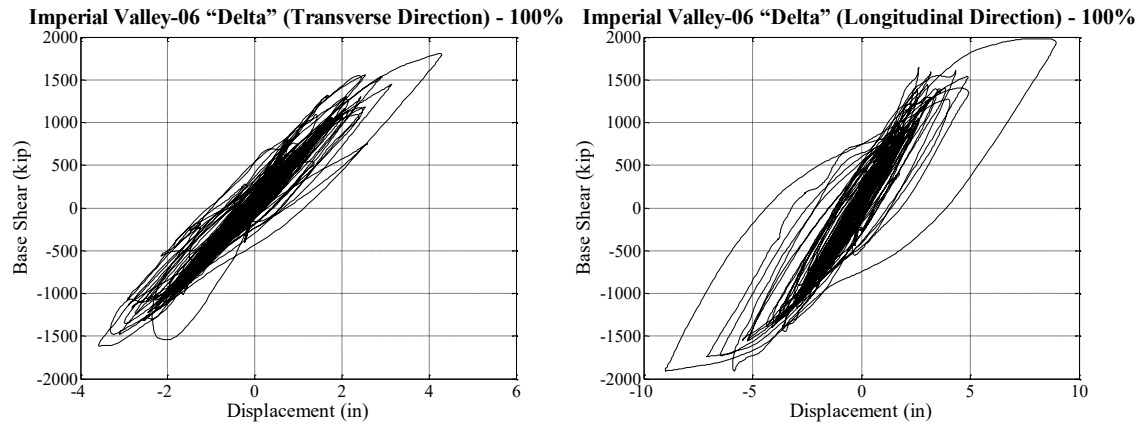
Earthquake	Station	RSN	Scale	Model 2		Model 3	
				Maximum Displacement (in)	Maximum Force (kips)	Maximum Displacement (in)	Maximum Force (kips)
Imperial Valley-06	Delta	169	1	0.02	6.80	0.02	9.93
Loma Prieta	Hollister Differential Array	778		0.02	6.95	0.02	10.20
Northridge-01	LA - Saturn St	1003		0.02	6.70	0.02	9.85
Imperial Valley-06	Bonds Corner	160		0.02	6.92	0.02	10.20
Chalfant Valley-02	Zack Brothers Ranch	558		0.01	6.70	0.02	9.78
Loma Prieta	Capitola	752		0.02	6.73	0.02	10.20
Northridge-01	Rinaldi Receiving Sta	1063		0.02	6.90	0.02	10.14
Northridge-01	Sylmar - Converter Sta	1084		0.01	6.75	0.02	9.89
Imperial Valley-06	Delta	169		1.5	0.02	6.80	0.02
Loma Prieta	Hollister Differential Array	778	0.02		7.00	0.02	10.23
Northridge-01	LA - Saturn St	1003	0.02		6.80	0.02	10.05
Imperial Valley-06	Bonds Corner	160	0.02		7.04	0.03	10.30
Chalfant Valley-02	Zack Brothers Ranch	558	0.02		6.73	0.02	9.90
Loma Prieta	Capitola	752	0.02		7.18		
Northridge-01	Rinaldi Receiving Sta	1063	0.02		7.00	0.03	10.26
Northridge-01	Sylmar - Converter Sta	1084	0.02		6.90	0.02	10.10

3.6 Concluding Remarks

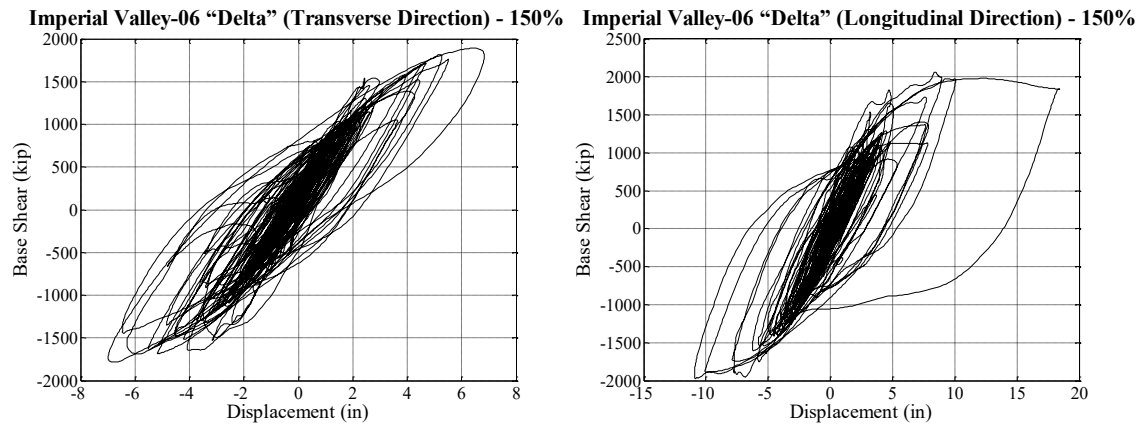
This chapter presented a numerical study to investigate the seismic response of headed anchors placed at two different pocket spacing of 4 ft and 6 ft. For this purpose, the number of headed anchors was first designed for live load and seismic forces, and later analyzed for eight different ground motions. The headed anchors were designed to resist the interface shear due to live load and the seismic forces generated in the deck. Headed anchors were designed for the maximum shear that was developed for two pocket spacing of 4 ft and 6 ft when the bridge is subjected to dead load and live load. Based on the interface shear demand, 12-#5 and 18-#5 headed anchors were required for the pocket spacing of 4 ft and 6 ft, respectively. Three finite element models with different properties of link element representing the headed anchors were analyzed. A rigid link element connection between the deck and girders was used in first model (Model 1). The second (Model 2) and third (Model 3) models used a link element with a properties equivalent to the design number of headed anchors spaced at 4 ft and 6 ft, respectively. Response spectrum analysis was performed on the models using design response spectrum.

The nonlinear response history analysis was also performed in the 3 models using eight different ground motions corresponding to 100% design level and 150% MCE level. Insignificant difference was observed in the overall seismic behavior due to the increase in pocket spacing from 4 ft to 6 ft. The finite element models with 4 ft and 6 ft spacing with 12-#5 and 18-#5 headed anchors, respectively, were found to show similar overall seismic behavior. Their seismic response were also similar to the Model 1. The forces in the anchors were investigated due to the 100% design level and 150% MCE

level ground motions. It was observed that the forces in the headed anchors were lower than the ultimate strength of the connectors. Thus, no failure in headed anchors were observed in either models.



(a)



(b)

Figure 3-32 Hysteresis Loop for Imperial Valley-06 "Delta" - Model 1 (a) 100% (b) 150%

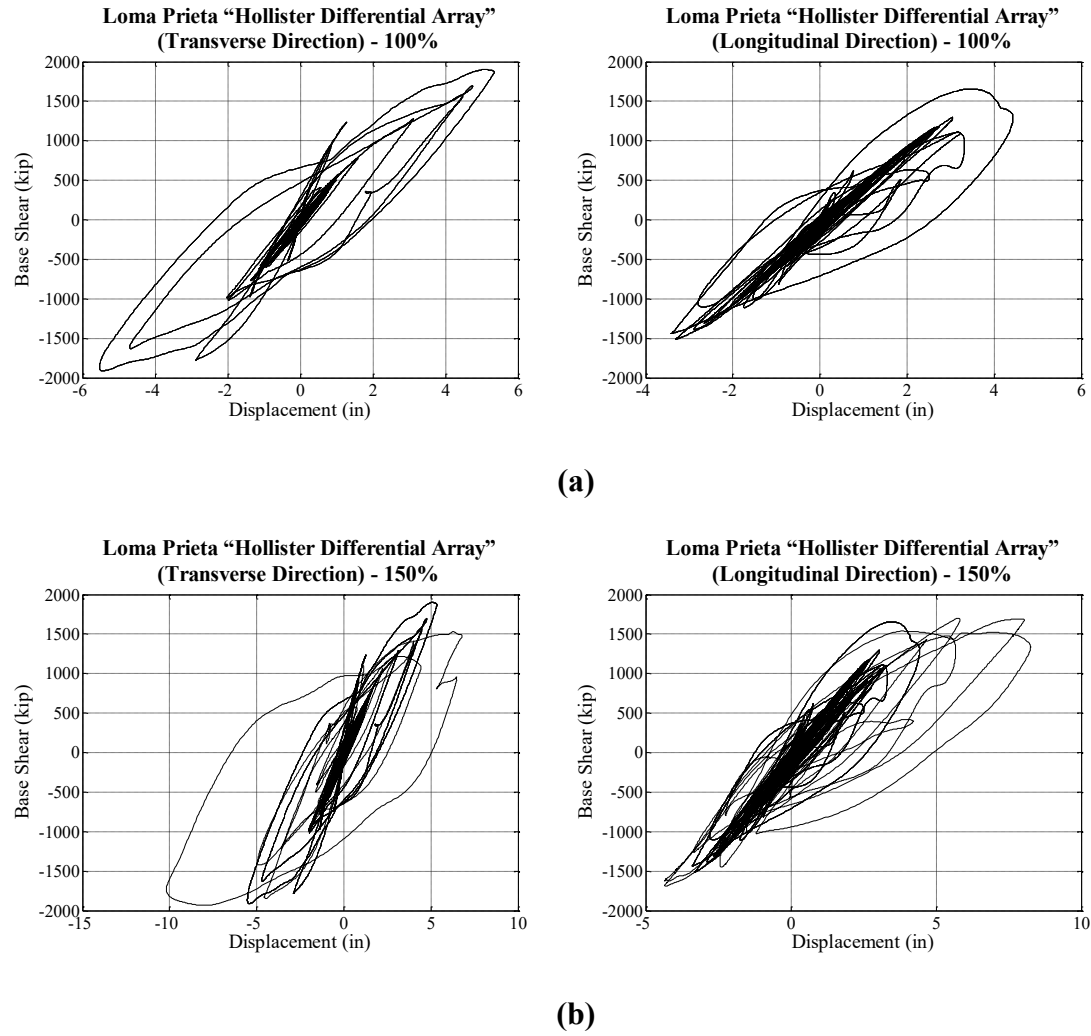
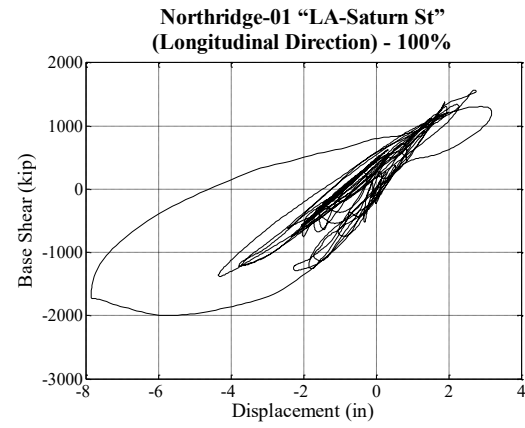
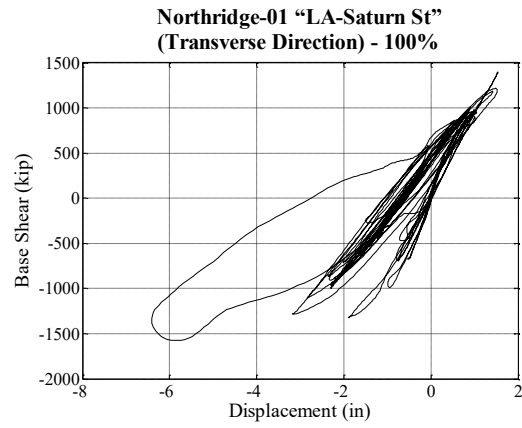
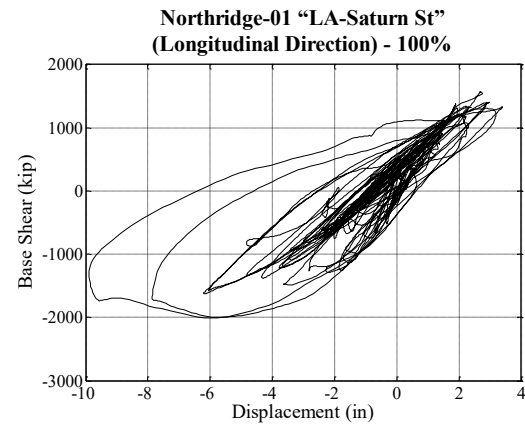
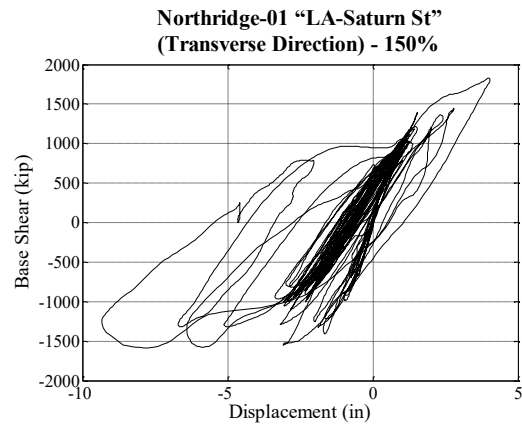


Figure 3-33 Hysteresis Loop for Loma Prieta "Hollister Differential Array" - Model 1 (a) 100% (b) 150%



(a)



(b)

Figure 3-34 Hysteresis Loop for Northridge-01 "LA-Saturn St" - Model 1 (a) 100% (b) 150%

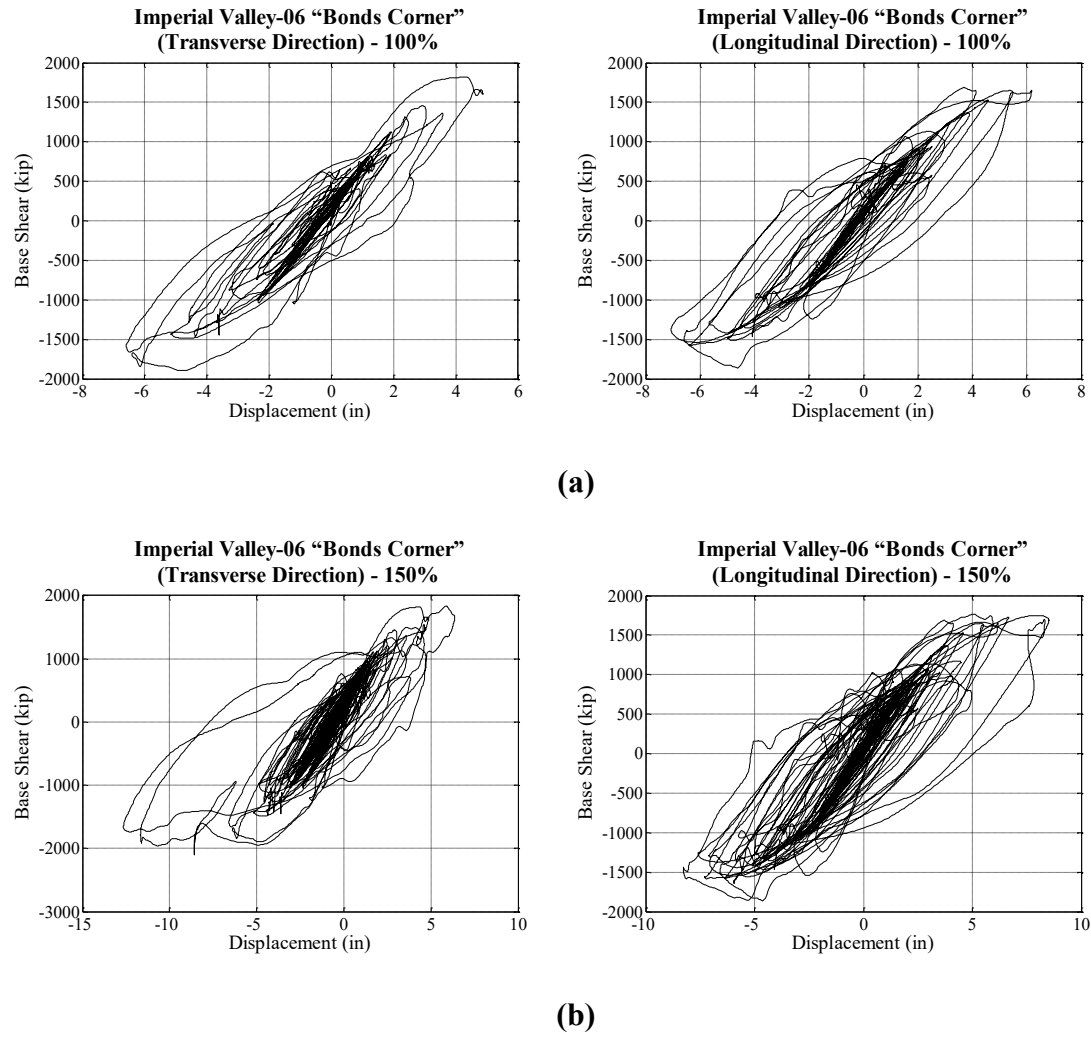


Figure 3-35 Hysteresis Loop for Imperial Valley-06 "Bonds Corner" - Model 1 (a) 100% (b) 150%

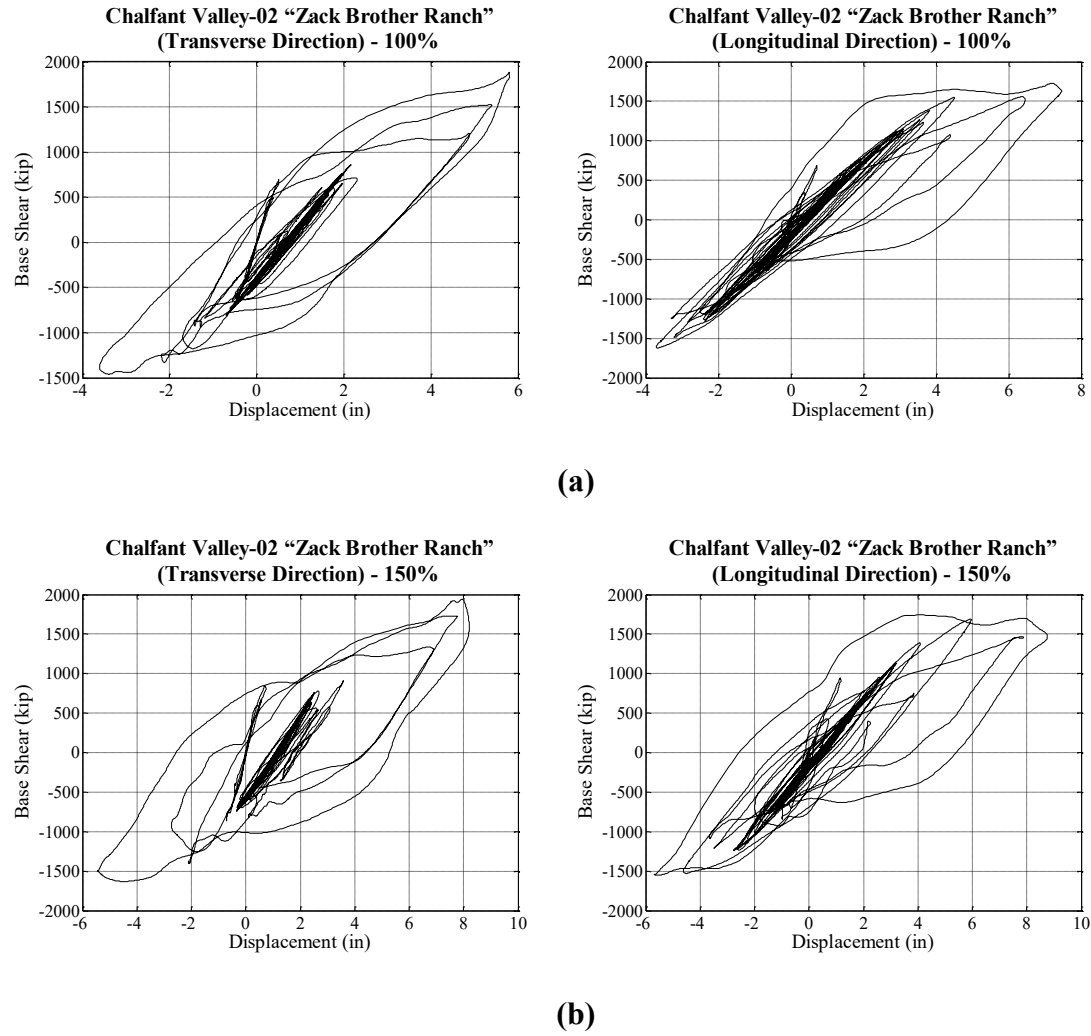
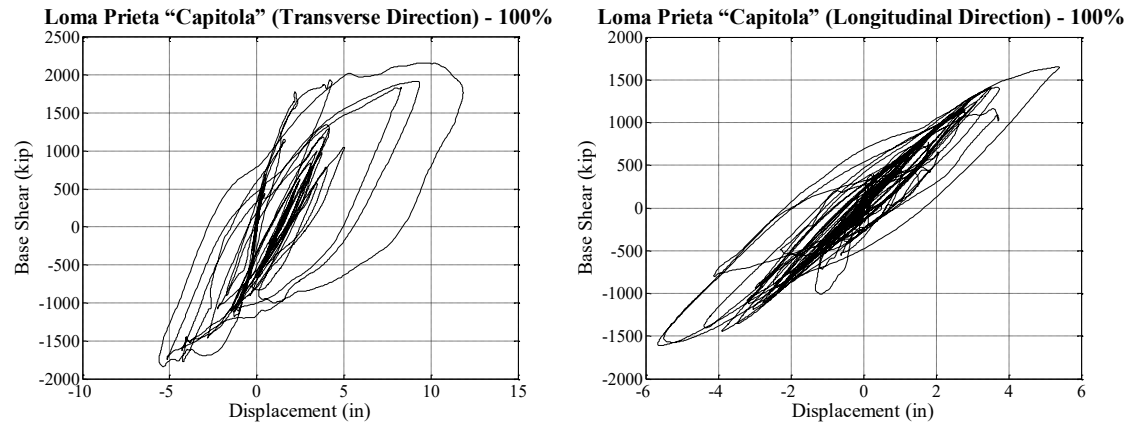
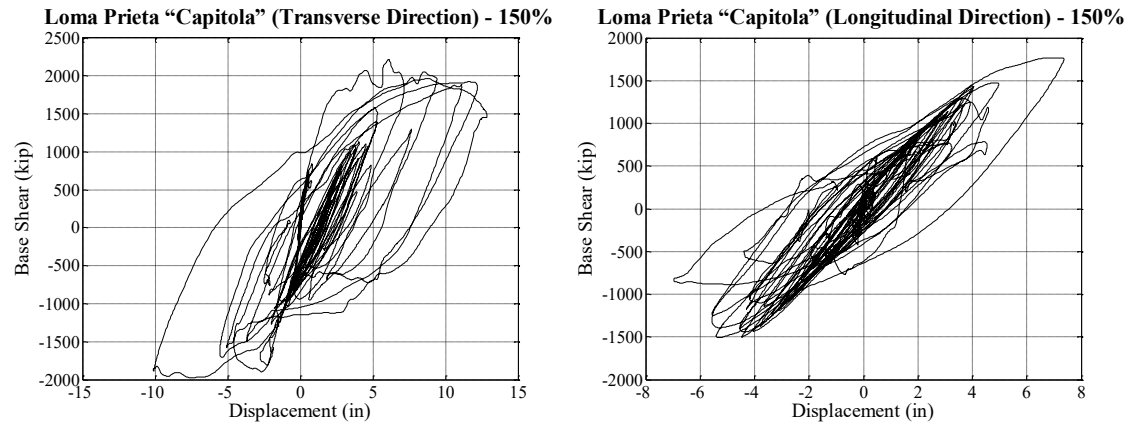


Figure 3-36 Hysteresis Loop for Chalfant Valley-02 "Zack Brother Ranch" - Model 1 (a) 100% (b) 150%



(a)



(b)

Figure 3-37 Hysteresis Loop for Loma Prieta "Capitola" - Model 1 (a) 100% (b) 150%

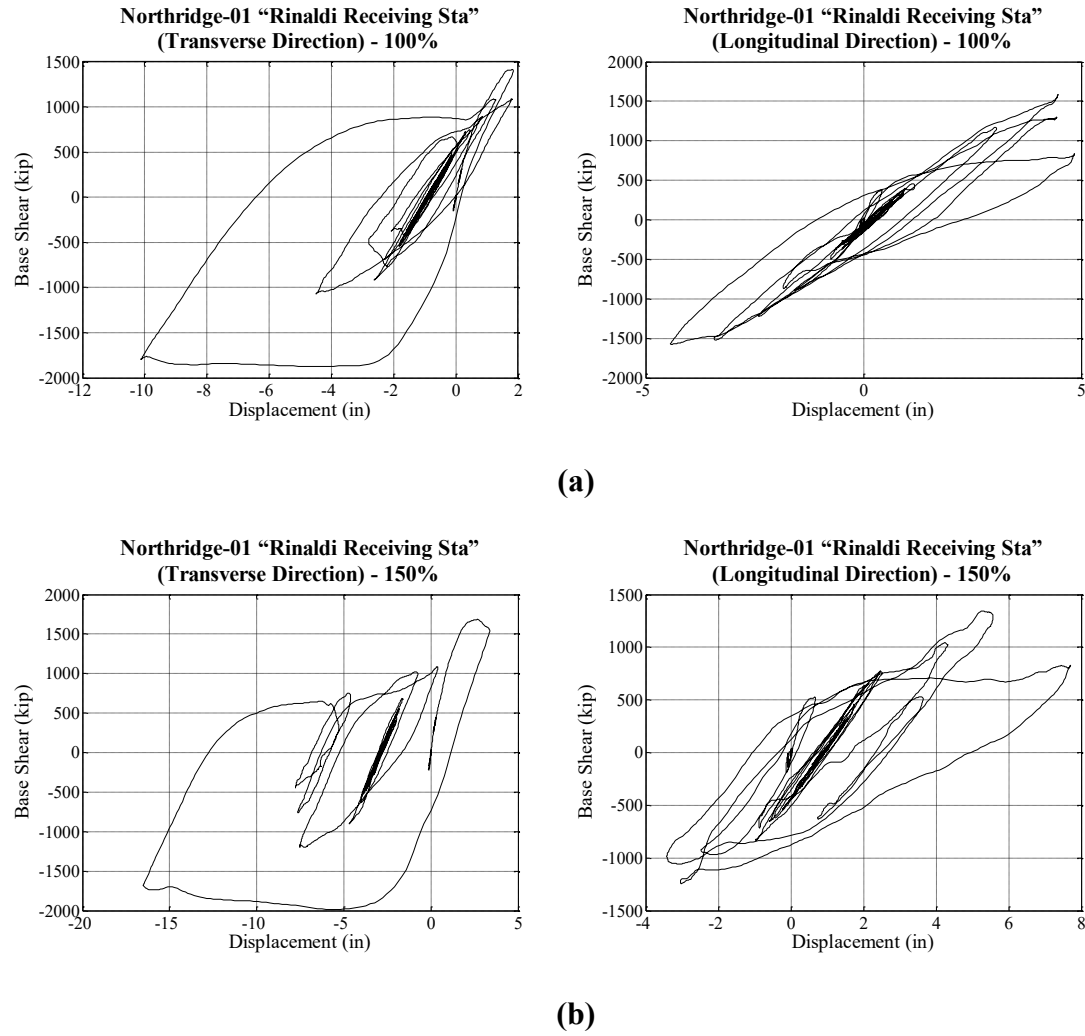


Figure 3-38 Hysteresis Loop for Northridge-01 "Rinaldi Receiving Sta" - Model 1 (a) 100% (b) 150%

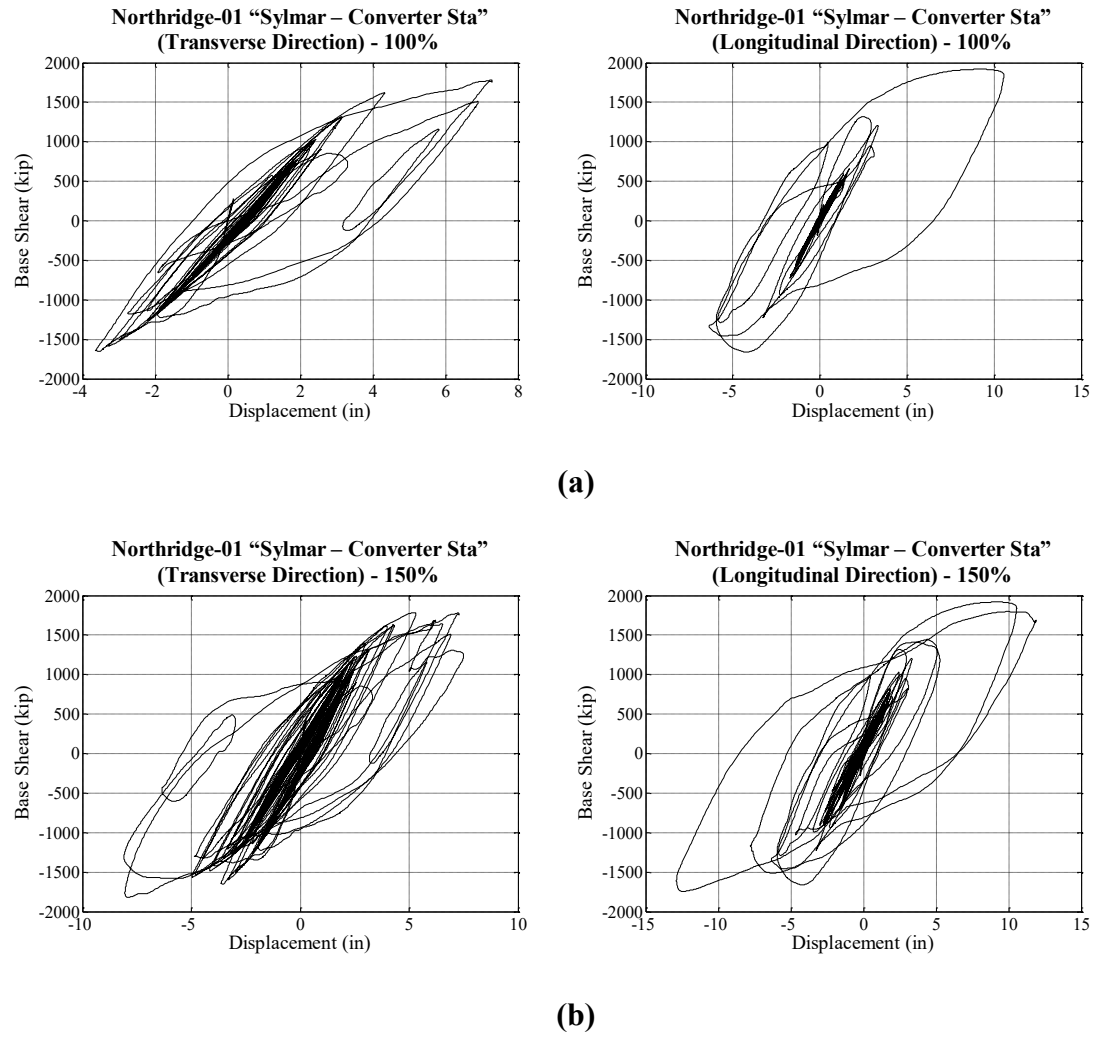
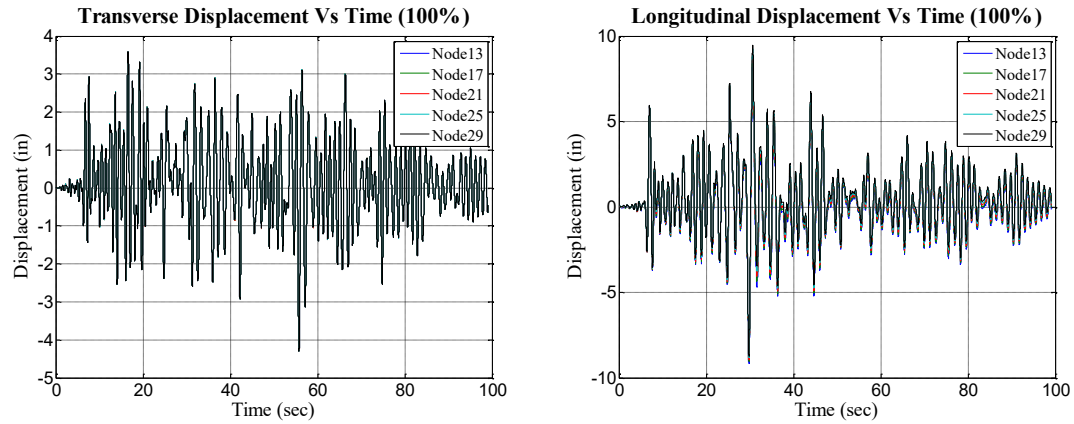
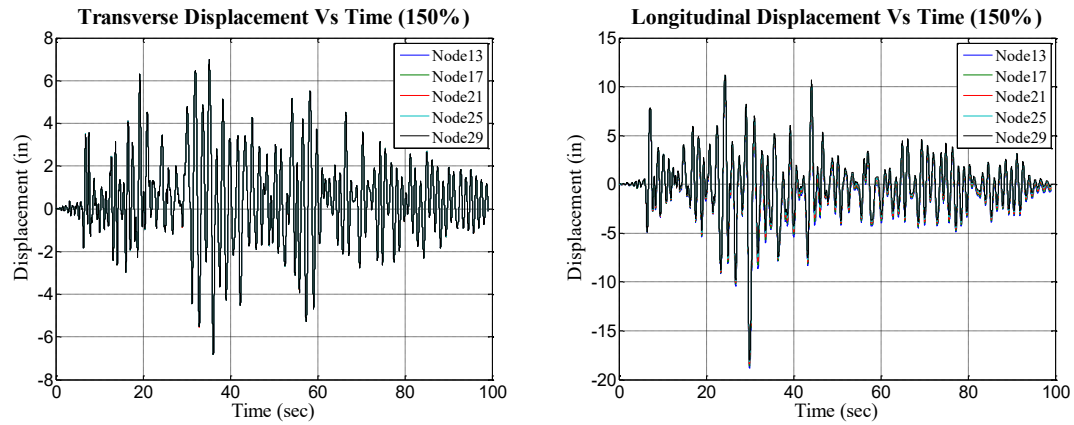


Figure 3-39 Hysteresis Loop for Northridge-01 "Sylmar-Converter Sta" - Model 1 (a) 100% (b) 150%

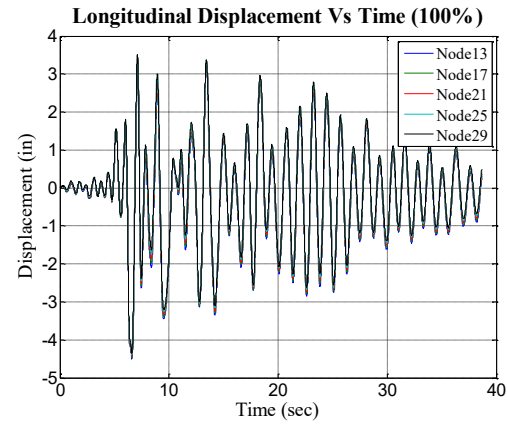
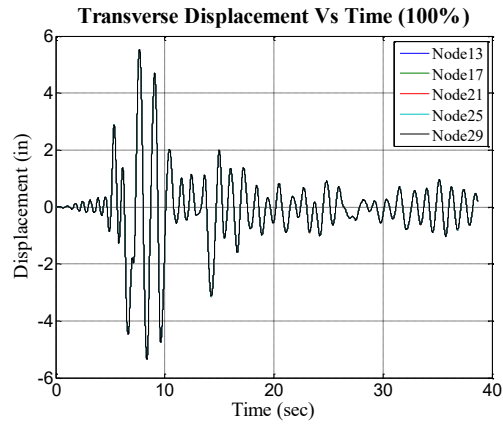


(a)

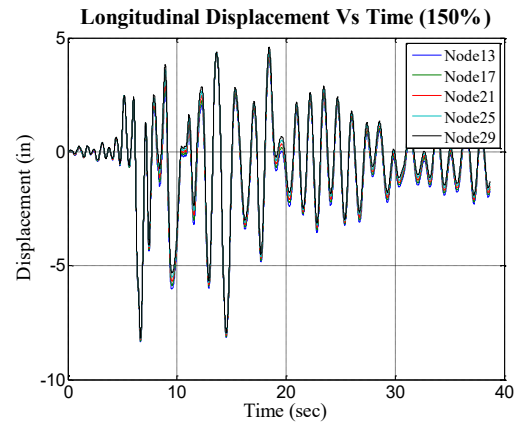
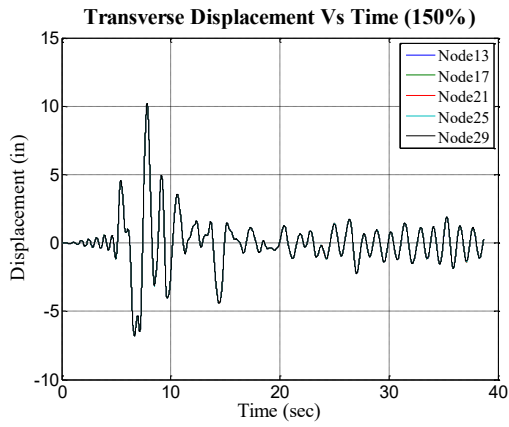


(b)

Figure 3-40 Displacement History for Imperial Valley-06 "Delta" - Model 1 (a) 100% (b) 150%

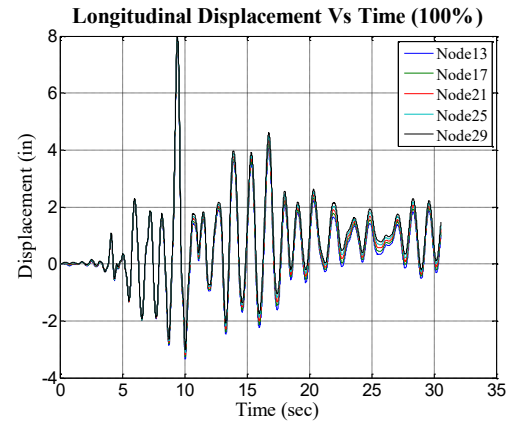
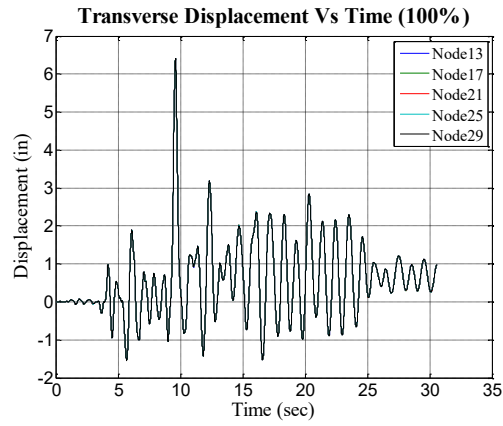


(a)

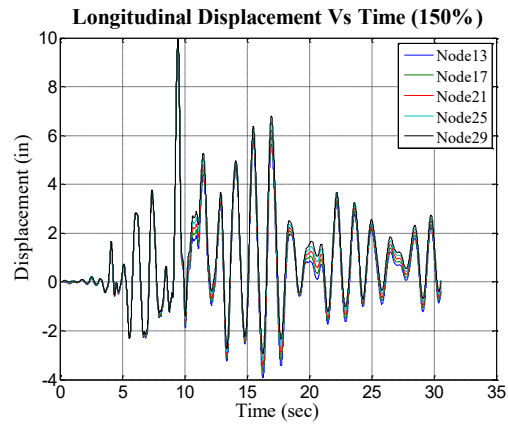
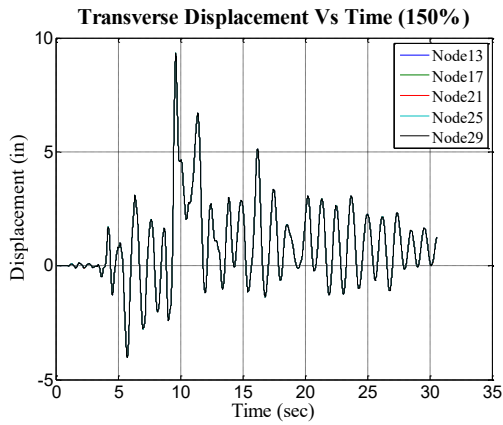


(b)

Figure 3-41 Displacement History for Loma Prieta "Hollister Differential Array" -Model 1 (a) 100% (b) 150%

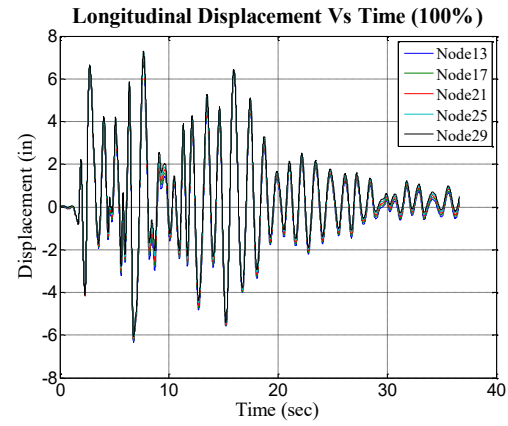
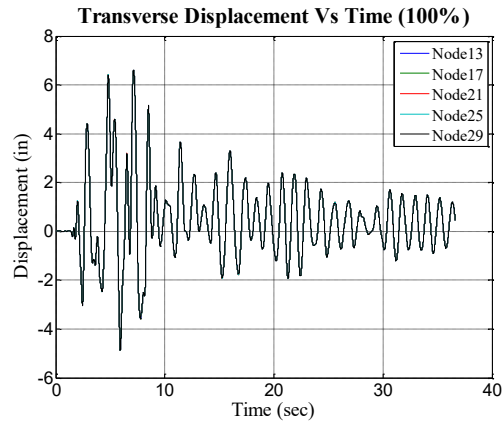


(a)

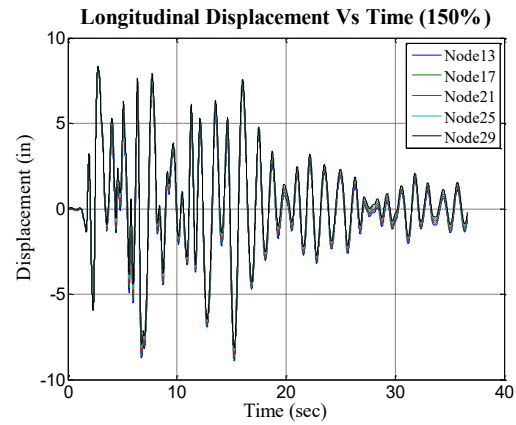
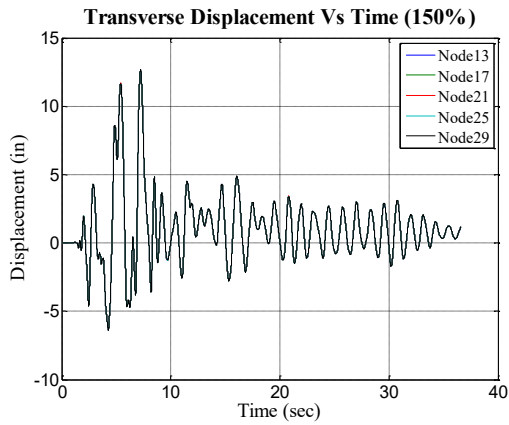


(b)

Figure 3-42 Displacement History for Northridge-01 "LA-Saturn St" - Model 1 (a) 100% (b) 150%

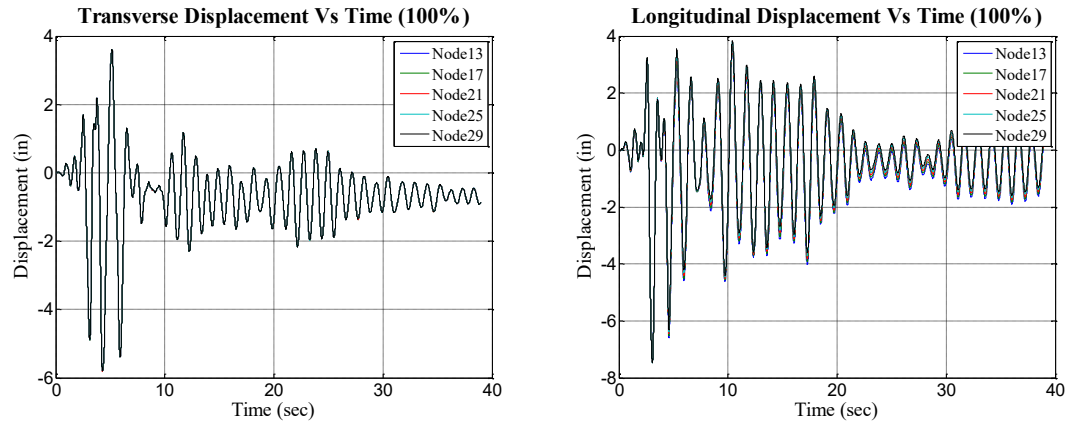


(a)

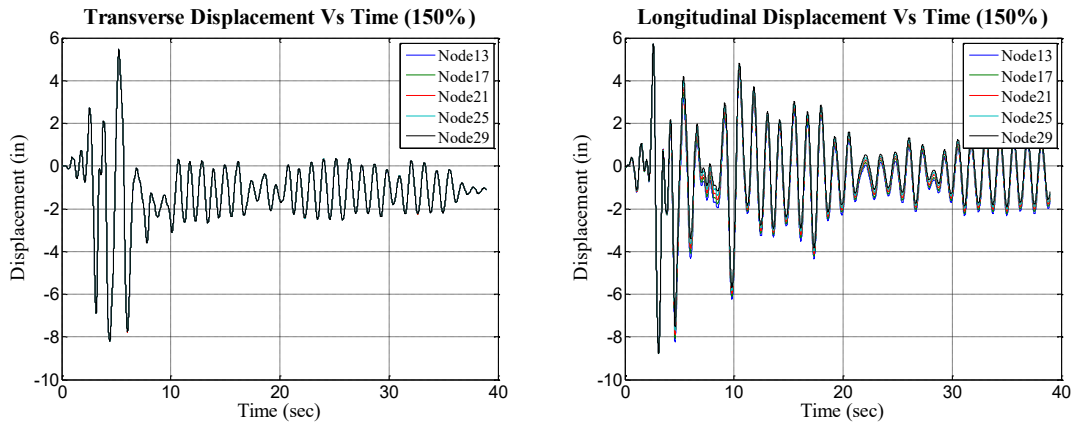


(b)

Figure 3-43 Displacement History for Imperial Valley-06 "Bonds Corner" - Model 1 (a) 100% (b) 150%

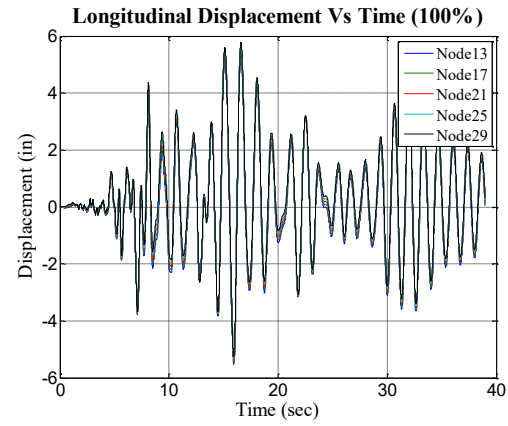
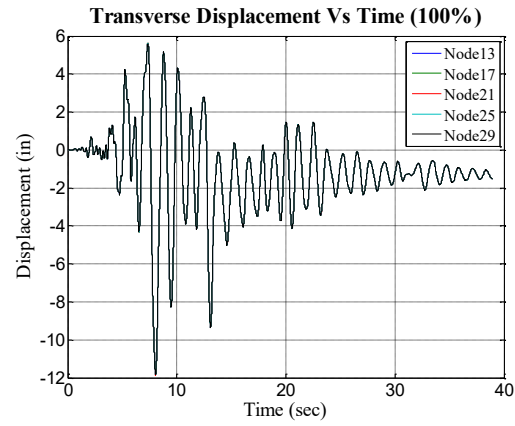


(a)

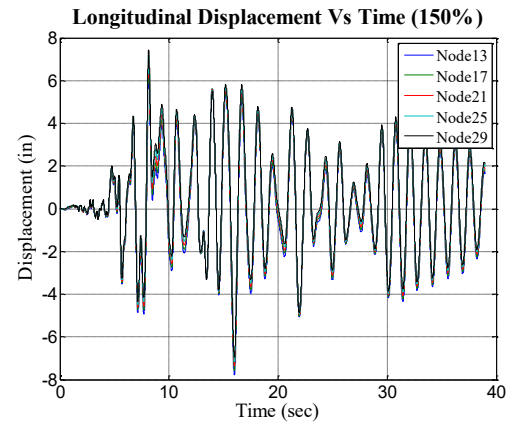
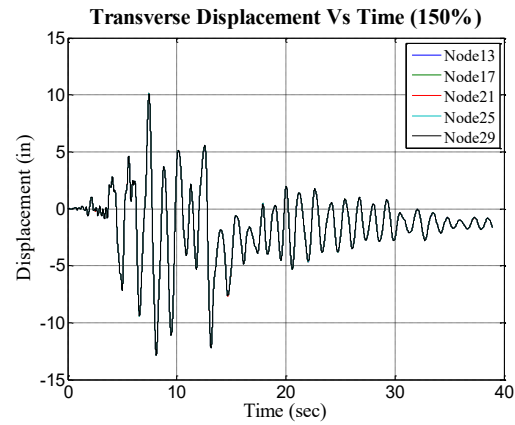


(b)

Figure 3-44 Displacement History for Chalfant Valley-02 "Zack Brother Ranch" -Model 1 (a) 100% (b) 150%

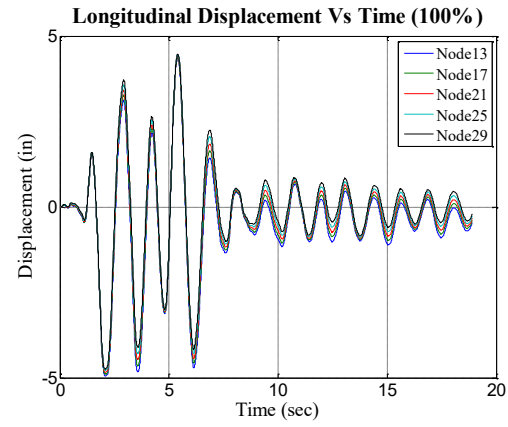
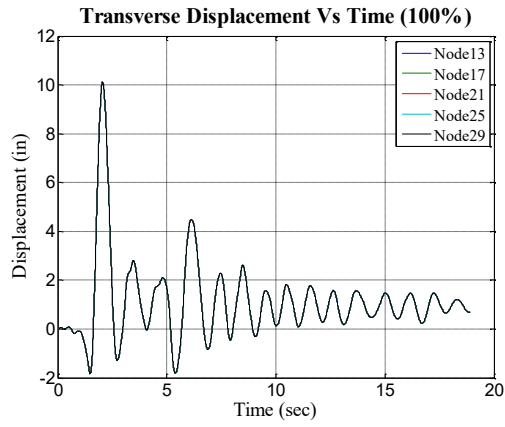


(a)

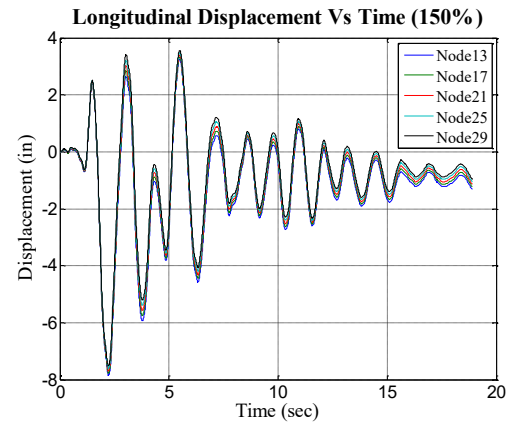
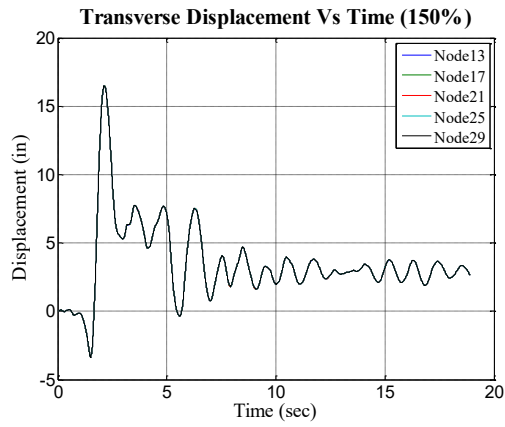


(b)

Figure 3-45 Displacement History for Loma Prieta "Capitola" - Model 1 (a) 100% (b) 150%

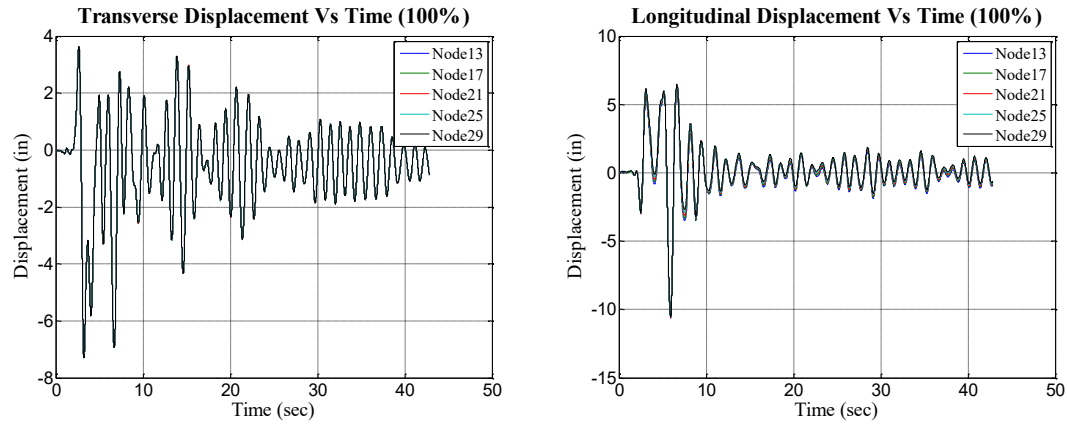


(a)

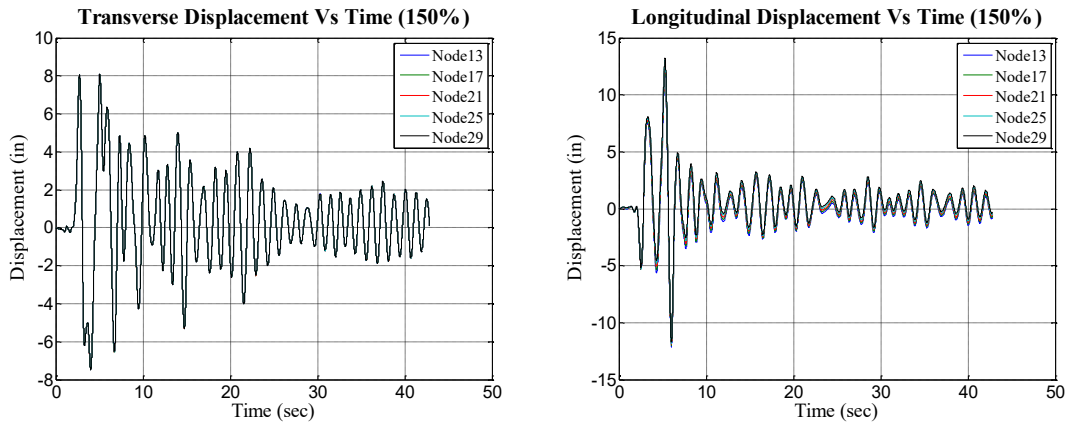


(b)

Figure 3-46 Displacement History for Northridge-01 "Rinaldi Receiving Sta" - Model 1 (a) 100% (b) 150%

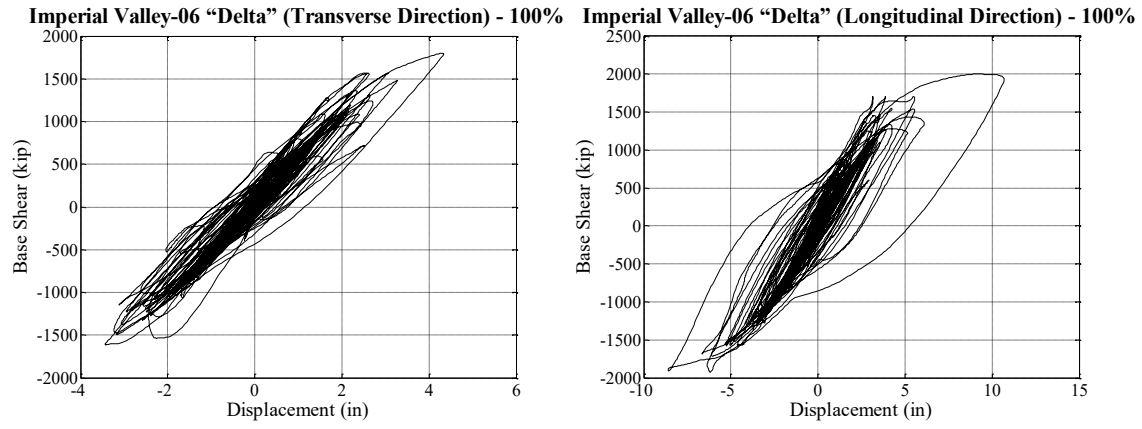


(a)

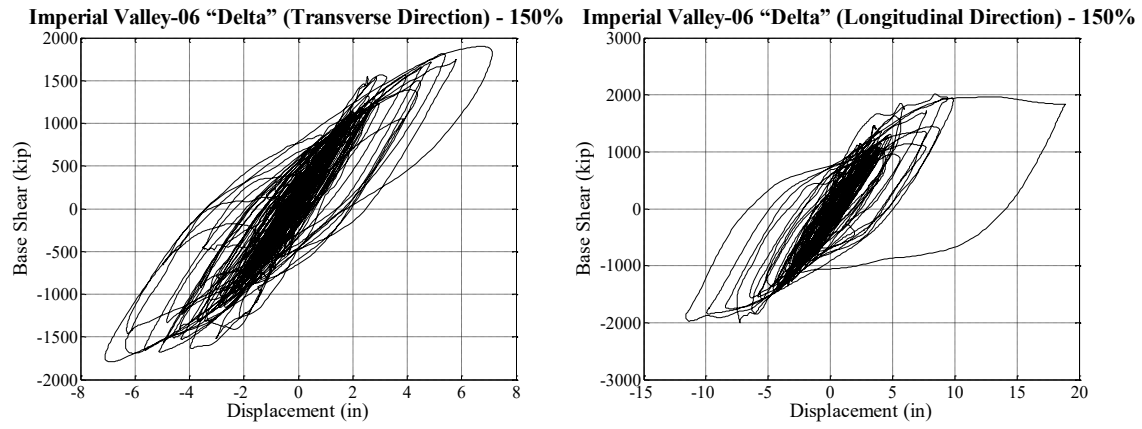


(b)

Figure 3-47 Displacement History for Northridge-01 "Sylmar-Converter Sta" - Model 1 (a) 100% (b) 150%



(a)



(b)

Figure 3-48 Hysteresis Loop for Imperial Valley-06 "Delta" - Model 2 (a) 100% (b) 150%

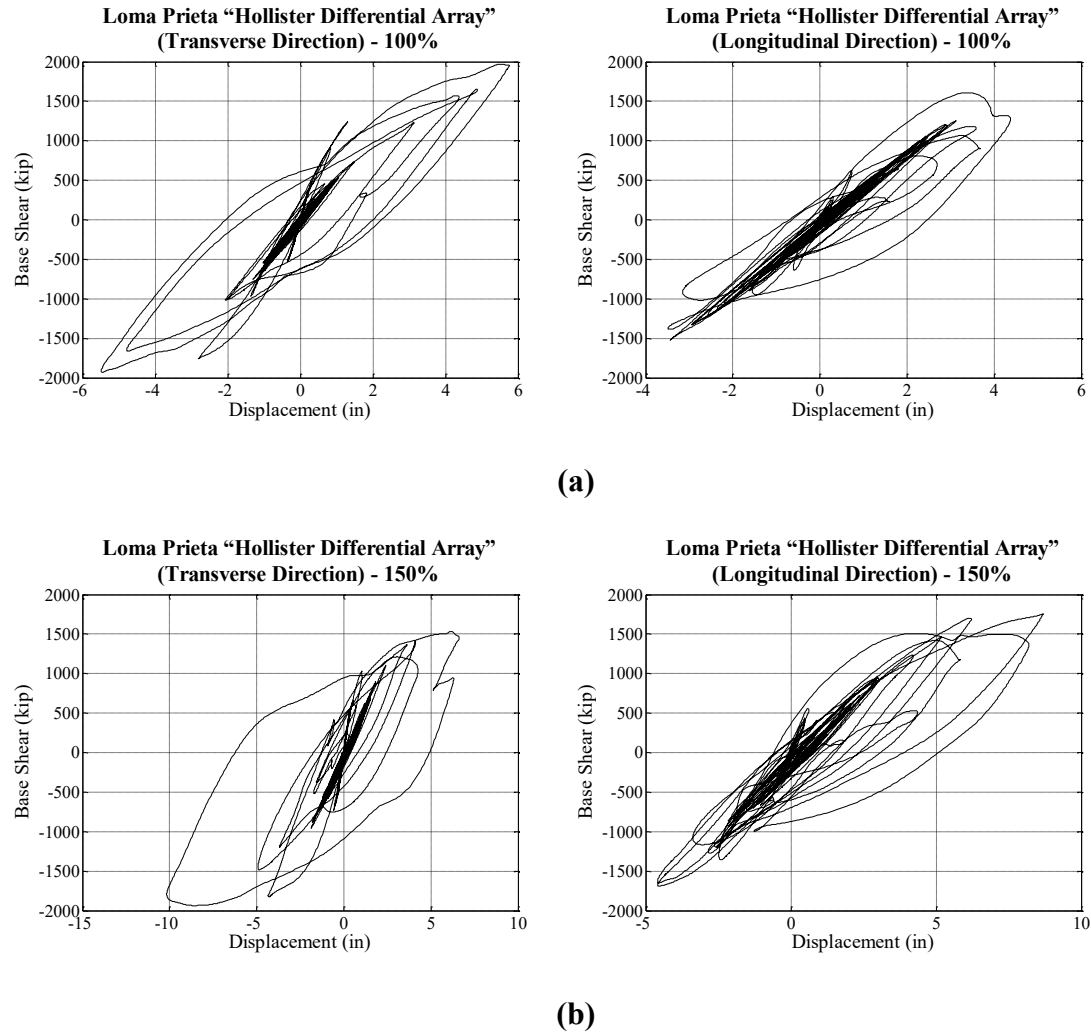


Figure 3-49 Hysteresis Loop for Loma Prieta "Hollister Differential Array" - Model 2 (a) 100% (b) 150%

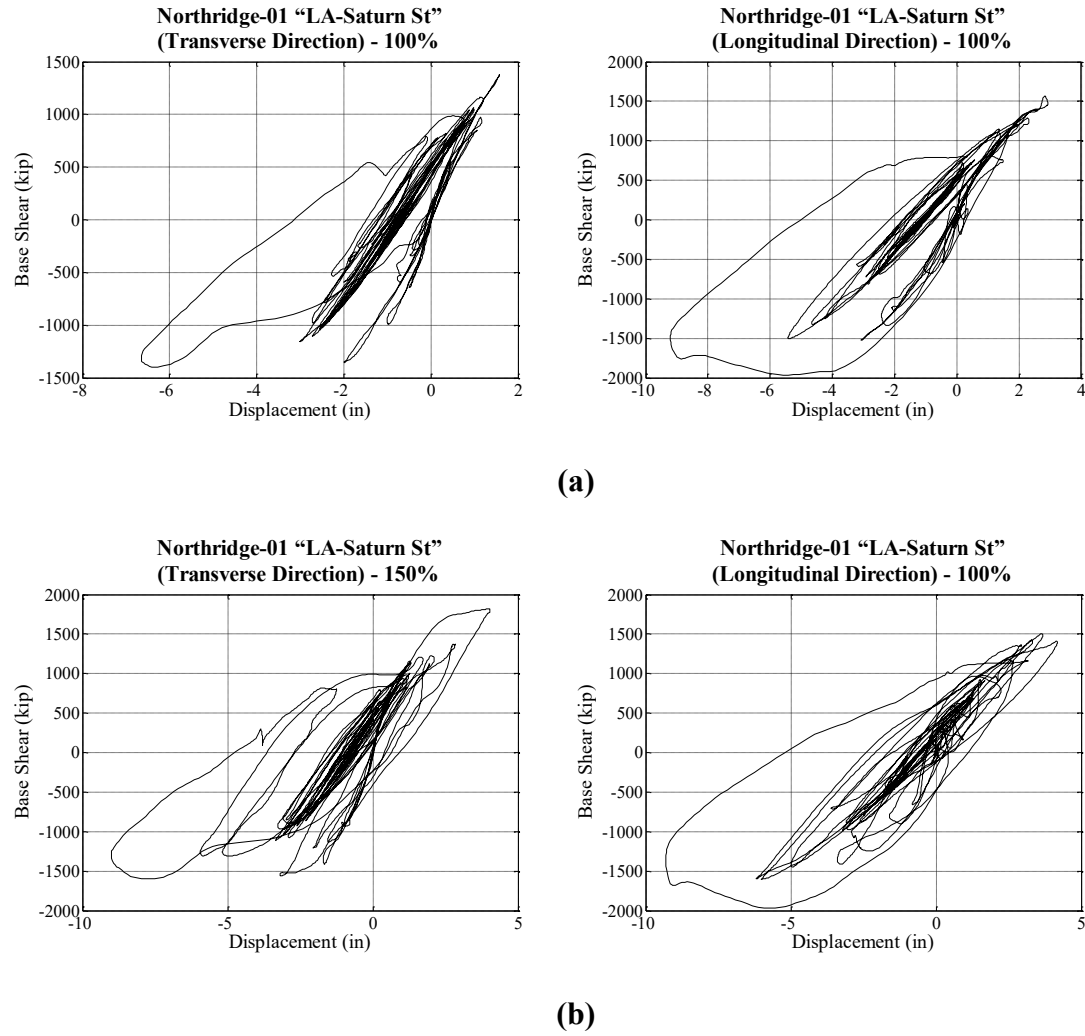


Figure 3-50 Hysteresis Loop for Northridge-01 "LA-Saturn St" - Model 2 (a) 100% (b) 150%

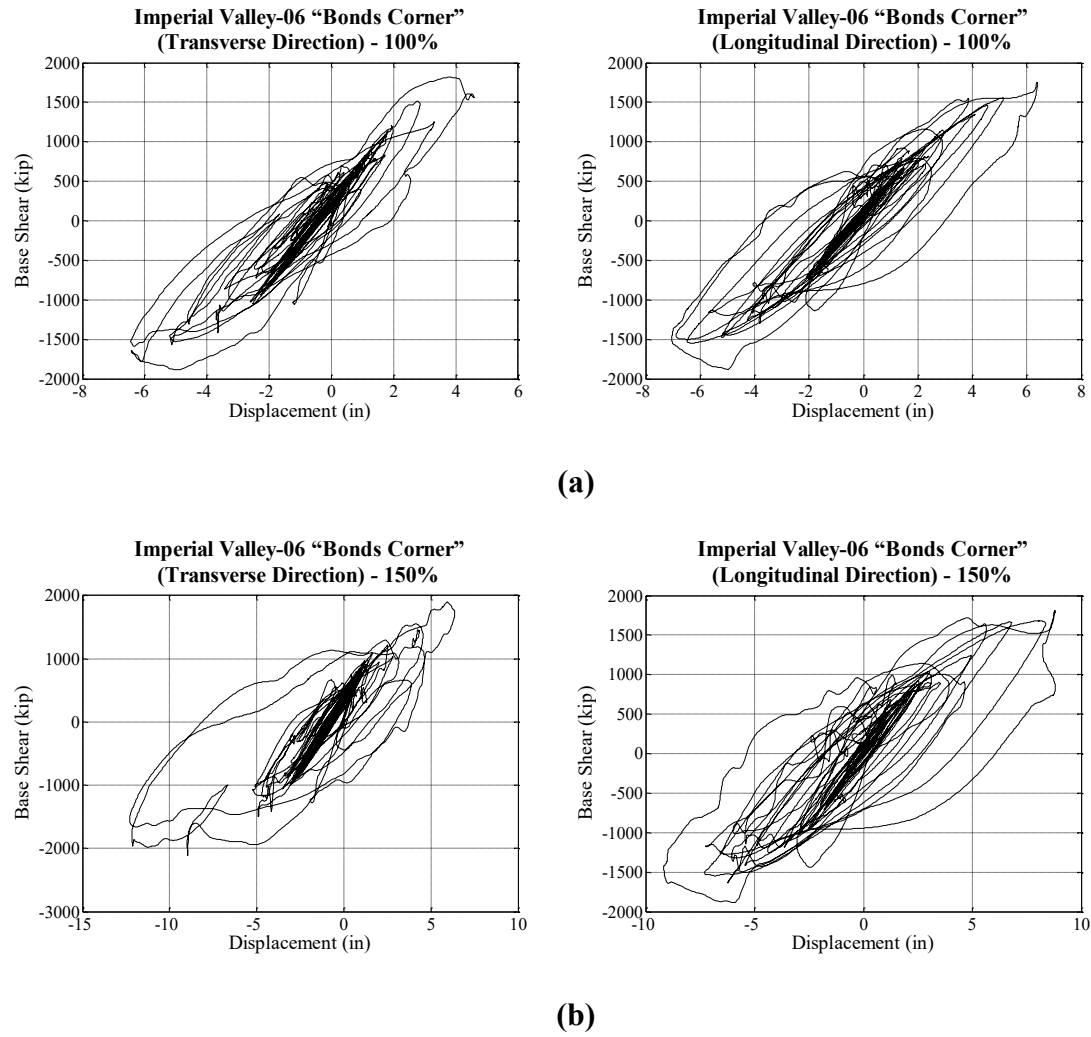


Figure 3-51 Hysteresis Loop for Imperial Valley-06 "Bonds Corner" - Model 2 (a) 100% (b) 150%

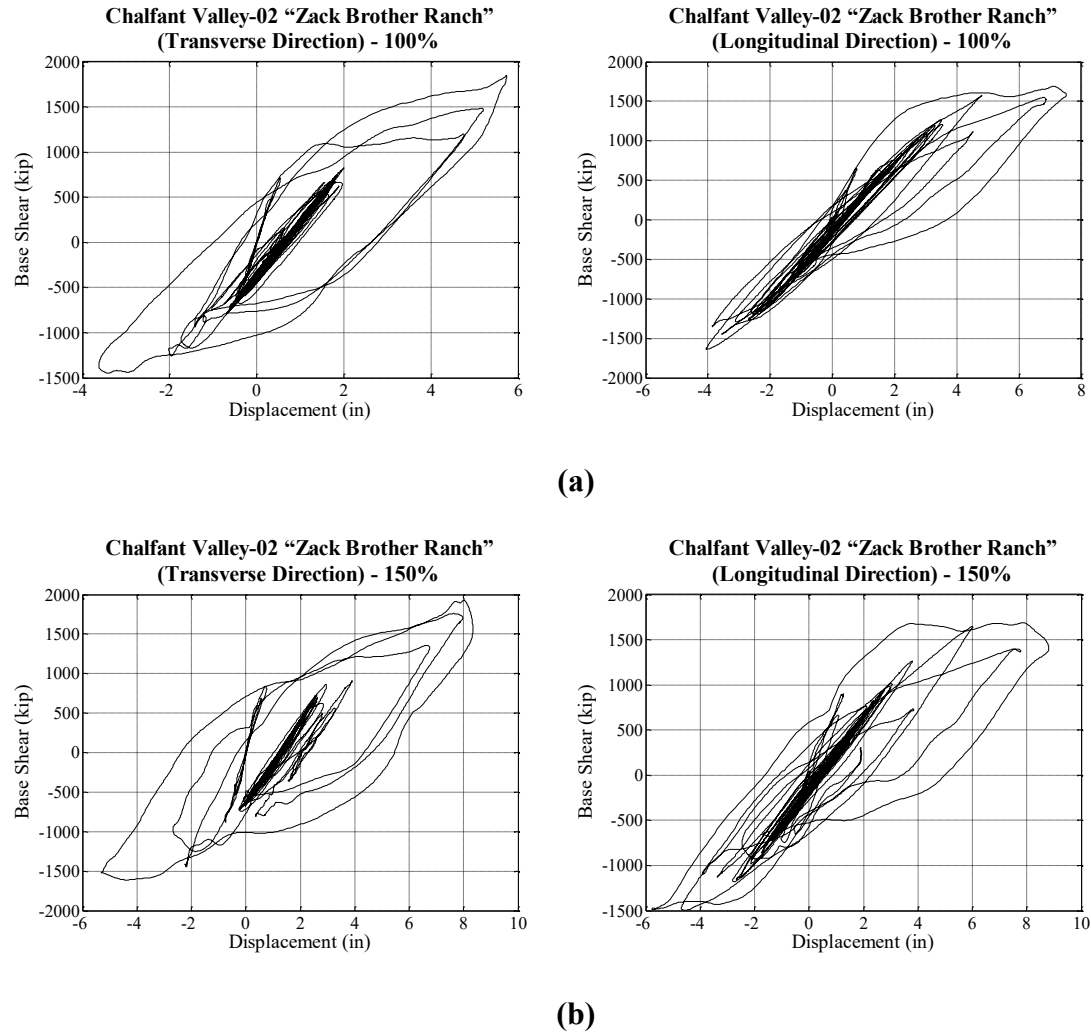
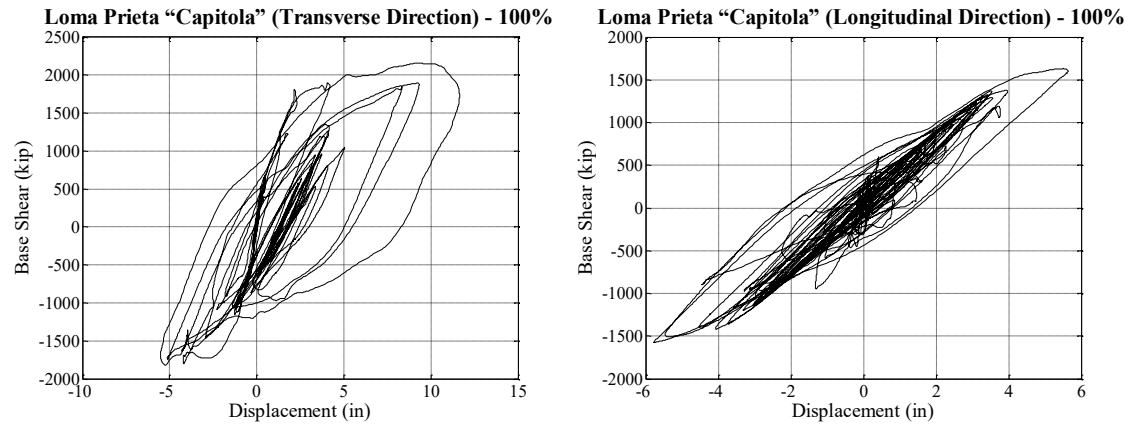
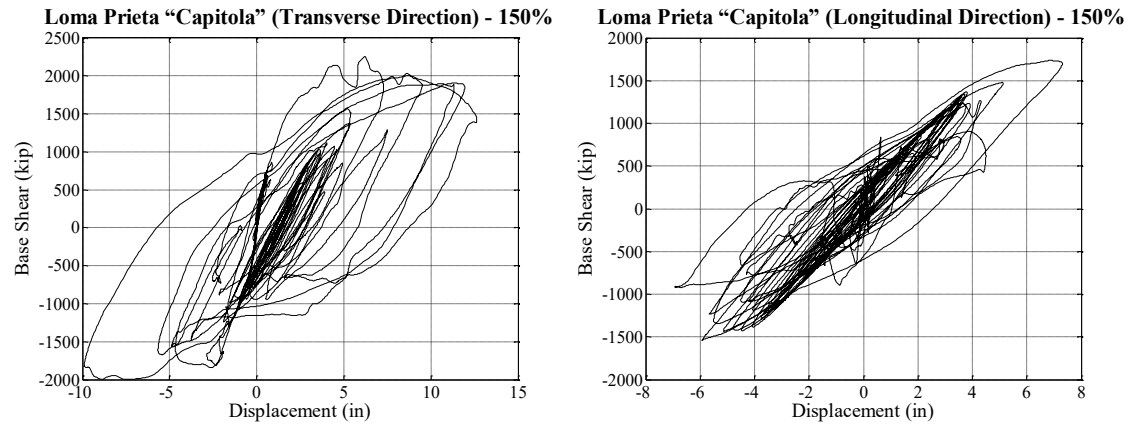


Figure 3-52 Hysteresis Loop for Chalfant Valley-02 "Zack Brother Ranch" - Model 2 (a) 100% (b) 150%

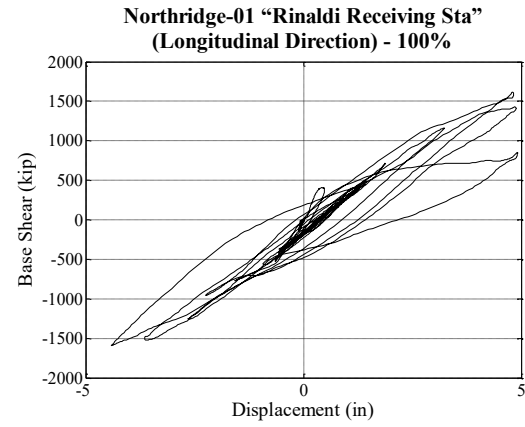
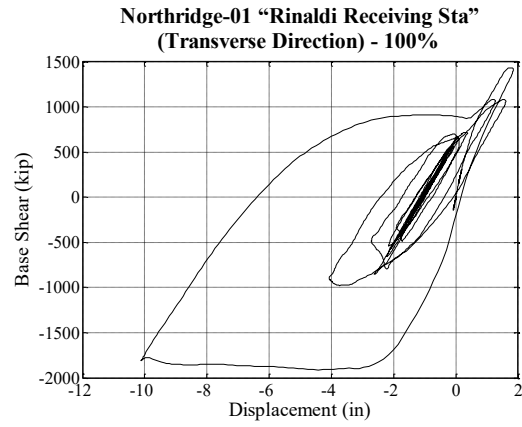


(a)

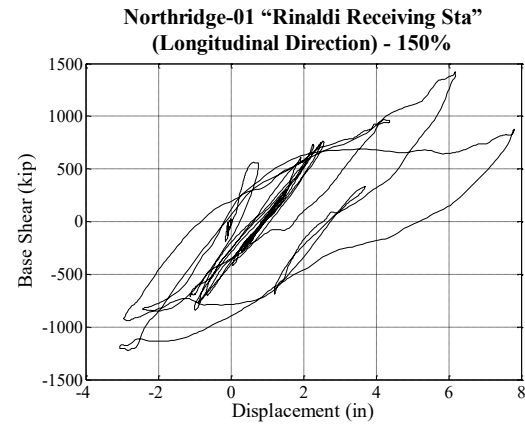
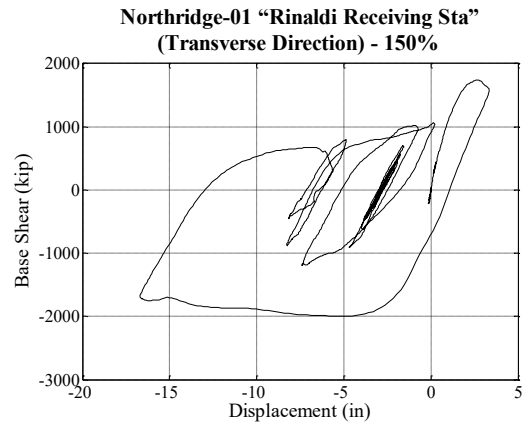


(b)

Figure 3-53 Hysteresis Loop for Loma Prieta "Capitola" - Model 2 (a) 100% (b) 150%



(a)



(b)

Figure 3-54 Hysteresis Loop for Northridge-01 "Rinaldi Receiving Sta" - Model 2 (a) 100% (b) 150%

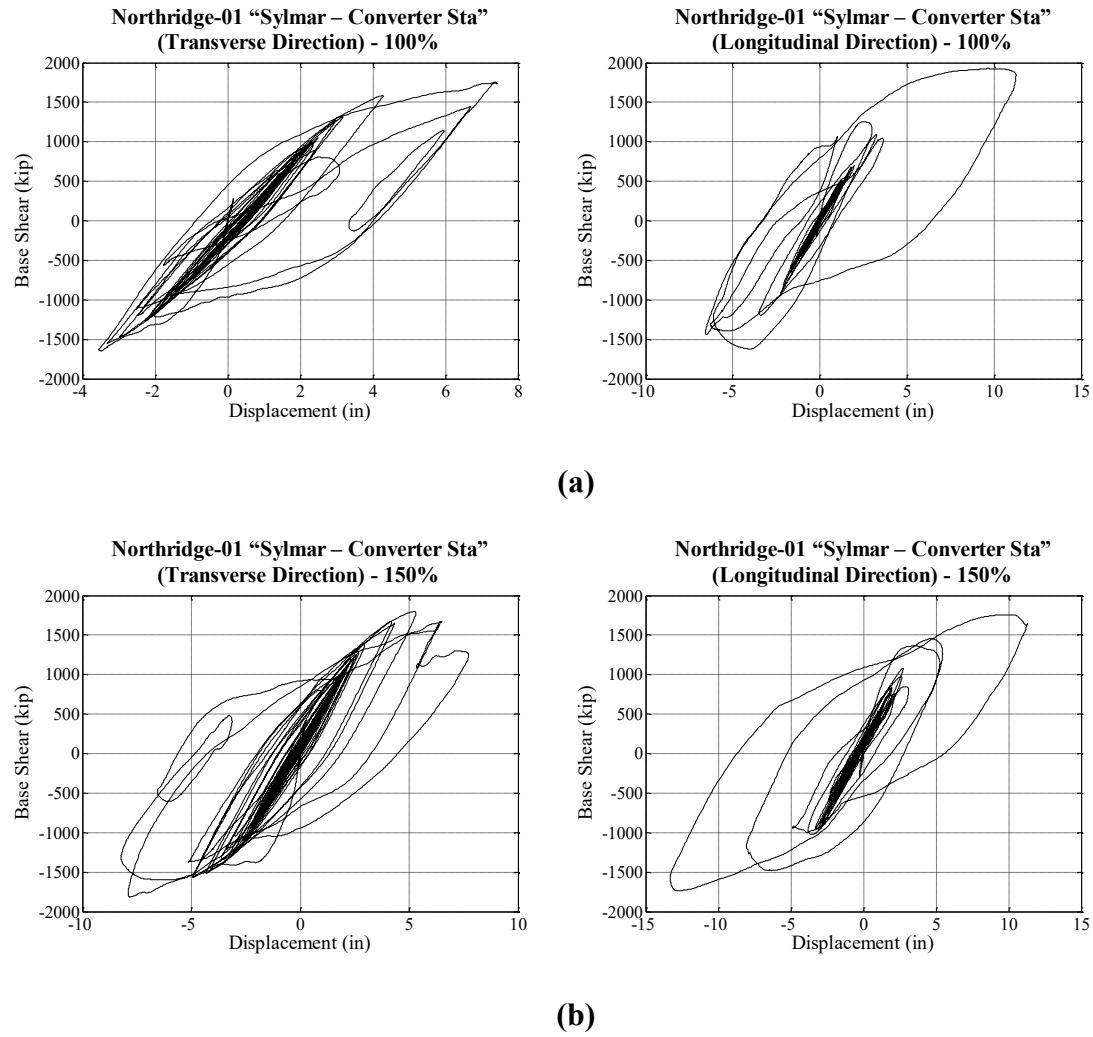
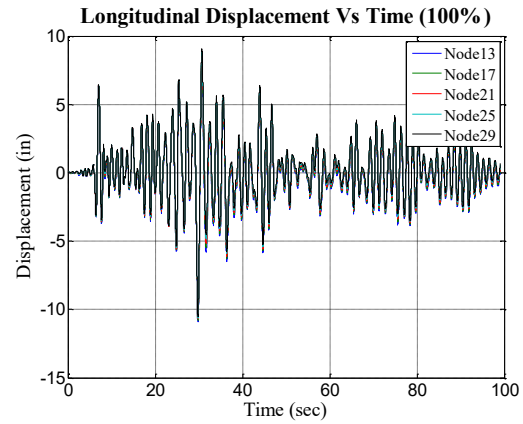
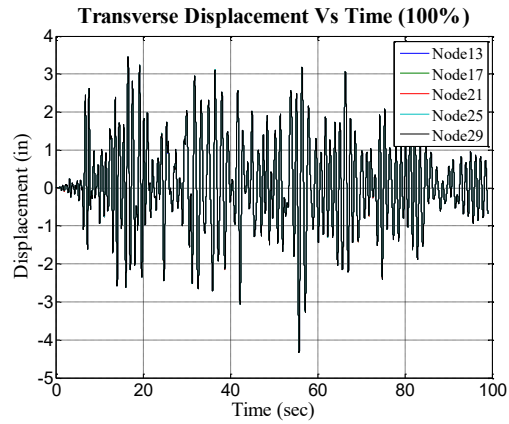
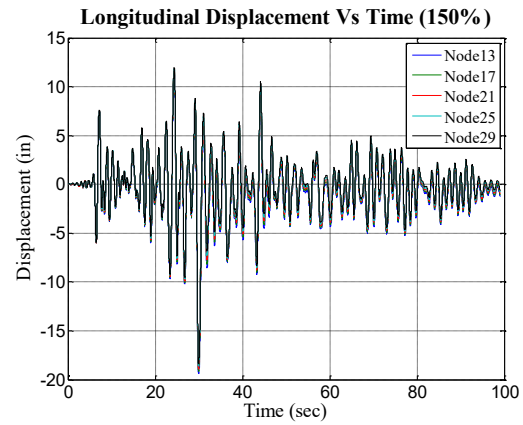
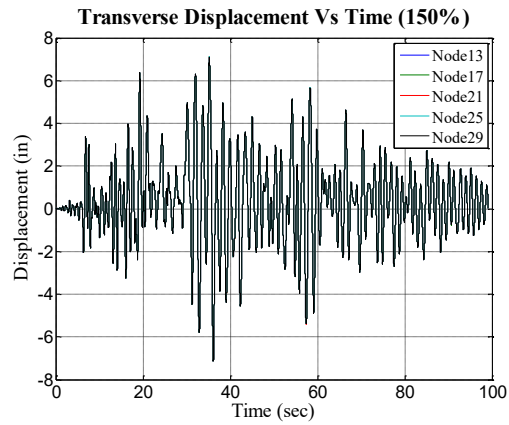


Figure 3-55 Hysteresis Loop for Northridge-01 "Sylmar-Converter Sta" - Model 2 (a) 100% (b) 150%

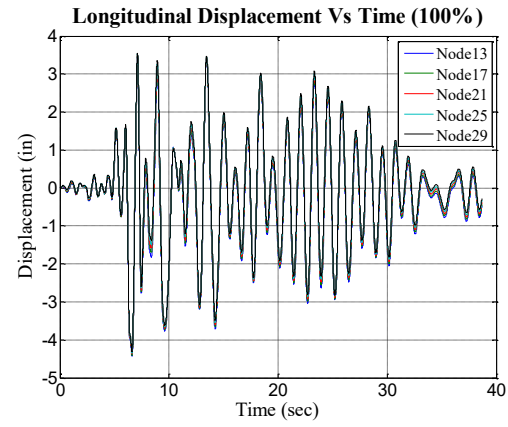
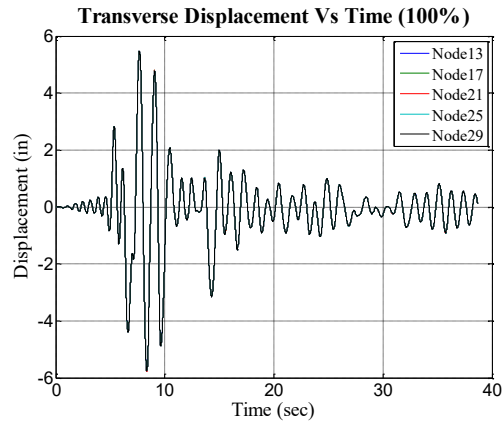


(a)

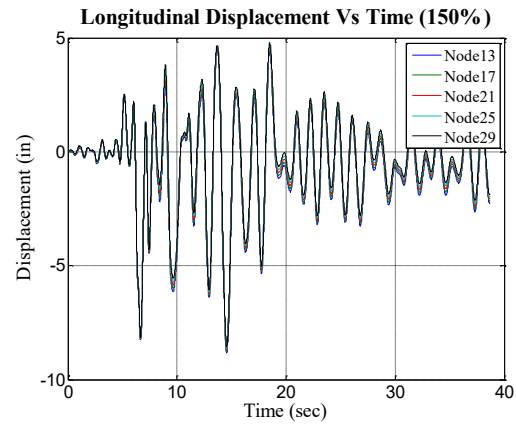
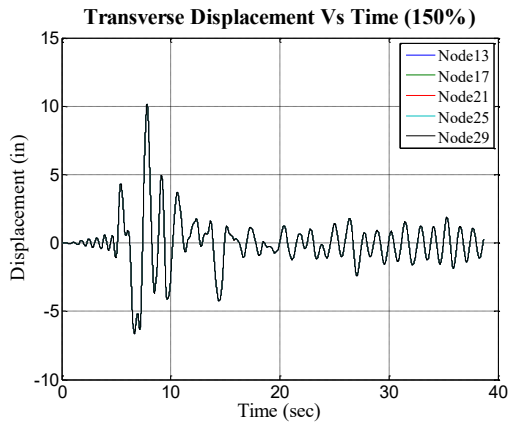


(b)

Figure 3-56 Displacement History for Imperial Valley-06 "Delta" - Model 2 (a) 100% (b) 150%

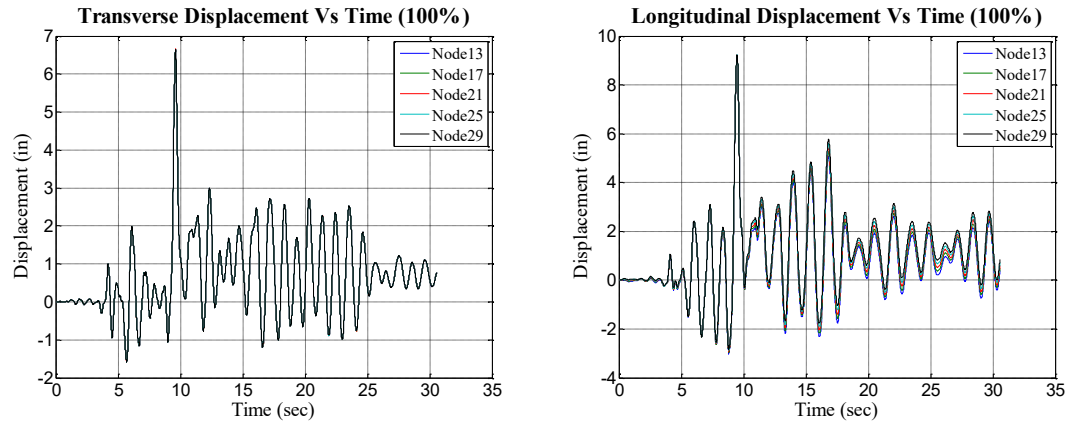


(a)

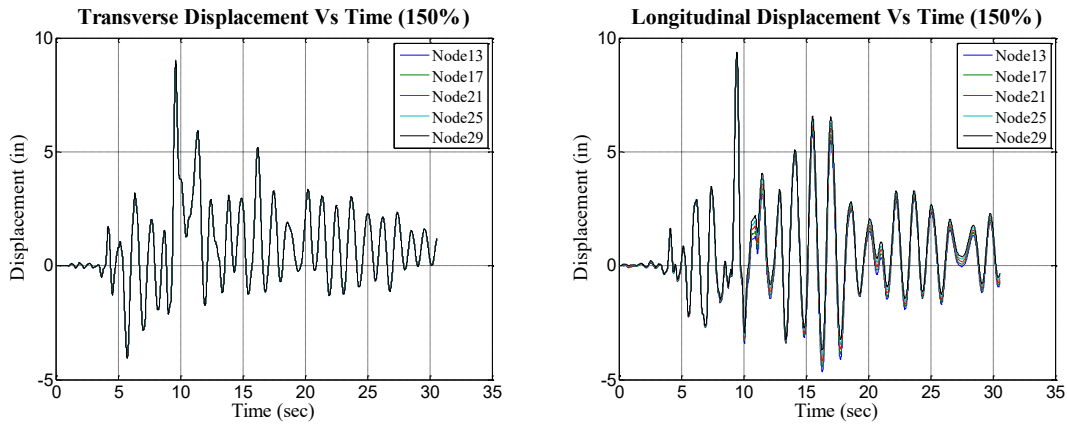


(b)

Figure 3-57 Displacement History for Loma Prieta "Hollister Differential Array" -Model 2 (a) 100% (b) 150%

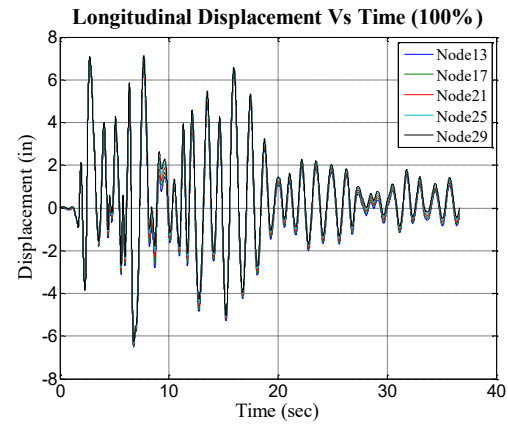
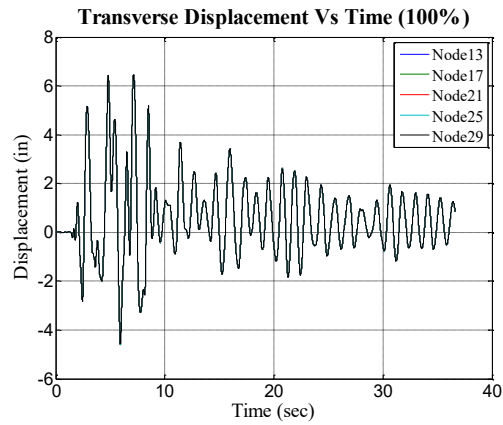


(a)

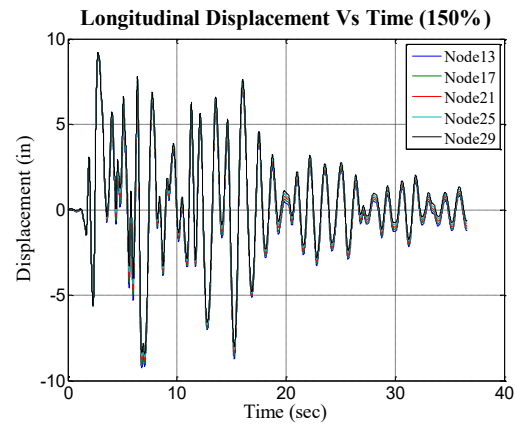
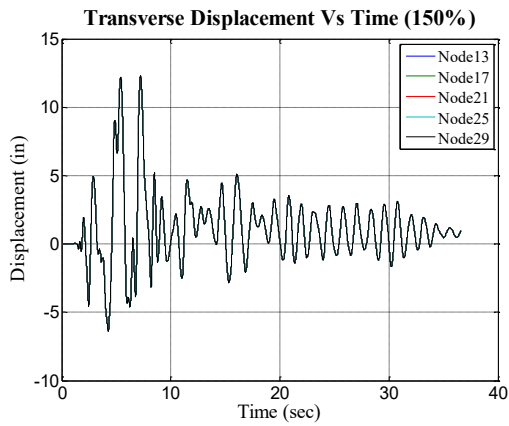


(b)

Figure 3-58 Displacement History for Northridge-01 "LA-Saturn St" - Model 2 (a) 100% (b) 150%

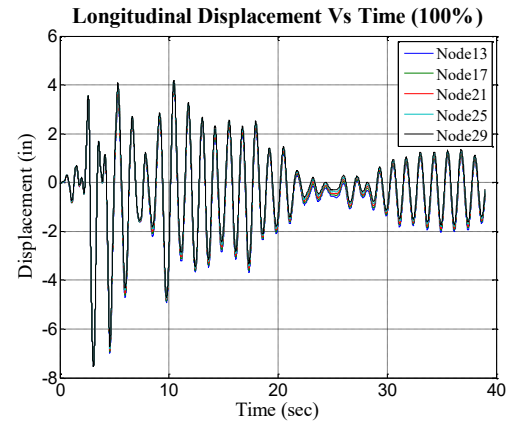
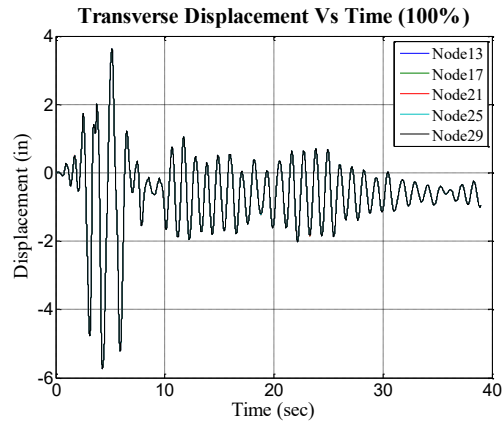


(a)

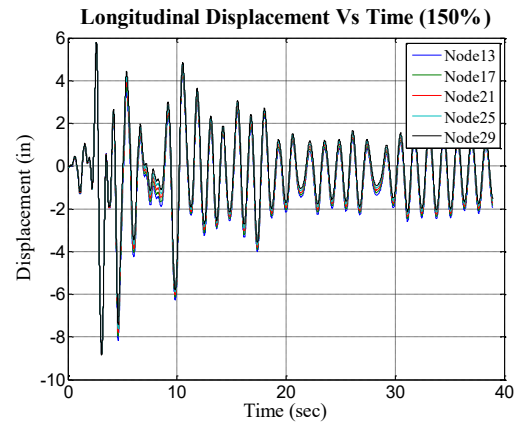
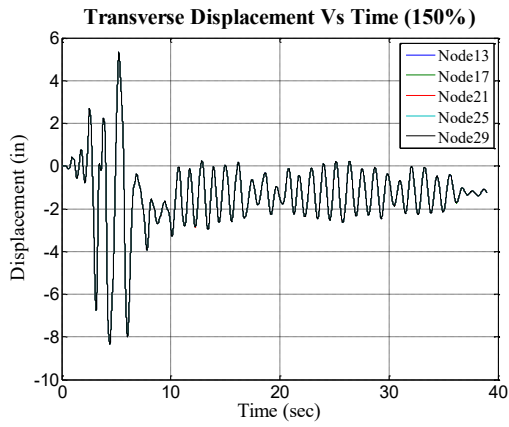


(b)

Figure 3-59 Displacement History for Imperial Valley-06 "Bonds Corner" - Model 2 (a) 100% (b) 150%

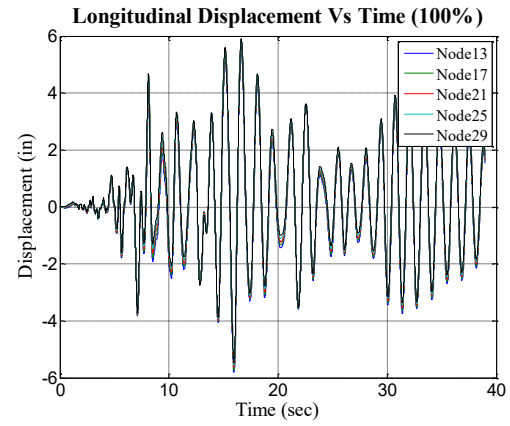
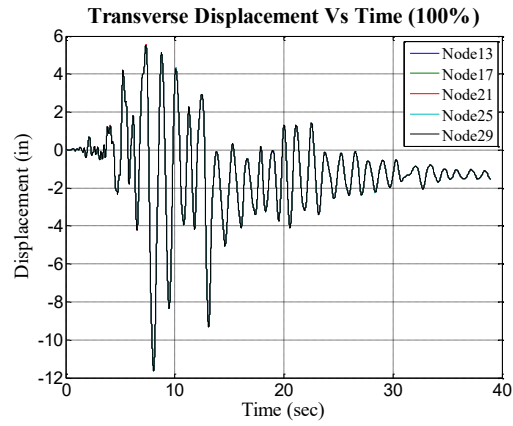


(a)

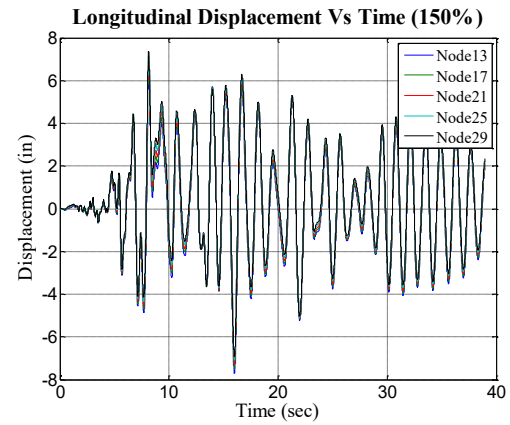
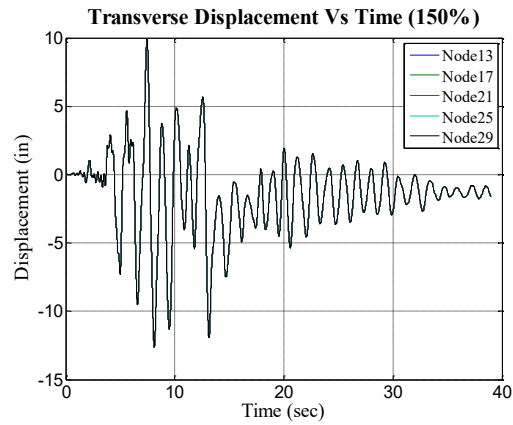


(b)

Figure 3-60 Displacement History for Chalfant Valley-02 "Zack Brother Ranch" -Model 2 (a) 100% (b) 150%

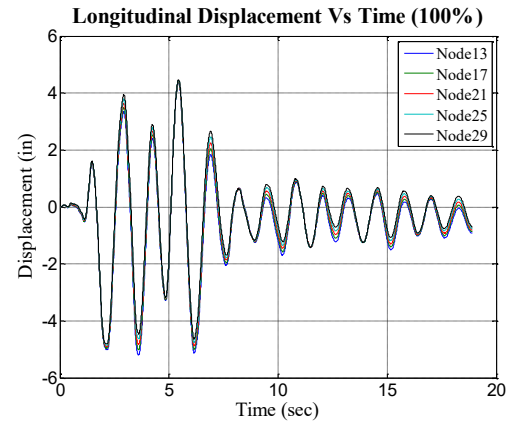
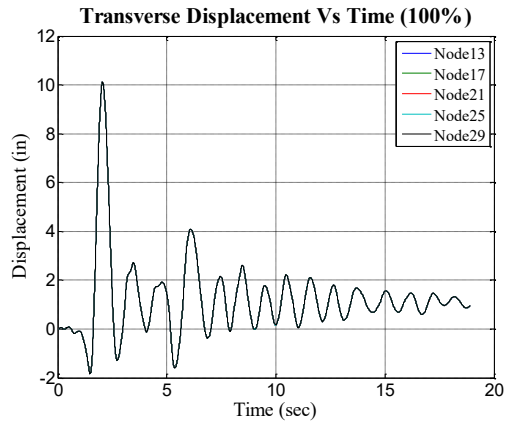


(a)

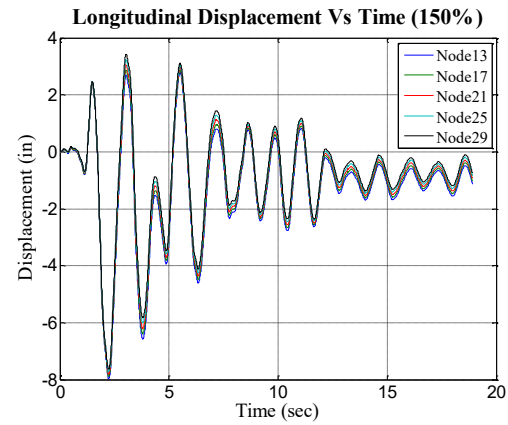
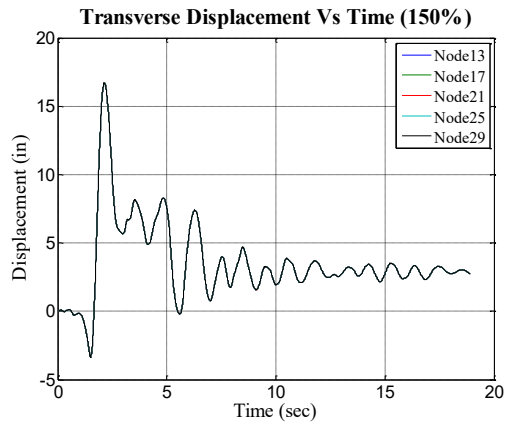


(b)

Figure 3-61 Displacement History for Loma Prieta "Capitola" - Model 2 (a) 100% (b) 150%

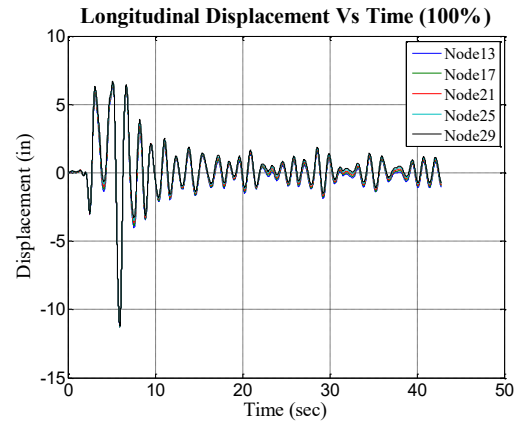
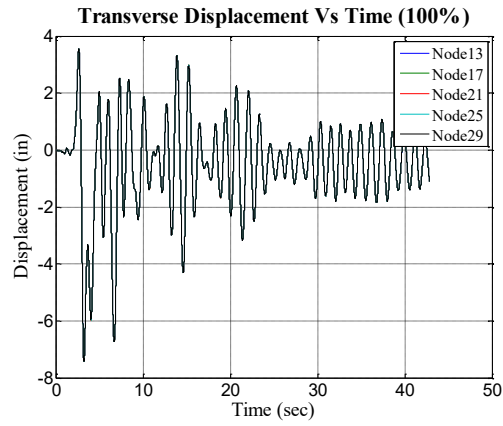


(a)

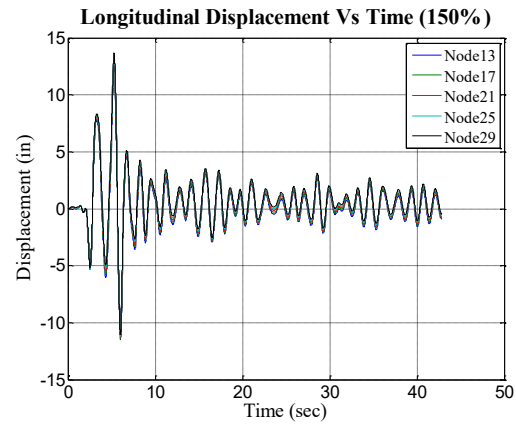
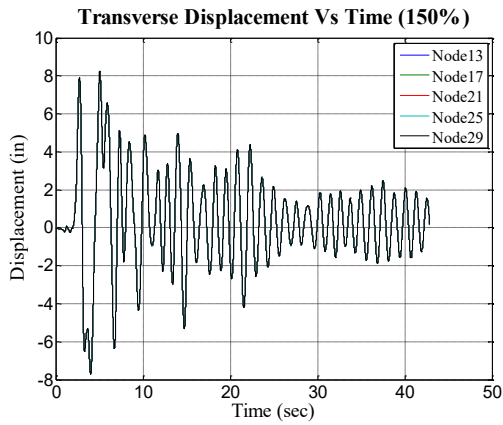


(b)

Figure 3-62 Displacement History for Northridge-01 "Rinaldi Receiving Sta" - Model 2 (a) 100% (b) 150%

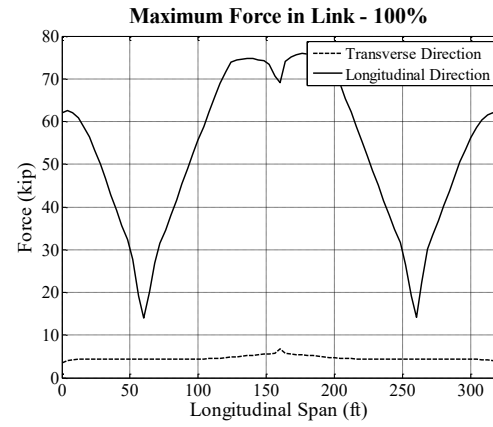
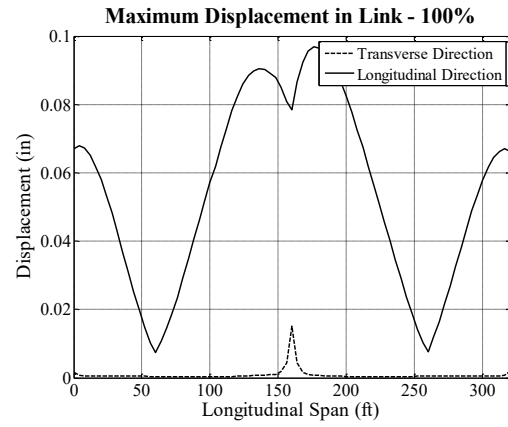


(a)

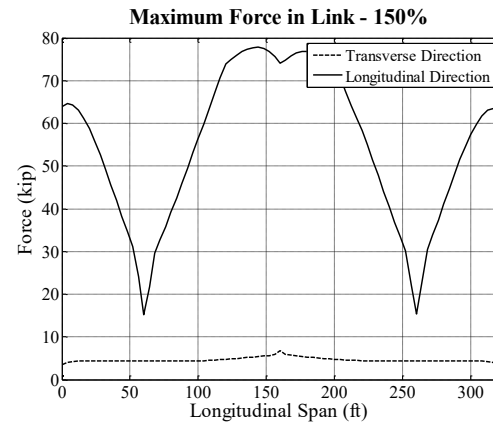
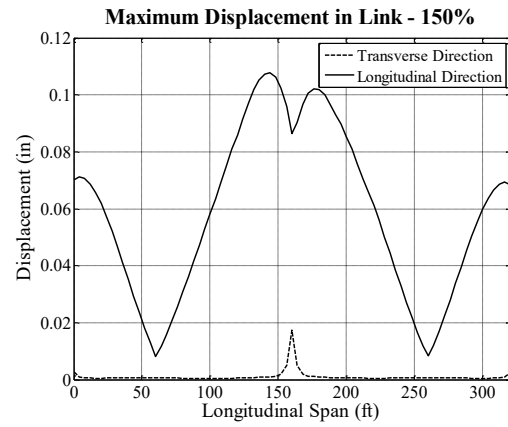


(b)

Figure 3-63 Displacement History for Northridge-01 "Sylmar-Converter Sta" - Model 2 (a) 100% (b) 150%

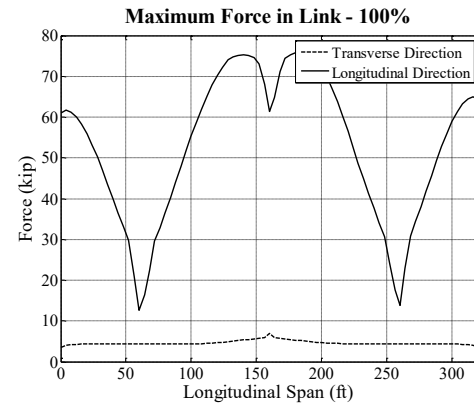
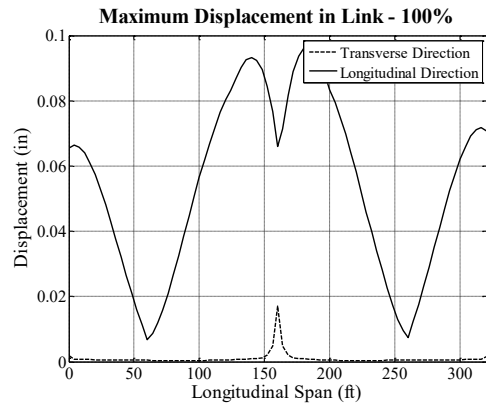


(a)

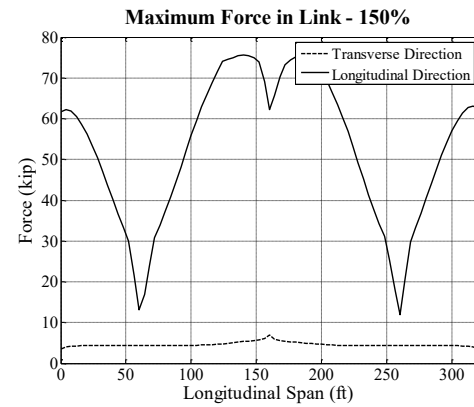
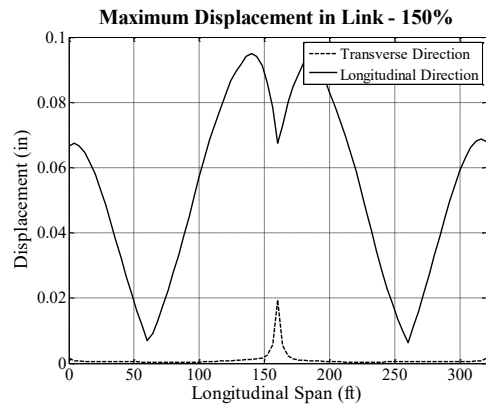


(b)

Figure 3-64 Maximum Link Force and Displacement for Imperial Valley-06 "Delta" - Model 2 (a) 100% (b) 150%



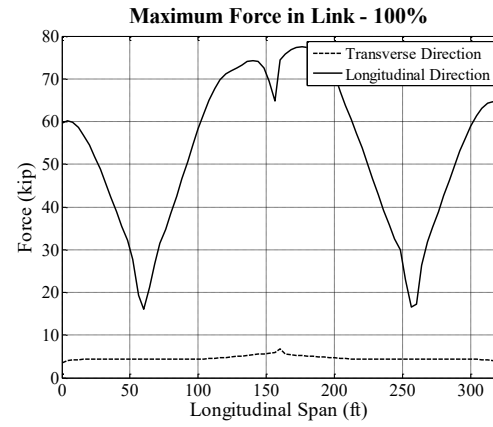
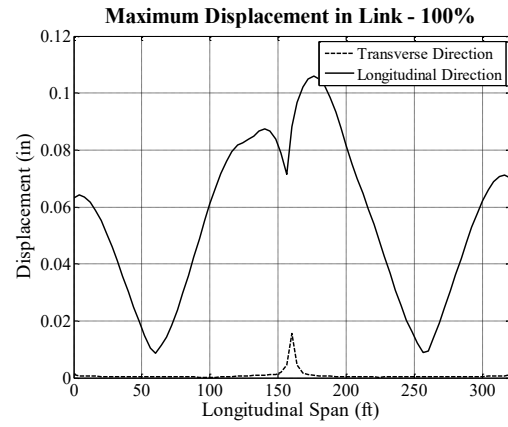
(a)



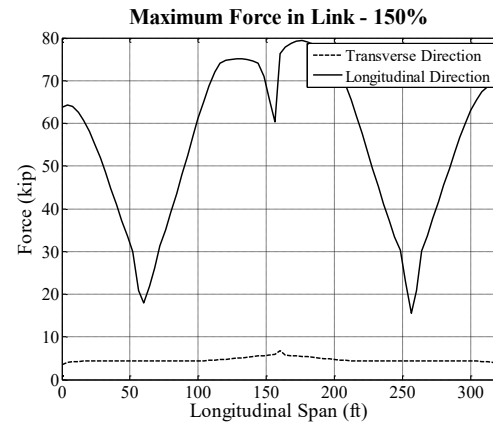
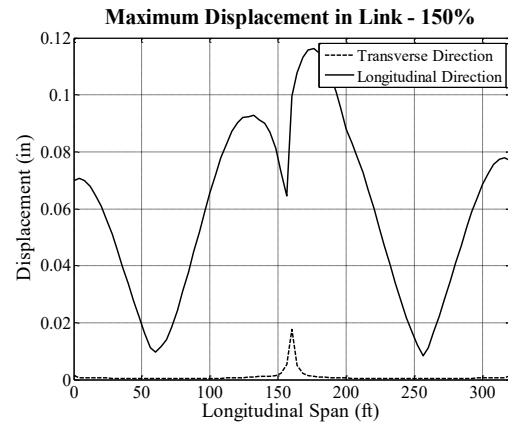
(b)

Figure 3-65 Maximum Link Force and Displacement for Loma Prieta "Hollister Differential Array" - Model 2 (a) 100%

(b) 150%

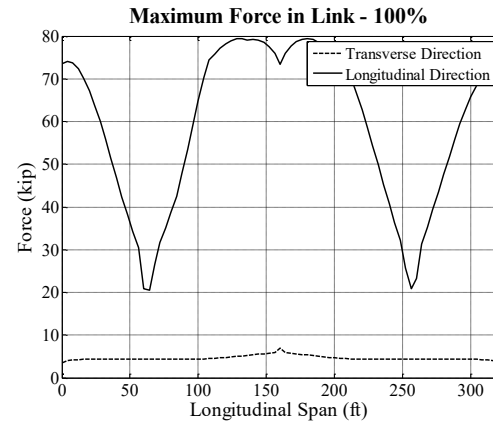
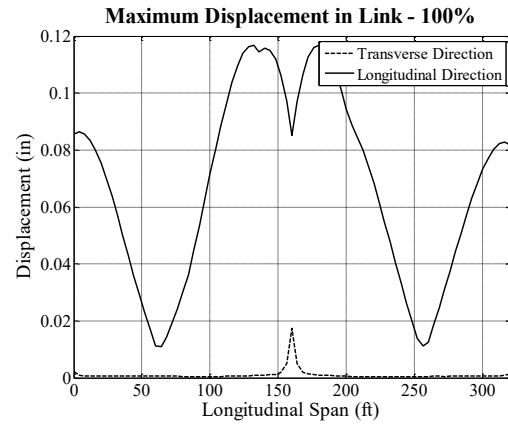


(a)

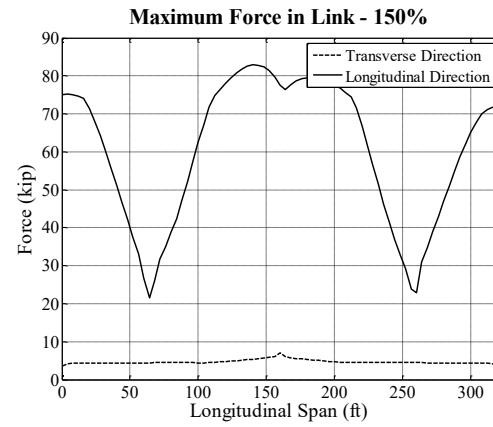
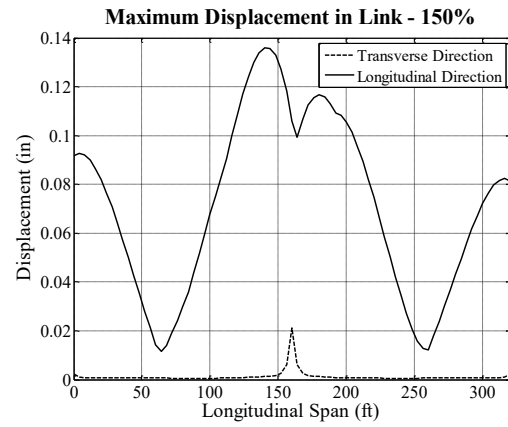


(b)

Figure 3-66 Maximum Link Force and Displacement for Northridge-01 "LA-Saturn St" - Model 2 (a) 100% (b) 150%

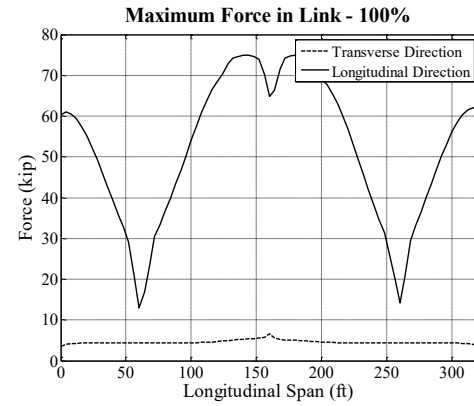
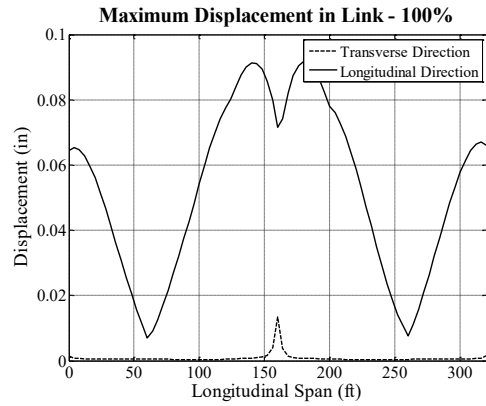


(a)

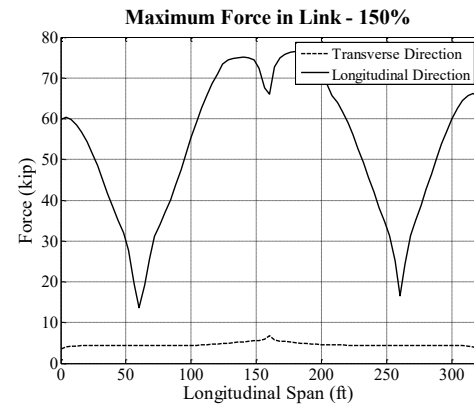
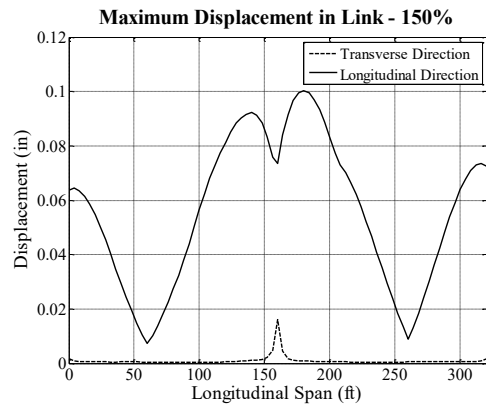


(b)

Figure 3-67 Maximum Link Force and Displacement for Imperial Valley-06 "Bonds Corner" - Model 2 (a) 100% (b) 150%



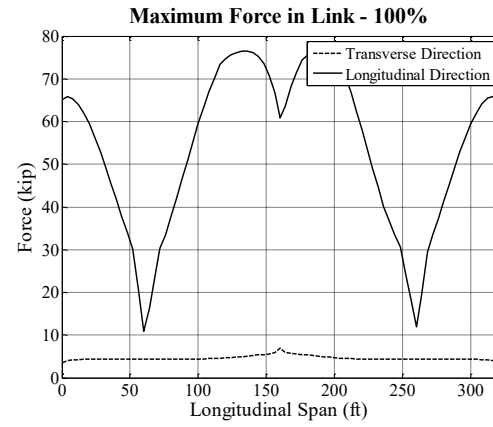
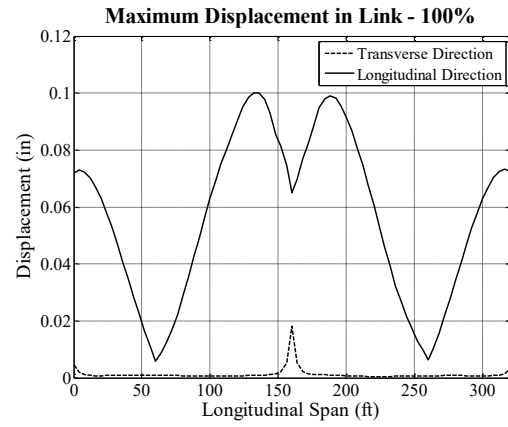
(a)



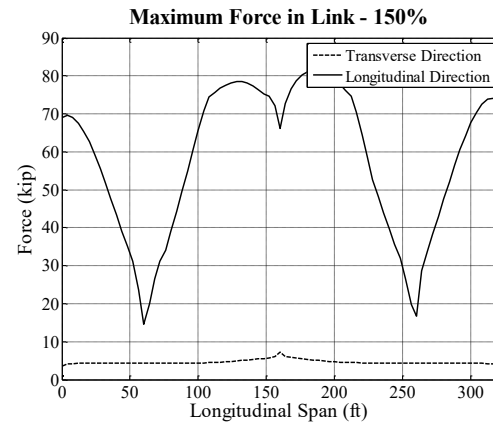
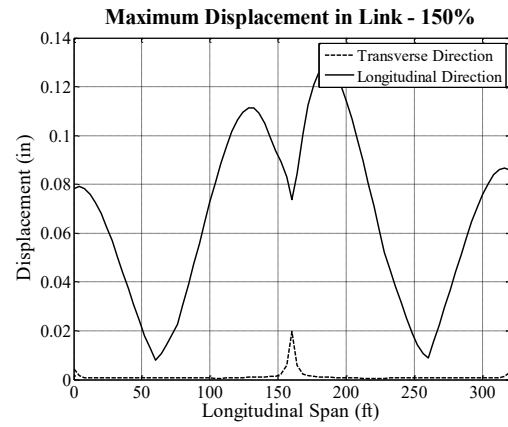
(b)

Figure 3-68 Maximum Link Force and Displacement for Chalfant Valley-02 "Zack Brother Ranch" - Model 2 (a) 100% (b)

150%

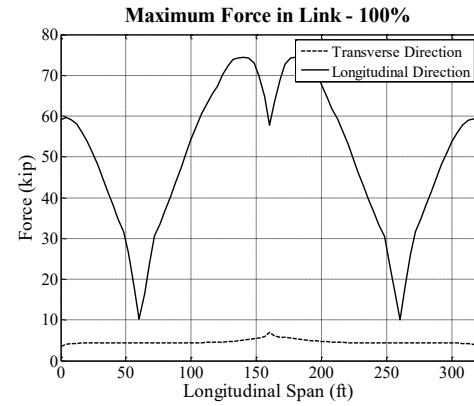
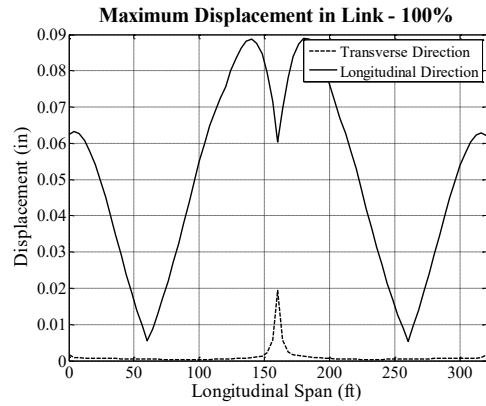


(a)

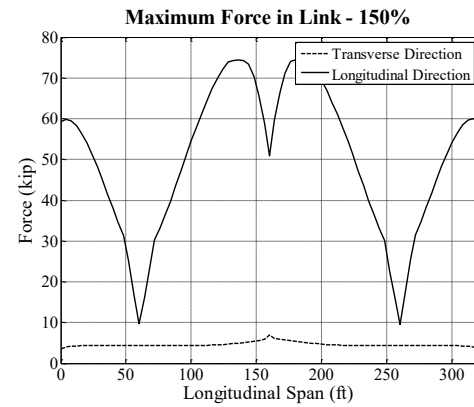
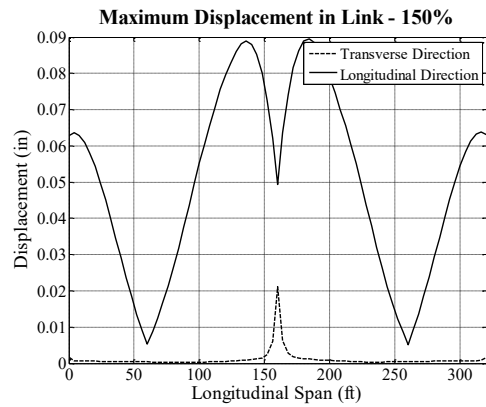


(b)

Figure 3-69 Maximum Link Force and Displacement for Loma Prieta "Capitola" -Model 2 (a) 100% (b) 150%



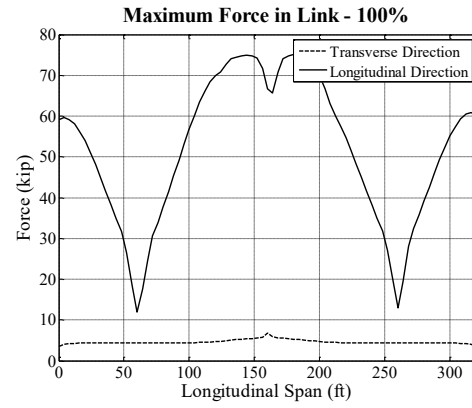
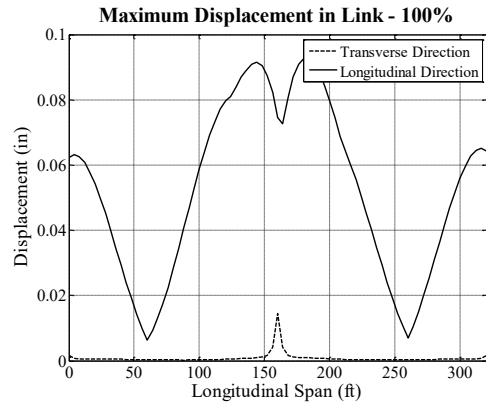
(a)



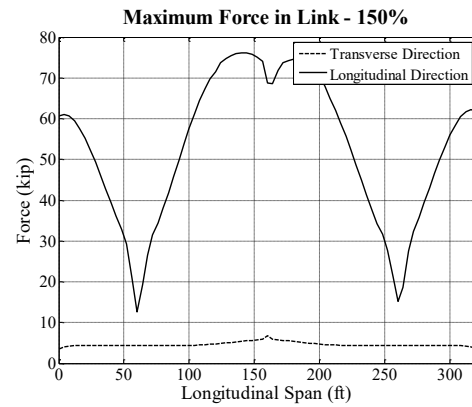
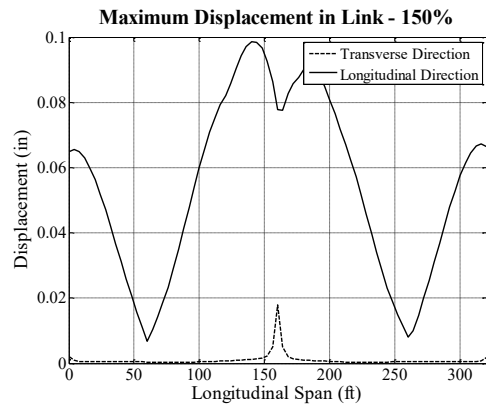
(b)

Figure 3-70 Maximum Link Force and Displacement for Northridge-01 "Rinaldi Receiving Sta" - Model 2 (a) 100% (b)

150%



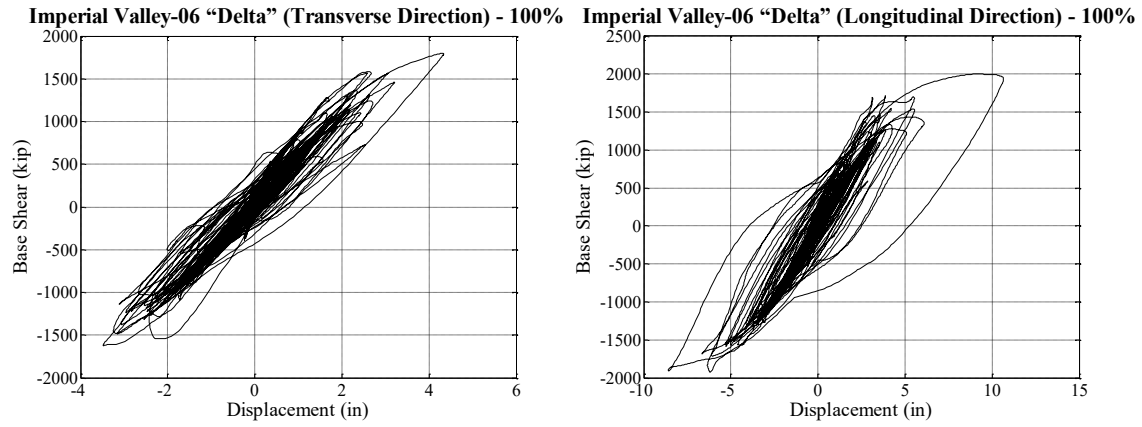
(a)



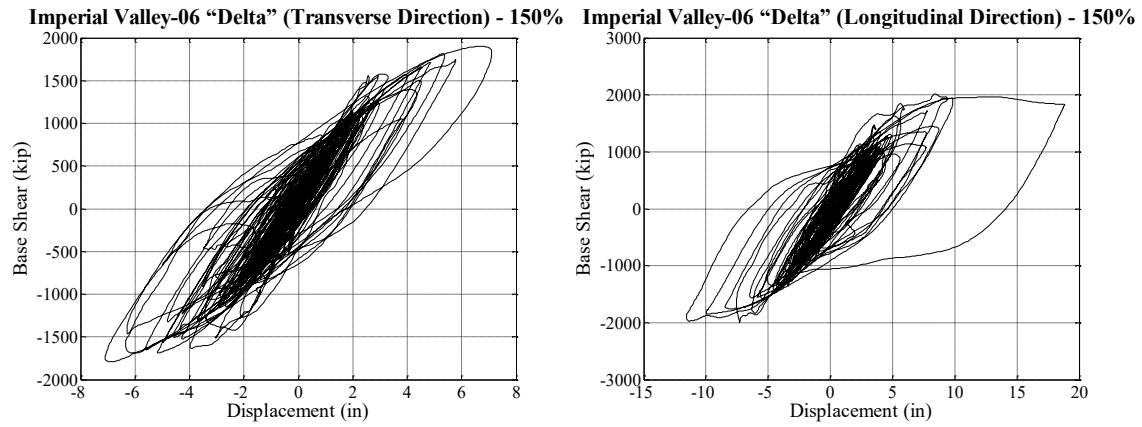
(b)

Figure 3-71 Maximum Link Force and Displacement for Northridge-01 "Sylmar-Converter Sta" - Model 2 (a) 100% (b)

150%



(a)



(b)

Figure 3-72 Hysteresis Loop for Imperial Valley-06 "Delta" - Model 3 (a) 100% (b) 150%

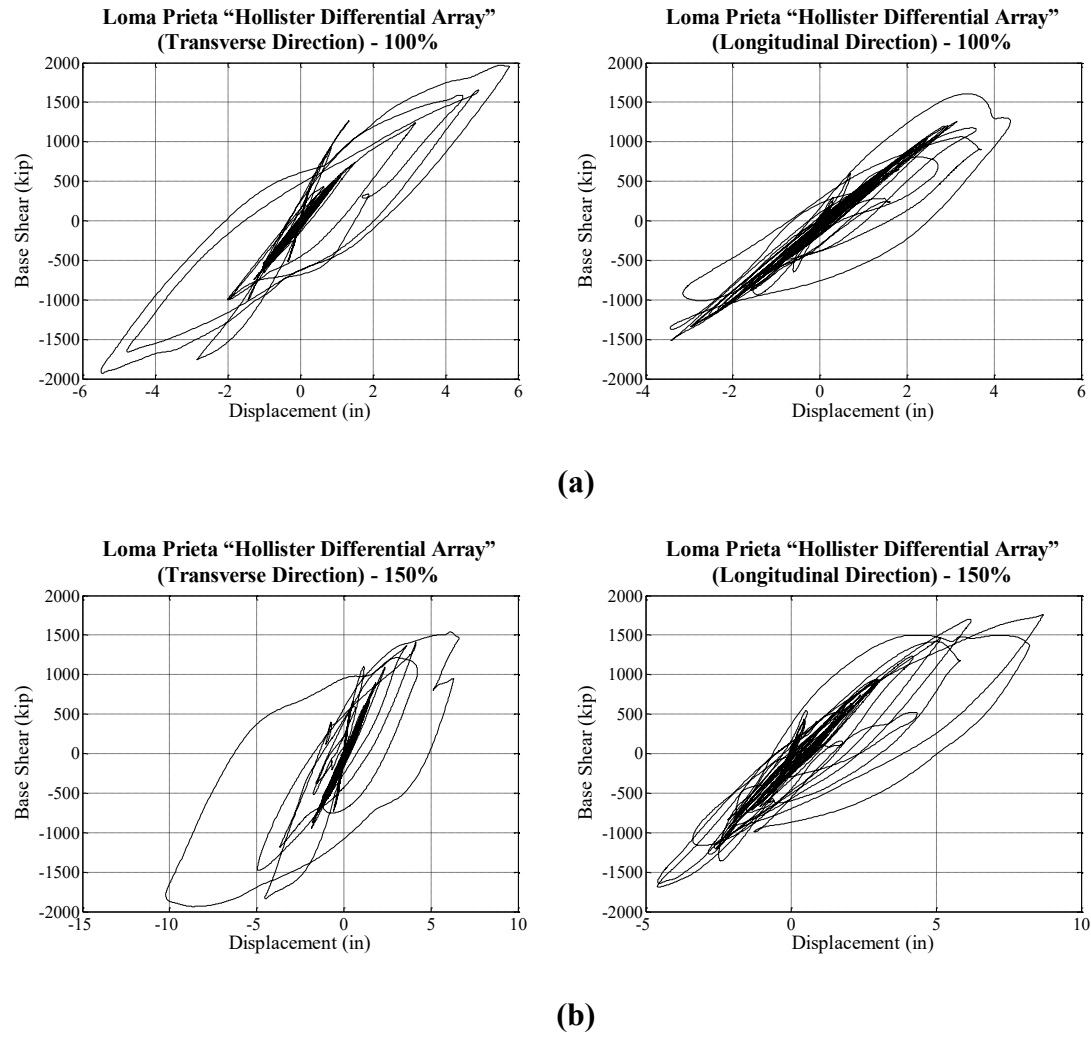


Figure 3-73 Hysteresis Loop for Loma Prieta "Hollister Differential Array" - Model 3 (a) 100% (b) 150%

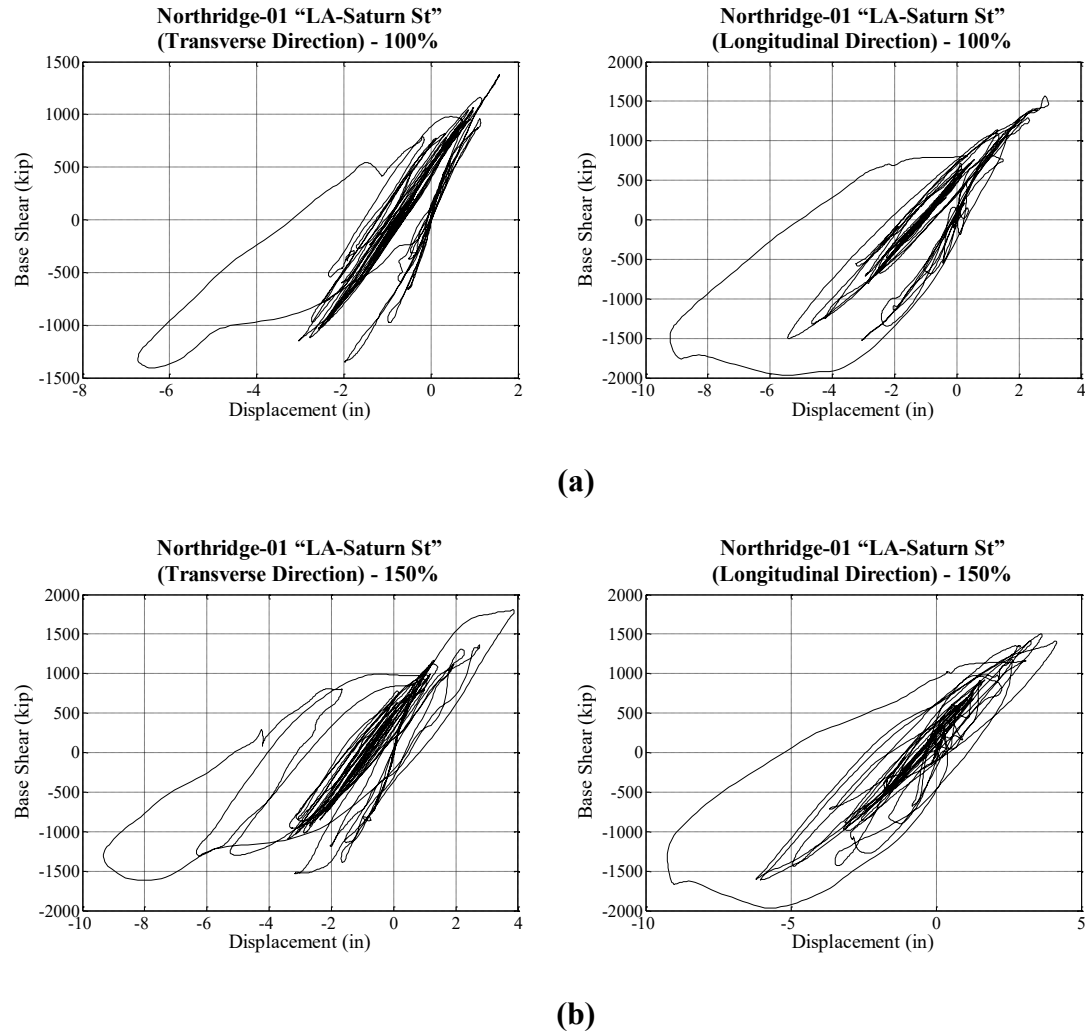


Figure 3-74 Hysteresis Loop for Northridge-01 "LA-Saturn St" - Model 3 (a) 100% (b) 150%

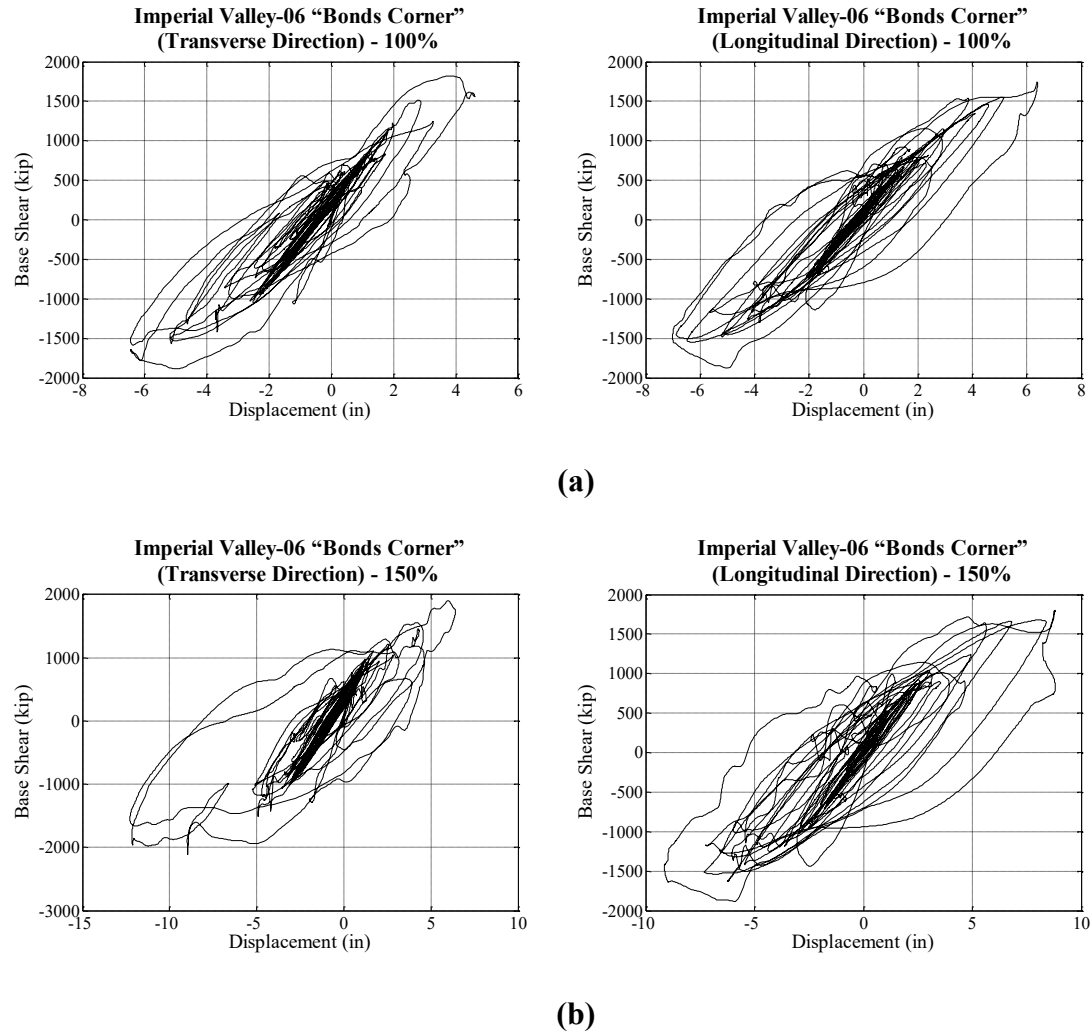


Figure 3-75 Hysteresis Loop for Imperial Valley-06 "Bonds Corner" - Model 3 (a) 100% (b) 150%

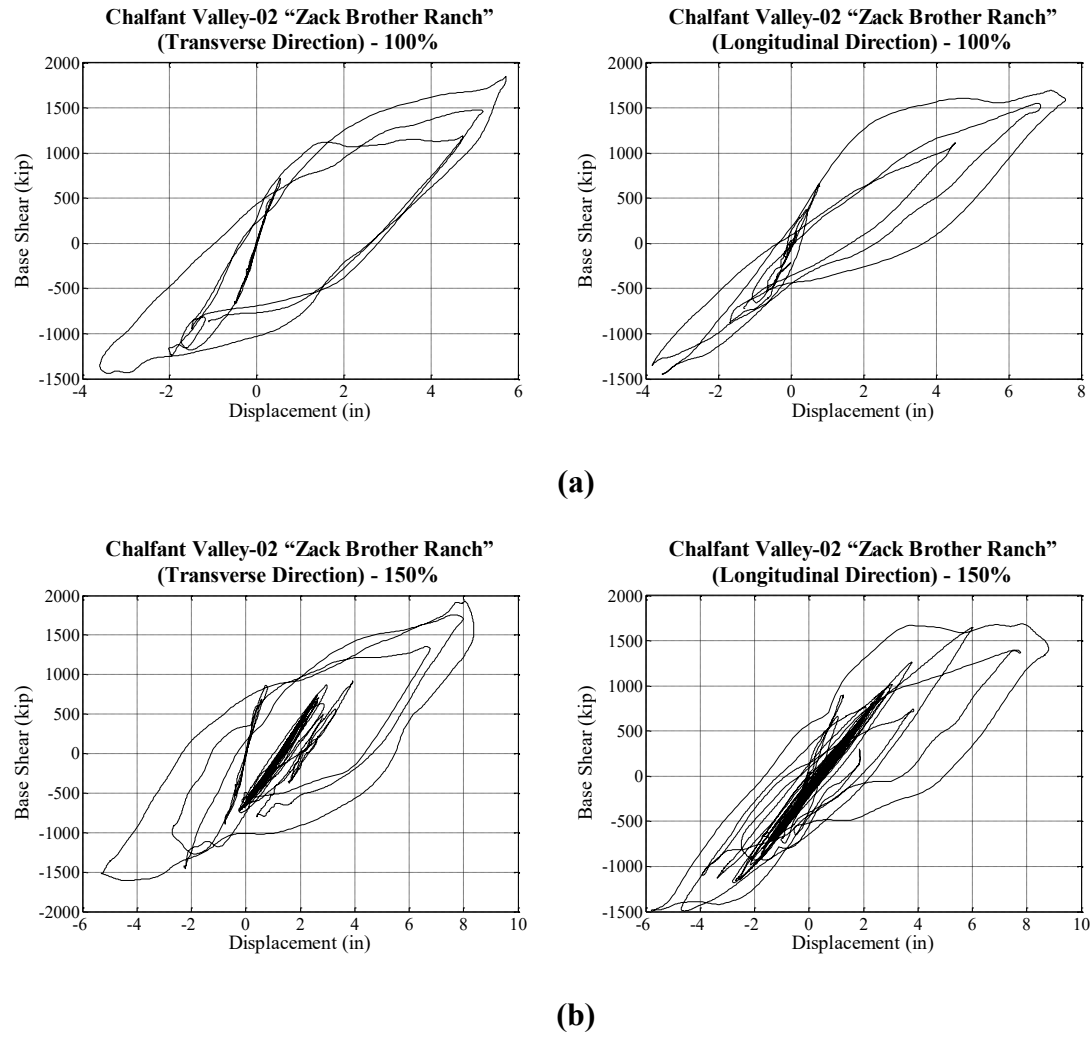


Figure 3-76 Hysteresis Loop for Chalfant Valley-02 "Zack Brother Ranch" - Model 3 (a) 100% (b) 150%

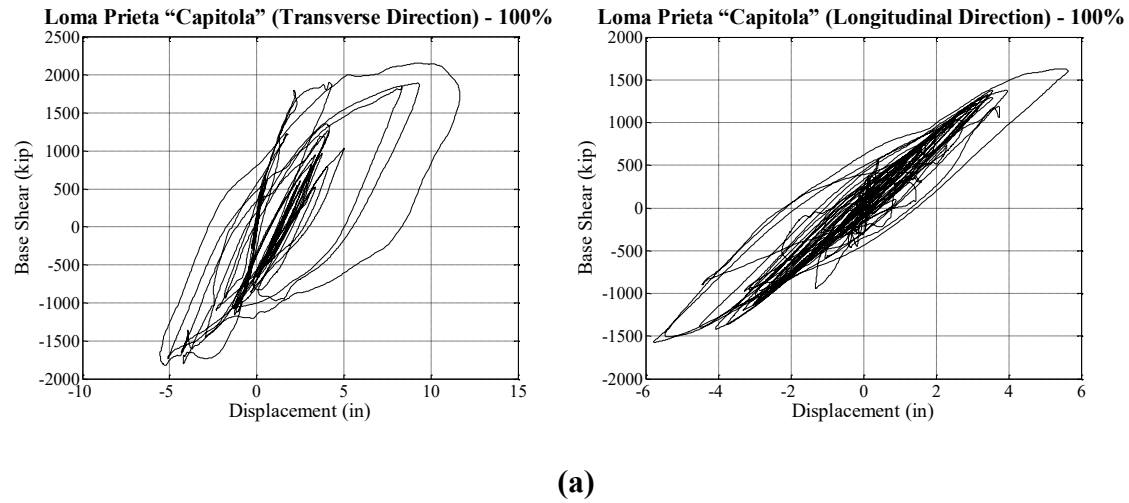
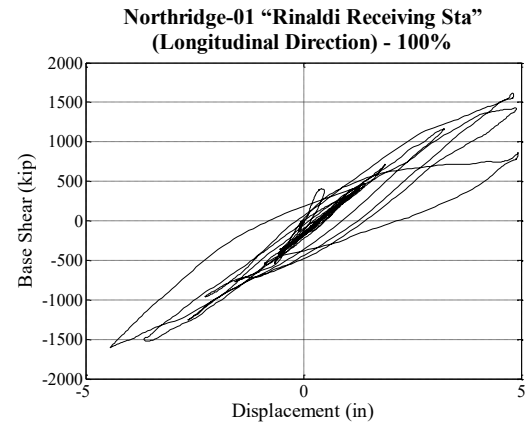
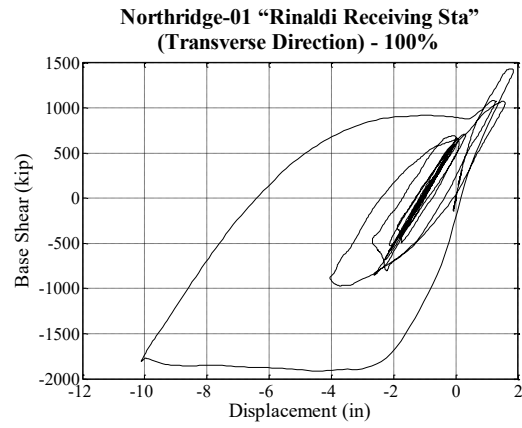
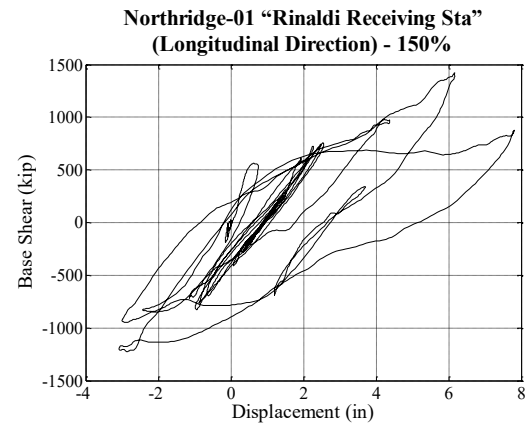
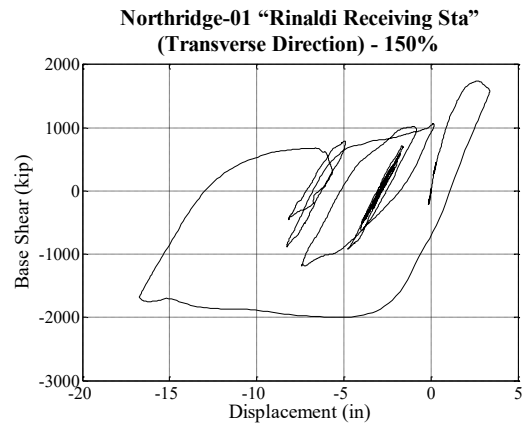


Figure 3-77 Hysteresis Loop for Loma Prieta "Capitola" - Model 3 (a) 100%



(a)



(b)

Figure 3-78 Hysteresis Loop for Northridge-01 "Rinaldi Receiving Sta" - Model 3 (a) 100% (b) 150%

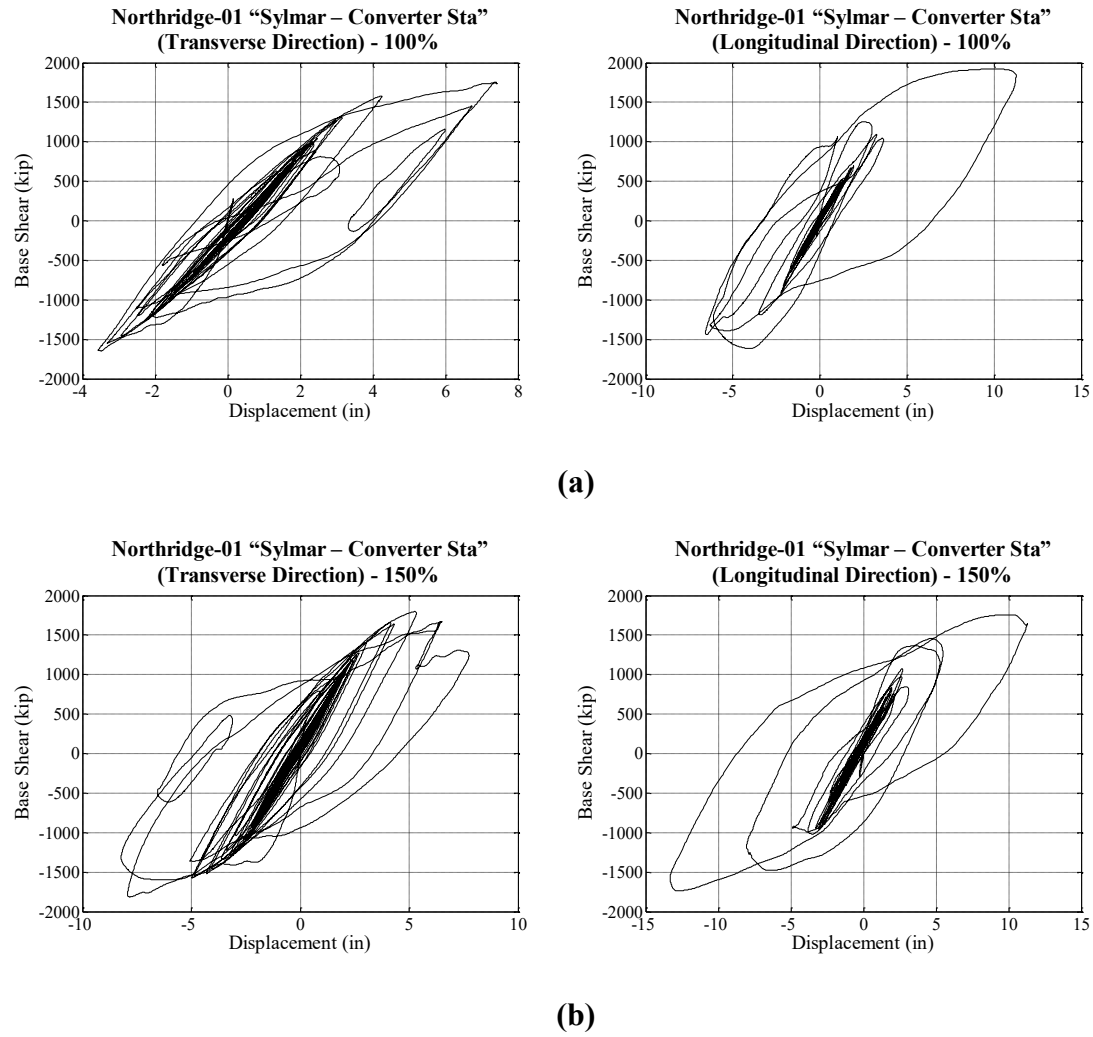
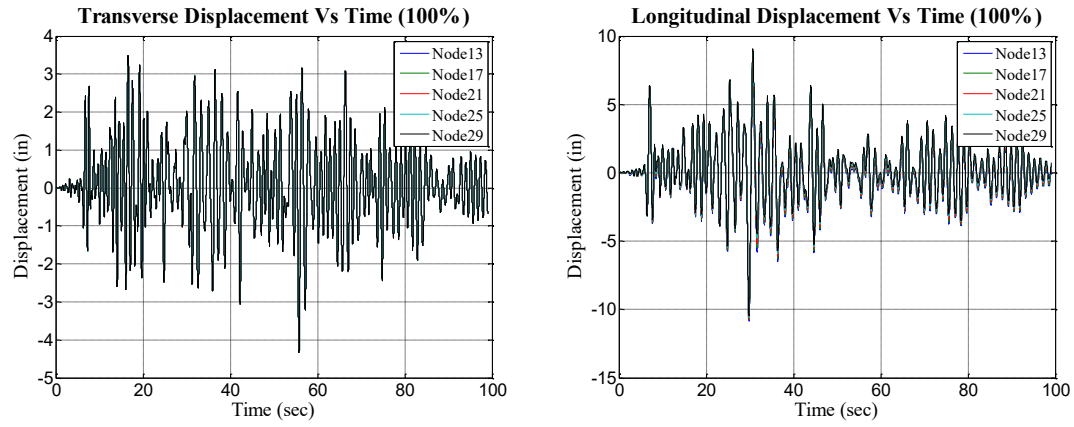
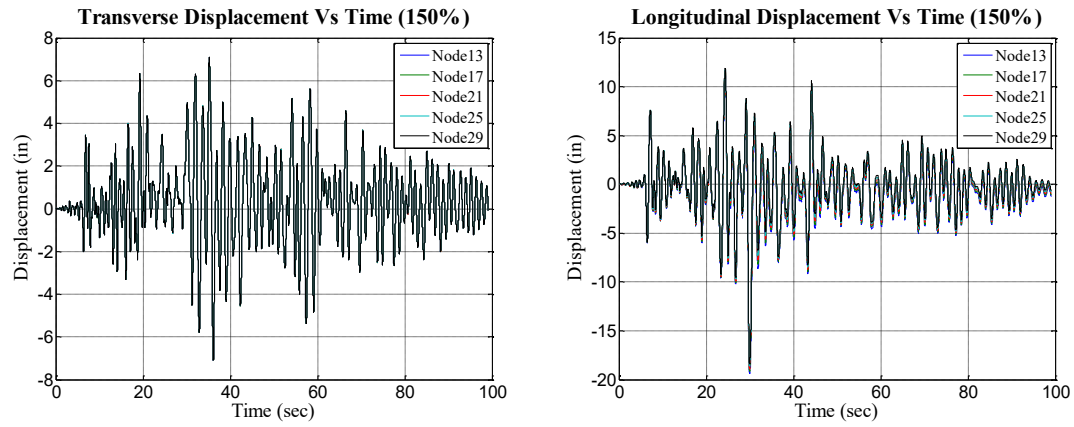


Figure 3-79 Hysteresis Loop for Northridge-01 "Sylmar-Converter Sta" - Model 3 (a) 100% (b) 150%

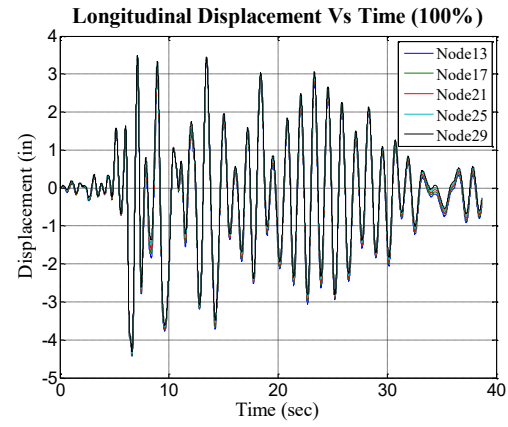
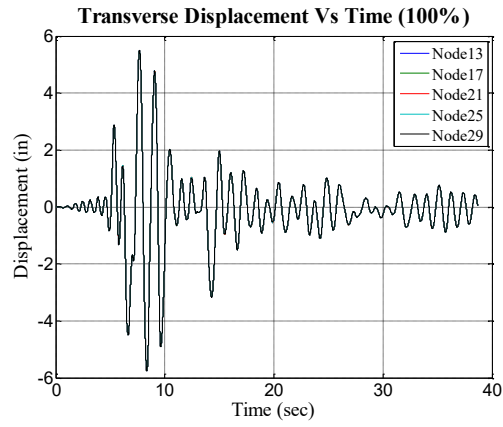


(a)

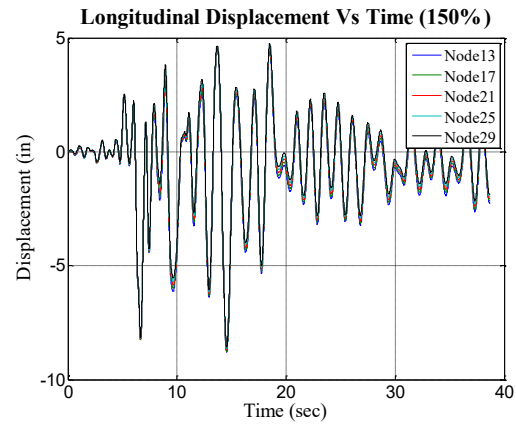
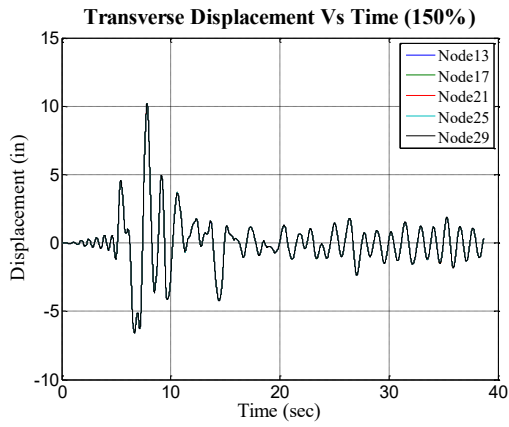


(b)

Figure 3-80 Displacement History for Imperial Valley-06 "Delta" - Model 3 (a) 100% (b) 150%

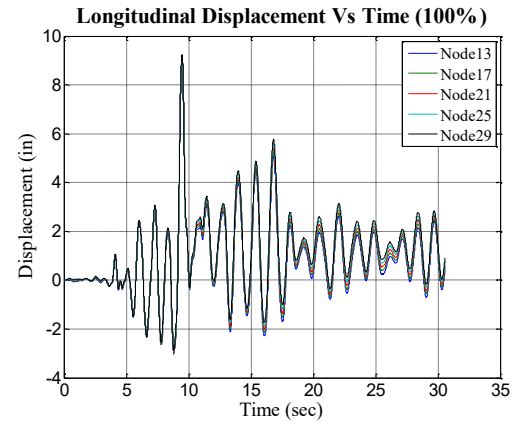
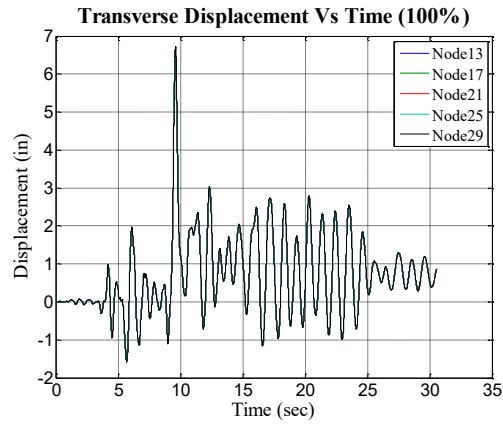


(a)

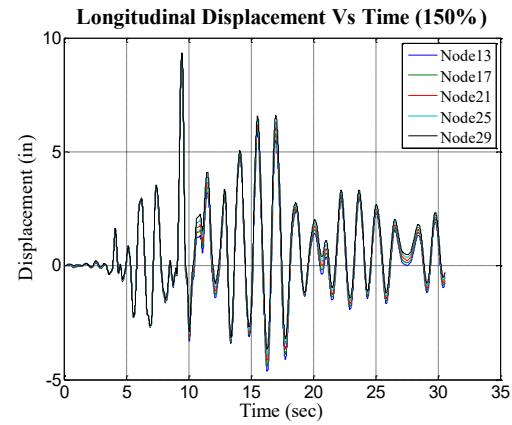
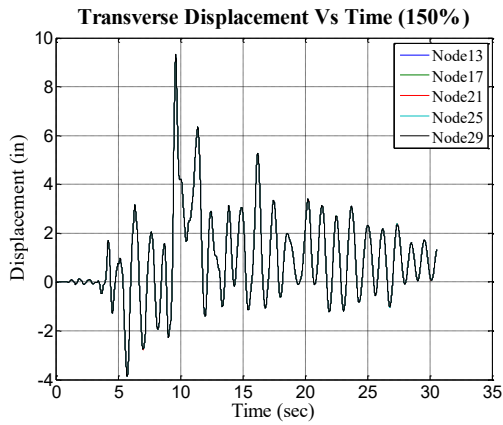


(b)

Figure 3-81 Displacement History for Loma Prieta "Hollister Differential Array" -Model 3 (a) 100% (b) 150%

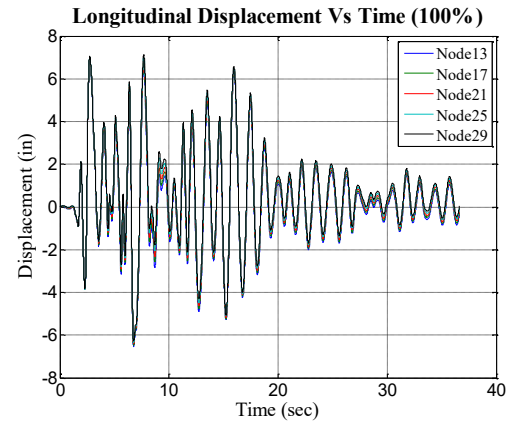
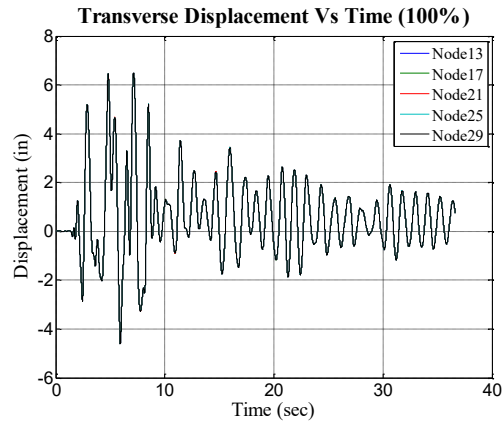


(a)

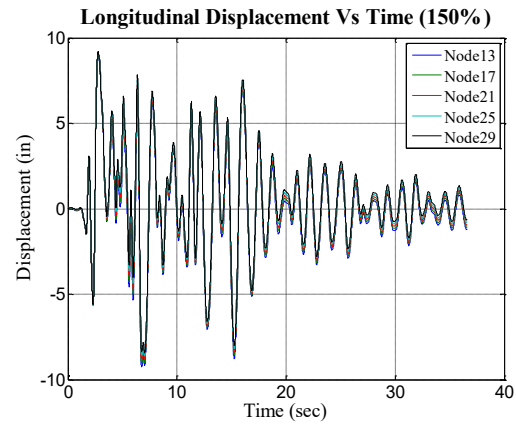
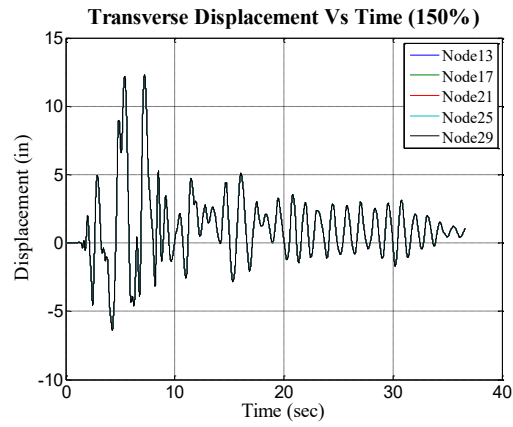


(b)

Figure 3-82 Displacement History for Northridge-01 "LA-Saturn St" - Model 3 (a) 100% (b) 150%

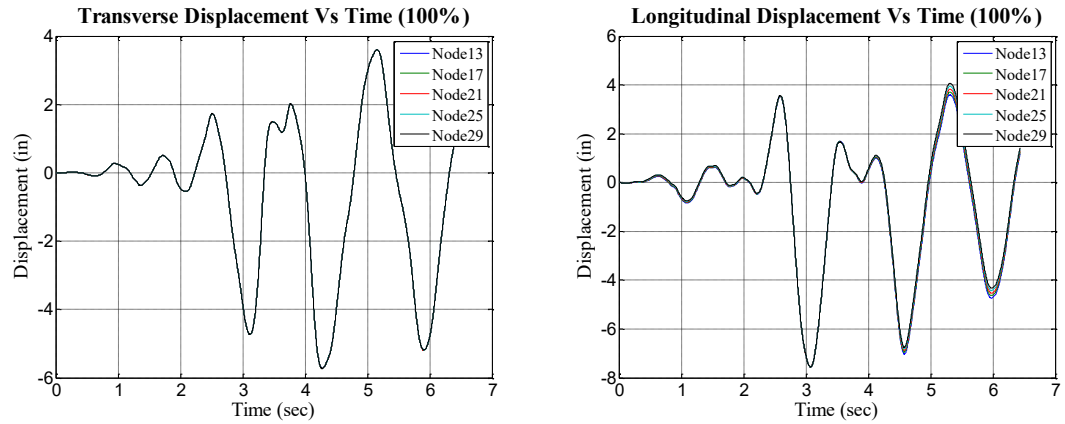


(a)

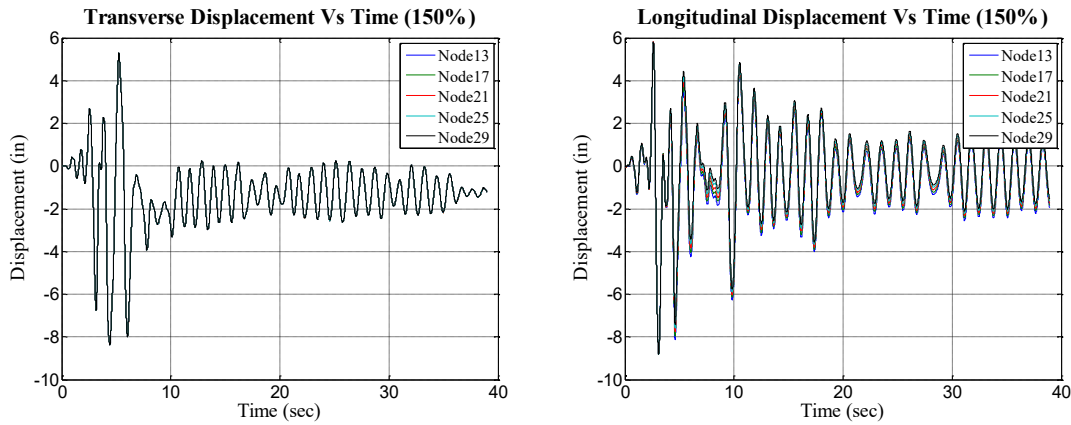


(b)

Figure 3-83 Displacement History for Imperial Valley-06 "Bonds Corner" - Model 3 (a) 100% (b) 150%

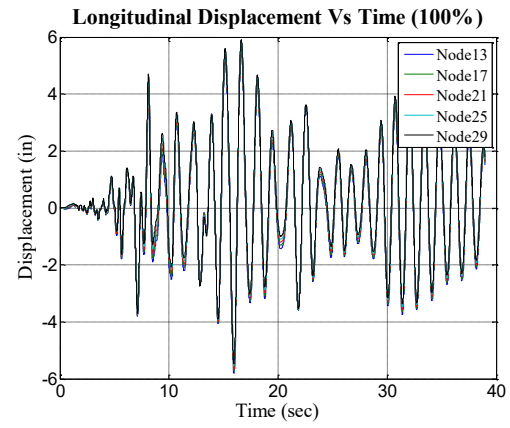
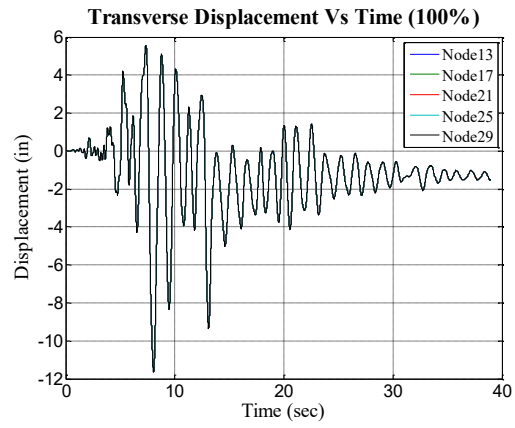


(a)



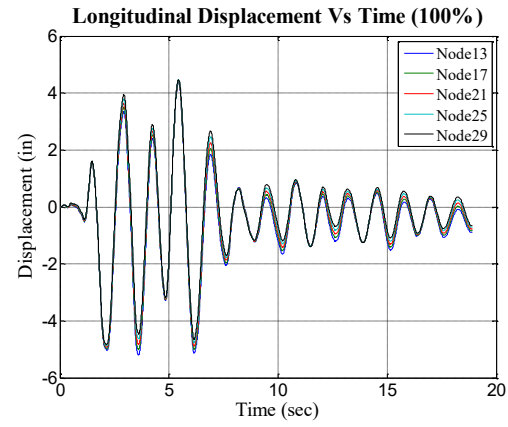
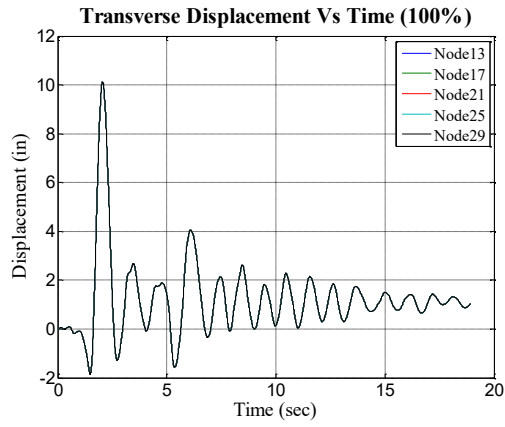
(b)

Figure 3-84 Displacement History for Chalfant Valley-02 "Zack Brother Ranch" -Model 3 (a) 100% (b) 150%

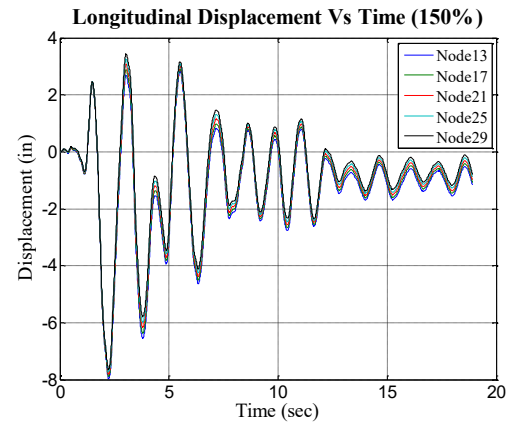
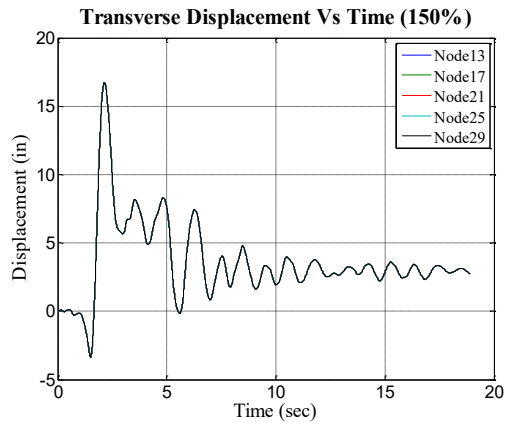


(a)

Figure 3-85 Displacement History for Loma Prieta "Capitola" - Model 3 (a) 100%

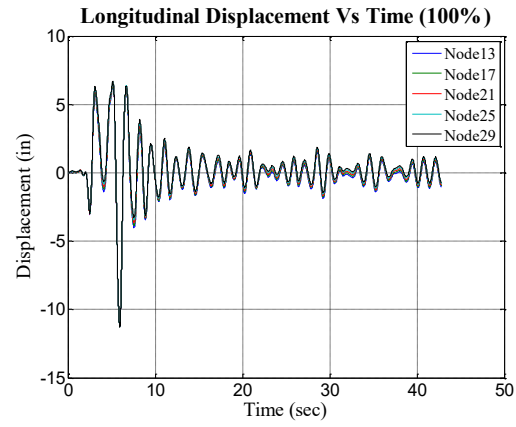
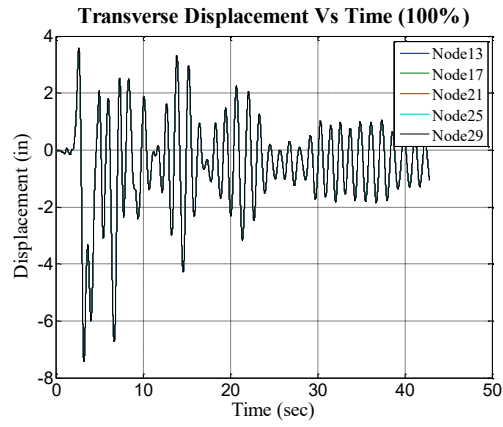


(a)

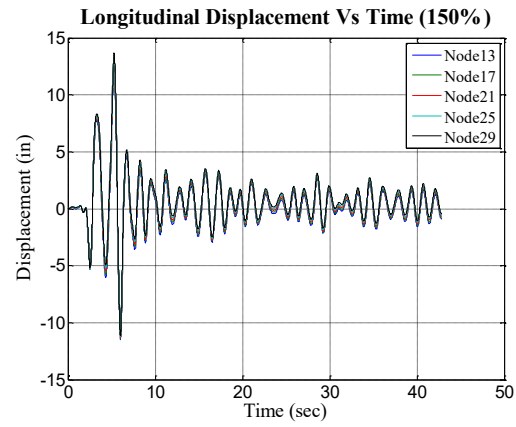
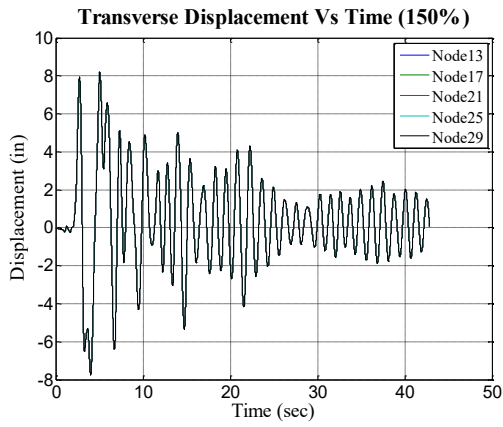


(b)

Figure 3-86 Displacement History for Northridge-01 "Rinaldi Receiving Sta" - Model 3 (a) 100% (b) 150%

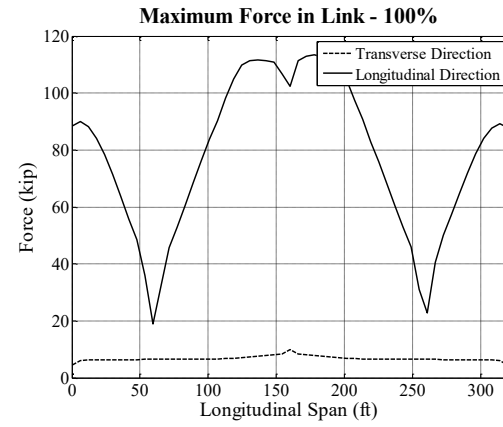
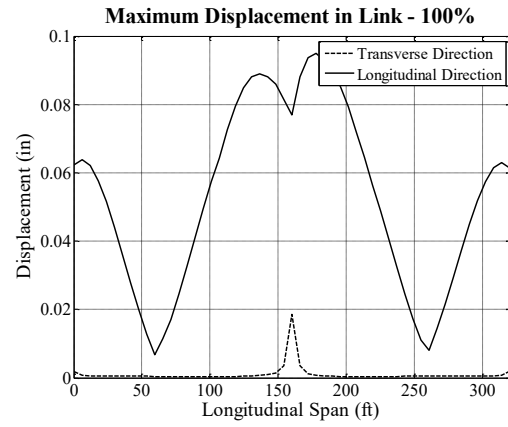


(a)

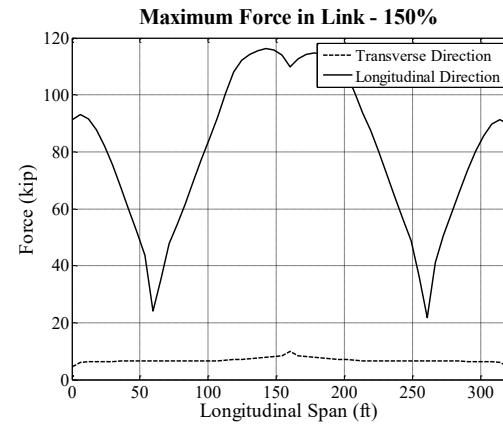
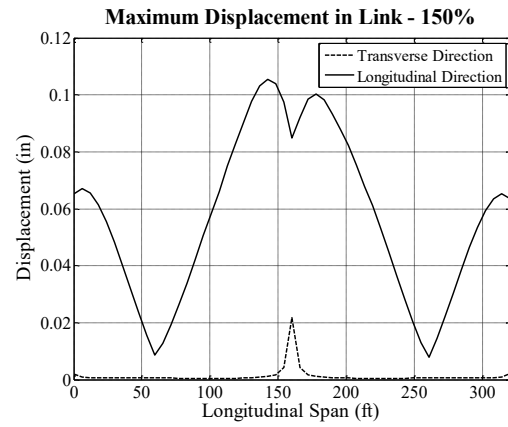


(b)

Figure 3-87 Displacement History for Northridge-01 "Sylmar-Converter Sta" - Model 3 (a) 100% (b) 150%

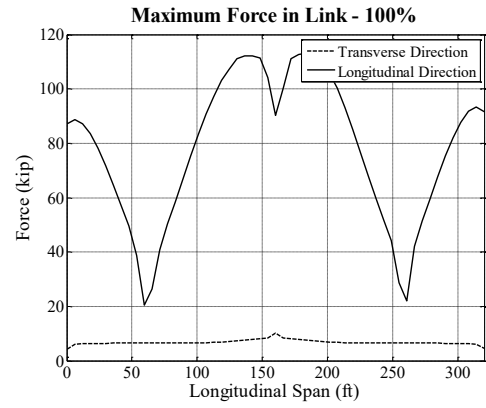
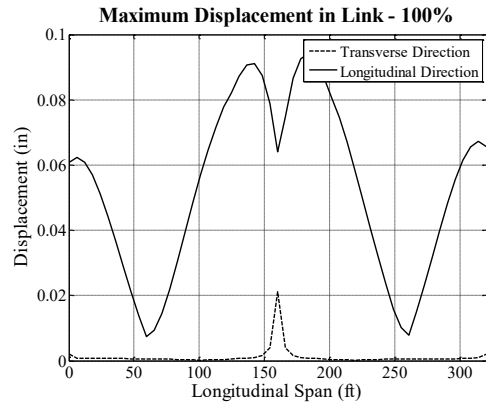


(a)

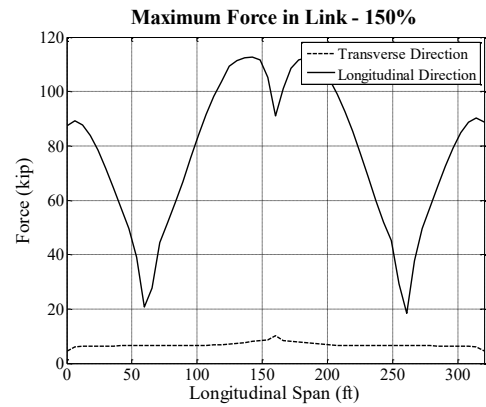
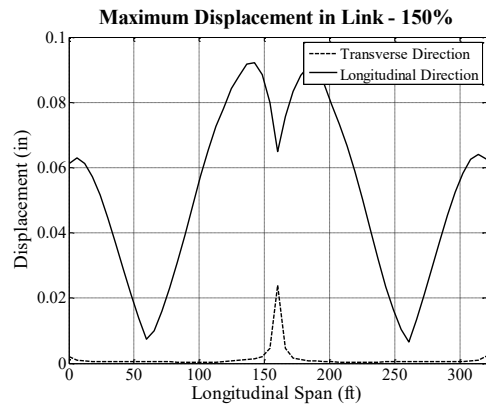


(b)

Figure 3-88 Maximum Link Force and Displacement for Imperial Valley-06 "Delta" - Model 3 (a) 100% (b) 150%



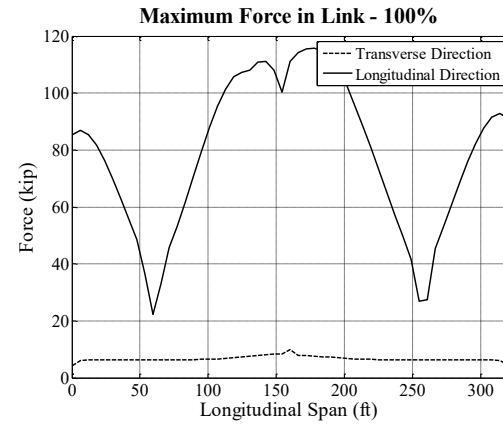
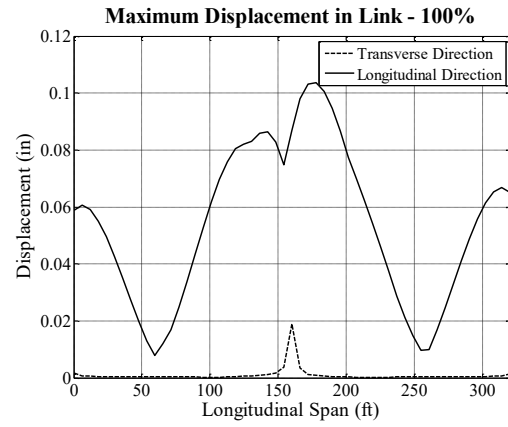
(a)



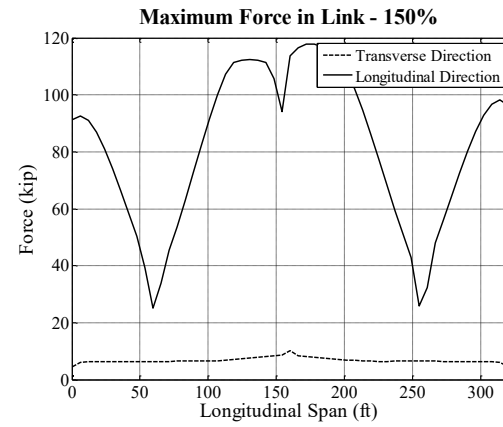
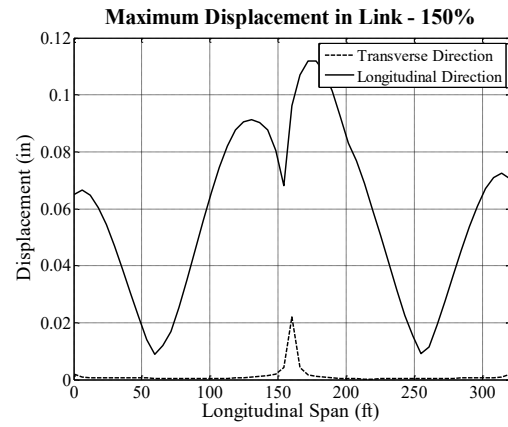
(b)

Figure 3-89 Maximum Link Force and Displacement for Loma Prieta "Hollister Differential Array" - Model 3 (a) 100%

(b) 150%

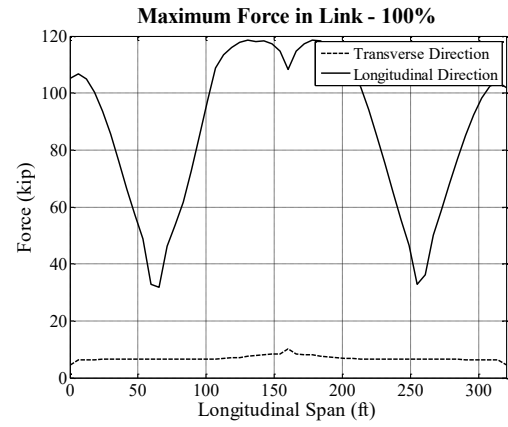
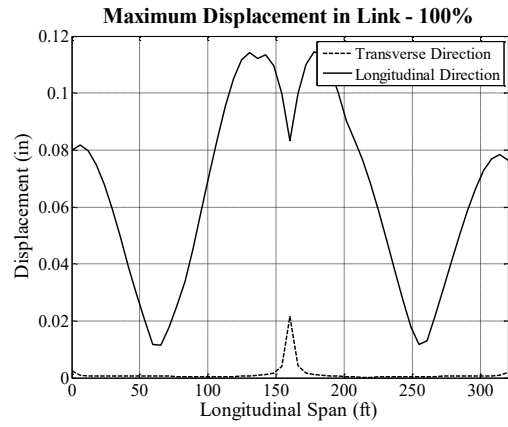


(a)

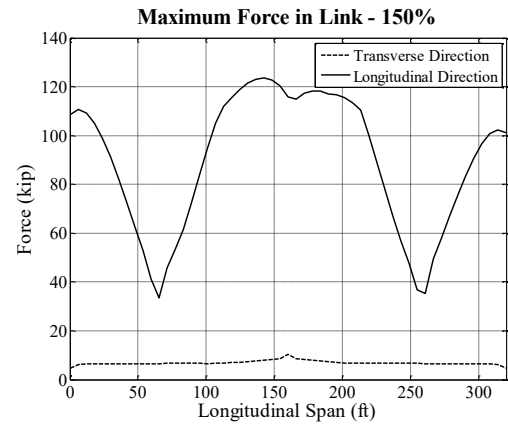
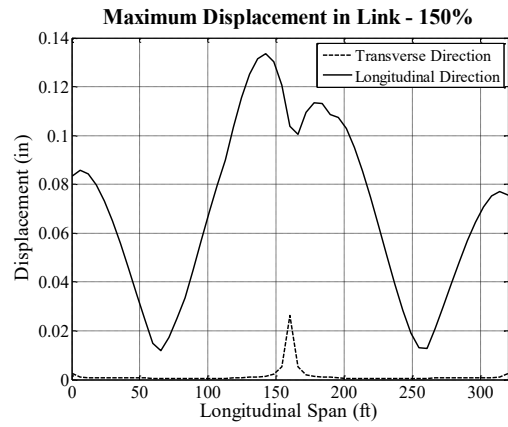


(b)

Figure 3-90 Maximum Link Force and Displacement for Northridge-01 "LA-Saturn St" - Model 3 (a) 100% (b) 150%

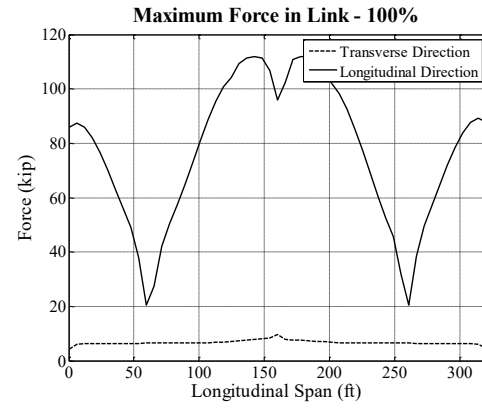
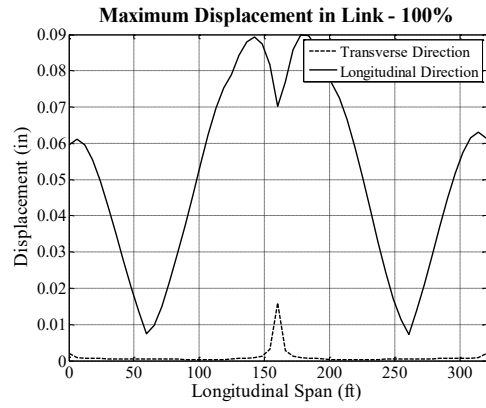


(a)

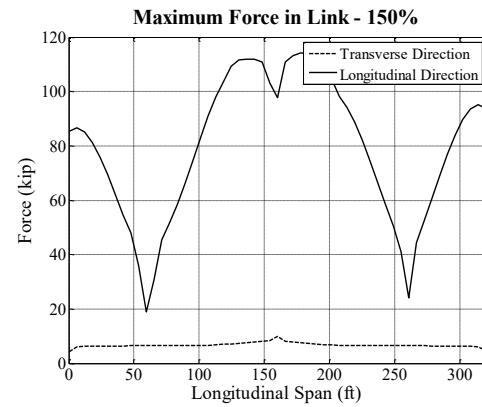
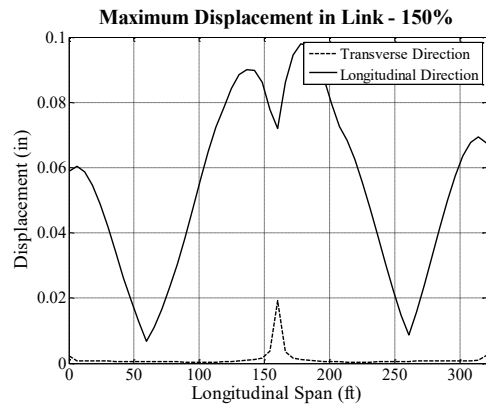


(b)

Figure 3-91 Maximum Link Force and Displacement for Imperial Valley-06 "Bonds Corner" - Model 3 (a) 100% (b) 150%



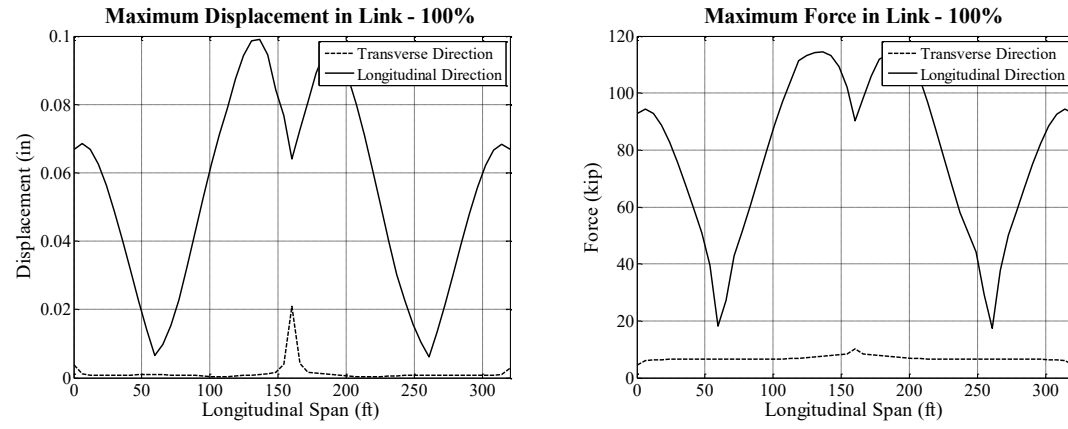
(a)



(b)

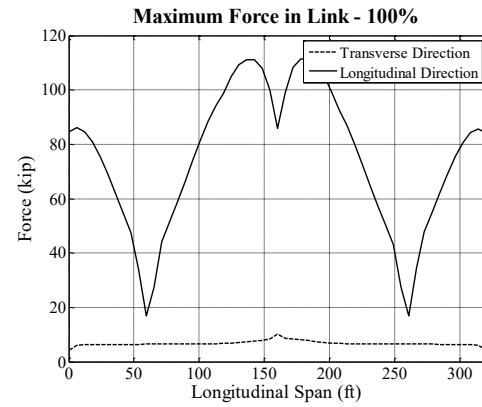
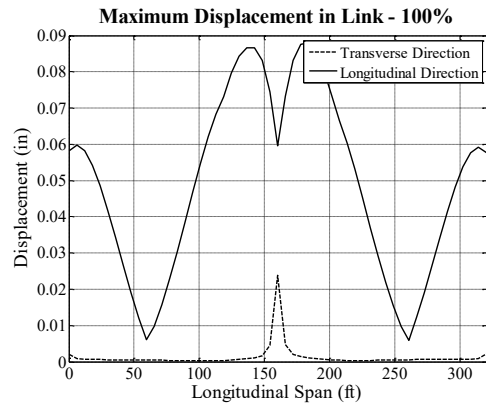
Figure 3-92 Maximum Link Force and Displacement for Chalfant Valley-02 "Zack Brother Ranch" - Model 3 (a) 100% (b)

150%

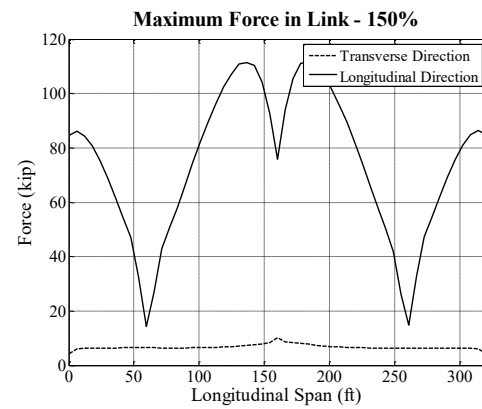
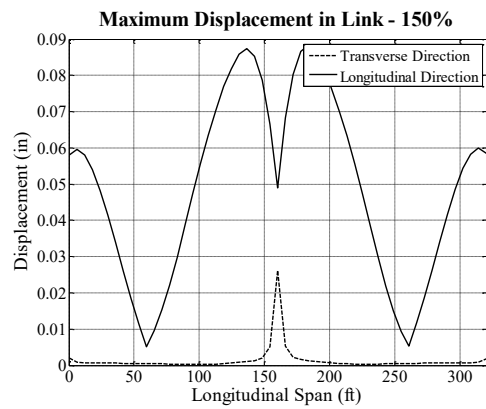


(a)

Figure 3-93 Maximum Link Force and Displacement for Loma Prieta "Capitola" -Model 3 (a) 100%



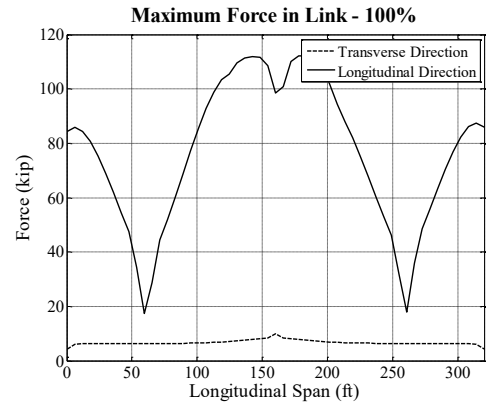
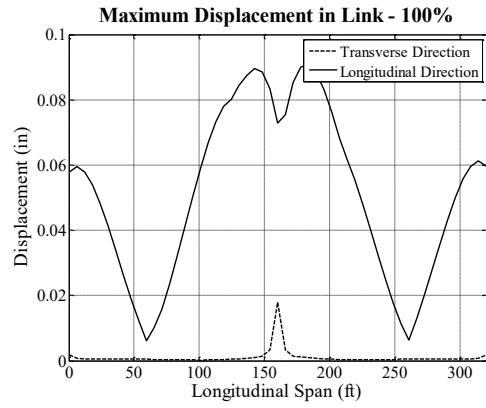
(a)



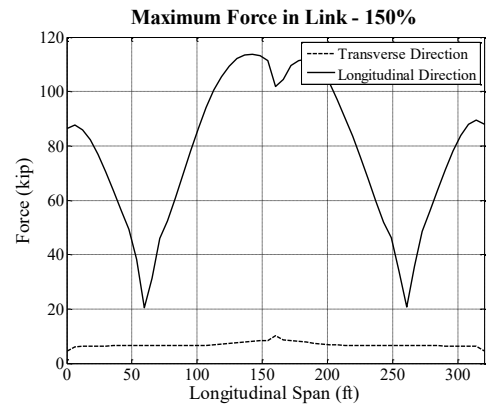
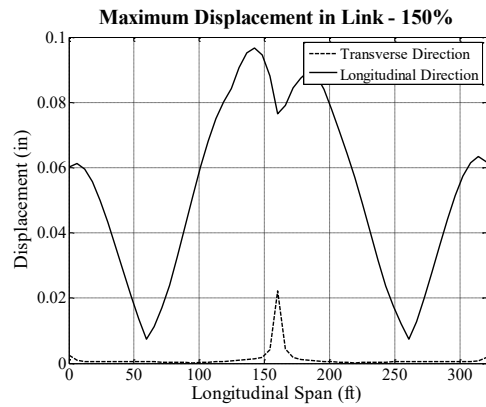
(b)

Figure 3-94 Maximum Link Force and Displacement for Northridge-01 "Rinaldi Receiving Sta" - Model 3 (a) 100% (b)

150%



(a)



(b)

Figure 3-95 Maximum Link Force and Displacement for Northridge-01 "Sylmar-Converter Sta" - Model 3 (a) 100% (b)

150%

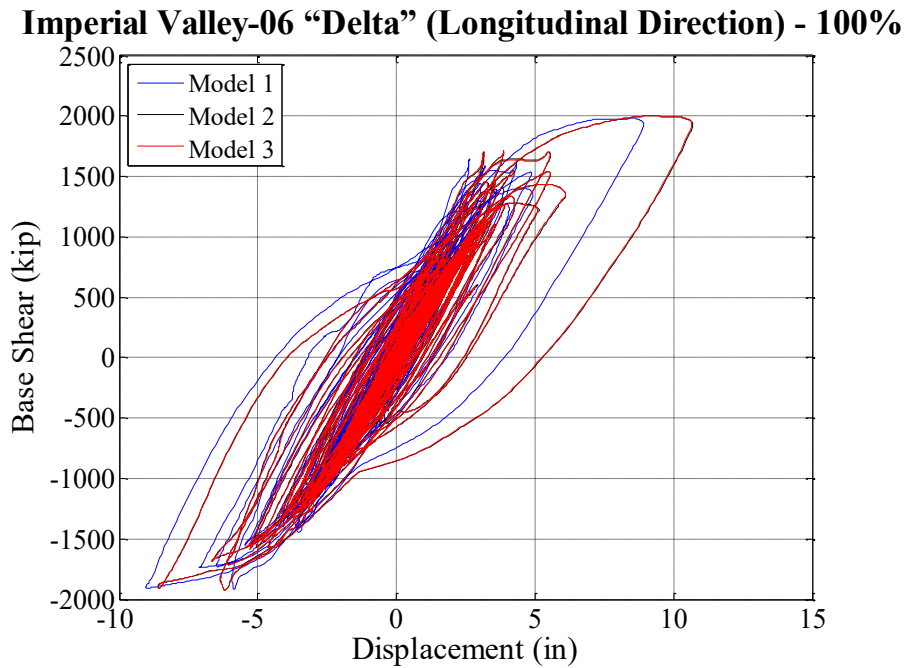
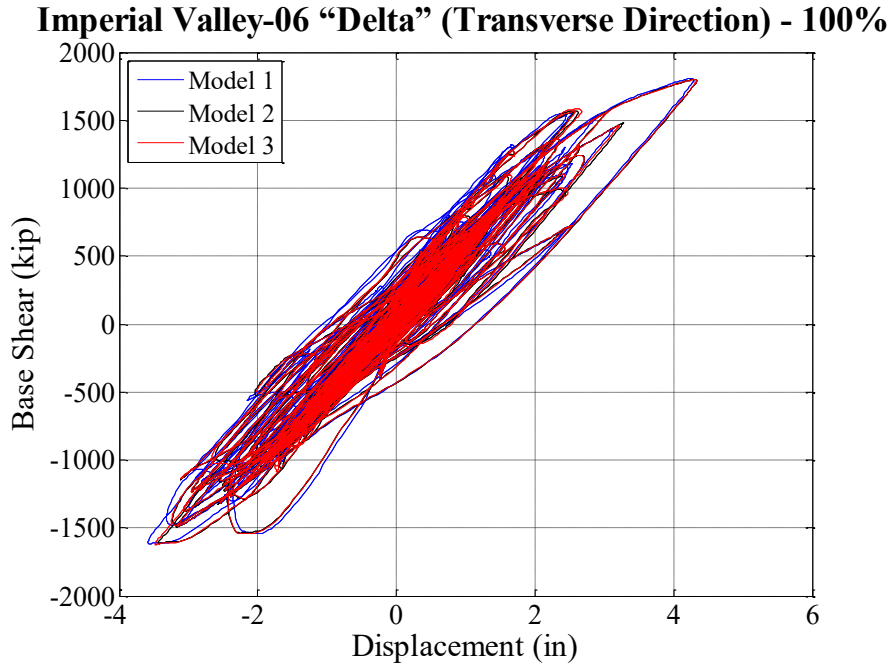


Figure 3-96 Comparison of Hysteresis Loop for Imperial Valley-06 "Delta" (100%)

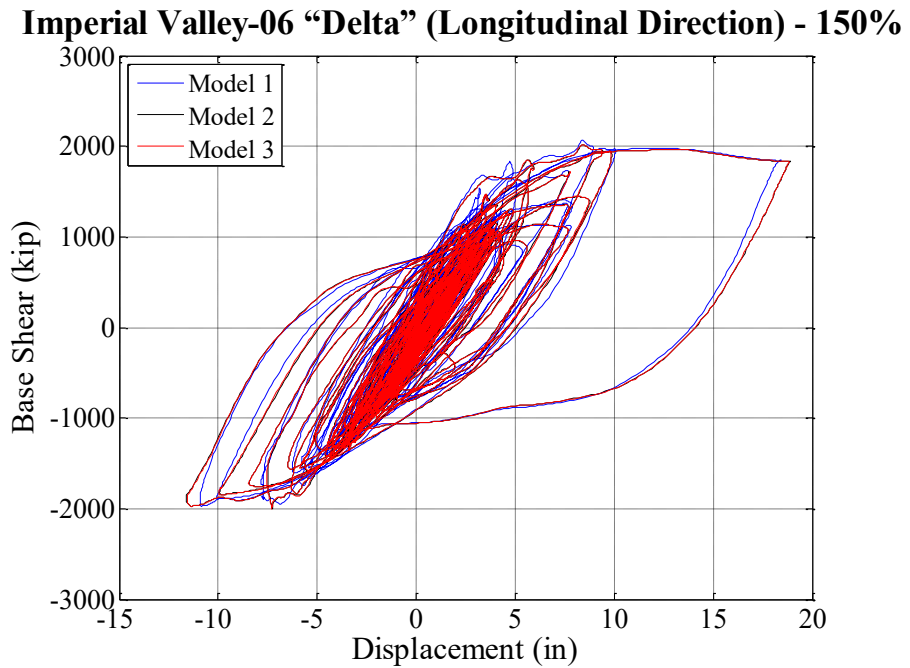
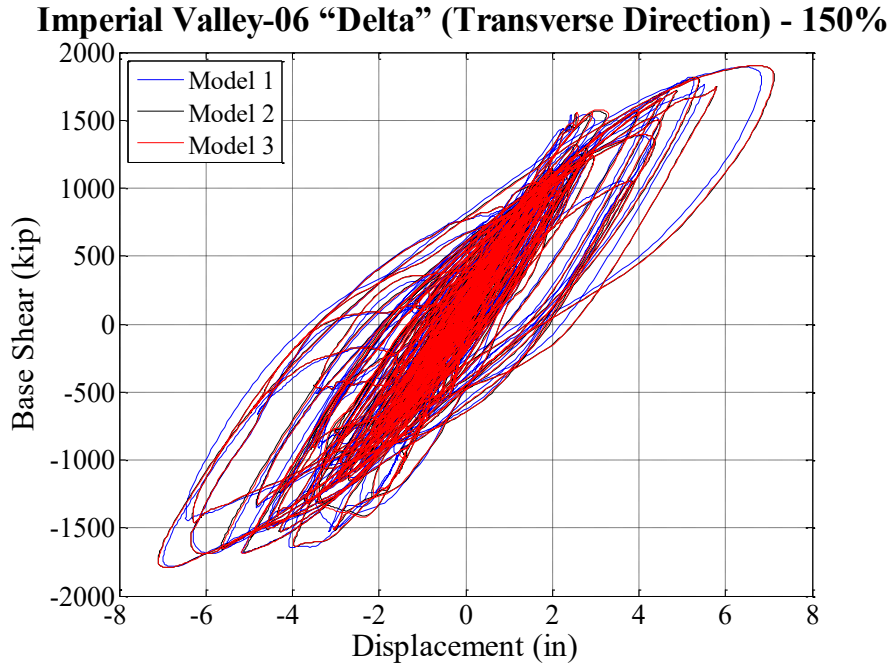


Figure 3-97 Comparison of Hysteresis Loop for Imperial Valley-06 "Delta" (150%)

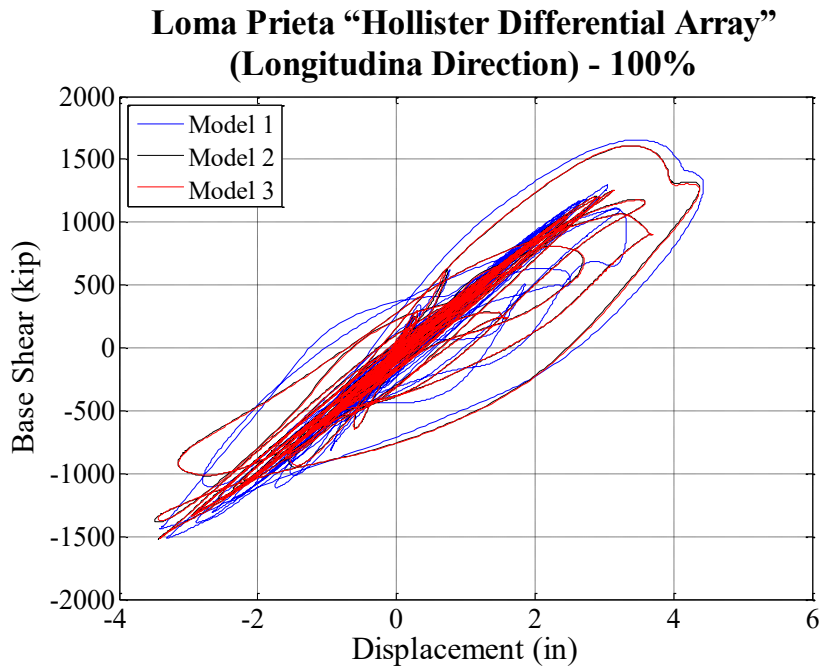
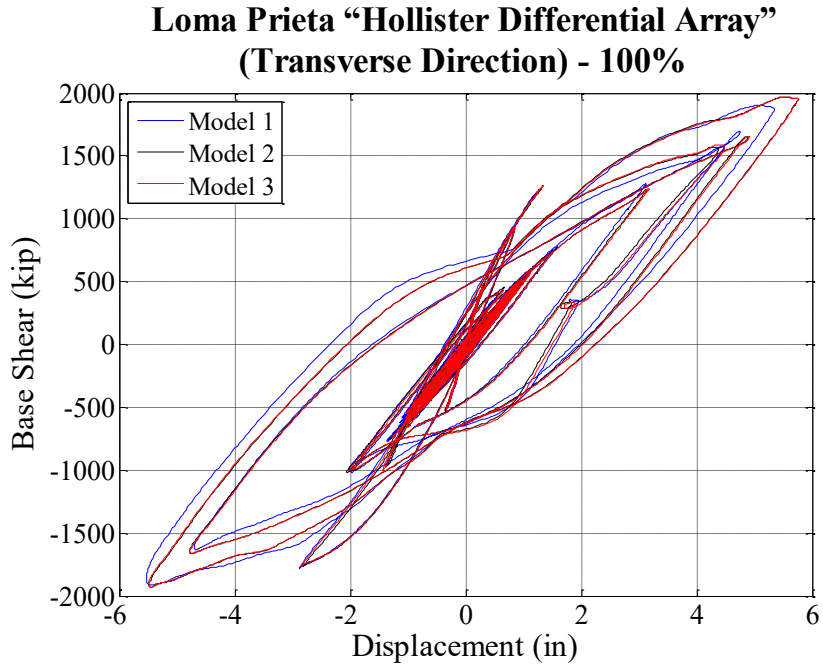


Figure 3-98 Comparison of Hysteresis Loop for Loma Prieta "Hollister Differential Array" (100%)

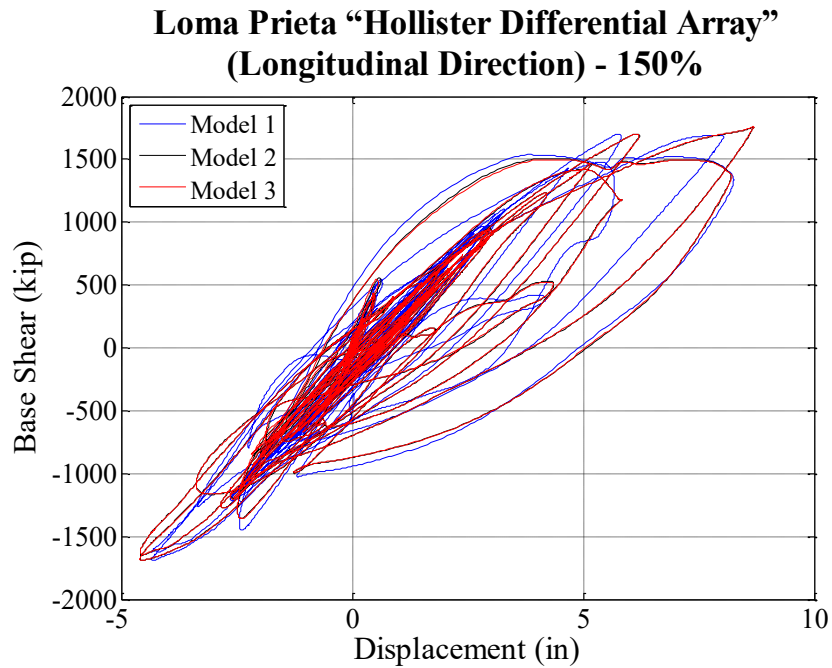
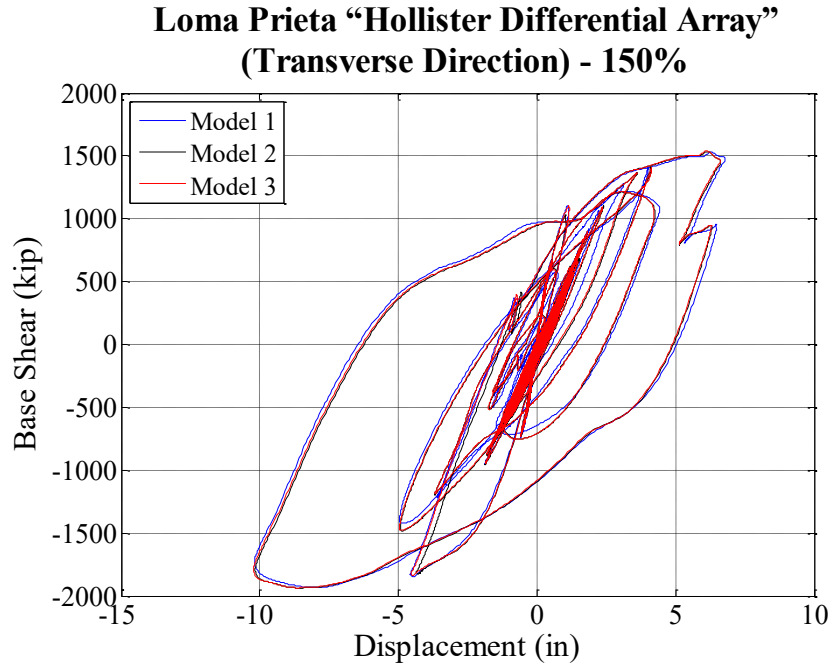
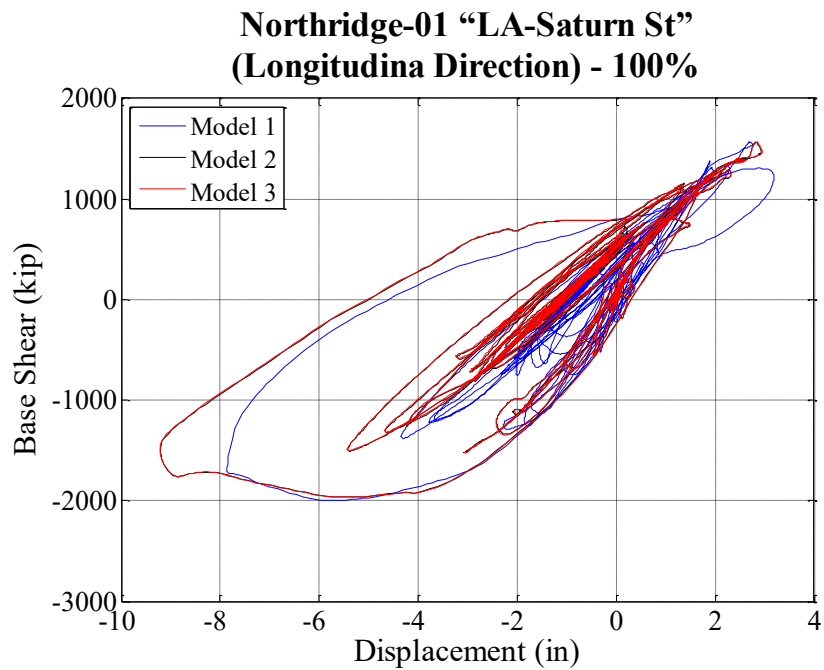
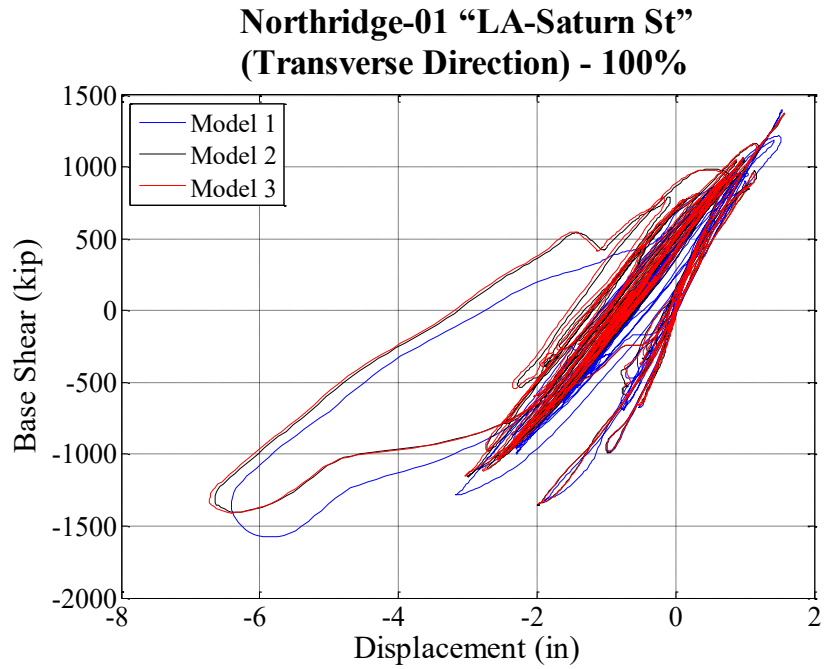
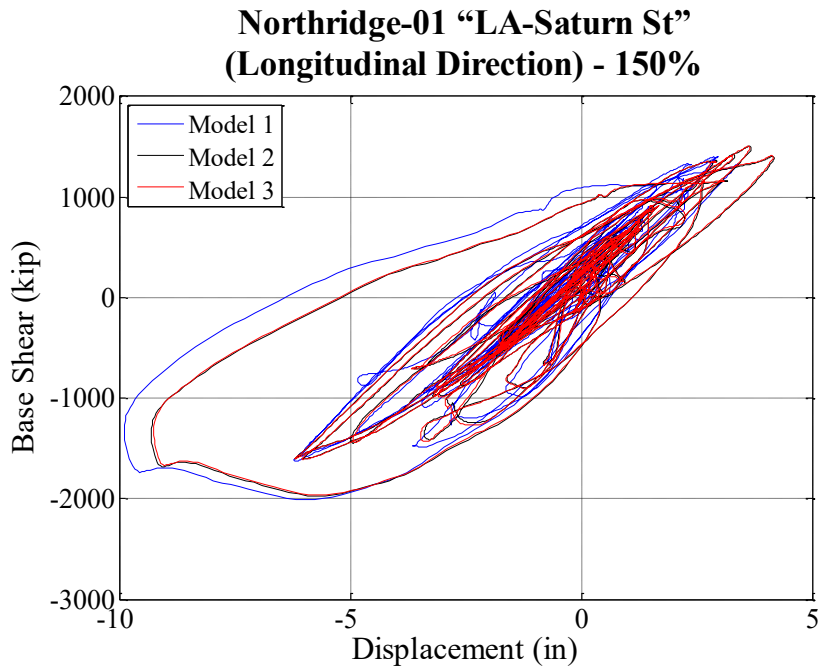
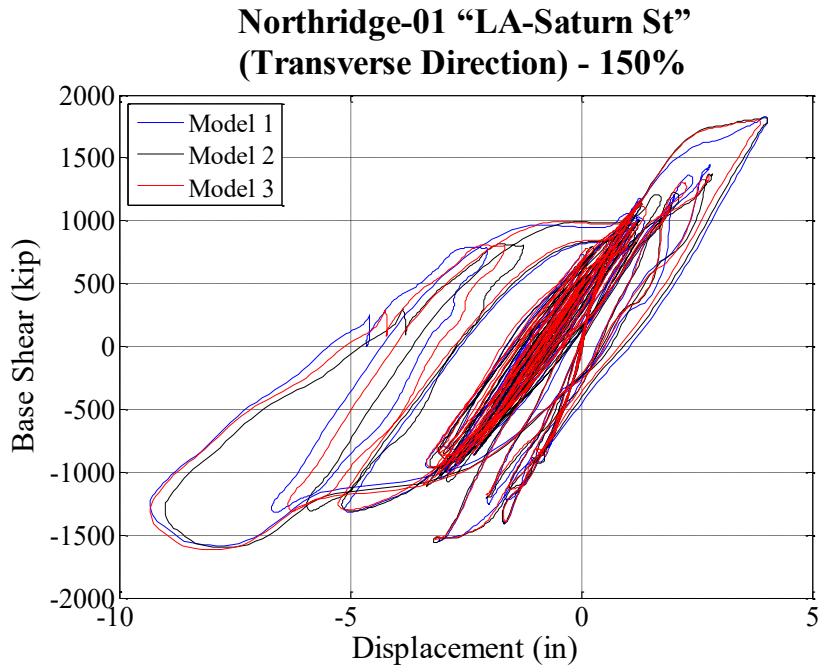


Figure 3-99 Comparison of Hysteresis Loop for Loma Prieta "Hollister Differential Array" (150%)



**Figure 3-100 Comparison of Hysteresis Loop for Northridge-01 "LA-Saturn St"
(100%)**



**Figure 3-101 Comparison of Hysteresis Loop for Northridge-01 "LA-Saturn St"
(150%)**

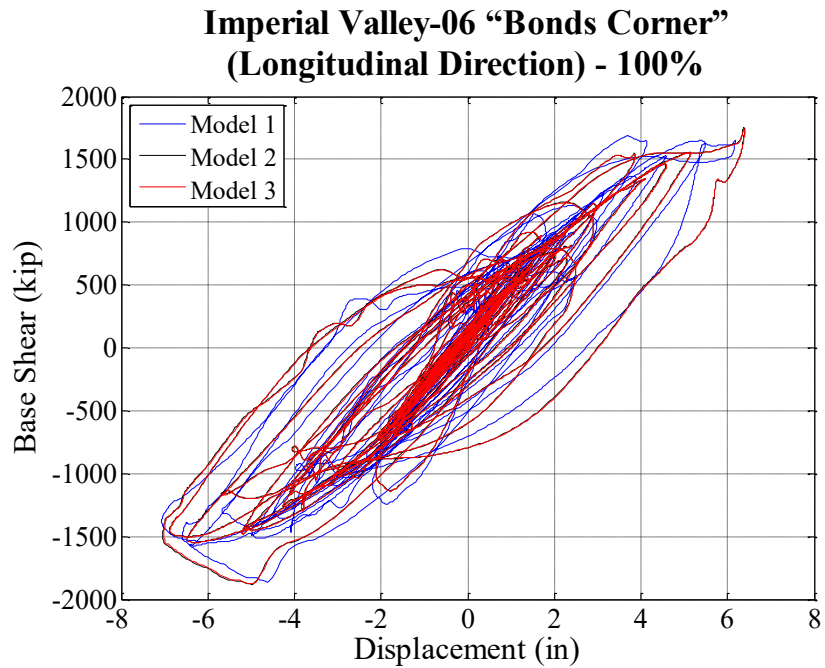
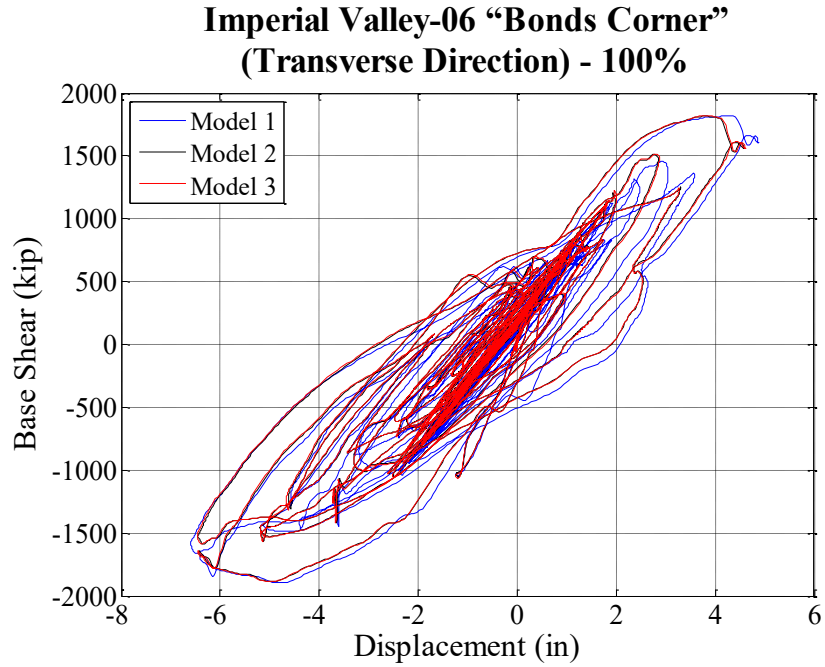


Figure 3-102 Comparison of Hysteresis Loop for Imperial Valley-06 "Bonds Corner" (100%)

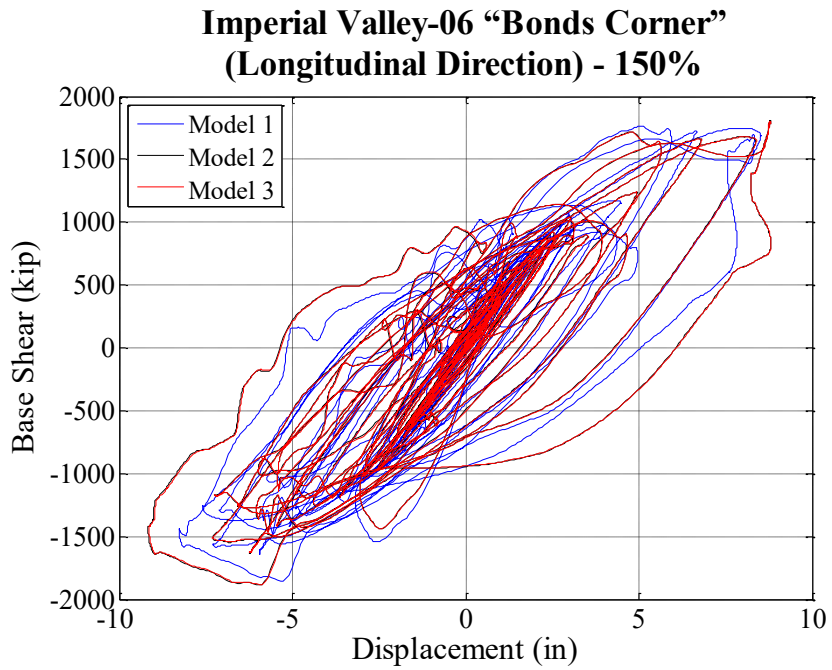
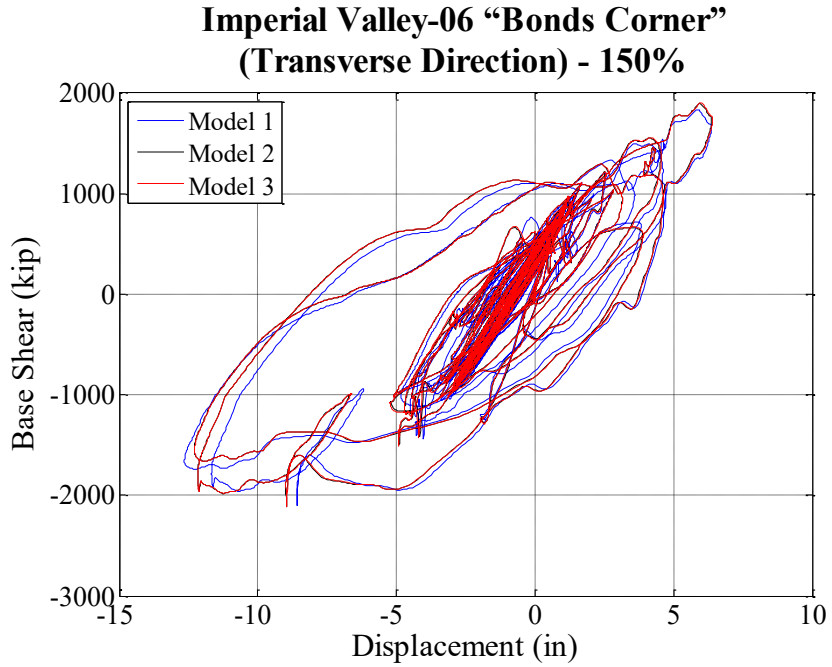
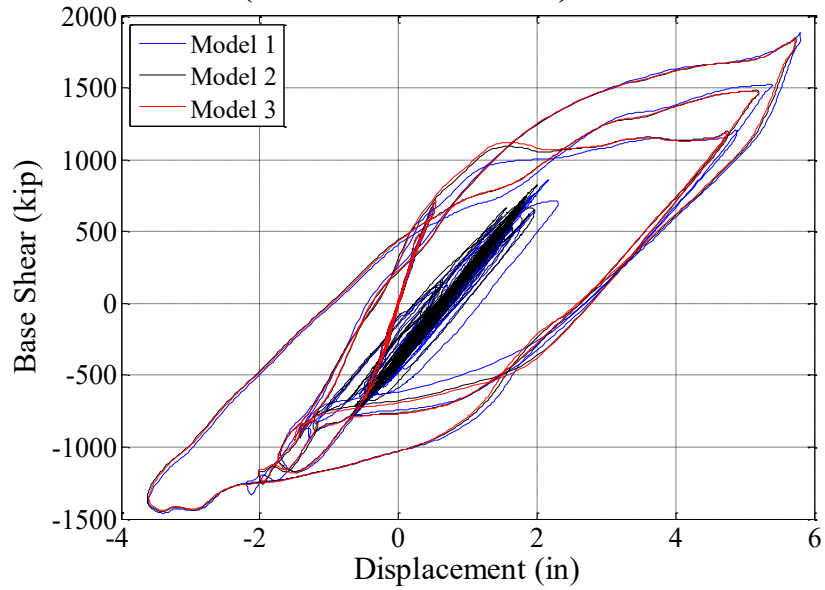


Figure 3-103 Comparison of Hysteresis Loop for Imperial Valley-06 "Bonds Corner" (150%)

**Chalfant Valley-02 "Zack Brother Ranch"
(Transverse Direction) - 100%**



**Chalfant Valley-02 "Zack Brother Ranch"
(Longitudinal Direction) - 100%**

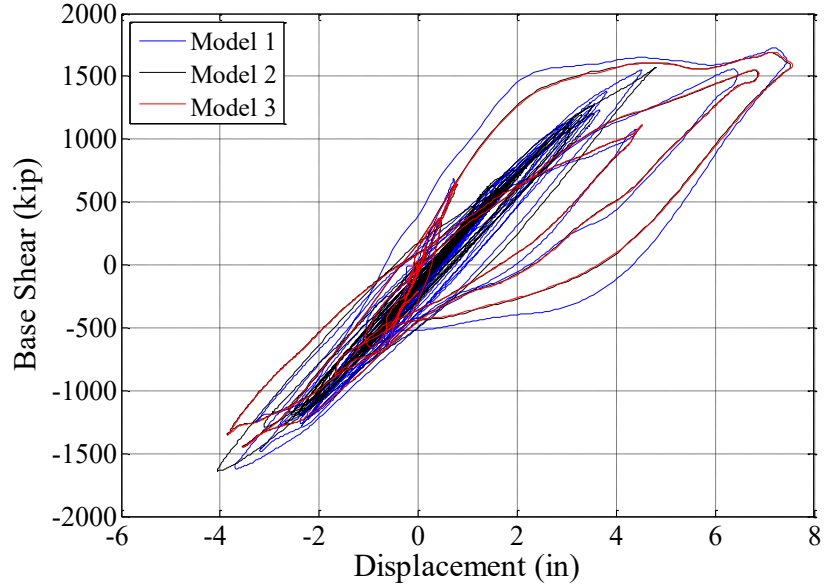
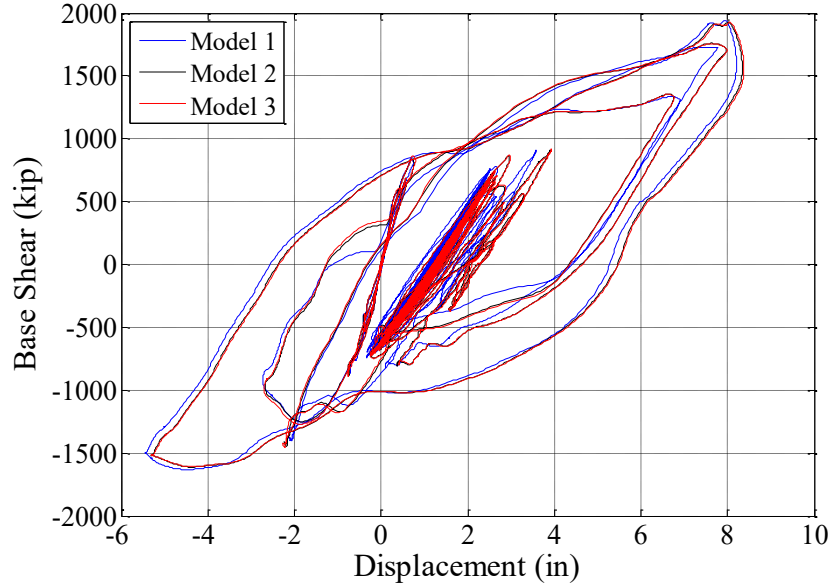


Figure 3-104 Comparison of Hysteresis Loop for Chalfant Valley-02 "Zack Brother Ranch" (100%)

**Chalfant Valley-02 "Zack Brother Ranch"
(Transverse Direction) - 150%**



**Chalfant Valley-02 "Zack Brother Ranch"
(Longitudinal Direction) - 150%**

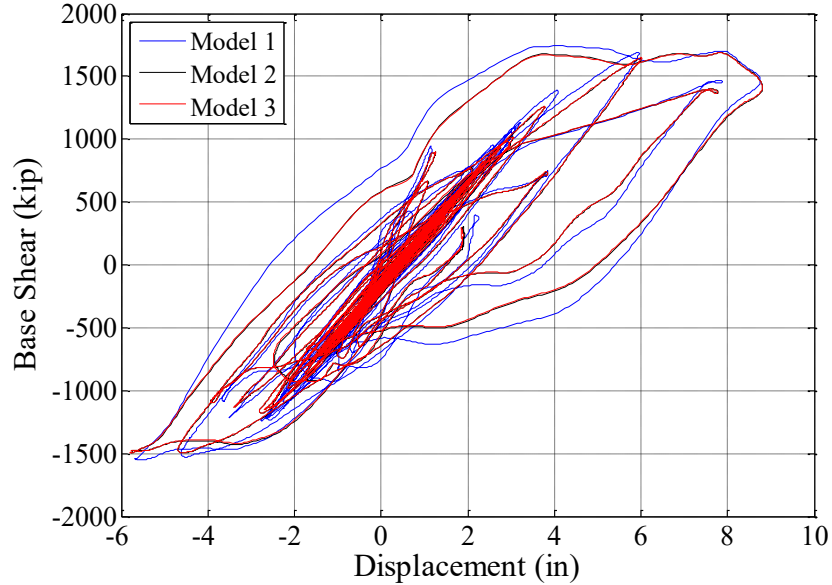
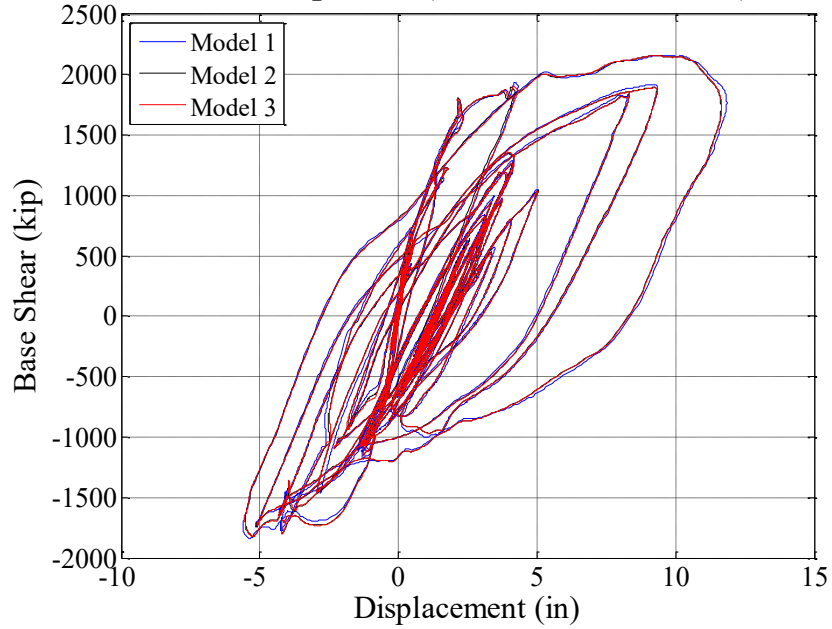


Figure 3-105 Comparison of Hysteresis Loop for Chalfant Valley-02 "Zack Brother Ranch" (150%)

Loma Prieta "Capitola" (Transverse Direction) - 100%



Loma Prieta "Capitola" (Longitudinal Direction) - 100%

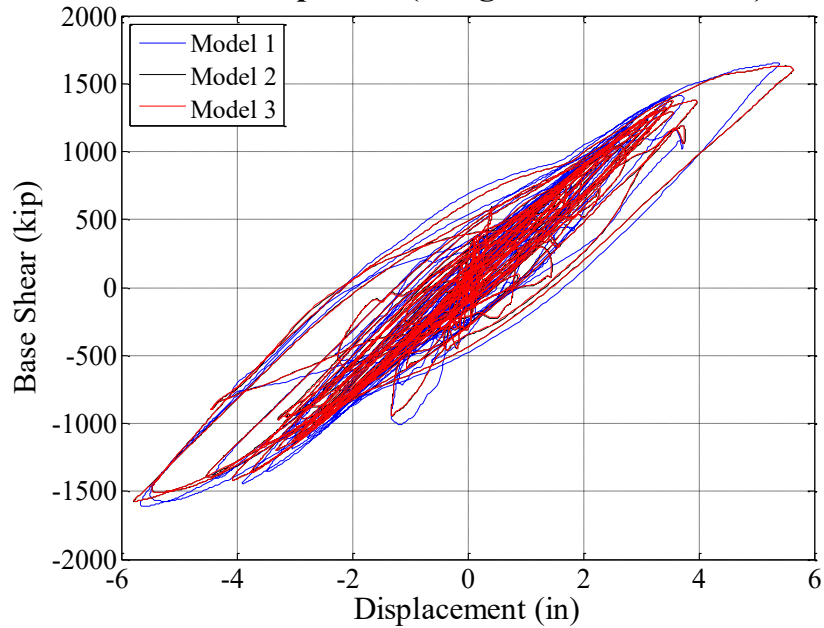


Figure 3-106 Comparison of Hysteresis Loop for Loma Prieta "Capitola" (100%)

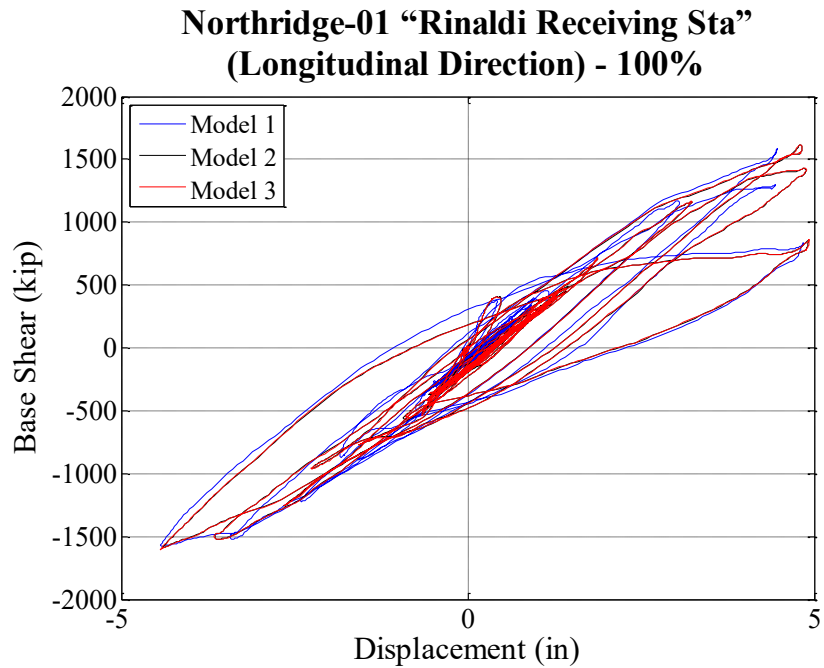
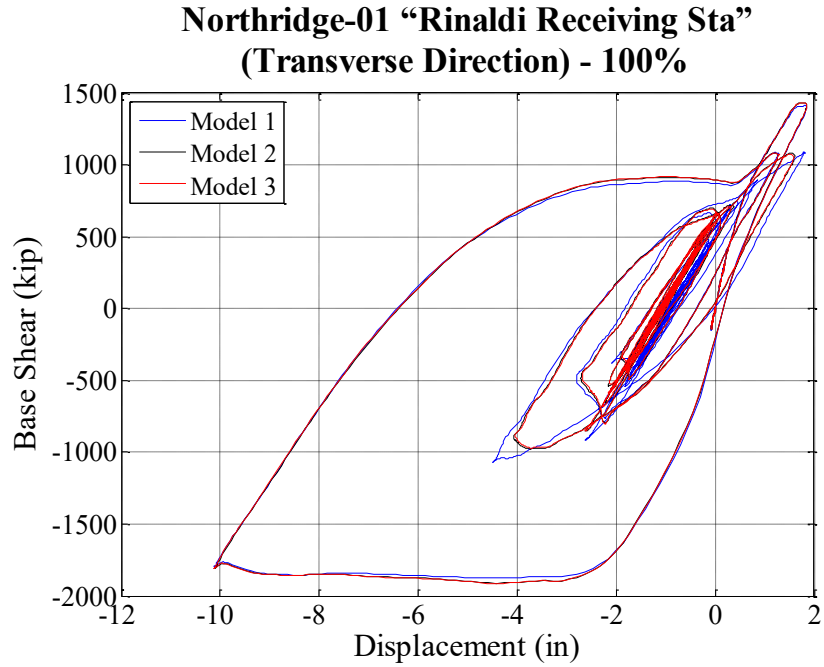


Figure 3-107 Comparison of Hysteresis Loop for Northridge-01 "Rinaldi Receiving Sta" (100%)

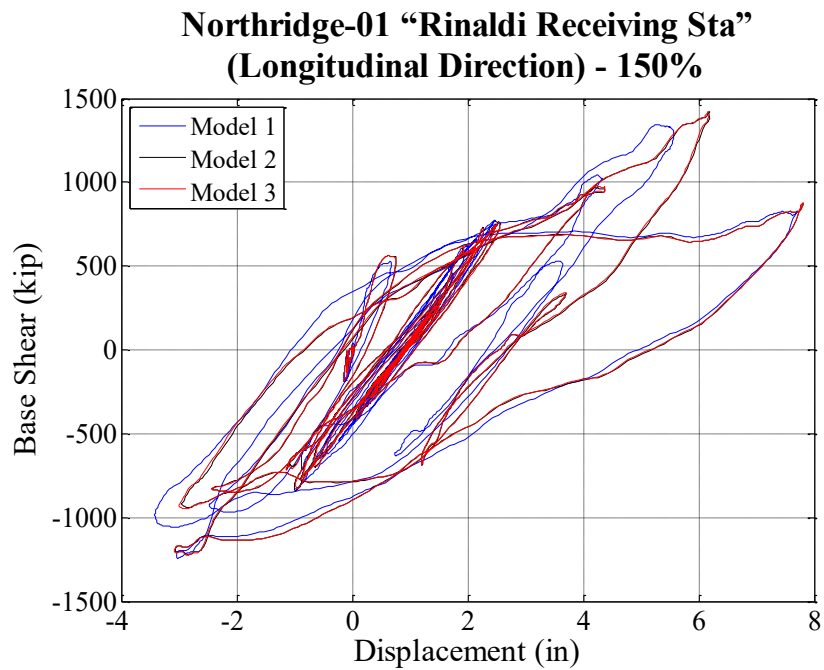
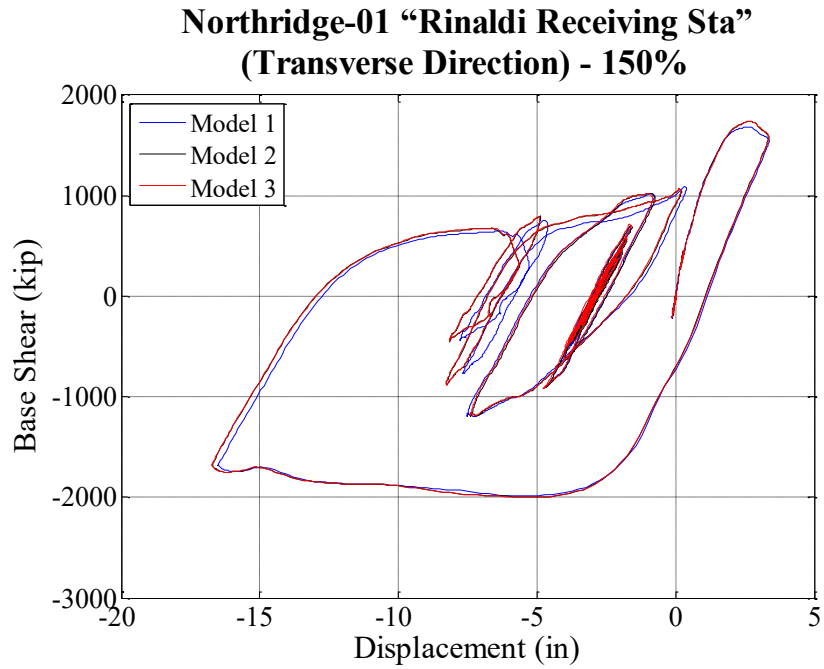


Figure 3-108 Comparison of Hysteresis Loop for Northridge-01 "Rinaldi Receiving Sta" (150%)

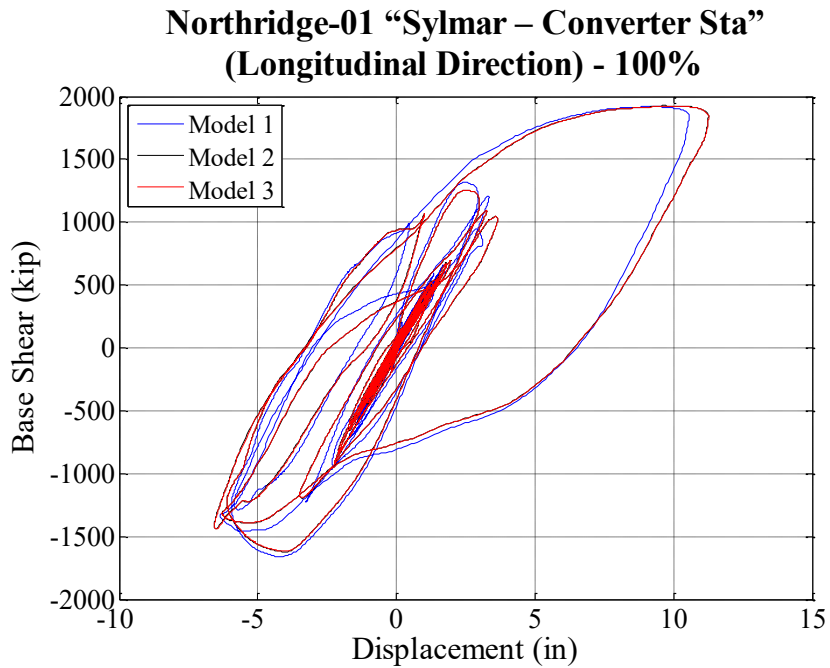
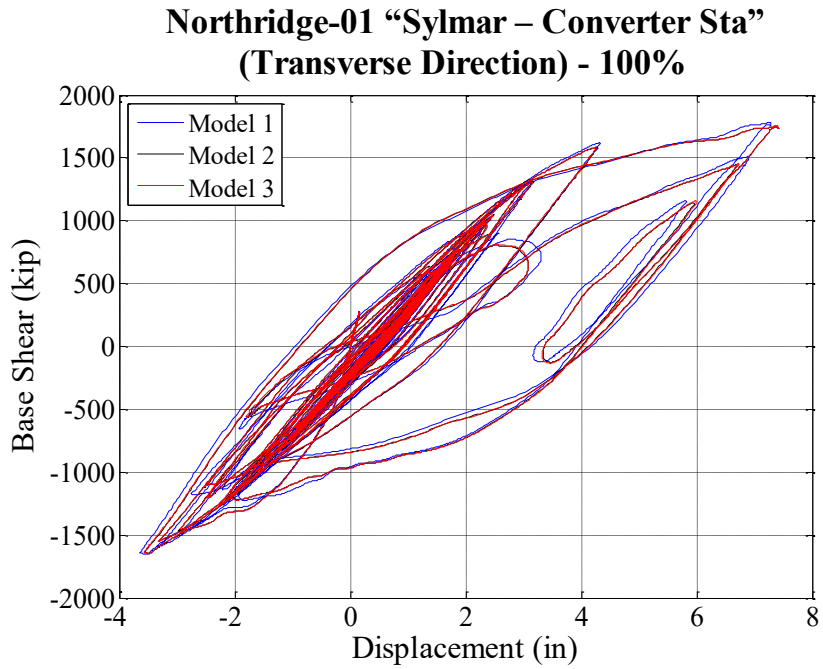
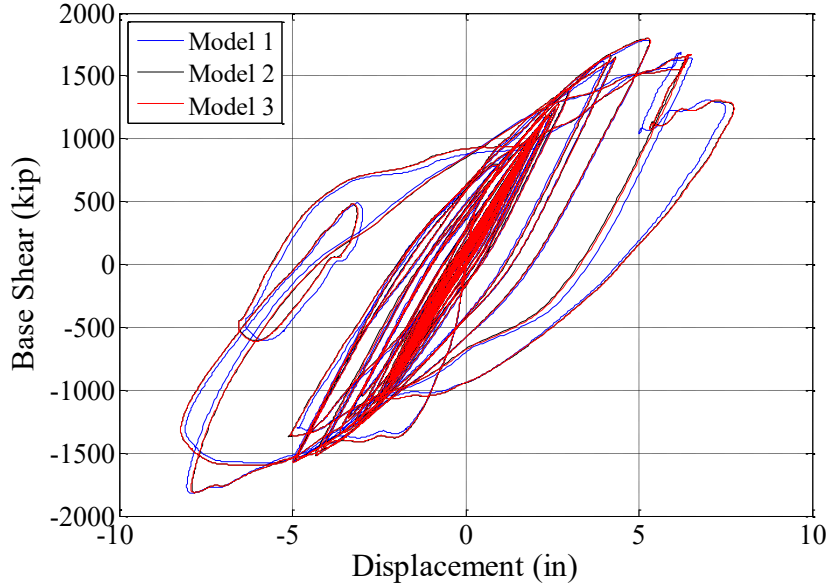


Figure 3-109 Comparison of Hysteresis Loop for Northridge-01 "Sylmar-Converter Sta" (100%)

**Northridge-01 "Sylmar – Converter Sta"
(Transverse Direction) - 150%**



**Northridge-01 "Sylmar – Converter Sta"
(Longitudinal Direction) - 150%**

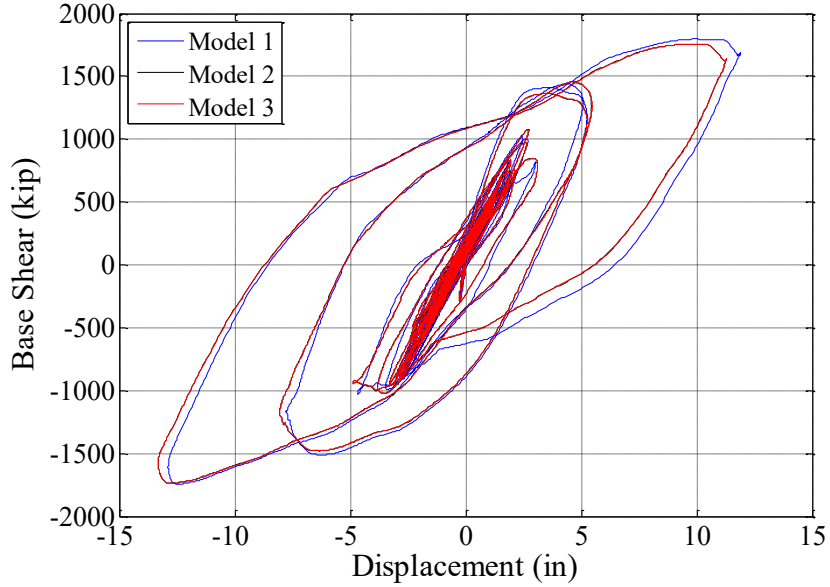


Figure 3-110 Comparison of Hysteresis Loop for Northridge-01 "Sylmar-Converter Sta" (150%)

4. Summary, Conclusions, and Recommendations for Future Research

4.1 Summary

The primary objective of this study was to develop and design prefabricated precast bridge decks connections to precast longitudinal girders. These prefabricated decks also offer the ability to be replaced during the life span of the bridge while maintaining the serviceability and seismic resiliency of the bridge.

To perform the analytical investigation on bridges with prefabricated decks, the properties of the anchors that connect the deck to the girders were needed. An experimental study was conducted on headed anchors to determine their shear, pullout strength, and stiffness. Nine push-out shear specimens were tested to identify the strength and the lateral stiffness of the anchors embedded in different types of grout or concrete. The filler material is referred to as “grout” in this document. The group effect of the anchors and the effect of the anchor head area were also investigated. In addition to the shear tests, twelve pullout specimens were tested to study the pull-out behavior of the anchor and determine their rebar pullout strength and stiffness using various grouts. Another parameter of the study was the ease in the removal of the grout. After each test, the grout was removed from the pockets in the shear specimens using a chipping hammer and the time required for the removal was recorded.

The experimental test results on the anchors were used in an analytical investigation on a two-span bridge to determine the anchor seismic demand forces and the effect of the anchor spacing on the overall bridge seismic response and the anchor forces. Three different models were investigated for this purpose. In the first model,

rigid link elements were used to connect the decks and girders. In the second and third models, link elements spaced at 4 ft and 6 ft were assumed, with increased number of anchors in each pocket in the latter to provide the same shear resistance in the two cases. The number of anchors was designed for live load and seismic forces. Response spectrum analysis was performed on the bridge model to design the deck anchors. A nonlinear response history analyses was performed with eight different ground motions corresponding to 100% design level and 150% level, which is assumed as the "maximum considered earthquake," MCE.

4.2 Conclusions

Based on the results of the experimental investigation and analytical study presented in this document, the following conclusions are drawn:

- The failure mode of all shear test specimens was the fracture of the headed anchor at the interface of deck and girder.
- The types of grout had negligible effect on the ultimate shear capacity of the anchor.
- The anchor head area had negligible effect on the ultimate shear capacity of the anchor when the filler material was UHPC.
- The shear capacity of the headed anchors increased linearly when the number of anchors increased indicating no group effect.
- The failure mode for all pullout tests was the fracture of the anchor at the top of the grout indicating adequate embedment length.

- The type of grout and anchor head area had no effect on the pullout strength of the headed anchor.
- Out of the six different grout types investigated, Latex Concrete took the least amount of time to be removed from the pocket.
- Polyester Concrete and UHPC were the most difficult material to be removed from the pockets.
- Based on the time required and ease in removing the grout, 1428 HP, EucoSpeed, conventional concrete and latex concrete were recommended to facilitate future deck replacement.
- The ultimate shear strength of the anchors were similar to the AASHTO Section 6 anchor shear capacity equation.

—

- The effective shear stiffness of the headed anchors obtained from the test results was:

—

where, E is the modulus of elasticity of anchor, I_a is the moment of inertia of anchor, and L_{eff} is the effective length that is unrestrained for bending in anchor.

- The axial stiffness of the headed anchors obtained from the test results was:

—

where, A is the area of anchor, E is the modulus of elasticity of anchor, and L_2 is the length of the anchor embedded into the deck.

- The design provisions in AASHTO Section 6 for cast-in-place decks were found to be applicable to precast decks.
- Using the experimental results of the anchor stiffness in gravity load analysis showed that precast bridge decks were able to achieve approximately 70-75% of a full composite action. The mid-span deflection of the bridge increased by 44% with experimental anchor stiffness than full composite action due to the decrease in vertical stiffness of the bridge.
- The analytical investigation showed no difference in the overall seismic response of pockets spaced at 4 ft and 6 ft.
- The results of the nonlinear seismic analysis showed all anchor forces were substantially less than their ultimate capacity.

4.3 Recommendations for Future Research

A system experiment of a multi-span bridge models is recommended to investigate the composite action of precast decks using headed anchors. The lack of full composite action may affect the live load stresses in the longitudinal girders. In addition, the fatigue response of the headed anchors needs to be evaluated.

References

- AASHTO (2011). "AASHTO Guide Specifications for LRFD Seismic Bridge Design," Washington, D.C.
- AASHTO (2012). "AASHTO LRFD Bridge Design Specifications, Customary .S. Units (6th Edition)," Washington, D.C.
- ACI 318 (2011). "Building Code Requirements for Structural Concrete (ACI 318-11) and Commentary," ACI Committee 318, American Concrete Institute, Farmington Hills, MI.
- Assad, A., (2014). "Evaluating the Impact of Bridge Deck Removal Method on the Performance of Precast/Prestressed Concrete I-Girders," Masters of Science Thesis, University of Nebraska, Lincoln, Nebraska.
- ASTM C39/C39M-17a (2017). "Standard Test Method for Compressive Strength of Cylinder Concrete Specimens," West Conshohocken, PA.
- ASTM C109/C109M-16a (2016). "Standard Test Method for Compressive Strength of Hydraulic Cement Mortars (Using 2 in. or (50-mm) Cube Specimens)," West Conshohocken, PA.
- ASTM C143/C143M-15a (2015). "Standard Test Method for Slump of Hydraulic-Cement Concrete," West Conshohocken, PA.
- ASTM C469/C469M-14 (2014). "Standard Test Method for Static Modulus of Elasticity and Poisson's Ratio of Concrete in Compression," West Conshohocken, PA.
- ASTM E8/E8M-16a (2016). "Standard Test Methods for Tension Testing of Metallic Materials," West Conshohocken, PA.

- Badie, S. S, and Tadros, M. K., (2008). "Full-Depth Precast Concrete Bridge Deck Panel Systems," Report 584 by National Cooperative Highway Research Program.
- Cao, Q., Hwang, S., Khayat, K. H., and Morcous, G., (2016). "Design and Implementation of Self-Consolidating Concrete for Connecting Precast Concrete Deck Panels to Bridge Girders," Journal of Materials in Civil Engineering, Volume 28 Issue 8, August 2016.
- CSI, (2015). CSiBridge 2015, v. 15.0.0, Computer and Structures, Inc., Walnut Creek, CA.
- Hanna, K., Morcous, G., and Tadros, M.K., (2010). "Second Generation Precast Concrete Deck Panel (N DECK) System," Nebraska Department of Roads and University of Nebraska-Lincoln.
- Hida, S., (2015). "Reigo Road Overcrossing Lessons Learned on challenging bridge project north of Sacramento," ASPIRE Concrete Bridge Magazine, Spring 2015 Issue, pp. 12-14.
- Henley, M. D., (2009). "Shear Connections for the Development of a Full-Depth Precast Concrete Deck System," Master of Science Thesis, Texas A&M niver sity, College Station, Texas.
- Saiidi, M., J. Benjumea, and A. Itani, "Shake Table Performance of a Two-Span Concrete Bridge System Integrating Six ABC Connection Types," Workshop W-11, Accelerated Bridge Construction in Seismic Regions, National Accelerated Bridge Conference, Miami, Florida, December 2017.

- Mander, T. J, (2009). "Structural Performance of a Full-Depth Precast Concrete Bridge Deck System," Master of Science Thesis, Texas A&M University, College Station, Texas.
- Markowski, S. M., (2005). "Experimental and Analytical Study of Full-Depth Precast/Prestressed Concrete Deck Panels for Highway Bridges," Master's Thesis, University of Wisconsin-Madison, Madison, WI.
- Menkulasi, F. and Roberts-Wollmann, C. L., (2005) "Behavior of Horizontal Shear Connections for Full-Depth Precast Concrete Bridge Decks on Prestressed I-Girders," PCI Journal, V. 50, No. 3, May-June, pp. 60-73.
- Monzon, E. V., Wei, C., Buckle, I. G., and Itani, A. M., (2012) "Seismic Response of Curved Highway Bridge with Seismic Isolation and Hybrid Protective Systems," 15 WCEE LISBOA 2012.
- Morcous, G., Tadros, M.K., and Hatami, A., (2013). "Implementation of Precast Concrete Deck System NUDECK (2nd Generation)," NDOR.
- Oliva, M. G., Bank L. C., and Russell J.S., (2007). "Full Depth Precast Concrete Highway Bridge Decks," Report to the Wisconsin Department of Transportation, Wisconsin Department of Transportation (WisDOT), Wisconsin.
- OpenSees. (2017). "Open System for Earthquake Engineering Simulations," Version 2.4.1, Berkeley, CA, Available online: <http://opensees.berkeley.edu>.
- Perry, V. H., and Royce, M., (2010). "Innovative Field Cast UHPC Joints for Precast Bridge System," 3rd fib International Congress.
- Precast/Prestressed Concrete Institute (PCI), (2001). "Precast Deck Panel Guidelines," Report No. PCINER-01-PDPG.

- Precast Concrete Institute (PCI), (2011a). "Full Depth Deck Panels Guidelines for Accelerated Bridge Deck Replacement or Construction," Report No. PCINER-11-FDDP, Second Edition.
- Precast Concrete Institute (PCI), (2011b). "State-of-the-Art Report on Full-Depth Precast Concrete Bridge Deck Panels," First Edition.
- Ramey, G. Ed., and Umphrey, J. (2006). "Rapid Rehabilitation/Replacement of Bridge Decks – Phase II," Research Project 930-436, Highway Research Center and Department of Civil Engineering at Auburn University.
- Scholz, D.P., Wallenfelsz, J.A., Lijeron, C., and Roberts-Wollmann, C.L. (2007). "Recommendations for the connection between full-depth precast bridge deck panel systems and precast I-beams," Report No. 07-CR17, Virginia Transportation Research Council, Charlottesville, Vir. Sullivan, S. (2007). "Construction and Behavior of Precast Bridge Deck Panel Systems", Ph.D. Dissertation, Virginia Tech.
- Shahawym, M. A., (2003). "Prefabricated Bridge Elements and Systems to Limit Traffic Disruption during Construction," NCHRP Synthesis 324, Transportation Research Board, Washington, DC.
- Sullivan, S., (2007). "Construction and Behavior of Precast Bridge Deck Panel Systems," Virginia Polytechnic Institute and State University, Blacksburg, Virginia.
- Tadros, M. K., and Baishya, M. C., (1998). "Rapid Replacement of Bridge Decks," NCHRP Report 407, Transportation Research Board, National Research Council, Washington, D. C.
- Tawadroud, R., (2017). "Design of Shear Pocket Connections in Full-Depth Precast Concrete Bridge Deck Systems," University of Nebraska, Lincoln, Nebraska.

List of CCEER Publications

Report No. Publication

- CCEER-84-1 Saiidi, M., and R. Lawver, “User's Manual for LZAK-C64, A Computer Program to Implement the Q-Model on Commodore 64,” Civil Engineering Department, Report No. CCEER-84-1, University of Nevada, Reno, January 1984.
- CCEER-84-1 Reprint Douglas, B., Norris, G., Saiidi, M., Dodd, L., Richardson, J. and Reid, W., “Simple Bridge Models for Earthquakes and Test Data,” Civil Engineering Department, Report No. CCEER-84-1 Reprint, University of Nevada, Reno, January 1984.
- CCEER-84-2 Douglas, B. and T. Iwasaki, “Proceedings of the First SA -Japan Bridge Engineering Workshop,” held at the Public Works Research Institute, Tsukuba, Japan, Civil Engineering Department, Report No. CCEER-84-2, University of Nevada, Reno, April 1984.
- CCEER-84-3 Saiidi, M., J. Hart, and B. Douglas, “Inelastic Static and Dynamic Analysis of Short R/C Bridges Subjected to Lateral Loads,” Civil Engineering Department, Report No. CCEER-84-3, University of Nevada, Reno, July 1984.
- CCEER-84-4 Douglas, B., “A Proposed Plan for a National Bridge Engineering Laboratory,” Civil Engineering Department, Report No. CCEER-84-4, University of Nevada, Reno, December 1984.
- CCEER-85-1 Norris, G. and P. Abdollahiaee, “Laterally Loaded Pile Response: Studies with the Strain Wedge Model,” Civil Engineering Department, Report No. CCEER-85-1, University of Nevada, Reno, April 1985.
- CCEER-86-1 Ghosn, G. and M. Saiidi, “A Simple Hysteretic Element for Biaxial Bending of R/C in NEABS-86,” Civil Engineering Department, Report No. CCEER-86-1, University of Nevada, Reno, July 1986.
- CCEER-86-2 Saiidi, M., R. Lawver, and J. Hart, “User's Manual of ISADAB and SIBA, Computer Programs for Nonlinear Transverse Analysis of Highway Bridges Subjected to Static and Dynamic Lateral Loads,” Civil Engineering Department, Report No. CCEER-86-2, University of Nevada, Reno, September 1986.

- CCEER-87-1 Siddharthan, R., "Dynamic Effective Stress Response of Surface and Embedded Footings in Sand," Civil Engineering Department, Report No. CCEER-86-2, University of Nevada, Reno, June 1987.
- CCEER-87-2 Norris, G. and R. Sack, "Lateral and Rotational Stiffness of Pile Groups for Seismic Analysis of Highway Bridges," Civil Engineering Department, Report No. CCEER-87-2, University of Nevada, Reno, June 1987.
- CCEER-88-1 Orié, J. and M. Saiidi, "A Preliminary Study of One-Way Reinforced Concrete Pier Hinges Subjected to Shear and Flexure," Civil Engineering Department, Report No. CCEER-88-1, University of Nevada, Reno, January 1988.
- CCEER-88-2 Orié, D., M. Saiidi, and B. Douglas, "A Micro-CAD System for Seismic Design of Regular Highway Bridges," Civil Engineering Department, Report No. CCEER-88-2, University of Nevada, Reno, June 1988.
- CCEER-88-3 Orié, D. and M. Saiidi, "User's Manual for Micro-SARB, a Microcomputer Program for Seismic Analysis of Regular Highway Bridges," Civil Engineering Department, Report No. CCEER-88-3, University of Nevada, Reno, October 1988.
- CCEER-89-1 Douglas, B., M. Saiidi, R. Hayes, and G. Holcomb, "A Comprehensive Study of the Loads and Pressures Exerted on Wall Forms by the Placement of Concrete," Civil Engineering Department, Report No. CCEER-89-1, University of Nevada, Reno, February 1989.
- CCEER-89-2 Richardson, J. and B. Douglas, "Dynamic Response Analysis of the Dominion Road Bridge Test Data," Civil Engineering Department, Report No. CCEER-89-2, University of Nevada, Reno, March 1989.
- CCEER-89-2 Vrontinos, S., M. Saiidi, and B. Douglas, "A Simple Model to Predict the Ultimate Response of R/C Beams with Concrete Overlays," Civil Engineering Department, Report NO. CCEER-89-2, University of Nevada, Reno, June 1989.
- CCEER-89-3 Ebrahimpour, A. and P. Jagadish, "Statistical Modeling of Bridge Traffic Loads - A Case Study," Civil Engineering Department, Report No. CCEER-89-3, University of Nevada, Reno, December 1989.
- CCEER-89-4 Shields, J. and M. Saiidi, "Direct Field Measurement of Prestress Losses in Box Girder Bridges," Civil Engineering Department, Report No. CCEER-89-4, University of Nevada, Reno, December 1989.

- CCEER-90-1 Saiidi, M., E. Maragakis, G. Ghusn, Y. Jiang, and D. Schwartz, "Survey and Evaluation of Nevada's Transportation Infrastructure, Task 7.2 - Highway Bridges, Final Report," Civil Engineering Department, Report No. CCEER 90-1, University of Nevada, Reno, October 1990.
- CCEER-90-2 Abdel-Ghaffar, S., E. Maragakis, and M. Saiidi, "Analysis of the Response of Reinforced Concrete Structures During the Whittier Earthquake 1987," Civil Engineering Department, Report No. CCEER 90-2, University of Nevada, Reno, October 1990.
- CCEER-91-1 Saiidi, M., E. Hwang, E. Maragakis, and B. Douglas, "Dynamic Testing and the Analysis of the Flamingo Road Interchange," Civil Engineering Department, Report No. CCEER-91-1, University of Nevada, Reno, February 1991.
- CCEER-91-2 Norris, G., R. Siddharthan, Z. Zafir, S. Abdel-Ghaffar, and P. Gowda, "Soil-Foundation-Structure Behavior at the Oakland Outer Harbor Wharf," Civil Engineering Department, Report No. CCEER-91-2, University of Nevada, Reno, July 1991.
- CCEER-91-3 Norris, G., "Seismic Lateral and Rotational Pile Foundation Stiffnesses at Cypress," Civil Engineering Department, Report No. CCEER-91-3, University of Nevada, Reno, August 1991.
- CCEER-91-4 O'Connor, D. and M. Saiidi, "A Study of Protective Overlays for Highway Bridge Decks in Nevada, with Emphasis on Polyester-Styrene Polymer Concrete," Civil Engineering Department, Report No. CCEER-91-4, University of Nevada, Reno, October 1991.
- CCEER-91-5 O'Connor, D.N. and M. Saiidi, "Laboratory Studies of Polyester-Styrene Polymer Concrete Engineering Properties," Civil Engineering Department, Report No. CCEER-91-5, University of Nevada, Reno, November 1991.
- CCEER-92-1 Straw, D.L. and M. Saiidi, "Scale Model Testing of One-Way Reinforced Concrete Pier Hinges Subject to Combined Axial Force, Shear and Flexure," edited by D.N. O'Connor, Civil Engineering Department, Report No. CCEER-92-1, University of Nevada, Reno, March 1992.
- CCEER-92-2 Wehbe, N., M. Saiidi, and F. Gordaninejad, "Basic Behavior of Composite Sections Made of Concrete Slabs and Graphite Epoxy Beams," Civil Engineering Department, Report No. CCEER-92-2, University of Nevada, Reno, August 1992.

- CCEER-92-3 Saiidi, M. and E. Hutchens, "A Study of Prestress Changes in A Post-Tensioned Bridge During the First 30 Months," Civil Engineering Department, Report No. CCEER-92-3, University of Nevada, Reno, April 1992.
- CCEER-92-4 Saiidi, M., B. Douglas, S. Feng, E. Hwang, and E. Maragakis, "Effects of Axial Force on Frequency of Prestressed Concrete Bridges," Civil Engineering Department, Report No. CCEER-92-4, University of Nevada, Reno, August 1992.
- CCEER-92-5 Siddharthan, R., and Z. Zafir, "Response of Layered Deposits to Traveling Surface Pressure Waves," Civil Engineering Department, Report No. CCEER-92-5, University of Nevada, Reno, September 1992.
- CCEER-92-6 Norris, G., and Z. Zafir, "Liquefaction and Residual Strength of Loose Sands from Drained Triaxial Tests," Civil Engineering Department, Report No. CCEER-92-6, University of Nevada, Reno, September 1992.
- CCEER-92-6-A Norris, G., Siddharthan, R., Zafir, Z. and Madhu, R. "Liquefaction and Residual Strength of Sands from Drained Triaxial Tests," Civil Engineering Department, Report No. CCEER-92-6-A, University of Nevada, Reno, September 1992.
- CCEER-92-7 Douglas, B., "Some Thoughts Regarding the Improvement of the University of Nevada, Reno's National Academic Standing," Civil Engineering Department, Report No. CCEER-92-7, University of Nevada, Reno, September 1992.
- CCEER-92-8 Saiidi, M., E. Maragakis, and S. Feng, "An Evaluation of the Current Caltrans Seismic Restrainer Design Method," Civil Engineering Department, Report No. CCEER-92-8, University of Nevada, Reno, October 1992.
- CCEER-92-9 O'Connor, D., M. Saiidi, and E. Maragakis, "Effect of Hinge Restrainers on the Response of the Madrone Drive Undercrossing During the Loma Prieta Earthquake," Civil Engineering Department, Report No. CCEER-92-9, University of Nevada, Reno, February 1993.
- CCEER-92-10 O'Connor, D., and M. Saiidi, "Laboratory Studies of Polyester Concrete: Compressive Strength at Elevated Temperatures and Following Temperature Cycling, Bond Strength to Portland Cement Concrete, and Modulus of Elasticity," Civil Engineering Department, Report No. CCEER-92-10, University of Nevada, Reno, February 1993.

- CCEER-92-11 Wehbe, N., M. Saiidi, and D. O'Connor, "Economic Impact of Passage of Spent Fuel Traffic on Two Bridges in Northeast Nevada," Civil Engineering Department, Report No. CCEER-92-11, University of Nevada, Reno, December 1992.
- CCEER-93-1 Jiang, Y., and M. Saiidi, "Behavior, Design, and Retrofit of Reinforced Concrete One-way Bridge Column Hinges," edited by D. O'Connor, Civil Engineering Department, Report No. CCEER-93-1, University of Nevada, Reno, March 1993.
- CCEER-93-2 Abdel-Ghaffar, S., E. Maragakis, and M. Saiidi, "Evaluation of the Response of the Aptos Creek Bridge During the 1989 Loma Prieta Earthquake," Civil Engineering Department, Report No. CCEER-93-2, University of Nevada, Reno, June 1993.
- CCEER-93-3 Sanders, D.H., B.M. Douglas, and T.L. Martin, "Seismic Retrofit Prioritization of Nevada Bridges," Civil Engineering Department, Report No. CCEER-93-3, University of Nevada, Reno, July 1993.
- CCEER-93-4 Abdel-Ghaffar, S., E. Maragakis, and M. Saiidi, "Performance of Hinge Restrainers in the Huntington Avenue Overhead During the 1989 Loma Prieta Earthquake," Civil Engineering Department, Report No. CCEER-93-4, University of Nevada, Reno, June 1993.
- CCEER-93-5 Maragakis, E., M. Saiidi, S. Feng, and L. Flournoy, "Effects of Hinge Restrainers on the Response of the San Gregorio Bridge during the Loma Prieta Earthquake," (in final preparation) Civil Engineering Department, Report No. CCEER-93-5, University of Nevada, Reno.
- CCEER-93-6 Saiidi, M., E. Maragakis, S. Abdel-Ghaffar, S. Feng, and D. O'Connor, "Response of Bridge Hinge Restrainers during Earthquakes -Field Performance, Analysis, and Design," Civil Engineering Department, Report No. CCEER-93-6, University of Nevada, Reno, May 1993.
- CCEER-93-7 Wehbe, N., Saiidi, M., Maragakis, E., and Sanders, D., "Adequacy of Three Highway Structures in Southern Nevada for Spent Fuel Transportation," Civil Engineering Department, Report No. CCEER-93-7, University of Nevada, Reno, August 1993.
- CCEER-93-8 Roybal, J., Sanders, D.H., and Maragakis, E., "Vulnerability Assessment of Masonry in the Reno-Carson City Urban Corridor," Civil Engineering Department, Report No. CCEER-93-8, University of Nevada, Reno, May 1993.

- CCEER-93-9 Zafir, Z. and Siddharthan, R., "MOVLOAD: A Program to Determine the Behavior of Nonlinear Horizontally Layered Medium Under Moving Load," Civil Engineering Department, Report No. CCEER-93-9, University of Nevada, Reno, August 1993.
- CCEER-93-10 O'Connor, D.N., Saiidi, M., and Maragakis, E.A., "A Study of Bridge Column Seismic Damage Susceptibility at the Interstate 80/U.S. 395 Interchange in Reno, Nevada," Civil Engineering Department, Report No. CCEER-93-10, University of Nevada, Reno, October 1993.
- CCEER-94-1 Maragakis, E., B. Douglas, and E. Abdelwahed, "Preliminary Dynamic Analysis of a Railroad Bridge," Report CCEER-94-1, January 1994.
- CCEER-94-2 Douglas, B.M., Maragakis, E.A., and Feng, S., "Stiffness Evaluation of Pile Foundation of Cazenovia Creek Overpass," Civil Engineering Department, Report No. CCEER-94-2, University of Nevada, Reno, March 1994.
- CCEER-94-3 Douglas, B.M., Maragakis, E.A., and Feng, S., "Summary of Pretest Analysis of Cazenovia Creek Bridge," Civil Engineering Department, Report No. CCEER-94-3, University of Nevada, Reno, April 1994.
- CCEER-94-4 Norris, G.M., Madhu, R., Valceschini, R., and Ashour, M., "Liquefaction and Residual Strength of Loose Sands from Drained Triaxial Tests," Report 2, Vol. 1&2, Civil Engineering Department, Report No. CCEER-94-4, University of Nevada, Reno, August 1994.
- CCEER-94-5 Saiidi, M., Hutchens, E., and Gardella, D., "Prestress Losses in a Post-Tensioned R/C Box Girder Bridge in Southern Nevada," Civil Engineering Department, CCEER-94-5, University of Nevada, Reno, August 1994.
- CCEER-95-1 Siddharthan, R., El-Gamal, M., and Maragakis, E.A., "Nonlinear Bridge Abutment, Verification, and Design Curves," Civil Engineering Department, CCEER-95-1, University of Nevada, Reno, January 1995.
- CCEER-95-2 Ashour, M. and Norris, G., "Liquefaction and drained Response Evaluation of Sands from Drained Formulation," Civil Engineering Department, Report No. CCEER-95-2, University of Nevada, Reno, February 1995.
- CCEER-95-3 Wehbe, N., Saiidi, M., Sanders, D. and Douglas, B., "Ductility of Rectangular Reinforced Concrete Bridge Columns with Moderate Confinement," Civil Engineering Department, Report No. CCEER-95-3, University of Nevada, Reno, July 1995.

- CCEER-95-4 Martin, T., Saiidi, M. and Sanders, D., "Seismic Retrofit of Column-Pier Cap Connections in Bridges in Northern Nevada," Civil Engineering Department, Report No. CCEER-95-4, University of Nevada, Reno, August 1995.
- CCEER-95-5 Darwish, I., Saiidi, M. and Sanders, D., "Experimental Study of Seismic Susceptibility Column-Footing Connections in Bridges in Northern Nevada," Civil Engineering Department, Report No. CCEER-95-5, University of Nevada, Reno, September 1995.
- CCEER-95-6 Griffin, G., Saiidi, M. and Maragakis, E., "Nonlinear Seismic Response of Isolated Bridges and Effects of Pier Ductility Demand," Civil Engineering Department, Report No. CCEER-95-6, University of Nevada, Reno, November 1995.
- CCEER-95-7 Acharya, S., Saiidi, M. and Sanders, D., "Seismic Retrofit of Bridge Footings and Column-Footing Connections," Civil Engineering Department, Report No. CCEER-95-7, University of Nevada, Reno, November 1995.
- CCEER-95-8 Maragakis, E., Douglas, B., and Sandirasegaram, ., "Full-Scale Field Resonance Tests of a Railway Bridge," A Report to the Association of American Railroads, Civil Engineering Department, Report No. CCEER-95-8, University of Nevada, Reno, December 1995.
- CCEER-95-9 Douglas, B., Maragakis, E. and Feng, S., "System Identification Studies on Cazenovia Creek Overpass," Report for the National Center for Earthquake Engineering Research, Civil Engineering Department, Report No. CCEER-95-9, University of Nevada, Reno, October 1995.
- CCEER-96-1 El-Gamal, M.E. and Siddharthan, R.V., "Programs to Computer Translational Stiffness of Seat-Type Bridge Abutment," Civil Engineering Department, Report No. CCEER-96-1, University of Nevada, Reno, March 1996.
- CCEER-96-2 Labia, Y., Saiidi, M. and Douglas, B., "Evaluation and Repair of Full-Scale Prestressed Concrete Box Girders," A Report to the National Science Foundation, Research Grant CMS-9201908, Civil Engineering Department, Report No. CCEER-96-2, University of Nevada, Reno, May 1996.

- CCEER-96-3 Darwish, I., Saiidi, M. and Sanders, D., “Seismic Retrofit of R/C Oblong Tapered Bridge Columns with Inadequate Bar Anchorage in Columns and Footings,” A Report to the Nevada Department of Transportation, Civil Engineering Department, Report No. CCEER-96-3, University of Nevada, Reno, May 1996.
- CCEER-96-4 Ashour, M., Pilling, R., Norris, G. and Perez, H., “The Prediction of Lateral Load Behavior of Single Piles and Pile Groups Using the Strain Wedge Model,” A Report to the California Department of Transportation, Civil Engineering Department, Report No. CCEER-96-4, University of Nevada, Reno, June 1996.
- CCEER-97-1-A Rimal, P. and Itani, A. “Sensitivity Analysis of Fatigue Evaluations of Steel Bridges,” Center for Earthquake Research, Department of Civil Engineering, University of Nevada, Reno, Nevada Report No. CCEER-97-1-A, September, 1997.
- CCEER-97-1-B Maragakis, E., Douglas, B., and Sandirasegaram, . “Full-Scale Field Resonance Tests of a Railway Bridge,” A Report to the Association of American Railroads, Civil Engineering Department, University of Nevada, Reno, May, 1996.
- CCEER-97-2 Wehbe, N., Saiidi, M., and D. Sanders, “Effect of Confinement and Flares on the Seismic Performance of Reinforced Concrete Bridge Columns,” Civil Engineering Department, Report No. CCEER-97-2, University of Nevada, Reno, September 1997.
- CCEER-97-3 Darwish, I., M. Saiidi, G. Norris, and E. Maragakis, “Determination of In-Situ Footing Stiffness Using Full-Scale Dynamic Field Testing,” A Report to the Nevada Department of Transportation, Structural Design Division, Carson City, Nevada, Report No. CCEER-97-3, University of Nevada, Reno, October 1997.
- CCEER-97-4-A Itani, A. “Cyclic Behavior of Richmond-San Rafael Tower Links,” Center for Civil Engineering Earthquake Research, Department of Civil Engineering, University of Nevada, Reno, Nevada, Report No. CCEER-97-4, August 1997.
- CCEER-97-4-B Wehbe, N., and M. Saiidi, “se r’s Manual for RCMC v. 1.2 : A Computer Program for Moment-Curvature Analysis of Confined and nc onfined Reinforced Concrete Sections,” Center for Civil Engineering Earthquake Research, Department of Civil Engineering, University of Nevada, Reno, Nevada, Report No. CCEER-97-4, November, 1997.

- CCEER-97-5 Isakovic, T., M. Saiidi, and A. Itani, "Influence of new Bridge Configurations on Seismic Performance," Department of Civil Engineering, University of Nevada, Reno, Report No. CCEER-97-5, September, 1997.
- CCEER-98-1 Itani, A., Vesco, T. and Dietrich, A., "Cyclic Behavior of "as Built" Laced Members With End Gusset Plates on the San Francisco Bay Bridge," Center for Civil Engineering Earthquake Research, Department of Civil Engineering, University of Nevada, Reno, Nevada Report No. CCEER-98-1, March, 1998.
- CCEER-98-2 G. Norris and M. Ashour, "Liquefaction and undrained Response Evaluation of Sands from Drained Formulation," Center for Civil Engineering Earthquake Research, Department of Civil Engineering, University of Nevada, Reno, Nevada, Report No. CCEER-98-2, May, 1998.
- CCEER-98-3 Qingbin, Chen, B. M. Douglas, E. Maragakis, and I. G. Buckle, "Extraction of Nonlinear Hysteretic Properties of Seismically Isolated Bridges from Quick-Release Field Tests," Center for Civil Engineering Earthquake Research, Department of Civil Engineering, University of Nevada, Reno, Nevada, Report No. CCEER-98-3, June, 1998.
- CCEER-98-4 Maragakis, E., B. M. Douglas, and C. Qingbin, "Full-Scale Field Capacity Tests of a Railway Bridge," Center for Civil Engineering Earthquake Research, Department of Civil Engineering, University of Nevada, Reno, Nevada, Report No. CCEER-98-4, June, 1998.
- CCEER-98-5 Itani, A., Douglas, B., and Woodgate, J., "Cyclic Behavior of Richmond-San Rafael Retrofitted Tower Leg," Center for Civil Engineering Earthquake Research, Department of Civil Engineering, University of Nevada, Reno. Report No. CCEER-98-5, June 1998
- CCEER-98-6 Moore, R., Saiidi, M., and Itani, A., "Seismic Behavior of New Bridges with Skew and Curvature," Center for Civil Engineering Earthquake Research, Department of Civil Engineering, University of Nevada, Reno. Report No. CCEER-98-6, October, 1998.
- CCEER-98-7 Itani, A and Dietrich, A, "Cyclic Behavior of Double Gusset Plate Connections," Center for Civil Engineering Earthquake Research, Department of Civil Engineering, University of Nevada, Reno, Nevada, Report No. CCEER-98-5, December, 1998.

- CCEER-99-1 Caywood, C., M. Saiidi, and D. Sanders, "Seismic Retrofit of Flared Bridge Columns with Steel Jackets," Civil Engineering Department, University of Nevada, Reno, Report No. CCEER-99-1, February 1999.
- CCEER-99-2 Mangoba, N., M. Mayberry, and M. Saiidi, "Prestress Loss in Four Box Girder Bridges in Northern Nevada," Civil Engineering Department, University of Nevada, Reno, Report No. CCEER-99-2, March 1999.
- CCEER-99-3 Abo-Shadi, N., M. Saiidi, and D. Sanders, "Seismic Response of Bridge Pier Walls in the Weak Direction," Civil Engineering Department, University of Nevada, Reno, Report No. CCEER-99-3, April 1999.
- CCEER-99-4 Buzick, A., and M. Saiidi, "Shear Strength and Shear Fatigue Behavior of Full-Scale Prestressed Concrete Box Girders," Civil Engineering Department, University of Nevada, Reno, Report No. CCEER-99-4, April 1999.
- CCEER-99-5 Randall, M., M. Saiidi, E. Maragakis and T. Isakovic, "Restrainer Design Procedures For Multi-Span Simply-Supported Bridges," Civil Engineering Department, University of Nevada, Reno, Report No. CCEER-99-5, April 1999.
- CCEER-99-6 Wehbe, N. and M. Saiidi, "User's Manual for RCMC v. 1.2, A Computer Program for Moment-Curvature Analysis of Confined and Unconfined Reinforced Concrete Sections," Civil Engineering Department, University of Nevada, Reno, Report No. CCEER-99-6, May 1999.
- CCEER-99-7 Burda, J. and A. Itani, "Studies of Seismic Behavior of Steel Base Plates," Civil Engineering Department, University of Nevada, Reno, Report No. CCEER-99-7, May 1999.
- CCEER-99-8 Ashour, M. and G. Norris, "Refinement of the Strain Wedge Model Program," Civil Engineering Department, University of Nevada, Reno, Report No. CCEER-99-8, March 1999.
- CCEER-99-9 Dietrich, A., and A. Itani, "Cyclic Behavior of Laced and Perforated Steel Members on the San Francisco-Oakland Bay Bridge," Civil Engineering Department, University of Nevada, Reno, Report No. CCEER-99-9, December 1999.
- CCEER 99-10 Itani, A., A. Dietrich, "Cyclic Behavior of Built-up Steel Members and their Connections," Civil Engineering Department, University of Nevada, Reno, Report No. CCEER-99-10, December 1999.

- CCEER 99-10-A Itani, A., E. Maragakis and P. He, "Fatigue Behavior of Riveted Open Deck Railroad Bridge Girders," Civil Engineering Department, University of Nevada, Reno, Report No. CCEER-99-10-A, August 1999.
- CCEER 99-11 Itani, A., J. Woodgate, "Axial and Rotational Ductility of Built up Structural Steel Members," Civil Engineering Department, University of Nevada, Reno, Report No. CCEER-99-11, December 1999.
- CCEER-99-12 Sgambelluri, M., Sanders, D.H., and Saiidi, M.S., "Behavior of One-Way Reinforced Concrete Bridge Column Hinges in the Weak Direction," Department of Civil Engineering, University of Nevada, Reno, Report No. CCEER-99-12, December 1999.
- CCEER-99-13 Laplace, P., Sanders, D.H., Douglas, B, and Saiidi, M, "Shake Table Testing of Flexure Dominated Reinforced Concrete Bridge Columns", Department of Civil Engineering, University of Nevada, Reno, Report No. CCEER-99-13, December 1999.
- CCEER-99-14 Ahmad M. Itani, Jose A. Zepeda, and Elizabeth A. Ware "Cyclic Behavior of Steel Moment Frame Connections for the Moscone Center Expansion," Department of Civil Engineering, University of Nevada, Reno, Report No. CCEER-99-14, December 1999.
- CCEER 00-1 Ashour, M., and Norris, G. "Unreinforced Lateral Pile and Pile Group Response in Saturated Sand," Civil Engineering Department, University of Nevada, Reno, Report No. CCEER-00-1, May 1999. January 2000.
- CCEER 00-2 Saiidi, M. and Wehbe, N., "A Comparison of Confinement Requirements in Different Codes for Rectangular, Circular, and Double-Spiral RC Bridge Columns," Civil Engineering Department, University of Nevada, Reno, Report No. CCEER-00-2, January 2000.
- CCEER 00-3 McElhaney, B., M. Saiidi, and D. Sanders, "Shake Table Testing of Flared Bridge Columns With Steel Jacket Retrofit," Civil Engineering Department, University of Nevada, Reno, Report No. CCEER-00-3, January 2000.
- CCEER 00-4 Martinovic, F., M. Saiidi, D. Sanders, and F. Gordaninejad, "Dynamic Testing of Non-Prismatic Reinforced Concrete Bridge Columns Retrofitted with FRP Jackets," Civil Engineering Department, University of Nevada, Reno, Report No. CCEER-00-4, January 2000.

- CCEER 00-5 Itani, A., and M. Saiidi, "Seismic Evaluation of Steel Joints for C LA Center for Health Science Westwood Replacement Hospital," Civil Engineering Department, University of Nevada, Reno, Report No. CCEER-00-5, February 2000.
- CCEER 00-6 Will, J. and D. Sanders, "High Performance Concrete sing Nevada Aggregates," Civil Engineering Department, ni versity of Nevada, Reno, Report No. CCEER-00-6, May 2000.
- CCEER 00-7 French, C., and M. Saiidi, "A Comparison of Static and Dynamic Performance of Models of Flared Bridge Columns," Civil Engineering Department, University of Nevada, Reno, Report No. CCEER-00-7, October 2000.
- CCEER 00-8 Itani, A., H. Sedarat, "Seismic Analysis of the AISI LRFD Design Example of Steel Highway Bridges," Civil Engineering Department, University of Nevada, Reno, Report No. CCEER 00-08, November 2000.
- CCEER 00-9 Moore, J., D. Sanders, and M. Saiidi, "Shake Table Testing of 1960's Two Column Bent with Hinges Bases," Civil Engineering Department, University of Nevada, Reno, Report No. CCEER 00-09, December 2000.
- CCEER 00-10 Asthana, M., D. Sanders, and M. Saiidi, "One-Way Reinforced Concrete Bridge Column Hinges in the Weak Direction," Civil Engineering Department, University of Nevada, Reno, Report No. CCEER 00-10, April 2001.
- CCEER 01-1 Ah Sha, H., D. Sanders, M. Saiidi, "Early Age Shrinkage and Cracking of Nevada Concrete Bridge Decks," Civil Engineering Department, University of Nevada, Reno, Report No. CCEER 01-01, May 2001.
- CCEER 01-2 Ashour, M. and G. Norris, "Pile Group program for Full Material Modeling a Progressive Failure," Civil Engineering Department, University of Nevada, Reno, Report No. CCEER 01-02, July 2001.
- CCEER 01-3 Itani, A., C. Lanaud, and P. Dusicka, "Non-Linear Finite Element Analysis of Built-p Shear Links," Civil Engineering Department, University of Nevada, Reno, Report No. CCEER 01-03, July 2001.
- CCEER 01-4 Saiidi, M., J. Mortensen, and F. Martinovic, "Analysis and Retrofit of Fixed Flared Columns with Glass Fiber-Reinforced Plastic Jacketing," Civil Engineering Department, University of Nevada, Reno, Report No. CCEER 01-4, August 2001
- CCEER 01-5 Not Published

- CCEER 01-6 Laplace, P., D. Sanders, and M. Saiidi, "Experimental Study and Analysis of Retrofitted Flexure and Shear Dominated Circular Reinforced Concrete Bridge Columns Subjected to Shake Table Excitation," Civil Engineering Department, University of Nevada, Reno, Report No. CCEER 01-6, June 2001.
- CCEER 01-7 Reppi, F., and D. Sanders, "Removal and Replacement of Cast-in-Place, Post-tensioned, Box Girder Bridge," Civil Engineering Department, University of Nevada, Reno, Report No. CCEER 01-7, December 2001.
- CCEER 02-1 Pulido, C., M. Saiidi, D. Sanders, and A. Itani, "Seismic Performance and Retrofitting of Reinforced Concrete Bridge Bents," Civil Engineering Department, University of Nevada, Reno, Report No. CCEER 02-1, January 2002.
- CCEER 02-2 Yang, Q., M. Saiidi, H. Wang, and A. Itani, "Influence of Ground Motion Incoherency on Earthquake Response of Multi-Support Structures," Civil Engineering Department, University of Nevada, Reno, Report No. CCEER 02-2, May 2002.
- CCEER 02-3 M. Saiidi, B. Gopalakrishnan, E. Reinhardt, and R. Siddharthan, "A Preliminary Study of Shake Table Response of A Two-Column Bridge Bent on Flexible Footings," Civil Engineering Department, University of Nevada, Reno, Report No. CCEER 02-03, June 2002.
- CCEER 02-4 Not Published
- CCEER 02-5 Banghart, A., Sanders, D., Saiidi, M., "Evaluation of Concrete Mixes for Filling the Steel Arches in the Galena Creek Bridge," Civil Engineering Department, University of Nevada, Reno, Report No. CCEER 02-05, June 2002.
- CCEER 02-6 Dusicka, P., Itani, A., Buckle, I. G., "Cyclic Behavior of Shear Links and Tower Shaft Assembly of San Francisco – Oakland Bay Bridge Tower," Civil Engineering Department, University of Nevada, Reno, Report No. CCEER 02-06, July 2002.
- CCEER 02-7 Mortensen, J., and M. Saiidi, "A Performance-Based Design Method for Confinement in Circular Columns," Civil Engineering Department, University of Nevada, Reno, Report No. CCEER 02-07, November 2002.

- CCEER 03-1 Wehbe, N., and M. Saiidi, “se r’s manual for SPMC v. 1.0 : A Computer Program for Moment-Curvature Analysis of Reinforced Concrete Sections with Interlocking Spirals,” Center for Civil Engineering Earthquake Research, Department of Civil Engineering, University of Nevada, Reno, Nevada, Report No. CCEER-03-1, May, 2003.
- CCEER 03-2 Wehbe, N., and M. Saiidi, “se r’s manual for RCMC v. 2.0 : A Computer Program for Moment-Curvature Analysis of Confined and nc onfined Reinforced Concrete Sections,” Center for Civil Engineering Earthquake Research, Department of Civil Engineering, University of Nevada, Reno, Nevada, Report No. CCEER-03-2, June, 2003.
- CCEER 03-3 Nada, H., D. Sanders, and M. Saiidi, “Seismic Performance of RC Bridge Frames with Architectural-Flared Columns,” Civil Engineering Department, University of Nevada, Reno, Report No. CCEER 03-3, January 2003.
- CCEER 03-4 Reinhardt, E., M. Saiidi, and R. Siddharthan, “Seismic Performance of a CFRP/ Concrete Bridge Bent on Flexible Footings,” Civil Engineering Department, University of Nevada, Reno, Report No. CCEER 03-4, August 2003.
- CCEER 03-5 Johnson, N., M. Saiidi, A. Itani, and S. Ladkany, “Seismic Retrofit of Octagonal Columns with Pedestal and One-Way Hinge at the Base,” Center for Civil Engineering Earthquake Research, Department of Civil Engineering, University of Nevada, Reno, Nevada, and Report No. CCEER-03-5, August 2003.
- CCEER 03-6 Mortensen, C., M. Saiidi, and S. Ladkany, “Creep and Shrinkage Losses in Highly Variable Climates,” Center for Civil Engineering Earthquake Research, Department of Civil Engineering, University of Nevada, Reno, Report No. CCEER-03-6, September 2003.
- CCEER 03- 7 Ayoub, C., M. Saiidi, and A. Itani, “A Study of Shape-Memory-Alloy-Reinforced Beams and Cubes,” Center for Civil Engineering Earthquake Research, Department of Civil Engineering, University of Nevada, Reno, Nevada, Report No. CCEER-03-7, October 2003.
- CCEER 03-8 Chandane, S., D. Sanders, and M. Saiidi, “Static and Dynamic Performance of RC Bridge Bents with Architectural-Flared Columns,” Center for Civil Engineering Earthquake Research, Department of Civil Engineering, University of Nevada, Reno, Nevada, Report No. CCEER-03-8, November 2003.

- CCEER 04-1 Olaegbe, C., and Saiidi, M., "Effect of Loading History on Shake Table Performance of A Two-Column Bent with Infill Wall," Center for Civil Engineering Earthquake Research, Department of Civil Engineering, University of Nevada, Reno, Nevada, Report No. CCEER-04-1, January 2004.
- CCEER 04-2 Johnson, R., Maragakis, E., Saiidi, M., and DesRoches, R., "Experimental Evaluation of Seismic Performance of SMA Bridge Restrainers," Center for Civil Engineering Earthquake Research, Department of Civil Engineering, University of Nevada, Reno, Nevada, Report No. CCEER-04-2, February 2004.
- CCEER 04-3 Moustafa, K., Sanders, D., and Saiidi, M., "Impact of Aspect Ratio on Two-Column Bent Seismic Performance," Center for Civil Engineering Earthquake Research, Department of Civil Engineering, University of Nevada, Reno, Nevada, Report No. CCEER-04-3, February 2004.
- CCEER 04-4 Maragakis, E., Saiidi, M., Sanchez-Camargo, F., and Elfass, S., "Seismic Performance of Bridge Restrainers At In-Span Hinges," Center for Civil Engineering Earthquake Research, Department of Civil Engineering, University of Nevada, Reno, Nevada, Report No. CCEER-04-4, March 2004.
- CCEER 04-5 Ashour, M., Norris, G. and Elfass, S., "Analysis of Laterally Loaded Long or Intermediate Drilled Shafts of Small or Large Diameter in Layered Soil," Center for Civil Engineering Earthquake Research, Department of Civil Engineering, University of Nevada, Reno, Nevada, Report No. CCEER-04-5, June 2004.
- CCEER 04-6 Correal, J., Saiidi, M. and Sanders, D., "Seismic Performance of RC Bridge Columns Reinforced with Two Interlocking Spirals," Center for Civil Engineering Earthquake Research, Department of Civil Engineering, University of Nevada, Reno, Nevada, Report No. CCEER-04-6, August 2004.
- CCEER 04-7 Dusicka, P., Itani, A. and Buckle, I., "Cyclic Response and Low Cycle Fatigue Characteristics of Plate Steels," Center for Civil Engineering Earthquake Research, Department of Civil Engineering, University of Nevada, Reno, Nevada, Report No. CCEER-04-7, November 2004.
- CCEER 04-8 Dusicka, P., Itani, A. and Buckle, I., "Built-up Shear Links as Energy Dissipaters for Seismic Protection of Bridges," Center for Civil Engineering Earthquake Research, Department of Civil Engineering, University of Nevada, Reno, Nevada, Report No. CCEER-04-8, November 2004.

- CCEER 04-9 Sureshkumar, K., Saiidi, S., Itani, A. and Ladkany, S., "Seismic Retrofit of Two-Column Bents with Diamond Shape Columns," Center for Civil Engineering Earthquake Research, Department of Civil Engineering, University of Nevada, Reno, Nevada, Report No. CCEER-04-9, November 2004.
- CCEER 05-1 Wang, H. and Saiidi, S., "A Study of RC Columns with Shape Memory Alloy and Engineered Cementitious Composites," Center for Civil Engineering Earthquake Research, Department of Civil Engineering, University of Nevada, Reno, Nevada, Report No. CCEER-05-1, January 2005.
- CCEER 05-2 Johnson, R., Saiidi, S. and Maragakis, E., "A Study of Fiber Reinforced Plastics for Seismic Bridge Restrainers," Center for Civil Engineering Earthquake Research, Department of Civil Engineering, University of Nevada, Reno, Nevada, Report No. CCEER-05-2, January 2005.
- CCEER 05-3 Carden, L.P., Itani, A.M., Buckle, I.G., "Seismic Load Path in Steel Girder Bridge Superstructures," Center for Civil Engineering Earthquake Research, Department of Civil Engineering, University of Nevada, Reno, Nevada, Report No. CCEER-05-3, January 2005.
- CCEER 05-4 Carden, L.P., Itani, A.M., Buckle, I.G., "Seismic Performance of Steel Girder Bridge Superstructures with Ductile End Cross Frames and Seismic Isolation," Center for Civil Engineering Earthquake Research, Department of Civil Engineering, University of Nevada, Reno, Nevada, Report No. CCEER-05-4, January 2005.
- CCEER 05-5 Goodwin, E., Maragakis, M., Itani, A. and Luo, S., "Experimental Evaluation of the Seismic Performance of Hospital Piping Subassemblies," Center for Civil Engineering Earthquake Research, Department of Civil Engineering, University of Nevada, Reno, Nevada, Report No. CCEER-05-5, February 2005.
- CCEER 05-6 Zadeh M. S., Saiidi, S, Itani, A. and Ladkany, S., "Seismic Vulnerability Evaluation and Retrofit Design of Las Vegas Downtown Viaduct," Center for Civil Engineering Earthquake Research, Department of Civil Engineering, University of Nevada, Reno, Nevada, Report No. CCEER-05-6, February 2005.
- CCEER 05-7 Phan, V., Saiidi, S. and Anderson, J., "Near Fault (Near Field) Ground Motion Effects on Reinforced Concrete Bridge Columns," Center for Civil Engineering Earthquake Research, Department of Civil Engineering, University of Nevada, Reno, Nevada, Report No. CCEER-05-7, August 2005.

- CCEER 05-8 Carden, L., Itani, A. and Laplace, P., "Performance of Steel Props at the UNR Fire Science Academy subjected to Repeated Fire," Center for Civil Engineering Earthquake Research, Department of Civil Engineering, University of Nevada, Reno, Nevada, Report No. CCEER-05-8, August 2005.
- CCEER 05-9 Yamashita, R. and Sanders, D., "Shake Table Testing and an Analytical Study of Unbonded Prestressed Hollow Concrete Column Constructed with Precast Segments," Center for Civil Engineering Earthquake Research, Department of Civil Engineering, University of Nevada, Reno, Nevada, Report No. CCEER-05-9, August 2005.
- CCEER 05-10 Not Published
- CCEER 05-11 Carden, L., Itani, A., and Peckan, G., "Recommendations for the Design of Beams and Posts in Bridge Falsework," Center for Civil Engineering Earthquake Research, Department of Civil Engineering, University of Nevada, Reno, Nevada, Report No. CCEER-05-11, October 2005.
- CCEER 06-01 Cheng, Z., Saiidi, M., and Sanders, D., "Development of a Seismic Design Method for Reinforced Concrete Two-Way Bridge Column Hinges," Center for Civil Engineering Earthquake Research, Department of Civil Engineering, University of Nevada, Reno, Nevada, Report No. CCEER-06-01, February 2006.
- CCEER 06-02 Johnson, N., Saiidi, M., and Sanders, D., "Large-Scale Experimental and Analytical Studies of a Two-Span Reinforced Concrete Bridge System," Center for Civil Engineering Earthquake Research, Department of Civil Engineering, University of Nevada, Reno, Nevada, Report No. CCEER-06-02, March 2006.
- CCEER 06-03 Saiidi, M., Ghasemi, H. and Tiras, A., "Seismic Design and Retrofit of Highway Bridges," Proceedings, Second US-Turkey Workshop, Center for Civil Engineering Earthquake Research, Department of Civil Engineering, University of Nevada, Reno, Nevada, Report No. CCEER-06-03, May 2006.
- CCEER 07-01 O'Brien, M., Saiidi, M. and Sadrossadat-Zadeh, M., "A Study of Concrete Bridge Columns Using Innovative Materials Subjected to Cyclic Loading," Center for Civil Engineering Earthquake Research, Department of Civil Engineering, University of Nevada, Reno, Nevada, Report No. CCEER-07-01, January 2007.

- CCEER 07-02 Sadrossadat-Zadeh, M. and Saiidi, M., "Effect of Strain rate on Stress-Strain Properties and Yield Propagation in Steel Reinforcing Bars," Center for Civil Engineering Earthquake Research, Department of Civil Engineering, University of Nevada, Reno, Nevada, Report No. CCEER-07-02, January 2007.
- CCEER 07-03 Sadrossadat-Zadeh, M. and Saiidi, M., "Analytical Study of NEESR-SG 4-Span Bridge Model Using OpenSees," Center for Civil Engineering Earthquake Research, Department of Civil Engineering, University of Nevada, Reno, Nevada, Report No. CCEER-07-03, January 2007.
- CCEER 07-04 Nelson, R., Saiidi, M. and Zadeh, S., "Experimental Evaluation of Performance of Conventional Bridge Systems," Center for Civil Engineering Earthquake Research, Department of Civil Engineering, University of Nevada, Reno, Nevada, Report No. CCEER-07-04, October 2007.
- CCEER 07-05 Bahen, N. and Sanders, D., "Strut-and-Tie Modeling for Disturbed Regions in Structural Concrete Members with Emphasis on Deep Beams," Center for Civil Engineering Earthquake Research, Department of Civil Engineering, University of Nevada, Reno, Nevada, Report No. CCEER-07-05, December 2007.
- CCEER 07-06 Choi, H., Saiidi, M. and Somerville, P., "Effects of Near-Fault Ground Motion and Fault-Rupture on the Seismic Response of Reinforced Concrete Bridges," Center for Civil Engineering Earthquake Research, Department of Civil Engineering, University of Nevada, Reno, Nevada, Report No. CCEER-07-06, December 2007.
- CCEER 07-07 Ashour M. and Norris, G., "Report and User Manual on Strain Wedge Model Computer Program for Files and Large Diameter Shafts with LRFD Procedure," Center for Civil Engineering Earthquake Research, Department of Civil Engineering, University of Nevada, Reno, Nevada, Report No. CCEER-07-07, October 2007.
- CCEER 08-01 Doyle, K. and Saiidi, M., "Seismic Response of Telescopic Pipe Pin Connections," Center for Civil Engineering Earthquake Research, Department of Civil Engineering, University of Nevada, Reno, Nevada, Report No. CCEER-08-01, February 2008.
- CCEER 08-02 Taylor, M. and Sanders, D., "Seismic Time History Analysis and Instrumentation of the Galena Creek Bridge," Center for Civil Engineering Earthquake Research, Department of Civil Engineering, University of Nevada, Reno, Nevada, Report No. CCEER-08-02, April 2008.

- CCEER 08-03 Abdel-Mohti, A. and Pekcan, G., "Seismic Response Assessment and Recommendations for the Design of Skewed Post-Tensioned Concrete Box-Girder Highway Bridges," Center for Civil Engineering Earthquake Research, Department of Civil and Environmental Engineering, University of Nevada, Reno, Nevada, Report No. CCEER-08-03, September 2008.
- CCEER 08-04 Saiidi, M., Ghasemi, H. and Hook, J., "Long Term Bridge Performance Monitoring, Assessment & Management," Proceedings, FHWA/NSF Workshop on Future Directions," Center for Civil Engineering Earthquake Research, Department of Civil and Environmental Engineering, University of Nevada, Reno, Nevada, Report No. CCEER 08-04, September 2008.
- CCEER 09-01 Brown, A., and Saiidi, M., "Investigation of Near-Fault Ground Motion Effects on Substandard Bridge Columns and Bents," Center for Civil Engineering Earthquake Research, Department of Civil and Environmental Engineering, University of Nevada, Reno, Nevada, Report No. CCEER-09-01, July 2009.
- CCEER 09-02 Linke, C., Pekcan, G., and Itani, A., "Detailing of Seismically Resilient Special Truss Moment Frames," Center for Civil Engineering Earthquake Research, Department of Civil and Environmental Engineering, University of Nevada, Reno, Nevada, Report No. CCEER-09-02, August 2009.
- CCEER 09-03 Hillis, D., and Saiidi, M., "Design, Construction, and Nonlinear Dynamic Analysis of Three Bridge Bents s ed in a Bridge System Test," Center for Civil Engineering Earthquake Research, Department of Civil and Environmental Engineering, University of Nevada, Reno, Nevada, Report No. CCEER-09-03, August 2009.
- CCEER 09-04 Bahrami, H., Itani, A., and Buckle, I., "Guidelines for the Seismic Design of Ductile End Cross Frames in Steel Girder Bridge Superstructures," Center for Civil Engineering Earthquake Research, Department of Civil and Environmental Engineering, University of Nevada, Reno, Nevada, Report No. CCEER-09-04, September 2so009.
- CCEER 10-01 Zaghi, A. E., and Saiidi, M., "Seismic Design of Pipe-Pin Connections in Concrete Bridges," Center for Civil Engineering Earthquake Research, Department of Civil and Environmental Engineering, University of Nevada, Reno, Nevada, Report No. CCEER-10-01, January 2010.
- CCEER 10-02 Pooranampillai, S., Elfass, S., and Norris, G., "Laboratory Study to Assess Load Capacity Increase of Drilled Shafts through Post Grouting," Center for Civil Engineering Earthquake Research, Department of Civil and Environmental Engineering, University of Nevada, Reno, Nevada, Report No. CCEER-10-02, January 2010.

- CCEER 10-03 Itani, A., Grubb, M., and Monzon, E, “Proposed Seismic Provisions and Commentary for Steel Plate Girder Superstructures,” Center for Civil Engineering Earthquake Research, Department of Civil and Environmental Engineering, University of Nevada, Reno, Nevada, Report No. CCEER-10-03, June 2010.
- CCEER 10-04 Cruz-Noguez, C., Saiidi, M., “Experimental and Analytical Seismic Studies of a Four-Span Bridge System with Innovative Materials,” Center for Civil Engineering Earthquake Research, Department of Civil and Environmental Engineering, University of Nevada, Reno, Nevada, Report No. CCEER-10-04, September 2010.
- CCEER 10-05 Vosooghi, A., Saiidi, M., “Post-Earthquake Evaluation and Emergency Repair of Damaged RC Bridge Columns Using CFRP Materials,” Center for Civil Engineering Earthquake Research, Department of Civil and Environmental Engineering, University of Nevada, Reno, Nevada, Report No. CCEER-10-05, September 2010.
- CCEER 10-06 Ayoub, M., Sanders, D., “Testing of Pile Extension Connections to Slab Bridges,” Center for Civil Engineering Earthquake Research, Department of Civil and Environmental Engineering, University of Nevada, Reno, Nevada, Report No. CCEER-10-06, October 2010.
- CCEER 10-07 Builes-Mejia, J. C. and Itani, A., “Stability of Bridge Column Rebar Cages during Construction,” Center for Civil Engineering Earthquake Research, Department of Civil and Environmental Engineering, University of Nevada, Reno, Nevada, Report No. CCEER-10-07, November 2010.
- CCEER 10-08 Monzon, E.V., “Seismic Performance of Steel Plate Girder Bridges with Integral Abutments,” Center for Civil Engineering Earthquake Research, Department of Civil and Environmental Engineering, University of Nevada, Reno, Nevada, Report No. CCEER-10-08, November 2010.
- CCEER 11-01 Motaref, S., Saiidi, M., and Sanders, D., “Seismic Response of Precast Bridge Columns with Energy Dissipating Joints,” Center for Civil Engineering Earthquake Research, Department of Civil and Environmental Engineering, University of Nevada, Reno, Nevada, Report No. CCEER-11-01, May 2011.
- CCEER 11-02 Harrison, N. and Sanders, D., “Preliminary Seismic Analysis and Design of Reinforced Concrete Bridge Columns for Curved Bridge Experiments,” Center for Civil Engineering Earthquake Research, Department of Civil and Environmental Engineering, University of Nevada, Reno, Nevada, Report No. CCEER-11-02, May 2011.

- CCEER 11-03 Vallejera, J. and Sanders, D., “Instrumentation and Monitoring the Galena Creek Bridge,” Center for Civil Engineering Earthquake Research, Department of Civil and Environmental Engineering, University of Nevada, Reno, Nevada, Report No. CCEER-11-03, September 2011.
- CCEER 11-04 Levi, M., Sanders, D., and Buckle, I., “Seismic Response of Columns in Horizontally Curved Bridges,” Center for Civil Engineering Earthquake Research, Department of Civil and Environmental Engineering, University of Nevada, Reno, Nevada, Report No. CCEER-11-04, December 2011.
- CCEER 12-01 Saiidi, M., “NSF International Workshop on Bridges of the Future – Wide Spread Implementation of Innovation,” Center for Civil Engineering Earthquake Research, Department of Civil and Environmental Engineering, University of Nevada, Reno, Nevada, Report No. CCEER-12-01, January 2012.
- CCEER 12-02 Larkin, A.S., Sanders, D., and Saiidi, M., “nbon ded Prestressed Columns for Earthquake Resistance,” Center for Civil Engineering Earthquake Research, Department of Civil and Environmental Engineering, University of Nevada, Reno, Nevada, Report No. CCEER-12-02, January 2012.
- CCEER 12-03 Arias-Acosta, J. G., Sanders, D., “Seismic Performance of Circular and Interlocking Spirals RC Bridge Columns under Bidirectional Shake Table Loading Part 1,” Center for Civil Engineering Earthquake Research, Department of Civil and Environmental Engineering, University of Nevada, Reno, Nevada, Report No. CCEER-12-03, September 2012.
- CCEER 12-04 Cukrov, M.E., Sanders, D., “Seismic Performance of Prestressed Pile-To-Bent Cap Connections,” Center for Civil Engineering Earthquake Research, Department of Civil and Environmental Engineering, University of Nevada, Reno, Nevada, Report No. CCEER-12-04, September 2012.
- CCEER 13-01 Carr, T. and Sanders, D., “Instrumentation and Dynamic Characterization of the Galena Creek Bridge,” Center for Civil Engineering Earthquake Research, Department of Civil and Environmental Engineering, University of Nevada, Reno, Nevada, Report No. CCEER-13-01, January 2013.
- CCEER 13-02 Vosooghi, A. and Buckle, I., “Evaluation of the Performance of a Conventional Four-Span Bridge During Shake Table Tests,” Center for Civil Engineering Earthquake Research, Department of Civil and Environmental Engineering, University of Nevada, Reno, Nevada, Report No. CCEER-13-02, January 2013.

- CCEER 13-03 Amiriormozaki, E. and Pekcan, G., "Analytical Fragility Curves for Horizontally Curved Steel Girder Highway Bridges," Center for Civil Engineering Earthquake Research, Department of Civil and Environmental Engineering, University of Nevada, Reno, Nevada, Report No. CCEER-13-03, February 2013.
- CCEER 13-04 Almer, K. and Sanders, D., "Longitudinal Seismic Performance of Precast Bridge Girders Integrally Connected to a Cast-in-Place Bentcap," Center for Civil Engineering Earthquake Research, Department of Civil and Environmental Engineering, University of Nevada, Reno, Nevada, Report No. CCEER-13-04, April 2013.
- CCEER 13-05 Monzon, E.V., Itani, A.I., and Buckle, I.G., "Seismic Modeling and Analysis of Curved Steel Plate Girder Bridges," Center for Civil Engineering Earthquake Research, Department of Civil and Environmental Engineering, University of Nevada, Reno, Nevada, Report No. CCEER-13-05, April 2013.
- CCEER 13-06 Monzon, E.V., Buckle, I.G., and Itani, A.I., "Seismic Performance of Curved Steel Plate Girder Bridges with Seismic Isolation," Center for Civil Engineering Earthquake Research, Department of Civil and Environmental Engineering, University of Nevada, Reno, Nevada, Report No. CCEER-13-06, April 2013.
- CCEER 13-07 Monzon, E.V., Buckle, I.G., and Itani, A.I., "Seismic Response of Isolated Bridge Superstructure to Incoherent Ground Motions," Center for Civil Engineering Earthquake Research, Department of Civil and Environmental Engineering, University of Nevada, Reno, Nevada, Report No. CCEER-13-07, April 2013.
- CCEER 13-08 Haber, Z.B., Saiidi, M.S., and Sanders, D.H., "Precast Column-Footing Connections for Accelerated Bridge Construction in Seismic Zones," Center for Civil Engineering Earthquake Research, Department of Civil and Environmental Engineering, University of Nevada, Reno, Nevada, Report No. CCEER-13-08, April 2013.
- CCEER 13-09 Ryan, K.L., Coria, C.B., and Dao, N.D., "Large Scale Earthquake Simulation of a Hybrid Lead Rubber Isolation System Designed under Nuclear Seismicity Considerations," Center for Civil Engineering Earthquake Research, Department of Civil and Environmental Engineering, University of Nevada, Reno, Nevada, Report No. CCEER-13-09, April 2013.

- CCEER 13-10 Wibowo, H., Sanford, D.M., Buckle, I.G., and Sanders, D.H., “The Effect of Live Load on the Seismic Response of Bridges,” Center for Civil Engineering Earthquake Research, Department of Civil and Environmental Engineering, University of Nevada, Reno, Nevada, Report No. CCEER-13-10, May 2013.
- CCEER 13-11 Sanford, D.M., Wibowo, H., Buckle, I.G., and Sanders, D.H., “Preliminary Experimental Study on the Effect of Live Load on the Seismic Response of Highway Bridges,” Center for Civil Engineering Earthquake Research, Department of Civil and Environmental Engineering, University of Nevada, Reno, Nevada, Report No. CCEER-13-11, May 2013.
- CCEER 13-12 Saad, A.S., Sanders, D.H., and Buckle, I.G., “Assessment of Foundation Rocking Behavior in Reducing the Seismic Demand on Horizontally Curved Bridges,” Center for Civil Engineering Earthquake Research, Department of Civil and Environmental Engineering, University of Nevada, Reno, Nevada, Report No. CCEER-13-12, June 2013.
- CCEER 13-13 Ardakani, S.M.S. and Saiidi, M.S., “Design of Reinforced Concrete Bridge Columns for Near-Fault Earthquakes,” Center for Civil Engineering Earthquake Research, Department of Civil and Environmental Engineering, University of Nevada, Reno, Nevada, Report No. CCEER-13-13, July 2013.
- CCEER 13-14 Wei, C. and Buckle, I., “Seismic Analysis and Response of Highway Bridges with Hybrid Isolation,” Center for Civil Engineering Earthquake Research, Department of Civil and Environmental Engineering, University of Nevada, Reno, Nevada, Report No. CCEER-13-14, August 2013.
- CCEER 13-15 Wibowo, H., Buckle, I.G., and Sanders, D.H., “Experimental and Analytical Investigations on the Effects of Live Load on the Seismic Performance of a Highway Bridge,” Center for Civil Engineering Earthquake Research, Department of Civil and Environmental Engineering, University of Nevada, Reno, Nevada, Report No. CCEER-13-15, August 2013.
- CCEER 13-16 Itani, A.M., Monzon, E.V., Grubb, M., and Amirhormozaki, E. “Seismic Design and Nonlinear Evaluation of Steel I-Girder Bridges with Ductile End Cross-Frames,” Center for Civil Engineering Earthquake Research, Department of Civil and Environmental Engineering, University of Nevada, Reno, Nevada, Report No. CCEER-13-16, September 2013.

- CCEER 13-17 Kavianipour, F. and Saiidi, M.S., “Experimental and Analytical Seismic Studies of a Four-span Bridge System with Composite Piers,” Center for Civil Engineering Earthquake Research, Department of Civil and Environmental Engineering, University of Nevada, Reno, Nevada, Report No. CCEER-13-17, September 2013.
- CCEER 13-18 Mohebbi, A., Ryan, K., and Sanders, D., “Seismic Response of a Highway Bridge with Structural Fuses for Seismic Protection of Piers,” Center for Civil Engineering Earthquake Research, Department of Civil and Environmental Engineering, University of Nevada, Reno, Nevada, Report No. CCEER-13-18, December 2013.
- CCEER 13-19 Guzman Pujols, Jean C., Ryan, K.L., “Development of Generalized Fragility Functions for Seismic Induced Content Disruption,” Center for Civil Engineering Earthquake Research, Department of Civil and Environmental Engineering, University of Nevada, Reno, Nevada, Report No. CCEER-13-19, December 2013.
- CCEER 14-01 Salem, M. M. A., Pekcan, G., and Itani, A., “Seismic Response Control Of Structures Using Semi-Active and Passive Variable Stiffness Devices,” Center for Civil Engineering Earthquake Research, Department of Civil and Environmental Engineering, University of Nevada, Reno, Nevada, Report No. CCEER-14-01, May 2014.
- CCEER 14-02 Saini, A. and Saiidi, M., “Performance-Based Probabilistic Damage Control Approach for Seismic Design of Bridge Columns,” Center For Civil Engineering Earthquake Research, Department Of Civil and Environmental Engineering, University of Nevada, Reno, Nevada, Report No. CCEER-14-02, May 2014.
- CCEER 14-03 Saini, A. and Saiidi, M., “Post Earthquake Damage Repair of Various Reinforced Concrete Bridge Components,” Center For Civil Engineering Earthquake Research, Department Of Civil and Environmental Engineering, University of Nevada, Reno, Nevada, Report No. CCEER-14-03, May 2014.
- CCEER 14-04 Monzon, E.V., Itani, A.M., and Grubb, M.A., “Nonlinear Evaluation of the Proposed Seismic Design Procedure for Steel Bridges with Ductile End Cross Frames,” Center For Civil Engineering Earthquake Research, Department Of Civil and Environmental Engineering, University of Nevada, Reno, Nevada, Report No. CCEER-14-04, July 2014.
- CCEER 14-05 Nakashoji, B. and Saiidi, M.S., “Seismic Performance of Square Nickel-Titanium Reinforced ECC Columns with Headed Couplers,” Center For Civil Engineering Earthquake Research, Department Of Civil and

Environmental Engineering, University of Nevada, Reno, Nevada, Report No. CCEER-14-05, July 2014.

CCEER 14-06 Tazarv, M. and Saiidi, M.S., “Next Generation of Bridge Columns for Accelerated Bridge Construction in High Seismic Zones,” Center For Civil Engineering Earthquake Research, Department Of Civil and Environmental Engineering, University of Nevada, Reno, Nevada, Report No. CCEER-14-06, August 2014.

CCEER 14-07 Mehrsoroush, A. and Saiidi, M.S., “Experimental and Analytical Seismic Studies of Bridge Piers with Innovative Pipe Pin Column-Footing Connections and Precast Cap Beams,” Center For Civil Engineering Earthquake Research, Department Of Civil and Environmental Engineering, University of Nevada, Reno, Nevada, Report No. CCEER-14-07, December 2014.

CCEER 15-01 Dao, N.D. and Ryan, K.L., “Seismic Response of a Full-scale 5-story Steel Frame Building Isolated by Triple Pendulum Bearings under 3D Excitations,” Center For Civil Engineering Earthquake Research, Department Of Civil and Environmental Engineering, University of Nevada, Reno, Nevada, Report No. CCEER-15-01, January 2015.

CCEER 15-02 Allen, B.M. and Sanders, D.H., “Post-Tensioning Duct Air Pressure Testing Effects on Web Cracking,” Center For Civil Engineering Earthquake Research, Department Of Civil and Environmental Engineering, University of Nevada, Reno, Nevada, Report No. CCEER-15-02, January 2015.

CCEER 15-03 Akl, A. and Saiidi, M.S., “Time-Dependent Deflection of In-Span Hinges in Prestressed Concrete Box Girder Bridges,” Center For Civil Engineering Earthquake Research, Department Of Civil and Environmental Engineering, University of Nevada, Reno, Nevada, Report No. CCEER-15-03, May 2015.

CCEER 15-04 Zargar Shotorbani, H. and Ryan, K., “Analytical and Experimental Study of Gap Damper System to Limit Seismic Isolator Displacements in Extreme Earthquakes,” Center For Civil Engineering Earthquake Research, Department Of Civil and Environmental Engineering, University of Nevada, Reno, Nevada, Report No. CCEER-15-04, June 2015.

- CCEER 15-05 Wieser, J., Maragakis, E.M., and Buckle, I., “Experimental and Analytical Investigation of Seismic Bridge-Abutment Interaction in a Curved Highway Bridge,” Center For Civil Engineering Earthquake Research, Department Of Civil and Environmental Engineering, University of Nevada, Reno, Nevada, Report No. CCEER-15-05, July 2015.
- CCEER 15-06 Tazarv, M. and Saiidi, M.S., “Design and Construction of Precast Bent Caps with Pocket Connections for High Seismic Regions,” Center For Civil Engineering Earthquake Research, Department Of Civil and Environmental Engineering, University of Nevada, Reno, Nevada, Report No. CCEER-15-06, August 2015.
- CCEER 15-07 Tazarv, M. and Saiidi, M.S., “Design and Construction of Bridge Columns Incorporating Mechanical Bar Splices in Plastic Hinge Zones,” Center For Civil Engineering Earthquake Research, Department Of Civil and Environmental Engineering, University of Nevada, Reno, Nevada, Report No. CCEER-15-07, August 2015.
- CCEER 15-08 Sarraf Shirazi, R., Pekcan, G., and Itani, A.M., “Seismic Response and Analytical Fragility Functions for Curved Concrete Box-Girder Bridges,” Center For Civil Engineering Earthquake Research, Department Of Civil and Environmental Engineering, University of Nevada, Reno, Nevada, Report No. CCEER-15-08, December 2015.
- CCEER 15-09 Coria, C.B., Ryan, K.L., and Dao, N.D., “Response of Lead Rubber Bearings in a Hybrid Isolation System During a Large Scale Shaking Experiment of an Isolated Building,” Center For Civil Engineering Earthquake Research, Department Of Civil and Environmental Engineering, University of Nevada, Reno, Nevada, Report No. CCEER-15-09, December 2015.
- CCEER 16-01 Mehraein, M and Saiidi, M.S., “Seismic Performance of Bridge Column-Pile-Shaft Pin Connections for Application in Accelerated Bridge Construction,” Center For Civil Engineering Earthquake Research, Department Of Civil and Environmental Engineering, University of Nevada, Reno, Nevada, Report No. CCEER-16-01, May 2016.
- CCEER 16-02 Varela Fontecha, S. and Saiidi, M.S., “Resilient Earthquake-Resistant Bridges Designed For Disassembly,” Center For Civil Engineering Earthquake Research, Department Of Civil and Environmental Engineering, University of Nevada, Reno, Nevada, Report No. CCEER-16-02, May 2016.

- CCEER 16-03 Mantawy, I. M, and Sanders, D. H., “Assessment of an Earthquake Resilient Bridge with Pretensioned, Rocking Columns,” Center For Civil Engineering Earthquake Research, Department Of Civil and Environmental Engineering, University of Nevada, Reno, Nevada, Report No. CCEER-16-03, May 2016.
- CCEER 16-04 Mohammed, M, Biasi, G., and Sanders, D., “Post-earthquake Assessment of Nevada Bridges using ShakeMap/ShakeCast,” Center For Civil Engineering Earthquake Research, Department Of Civil and Environmental Engineering, University of Nevada, Reno, Nevada, Report No. CCEER-16-04, May 2016.
- CCEER 16-05 Jones, J, Ryan, K., and Saiidi, M, “Toward Successful Implementation of Prefabricated Deck Panels to Accelerate the Bridge Construction Process,” Center For Civil Engineering Earthquake Research, Department Of Civil and Environmental Engineering, University of Nevada, Reno, Nevada, Report No. CCEER-16-05, August 2016.
- CCEER 16-06 Mehrsoroush, A. and Saiidi, M., “Probabilistic Seismic Damage Assessment for Sub-standard Bridge Columns,” Center For Civil Engineering Earthquake Research, Department Of Civil and Environmental Engineering, University of Nevada, Reno, Nevada, Report No. CCEER-16-06, November 2016.
- CCEER 16-07 Nielsen, T., Maree, A., and Sanders, D., “Experimental Investigation into the Long-Term Seismic Performance of Dry Storage Casks,” Center For Civil Engineering Earthquake Research, Department Of Civil and Environmental Engineering, University of Nevada, Reno, Nevada, Report No. CCEER-16-07, December 2016.
- CCEER 16-08 Wu, S., Buckle, I., and Itani, A., “Effect of Skew on Seismic Performance of Bridges with Seat-Type Abutments,” Center For Civil Engineering Earthquake Research, Department Of Civil and Environmental Engineering, University of Nevada, Reno, Nevada, Report No. CCEER-16-08, December 2016.
- CCEER 16-09 Mohammed, M., and Sanders, D., “Effect of Earthquake Duration on Reinforced Concrete Bridge Columns,” Center For Civil Engineering Earthquake Research, Department Of Civil and Environmental Engineering, University of Nevada, Reno, Nevada, Report No. CCEER-16-09, December 2016.

- CCEER 16-10 Guzman Pujols, J., and Ryan, K., "Slab Vibration and Horizontal-Vertical Coupling in the Seismic Response of Irregular Base-Isolated and Conventional Buildings," Center For Civil Engineering Earthquake Research, Department Of Civil and Environmental Engineering, University of Nevada, Reno, Nevada, Report No. CCEER-16-10, December 2016.
- CCEER 17-01 White, L., Ryan, K., and Buckle, I., "Thermal Gradients in Southwestern United States and the Effect on Bridge Bearing Loads," Center For Civil Engineering Earthquake Research, Department Of Civil and Environmental Engineering, University of Nevada, Reno, Nevada, Report No. CCEER-17-01, May 2017.
- CCEER 17-02 Mohebbi, A., Saiidi, M., and Itani, A., "Development and Seismic Evaluation of Pier Systems w/Pocket Connections, CFRP Tendons, and ECC/ HPC Columns," Center For Civil Engineering Earthquake Research, Department Of Civil and Environmental Engineering, University of Nevada, Reno, Nevada, Report No. CCEER-17-02, May 2017.
- CCEER 17-03 Mehrsoroush, A., Saiidi, M., and Ryan, K., "Development of Earthquake-resistant Precast Pier Systems for Accelerated Bridge Construction in Nevada," Center For Civil Engineering Earthquake Research, Department Of Civil and Environmental Engineering, University of Nevada, Reno, Nevada, Report No. CCEER-17-03, June 2017.
- CCEER 17-04 Abdollahi, B., Saiidi, M., Siddharthan, R., and Elfass, S., "Shake Table Studies on Soil-Abutment-Structure Interaction in Skewed Bridges," Center For Civil Engineering Earthquake Research, Department Of Civil and Environmental Engineering, University of Nevada, Reno, Nevada, Report No. CCEER-17-04, July 2017.
- CCEER 17-05 Shrestha, G., Itani, A., and Saiidi, M., "Seismic Performance of Precast Full-Depth Decks in Accelerated Bridge Construction," Center For Civil Engineering Earthquake Research, Department Of Civil and Environmental Engineering, University of Nevada, Reno, Nevada, Report No. CCEER-17-05, July 2018.